

**University of Strathclyde**

**Department of Naval Architecture, Ocean and Marine Engineering**

**ON THE SAFETY OF LNG-  
FUELLED SHIPS**

by

**Byongug Jeong**

A thesis presented in fulfilment of the requirements for the degree  
of Doctor of Philosophy

June

2018

This thesis is the result of the author's original research. It has been composed by the author and has not been previously submitted for examination which has led to the award of a degree.

The copyright of this thesis belongs to the author under the terms of the United Kingdom Copyright Acts as qualified by University of Strathclyde Regulation 3.50. Due acknowledgement must always be made of the use of any material contained in, or derived from, this thesis.

*To my Lord,*

*To my parents, Taeho Jeong & Myeonghwa Choi*

*To my wife, Hyosung Jung*

*To my children, Ahjin and Eunwoo Jeong*

## **ABSTRACT**

With an increasing pressure to use cleaner fuels in shipping, LNG has become a realistic marine fuel of choice by many ship-owners. Although it will undoubtedly contribute towards cleaner shipping, there is a general concern about the safety of its use. Such fears are based on the fact that an accidental release of this flammable mixture may lead to potential incidents, in particular, of fire and explosion. In this context, ensuring the safety is one of the most crucial tasks for the industry in adopting LNG as a marine fuel. It is hardly surprising, therefore, that several rules, regulations, standards and guidelines have been produced at both international and local level. Nevertheless, due largely to the brevity of their history, the existing regulations and class rules appear to have some limitations and shortcomings, in particular, they lack explicit requirements in quantitative terms. It is true that there are rules and guidance for design and operation of LNG process systems in chemical industry with a relatively long history, and they can to some extent be used to safeguard the use of LNG as a fuel, but the arrival of LNG-fuelled ships has made it essential and urgent that their safety should be investigated in detail.

In an effort to examine the existing regulations more intimately a conceptual design exercise to retrofit a 300,000 DWT very large ore carrier to use LNG as one of the marine fuels was carried out in accordance with current regulations. Although it was felt that the most hazardous areas of such a ship are with the fuel preparation room with high-pressure fuel supply system and the bunkering systems, the current regulations were not of much help during this process.

In order to obtain meaningful insights into their threats, the safety of these critical areas were systematically evaluated using quantitative risk assessment models that have been proven to be an effective and efficient tool for evaluating risks in oil/gas process systems.

It became obvious from the outset that an efficient computation tool is essential for the investigation. Consequently, the conventional quantitative risk assessment methods were modified and augmented to best suit the current problem and implemented in a computer program called Integrated Quantitative Risk

Assessment (IQRA). One of the main strengths of IQRA is that it can carry out the whole process of risk analysis from frequency calculation to evaluation of consequence in a seamless process, unlike existing software which require tedious post-processing to obtain the risk values. It has more than proven its worth during the course of this project.

LNG bunkering, at the two weakest ends (on-board LNG receiving point and LNG supplying point) were examined first. Usually such weak points are made relatively safe by imposing a ‘safety exclusion zone’ where non-essential personnel are not allowed entry during the process in question is in progress. However, there is no realistic regulation or guidance to help determining the extent of the zones. One of the few existing guidelines based on population-independent analysis requires an exclusion zone far too extensive and impossible to implement. A realistic method of determining the exclusion zones based on statistical quantitative risk assessment was developed and demonstrated in this thesis. An interesting fact discovered through this study was the fact that short duration bunkering at large scale tends to require smaller exclusion zones than smaller scale bunker for longer duration.

The next area to examine was the fuel preparation room with a high-pressure fuel gas supply system. In this study, an event tree analysis was used to identify events that may cause vapour cloud explosion. General frequency data from various sources was used, and fault tree analysis was applied. Consequence was analysed in terms of the impact from explosion using a CFD and an FEA program. It was found that the structure of some sections of the fuel preparation room must be strengthened in addition to the scantling required by the classification rules.

Additionally, the safety of a medium-sized floating regasification unit was investigated by applying a hierarchical system modelling method newly put forward in this thesis. It demonstrated the excellence of the hierarchical system modelling in assessing the overall risk of complex process systems. The results were compared to the recommendations produced by a benchmark HAZOP study and selective quantitative risk assessment method.

This project established and demonstrated the way that the quantitative risk assessment techniques can be used to investigate the safety of a variety of novel marine LNG plants. A series of studies have proven that the framework and

methodology developed in this thesis provides structured guidelines to conduct quantitative risk assessment associated with LNG-fuelled ships as well as LNG process systems regarding fire and explosion. The facility for parametric and sensitivity analyses have also been shown to be an excellent tool in gaining insight into the nature and characteristics of risks that are inherent in oil/gas process systems while improving understanding of contributing factors to risks and methods of mitigating them as well as points to note during quantitative risk assessment. It is thought that such a tool will be a very useful aid in future rule development.

Last but not least, the safety of people and ships in using and/or processing LNG is paramount. If it is agreed that enhancing the current regulations is an urgent task, it is expected that the results of the studies carried out in this thesis can make a significant contribution to decision-making and further regulatory framework for port authorities and rule-makers.

## **ACKNOWLEDGEMENTS**

Many waves of people have helped to bring this thesis to fruition. In the beginning, Dr Byung Suk Lee was a strong believer that there would be a need for this work to be done. His great encouragement moved this thesis off the starting line. His enthusiastic supervision and personal care for my three year Ph.D. duration made this work to be successful and even more valuable. I am deeply grateful for his anguish of trying to correct the unreadable English writing to be logical and academic.

Professor Peilin Zhou was who provided me with the opportunity that I could come to the University of Strathclyde and indulged myself into studying on the safety of LNG-fuelled ship. His financial/personal supports helped me to only focus on the research work. I would like to thank him for his guidance, consideration, and above all his fairness throughout the entire process. Besides, he has given me a new opportunity to expand my knowledge to a different academic area by appointing me as a research assistant for participating in the SHIPLY project through which I have improved my ability of teamwork for academic research and of collaboration with oversea project partners.

I would like to acknowledge the support of Mr Seungman Ha, who inspired me to be interested in this subject and Dr Juno Kwak who instructed me how to develop a software using LabVIEW.

I was fortunate to work and study with many of colleagues belonging to NAOME. Although not mentioning all their names here, I hope this thesis reflects my enormous respect for what they have done for me.

I also owe a different kind of debt to my family. My wife, Hyosung Jung, was the strongest supporter of my life as she never doubted on my decision. Without her dedication, I could not have achieved this academic fruits. I am so grateful that Ahjin and Eunwoo have successfully settled in and kept happiness in this Scotland environment. My parents always trusted and supported me. They never wanted me to be a person who they would want me to be. Instead, they let me to be a person who I would want to be. I believe that their absolute trust in me comes from the

greatest love. I cannot forget my parents-in-law as their love and support towards me was never less than those from my parents.

I am also grateful for the warmest support and encouragement from my precious Glasgow families and friends; Pastor Philip Everett and Lydia Everett, Pastor Sung-hun Kim, Dr Mingkyu Kim, Kevin Cho, Dae-seung Ahn, Jung-wha Lee, and a lot many others.

I owed too many people to write down all their names. Even though some names are not listed here, my appreciation towards them cannot be underestimated. Whether mentioned here or not, it is true that all of them made my Ph.D. years to be one of the happiest moments. Both my academic and personal accomplishments never could have come this far without their cheerful love and support. Thanks again for all the things that they have done to me.

I have to admit all my intuitions for this subject were originally from God who did not allow me to be discouraged. Instead, he always encouraged and inspired me to put a step forward no matter what difficulties had been placed before me. Therefore, he deserves to receive all my glory.

Last but not least, it is also important to mention that some ideas I describe in this thesis are not originally my own. Rather, I am an applicator to utilize the brilliant of work done by great scholars over the centuries into the marine field. Likewise, I hope that this thesis will help to transmit my knowledge and enthusiasm to new readers and future Ph.D. applicants.



## PUBLICATIONS

### IMO information documents

- Republic of Korea, 2016, IMO CCC3/INF. 13: Evaluation of safety zone for LNG bunkering station for LNG-fuelled ships, London, IMO.
- Republic of Korea, 2016, IMO CCC3/INF. 15: Quantitative risk assessment of fuel preparation room having high-pressure fuel gas supply system for LNG-fuelled ship, London, IMO.
- Republic of Korea, 2016, IMO CCC3/INF. 16: Quantitative risk assessment of LNG bunkering using parametric analysis, London, IMO.
- Republic of Korea, 2017, IMO CCC4/INF18: Study on Quantitative Risk Assessment of Medium-Sized Floating Regasification Unit

### Conferences

- Quantitative risk assessment of fuel preparation room having high-pressure fuel gas supply system for LNG-fuelled ship. EKC 2016, Berlin.
- Quantitative risk Assessment of FRU. WSOS 2016, Newcastle, UK.
- Introduction of rapid quantitative risk assessment software specific to oil / gas processing systems, EKC 2017, Sweden.

### Journals

- **Jeong, B.**, Lee, B.S., Zhou, P., Ha, S.-m., 2017. Evaluation of safety exclusion zone for LNG bunkering station on LNG-fuelled ships. *Journal of Marine Engineering & Technology*, P1-24, <http://dx.doi.org/10.1080/20464177.2017.1295786>
- **Jeong, B.**, Lee, B.S., Zhou, P. 2017. Quantitative risk assessment of fuel preparation room having high-pressure fuel gas supply system for LNG-fuelled ship. *Journal of Ocean Engineering* (137), P450-468, <https://doi.org/10.1016/j.oceaneng.2017.04.002>

- **Jeong, B.**, Lee, B.S., Zhou, P., Ha, S.-m., 2017. Quantitative Risk Assessment of Medium-Sized Floating Regasification Unit. Journal of Ocean Engineering, <https://doi.org/10.1016/j.oceaneng.2017.10.011>
- **Jeong, B.**, Lee, B.S., Zhou, P., Ha, S.-m., 2018. Determination of Safety Exclusion Zone for LNG Bunkering at Fuel-Supplying Point. Journal of Ocean Engineering. <https://doi.org/10.1016/j.oceaneng.2018.01.066>
- Park, S, **Jeong, B.**, Lee, B.S. Oterkus, S., Zhou, P., 2018. Structural Safety Evaluation of FLNG Liquefaction Modules against Potential Vapour Cloud Explosion. Journal of Ocean Engineering (149), P423-437. <https://doi.org/10.1016/j.oceaneng.2017.08.032>
- **Jeong, B.**, Wang, H., Oguz, E., Zhou P., 2018. An effective framework for life cycle and cost assessment for marine vessels aiming to select optimal propulsion systems Journal of Cleaner Production (187), P111-130. <https://doi.org/10.1016/j.jclepro.2018.03.184>
- Wang, H., Oguz, E., **Jeong, B.**, Zhou, P., 2017. Life cycle and cost analyses on ship hull maintenance strategy for a short route hybrid ferry, submitted to Ocean Engineering (*Accepted*)

#### **Additional Journals done during Ph.D. period**

- **Jeong, B.**, Wang, H., Oguz, E., Zhou P., 2017 Multi-criteria Decision Making for Marine Propulsion: Hybrid, Diesel Electrical and Diesel Mechanical Systems for Cost-Environment-Risk Perspectives, submitted to Journal of Applied Energy (*Under 2<sup>st</sup> review*)
- **Jeong, B.**, 2017. Comparative Analysis of SO<sub>x</sub> Emission-Compliant Options for Marine Vessels from Environmental Perspective, submitted to Journal of the Korea Society for Power System Engineering (*Under 2<sup>nd</sup> review*)
- Lee, J-u., **Jeong, B.**, 2017, Application of Strain Gauge Method for Investigating Influence of Ship Shaft Movement by Hydrodynamic Propeller Forces on Shaft Alignment. Submitted to Journal of Measurement (*under 2<sup>nd</sup> review*)

# CONTENTS

---

<b>ABSTRACT .....</b>	<b>I</b>
<b>ACKNOWLEDGEMENTS .....</b>	<b>IV</b>
<b>PUBLICATIONS.....</b>	<b>VI</b>
<b>CONTENTS .....</b>	<b>VIII</b>
<b>LIST OF FIGURES.....</b>	<b>XII</b>
<b>LIST OF TABLES.....</b>	<b>XVI</b>
<b>GLOSSARY .....</b>	<b>XVIII</b>
<b>1. INTRODUCTION.....</b>	<b>1</b>
1.1. Advent of LNG-fuelled ships .....	1
1.2. Safety concerns of LNG-fuelled ships.....	4
1.3. Outline of the thesis .....	6
<b>2. PROJECT AIM AND OBJECTIVES.....</b>	<b>8</b>
2.1. Aim and objectives.....	8
2.2. Tasks .....	9
<b>3. OVERVIEW OF SAFETY OF LNG-FUELLED SHIPS.....</b>	<b>13</b>
3.1. System description in LNG-fuelled ships .....	13
3.1.1. Bunkering system.....	14
3.1.2. LNG fuel tank .....	16
3.1.3. Fuel gas supply system (FGS system) .....	18
3.1.4. Dual-fuel engine (or multi-fuel engine).....	19
3.2. Safety of LNG-fuelled ships.....	19
<b>4. LITERATURE REVIEW.....</b>	<b>24</b>
4.1. Fire/explosion associated with LNG .....	24
4.2. Current regulations, rules, standards and guidelines.....	29
4.2.1. International regulations .....	30
4.2.2. Class rules .....	31
4.2.3. Other related standards and guidelines .....	32
4.3. Safety challenges on LNG-fuelled ship .....	34
4.3.1. Risks associated with LNG bunkering.....	34
4.3.2. Low risk for low pressure FGS system.....	40
4.3.3. High risk for high pressure FGS system .....	40
4.4. Overview of risk assessment to investigate the safety of LNG-fuelled ship .....	43
4.4.1. Hazard identification .....	44

---

4.4.2.	Risk analysis.....	45
4.5.	Concluding remarks .....	52
<b>5.</b>	<b>CONCEPTUAL DESIGN OF A CASE SHIP .....</b>	<b>53</b>
5.1.	Arrangement of overall LNG fuel system .....	54
5.1.1.	LNG storage tank .....	55
5.1.2.	Fuel preparation room .....	56
5.1.3.	Bunkering system.....	57
5.1.4.	Machinery room.....	59
<b>6.</b>	<b>METHODOLOGY.....</b>	<b>61</b>
6.1.	Introduction.....	61
6.1.1.	System modelling.....	63
6.1.2.	Approach to risk assessment.....	67
6.2.	Methods adopted for risk assessment .....	69
6.2.1.	Frequency analysis .....	70
6.2.2.	Consequence analysis.....	71
6.2.3.	Risk assessment.....	73
6.3.	Software implementation .....	78
<b>7.</b>	<b>OVERVIEW OF CONSEQUENCE ANALYSIS .....</b>	<b>84</b>
7.1.	Leak rate.....	84
7.2.	LNG spread/evaporation .....	85
7.2.1.	LNG spread model .....	86
7.2.2.	Evaporation model .....	89
7.3.	Jet fire model.....	94
7.4.	Flash fire (dispersion model).....	96
7.5.	VCE model.....	97
7.5.1.	TNT equivalency explosion model.....	97
7.5.2.	TNO multi-energy model .....	99
7.5.3.	Baker-Strehlow-Tang model (BST).....	100
7.6.	Pool fire model.....	102
<b>8.</b>	<b>ON-BOARD SAFETY EXCLUSION ZONE FOR LNG BUNKERING</b>	
	<b>109</b>	
8.1.	Introduction.....	109
8.2.	Case ships.....	109
8.3.	Fuel system design .....	111
8.3.1.	Case Ship 1.....	111
8.3.2.	Case Ship 2.....	112
8.4.	Risk assessment.....	115

8.4.1.	Frequency analysis .....	115
8.4.2.	Consequence analysis.....	118
8.4.3.	Assessment results.....	119
8.5.	Sensitivity/parametric analysis .....	125
8.5.1.	Sensitivity analysis for different data usage .....	125
8.5.2.	Parametric analysis for flow rate .....	129
8.5.3.	Comparison with deterministic approach .....	133
8.5.4.	Comparison with DNV GL risk criteria.....	134
8.6.	Concluding remarks .....	135
<b>9.</b>	<b>SAFETY EXCLUSION ZONE FOR LNG BUNKERING AT FUEL-SUPPLYING POINT .....</b>	<b>137</b>
9.1.	Introduction.....	137
9.2.	Description of study .....	137
9.2.1.	Identification of parameters.....	137
9.2.2.	Bunkering case design.....	138
9.2.3.	Approaches adopted .....	140
9.3.	Risk assessment.....	143
9.3.1.	Frequency analysis .....	143
9.3.2.	Consequence analysis.....	146
9.3.3.	Assessment results.....	148
9.4.	Concluding remarks .....	157
<b>10.</b>	<b>QUANTITATIVE RISK ASSESSMENT OF FPR WITH HP FGS SYSTEM.....</b>	<b>158</b>
10.1.	Introduction.....	158
10.2.	Description of study .....	158
10.2.1.	Ship information.....	158
10.2.2.	Approach adopted .....	162
10.3.	Risk assessment.....	164
10.3.1.	Frequency analysis .....	164
10.3.2.	Consequence analysis.....	169
10.3.3.	Assessment results.....	175
10.4.	Results of consequence analysis.....	179
10.5.	Sensitivity analysis .....	184
10.6.	Additional reference.....	187
10.7.	Concluding remarks .....	189
<b>11.</b>	<b>QUANTITATIVE RISK ASSESSMENT OF MEDIUM-SIZED FLOATING REGASIFICATION UNIT .....</b>	<b>191</b>

---

11.1.	Introduction .....	191
11.2.	Description of study .....	192
11.2.1.	Ship information.....	192
11.2.2.	Hierarchical system modelling .....	193
11.3.	Risk assessment.....	197
11.3.1.	Frequency analysis .....	197
11.3.2.	Consequence analysis.....	199
11.3.3.	Assessment results.....	201
11.4.	Parametric analysis (application of safety measures) .....	203
11.4.1.	Modification of frequency analysis .....	203
11.4.2.	Assessment results.....	206
11.4.3.	Comparison with selective quantitative risk assessment.....	208
11.5.	Concluding Remarks .....	210
<b>12.</b>	<b>DISCUSSION .....</b>	<b>211</b>
12.1.	Novelty of research .....	211
12.1.1.	As a tool for early design stages .....	212
12.1.2.	As a tool for rule-developing.....	214
12.2.	Contributions to industries .....	215
12.3.	Limitations and suggestions for future works.....	219
12.3.1.	Software development .....	219
12.3.2.	Further research.....	219
<b>13.</b>	<b>CONCLUSIONS .....</b>	<b>222</b>
	<b>REFERENCES .....</b>	<b>224</b>
	<b>APPENDIX A .....</b>	<b>232</b>
A.1.	Flash fire .....	232
A.2.	Impact of explosion.....	236
A.3.	Pool fire.....	238
	<b>APPENDIX B.....</b>	<b>240</b>
	<b>APPENDIX C .....</b>	<b>257</b>

## LIST OF FIGURES

Figure 2.1. Outline flowchart for the research work.....	9
Figure 3.1. Outline of system arrangement of LNG-fuelled ship (KR 2016). .....	14
Figure 3.2. Standard LNG bunkering options (modified based on ISO 2015c). .....	15
Figure 3.3. General outline of FGS system(modified based on (MAN Diesel 2015)). .....	19
Figure 4.1. History of IMO regulatory work for safety of LNG-fuelled ship (Ha 2017). .	31
Figure 4.2. Illustration of a safety exclusion zone for LNG bunkering (ISO 2015c). .....	38
Figure 4.3 Diagrammatic representation of fuel system on an LNG-fuelled container ship (Piellisch 2013). .....	42
Figure 4.4. Formal safety assessment (IMO 1997).....	44
Figure 4.5 HAZOP framework (Lee 2016; Rausand and Høyland 2004).....	47
Figure 4.6. Selective quantitative risk assessment framework (Dan et al. 2014). .....	50
Figure 5.1. Outline of LNG fuel system. ....	55
Figure 5.2. Arrangement of LNG storage tank for the case ship. ....	59
Figure 5.3. Conceptual design of LNG-fuelled ship.....	60
Figure 6.1. Outline flowchart risk assessment process. ....	62
Figure 6.2. An example of hierarchical system modelling for a complex system.....	63
Figure 6.3. An example of ET for a LNG leak. ....	66
Figure 6.4. Risk assessment with hierarchical system modelling. ....	67
Figure 6.5. An example of quantitative risk assessment using hierarchical system modelling. ....	69
Figure 6.6. An example of event tree (Dan et al., 2014; ISO, 2015; Jeong et al. 2017a). .	70
Figure 6.7. Process of consequence analysis. ....	72
Figure 6.8 Layout for population-independent analysis (Jeong et al. 2017a). .....	75
Figure 6.9. an example for estimating the F-N Curve from the complex system.....	78
Figure 6.10. Organisation of main components of IQRA software. ....	80
Figure 6.11. User interface of IQRA software. ....	81
Figure 6.12. Main strengths of IQRA software. ....	82
Figure 7.1. Box model used to indicate pool spreading behaviour. ....	86
Figure 7.2. Schematic representation of a pool spreading on land. ....	87
Figure 7.3. Heat flux versus excess temperature (Baumeister and Simon 1973; Basha et al. 2014).....	91
Figure 7.4. Normalised overpressure vs normalised distance for its use in TNO multi- energy model. ....	99
Figure 7.5. Dimensionless peak overpressure vs scaled distance for BST model (Melton and Marx 2009).....	101
Figure 8.1. Outline bunkering system designed for Case Ship 1. ....	112
Figure 8.2. Arrangement of the LNG fuel systems for Case ship 2. ....	112
Figure 8.3. Outline design of bunkering system for Case ship 2. ....	113
Figure 8.4. Leak frequency of proposed LNG bunkering systems. ....	115
Figure 8.5. An event tree for 3mm leak hole from LNG bunkering main system for Case Ship 1. ....	117
Figure 8.6. Example of critical distance for Group 1 for Case Ship 1. ....	119
Figure 8.7 Risk level of safety exclusion zones for Case Ship 1. ....	122
Figure 8.8 Risk level of safety exclusion zones for Case Ship 2. ....	123
Figure 8.9 Risk level of safety exclusion zones with respect to probability of fatalities. .	124

Figure 8.10. A modified event tree for 3mm leak hole from LNG bunkering main system for Case Ship 1.....	126
Figure 8.11 Risk level of safety exclusion zones with different scenarios and databases. ....	127
Figure 8.12 Risk level of safety exclusion zones with respect to congestion ratio. ....	128
Figure 8.13 Result of parametric analysis for velocity. ....	131
Figure 8.14. Result of parametric analysis for system size. ....	132
Figure 8.15. LFL boundary for deterministic approach – PPM over x direction. ....	133
Figure 8.16. Analysis results based on DNV GL guideline. ....	135
Figure 9.1. Concept of parametric risk analysis. ....	139
Figure 9.2. A flowchart of study based on IQRA software. ....	141
Figure 9.3. Assumed port population (unit: persons). ....	143
Figure 9.4. Leak frequency of various LNG bunkering systems (Case 1 – 5,000 m <sup>3</sup> ). ...	144
Figure 9.5. An event tree for 3mm leak hole from LNG bunkering with TTS (Case 1 – 5,000m <sup>3</sup> ). ....	146
Figure 9.6. Critical distance from accidents with respect to bunkering method. ....	148
Figure 9.7. Risk frequency for critical distances. ....	150
Figure 9.8. F-N curves for port population 1 (P_Case 1). ....	153
Figure 9.9. F-N curves for port population 2 (P_Case 2). ....	154
Figure 9.10. F-N curves for port population 3 (P_Case 3). ....	154
Figure 9.11. F-N curves for modified port population. ....	156
Figure 10.1. A proposed general arrangement of the LNG fuel system. ....	160
Figure 10.2. Concept design of the FGS system for the case ship. ....	161
Figure 10.3. FT for late isolation with one gas detector system. ....	168
Figure 10.4. FTA for ventilation failure. ....	168
Figure 10.5. Possible directions of explosion impact. ....	170
Figure 10.6. A 3D model of the FPR. ....	172
Figure 10.7. A 2D Model of the FPR. ....	172
Figure 10.8. Details of the FPR floor structure. ....	174
Figure 10.9. The stiffened bottom panel of the FPR for Case 1. ....	175
Figure 10.10. FTA showing the overall frequency of explosion. ....	178
Figure 10.11. Progress of explosion. ....	180
Figure 10.12. Maximum pressure on the floor at various distances from the ignition point. ....	181
Figure 10.13. Pressure load applied in FE analysis. ....	182
Figure 10.14. Shear stress on the floor: (a) Case 1; (b) Case 2; (c) Case 3; (d) Case 4... 183	183
Figure 10.15. Bending stress on the floor: (a) Case 1; (b) Case 2; (c) Case 3; (d) Case 4. ....	183
Figure 10.16. Equivalent stress on the floor: (a) Case 1; (b) Case 2; (c) Case 3; (d) Case 4. ....	184
Figure 10.17. Maximum pressure on the floor at various distances from the ignition points and methane compositions. ....	186
Figure 10.18. Ventilation analysis of FPR at 0.07 kg/s leak. ....	188
Figure 10.19. Mass fraction of CH <sub>4</sub> over time at 0.07 kg/s leak. ....	188
Figure 10.20. Mesh convergence test. ....	189
Figure 11.1. Case ship – JSK FRU (by courtesy of JSK Shipping Co., Ltd). ....	192
Figure 11.2. Regasification process. ....	193
Figure 11.3. Proposed process of evaluating the overall risk using the hierarchical modelling. ....	194
Figure 11.4. Simplified diagram of LNG regasification plant. ....	195



Figure 11.5. Hierarchical system modelling.....	196
Figure 11.6. Estimated leak frequency. ....	197
Figure 11.7. ET for 3mm leak hole for Sub-Group 1 of Sub-System 1. ....	199
Figure 11.8. Estimated leak rates. ....	200
Figure 11.9. Population in the terminal (by courtesy of JSK Shipping Co., Ltd). ....	201
Figure 11.10. Risk F-N graphs. ....	202
Figure 11.11. FT for late isolation with two gas detectors. ....	204
Figure 11.12. Modified ETs for 3mm leak hole for Sub-Group 1 of Sub-System 2. ....	205
Figure 11.13. F-N graphs of risk with safety measures incorporated in Sub-System 1. .	206
Figure 11.14. F-N graphs of risk with safety measures incorporated in Sub-System 2. .	207
Figure 11.15. F-N graphs of risk from selective quantitative risk assessment. ....	209
Figure 12.1. Design process, decision and knowledge availability (Koch and Castillo, 2017). ....	212
Figure 12.2. Traditional and ideal processes of safety evaluation for hazardous process systems. ....	213
Figure 12.3. Integrated process contributing to rule-development. ....	215
Figure 12.4. Summary of study on safety of on-board LNG bunkering. ....	216
Figure 12.5. Summary of study of safety of LNG bunkering at supplying ends. ....	216
Figure 12.6. Summary of study on the safety of FPR. ....	217
Figure 12.7. Summary of study on the safety of FRU. ....	218
Figure A.1. Gas concentration in response to x-distance. ....	233
Figure A.2. Gas concentration in response to x-distance. ....	234
Figure A.3. Gas concentration (Briggs. vs Van.). ....	235
Figure A.4. Explosion impact. ....	236
Figure A.5. Explosion impact (Lobato et al. 2009). ....	238
Figure A.6. Comparison of the results obtained with different models applied to standard damages (Lobato et al. 2009). ....	238
Figure A.7. Impact of pool fire. ....	239
Figure C.1. Comparison between static condition and transient condition. ....	240
Figure C.2. Stresses of Case 1 and 2 at the condition of 5% of methane mixture and 0.7m ignition point. ....	241
Figure C.3. Stresses of Case 3 and 4 at the condition of 5% of methane mixture and 0.7m ignition point. ....	242
Figure C.4. Stresses of Case 1 and 2 at the condition of 10% of methane mixture and 0.7m ignition point. ....	243
Figure C.5. Stresses of Case 3 and 4 at the condition of 10% of methane mixture and 0.7m ignition point. ....	244
Figure C.6. Stresses of Case 1 and 2 at the condition of 15% of methane mixture and 0.7m ignition point. ....	245
Figure C.7. Stresses of Case 3 and 4 at the condition of 15% of methane mixture and 0.7m ignition point. ....	246
Figure C.8. Stresses of Case 1 and 2 at the condition of 5% of methane mixture and 0.9m ignition point. ....	247
Figure C.9. Stresses of Case 3 and 4 at the condition of 5% of methane mixture and 0.9m ignition point. ....	248
Figure C.10. Stresses of Case 1 and 2 at the condition of 10% of methane mixture and 0.9m ignition point. ....	249
Figure C.11. Stresses of Case 3 and 4 at the condition of 10% of methane mixture and 0.9m ignition point. ....	250

Figure C.12. Stresses of Case 1 and 2 at the condition of 15% of methane mixture and 0.9m ignition point.....251

Figure C.13. Stresses of Case 3 and 4 at the condition of 15% of methane mixture and 0.9m ignition point.....252

Figure C.14. Stresses of Case 1 and 2 at the condition of 15% of methane mixture and 1.0m ignition point.....253

Figure C.15. Stresses of Case 3 and 4 at the condition of 5% of methane mixture and 1.0m ignition point.....254

Figure C.16. Stresses of Case 3 and 4 at the condition of 5% of methane mixture and 1.0m ignition point.....255

Figure C.17. Stresses of Case 3 and 4 at the condition of 15% of methane mixture and 1.0m ignition point.....256

## LIST OF TABLES

Table 3.1 Standard LNG fuel tanks (WPCI 2015).....	17
Table 3.2 Previous accidents involving LNG facilities. ....	21
Table 3.3 Previous accidents involving LNG carriers. ....	22
Table 4.1 LNG fire tests (Woodward and Pitbaldo 2010; Zabetakis 2965; May and McQueen 1973) .....	24
Table 5.1 General specifications of the case ship ( <i>by courtesy of Korean Resister</i> ).....	54
Table 7.1 Briggs sigmas.....	97
Table 7.2 Van Buijtenen. ....	97
Table 7.3 Mach numbers (Mw) for BST model .....	102
Table 7.4 Fuel reactivity vs burning velocity (Melton and Marx 2009). ....	102
Table 7.5 Obstacle density vs the volume blockage ratio (Melton and Marx 2009). ....	102
Table 7.6 View factor for a horizontal receiving surface (FH). ....	108
Table 7.7 View factor for a vertical receiving surface (FV). ....	108
Table 8.1 General specifications of the case ships (by courtesy of Korea Resister of Shipping). ....	110
Table 8.2 List of components in bunkering systems. ....	114
Table 8.3 Probability of Immediate Ignition (DNV, 2012b). ....	117
Table 8.4 Leak rates for various leak hole sizes (unit: kg/s).....	118
Table 8.5 Numerical result of frequency and consequence analysis.....	121
Table 8.6 Risk level of safety exclusion zones with respect to probability of fatalities (unit: /year). ....	124
Table 8.7 Risk level of safety exclusion zones with different scenarios and databases (unit: /year). ....	127
Table 8.8 Risk level of safety exclusion zones with respect to congestion ratio (unit: /year).....	128
Table 8.9 Annual bunkering time for varying fluid velocity. ....	129
Table 8.10 Result of parametric analysis for velocity (unit: /year).....	130
Table 8.11 Annual bunkering time for varying pipe size. ....	131
Table 8.12 Result of parametric analysis for piping size (unit: /year). ....	132
Table 8.13 Analysis results based on DNV GL guideline (unit: /bunkering). ....	134
Table 9.1 List of LNG bunkering equipment. ....	140
Table 9.2 Leak frequency of LNG bunkering systems with respect to capacity (unit:/year). ....	145
Table 9.3 Leak rates for various leak hole sizes (unit: kg/s).....	147
Table 9.4 Numerical result of frequency and consequence analysis.....	149
Table 9.5 Zones with less than tolerable risks. ....	151
Table 9.6 Summary of risk levels for various cases. ....	155
Table 9.7 Modified population (unit: persons). ....	156
Table 10.1 General specifications of the case ship (KR 2015a). ....	159
Table 10.2 Specifications of the FGS system.....	161
Table 10.3 Frequency of initial leak with respect to leak size. ....	165
Table 10.4 Reliability data for safety systems.....	167
Table 10.5 Probability of immediate ignition (DNV 2013).....	169
Table 10.6 Probability of delayed ignition (OGP 2010c). ....	169
Table 10.7 Model verification tests. ....	171
Table 10.8 CFD simulation conditions.....	172

---

Table 10.9 Stiffened designs for each case.....	174
Table 10.10 Result of ETA for various cases.....	175
Table 10.11 Summary of stresses for various scantlings.....	184
Table 10.12 Summary of stresses associated with alternative scenarios for various scantlings.....	187
Table 11.1 Results of selective quantitative risk assessment.....	209
Table 11.2 Summary of study results.....	210
Table A.1 Gas dispersion model (Yoon et al. vs IQRA software).....	232
Table A.2 CHEMS-PLUS vs IQRA software.....	233
Table A.3 Flash fire impact.....	236
Table A.4. Explosion impact.....	237
Table A.5 Explosion impact.....	236
Table A.6 Explosion impact.....	238
Table A.7 Pool fire impact.....	239
Table B.1 Comparison between static condition and transient condition.....	240

## GLOSSARY

ABS	American Bureau of Shipping
BOG	Boil-off gas
BST	Baker-Strehlow-Tang model
BV	Bureau Veritas
CEN	European Committee for Standardization
CFD	computational fluid dynamics
CFR	Code of Federal Regulations
CNG	compressed natural gas
DNV	Det Norske Veritas
DSEC	Daewoo Ship Engineering Company
ECA	Emission Control Area
ESD	emergency shut-down device
ERC	emergency release couplings
ETA	event tree analysis
FEA	finite element analysis
FGS	Fuel gas supply
FLACS	FLame ACceleration Simulator
FMCEA	failure modes, effects and criticality analysis
FPR	fuel preparation room
FRU	floating regasification unit
FSA	formal safety assessment
FTA	fault tree analysis
GL	Germanischer Lloyd
HAZID	hazard identification
HAZOP	hazard and operability study
HFO	heavy fuel oil
HP	high pressure
HSE	Health & Safety Executive
IGC Code	International Code for the Construction and Equipment of Ships carrying Liquefied Gases in Bulk
IGF Code	International Code of Safety for Ships using Gases or other Low-flashpoint Fuels
IGU	The International Gas Union
IMO	International Maritime Organization
ISO	International Organization of Standardization
IQRA	Integrated Quantitative Risk Assessment
KFX	Kameleon FireEx
KR	Korean Register of Shipping
LFL	lower flammable limit
LFS	LNG-fuelled ship
LNG	liquefied natural gas
LR	Lloyd's Register
LSFO	low sulphur fuel oil
MARPOL	The International Convention for the Prevention of Pollution from Ships
MGO	marine gas oil
MSC	Marine Safety Committee

NFPA	National Fire Protection Association
OSV	offshore service vessel
PHAST	Process hazard analysis / consequence analysis
P&ID	process and instrumentation diagrams
RH	relative humidity
SCR	selective catalytic reduction
SIGTTO	International Gas Tanker and Terminal Operators
SWIFT	structured what-if checklist technique
TEU	twenty-foot equivalent unit
UFL	upper flammable limit
VCE	vapour cloud explosion
VLOC	very large ore carriers

## 1. INTRODUCTION

### 1.1. Advent of LNG-fuelled ships

About 80 % of world trade relies on maritime transport engaging more than 90,000 marine vessels (UNCTAD 2015), last few decades have been a heady time for liquid petroleum products as the main marine fuel source for the simple reason that they were abundant, highly accessible, of high energy density, easy to handle and less costly than other fuel types.

The conventional liquid fuels, however, contain high levels of asphalt, carbon residues and sulphur/metallic compounds which are converted into air pollutants when burned. As a result, the seaborne-trade has been attributed to producing approximately 2.2 % of carbon dioxide (CO<sub>2</sub>), 13 % and 12 % of nitrous oxides (NO<sub>x</sub>) and sulphur oxides (SO<sub>x</sub>) on earth (IMO 2015).

With the worldwide green shipping movement, IMO MARPOL Annex VI, first adopted in 1973, has been updated in an effort to reduce such marine air pollutants contained in ships' exhaust gas. In particular, Regulation 14 of the MARPOL Annex VI requires progressive reduction in the emissions of SO<sub>x</sub> and particulate matters from ships, by introducing phased measures as below.

The sulphur content of any fuel oil used on board ships is not to exceed the following limits:

- 4.50 % m/m<sup>1</sup> prior to 1 January 2012
- 3.50 % m/m on and after 1 January 2012
- 0.50 % m/m on and after 1 January 2020

For ships operating within an Emission Control Area (ECA), the sulphur content of fuel oil used on board ships is not to exceed the following limits:

---

<sup>1</sup> Percentage of weight / weight

- 1.50 % m/m prior to 1 July 2010
- 1.00 % m/m on and after 1 July 2010
- 0.10 % m/m on and after 1 January 2015

Meanwhile, the European Commission has adopted Directive 2012/32/EU in 2012, in line with the IMO MARPOL Annex VI.

In order to be compliant with these regulations, ship operators will no longer be able to use conventional fuel oils from the effective dates as they exceed the allowed levels of sulphur contents, prompting them to seek for SO<sub>x</sub> reducing measures. There are three viable options at present: using marine gas oil (MGO)/low sulphur fuel oil (LSFO), installing a scrubber system on board, and using LNG as a marine fuel. In this context, a ship-owner planning today to build a ship has to choose one of them (Balland 2015).

At present, the vast majority of ships engaged in ECAs use the MGO option as it is perceived to be the easiest way, since it does not necessarily require system retrofitting and this fuel is widely available in ports. High price of MGO, however, may cause huge operational expenses in the long run (Ship&Bunker 2017).

Using exhaust-gas scrubbers to filter the sulphur contents from the conventional heavy fuel oil (HFO) is regarded a very promising solution for many ship-owners, but scrubbers are still a new and unproven technology in the marine industry and ships with scrubbers may be subject to reduced stability, since the exhaust gas treatment system has to be installed on top of the exhaust stack. Furthermore, such scrubbers use water in the cleaning process, and therefore further facilities are required to treat the resulting liquid and sludge waste. Economically, the scrubbers increase fuel consumption by between 1 and 3 % and the operational and maintenance costs are also not negligible (Semolinos 2011).

Given the drawbacks of the foregoing SO<sub>x</sub>-compliant options, using LNG becomes a very attractive alternative (MAN Diesel 2012). LNG is a cleaner energy source emitting far less harmful gases into the air than conventional liquid



fossil fuels, thereby reducing the concentration of SO<sub>x</sub> in exhaust gas to a virtually negligible level.

Using LNG as a marine fuel can also be advantageous for reducing NO<sub>x</sub> emissions determined by IMO MARPOL Annex VI Regulation 13 which makes it mandatory for new-build ships to reduce it by 80 % from 2020. In this regard LNG seems the only practical option to comply with the most stringent limit (IMO Tier III) without any secondary exhaust gas purifying system, although some dual fuel engines need to install an additional system to meet the Tier III requirements. Ships running on MGO or HFO in any case will need to install NO<sub>x</sub>-reducing systems such as selective catalytic reduction (SCR).

Technical advancement in gas engines, as well as the surge in US shale gas, has helped LNG-fuelled ships become a realistic option (Aymelek et al. 2014; IGU 2015). In addition, the narrowing price gaps between oil products and natural gas are attracting more ship owners to LNG. This development of diversification of fuel types is beginning to ease the overreliance on existing liquid and solid fossil fuels.

As a vivid evidence of this anticipation, the number of LNG-fuelled vessels has rapidly increased over the past few years. Before the 21<sup>st</sup> century, LNG was rarely used as a ship's fuel while a few small ships were propelled by compressed natural gas (CNG). As the beginning of 21<sup>st</sup> century, the first LNG-fuelled ship, a Norwegian ferry, was commissioned (Arnsdorf 2013). Four years later, in 2004, M/V 'VIKING AVANT', a platform supply ship, and its sister ship became the first LNG-fuelled support cargo ships (DNVGL 2015). Since the 2010s, this trend has extended to the deep sea ships. TOTE Maritime Ltd. started to operate the first LNG-fuelled 3,100 TEU container vessel between the Pacific Northwest and Alaska. Crowley Liner Services Ltd. has built two other LNG-fuelled ships that carry up to 2,400 TEUs and 400 units of automobiles and other wheeled cargo between Florida and Puerto Rico since 2013. Moreover, Matson Navigation also ordered two LNG-fuelled container ships to be delivered in 2018. In addition, United Arab Shipping Co., Ltd. is building 17 new ships – six 19,000 TEU ships and 11 ships with 15,000 TEU capacity – that will run on either LNG

or diesel and several European short-sea operators also are building LNG-fuelled ships (Aymelek et al. 2015).

Despite a short history, the world fleet of LNG-fuelled ships is steadily expanding from emissions control areas (ECA) in Northern Europe and North America into worldwide. As a result, more than one hundred of LNG-fuelled ships (LFSs) are presently constructed or operated since the world's first LFS emerged in 2000 (DNVGL 2015). According to a survey report on global new-build forecasts (LR 2012) it is expected that the number of LNG-fuelled ships will reach 700 accounting for approximately 4.2 % of global new builds of ships by 2025.

## 1.2. Safety concerns of LNG-fuelled ships

LNG is a cryogenic liquid that rapidly evaporates when exposed to normal atmospheric condition turning into gas (mainly methane) which gets mixed with air at the time of release. Such rapid phase transition phenomenon in itself can present some hazards, such as asphyxiation, cryogenic burns and structural damage. Furthermore, if this flammable mixture is ignited, fire and/or explosion can occur (ISO 2015a).

Therefore, such a low-flashpoint fuel posing safety challenges needs to be properly understood and handled. Not surprisingly International Maritime Organization (IMO) has developed The International Code of Safety for Ships using Gases or other Low-flashpoint Fuels (IGF Code) that contains mandatory provisions for ships using such fuels, with respect to the arrangement, installation, control and monitoring of ship's compartments, machinery, equipment and systems (IMO 2017). Several other international/local organisations and groups have also introduced regulations, rules, guidelines and standards associated with the safety of LNG-fuelled ships in order to minimize the potential risk of the LNG-fuelled ships.

Due largely to the brevity of its history, it is too early to compile meaningful accident statistics associated with LNG-fuelled ships. Because of this, it is difficult to find explicit quantitative safety requirements in the existing rules, regulations and guidelines concerning design and operation of LNG systems on board LNG-fuelled ships.

As LNG-fuelled ships become more numerous, the number of occurrences of accidents associated with LNG leak may increase as well. Therefore, identifying and assessing the potential risk of LNG-fuelled ships, and enhancing the regulations is an urgent task. The main base of the current regulations, rules, standards and guidelines associated with the safety of LNG-fuelled ships is the experience and knowledge of similar systems, such as LNG carriers. Therefore, they need to be reviewed and revamped based on proper systematic risk assessment of the LNG-fuelled ships. It is also true that there are some existing studies of investigation into the safety of LNG-fuelled ships, but all of them are too case-specific for their research findings to be translated into general regulations directly.

In this context, it is not thought to be too late to assess the risk in using LNG as a marine fuel and understand the level of risk as well as risk factors. The key issues to be addressed in such a process are as follows:

- limitations and shortcomings of current regulations;
- nature and scale of the risk of LNG systems on board vessels using LNG as a fuel; and
- providing insight to help rule-makers, designers and other decision-makers.

### 1.3. Outline of the thesis

This thesis consists of 13 chapters and 3 appendices.

**Chapter 2** presents the research aim and objectives with an outline of tasks to achieve them. An overview of the safety of LNG-fuelled ships was given in **Chapter 3**. An in-depth literature review of publications on all aspects of safety of systems associated with LNG is given in **Chapter 4**. In this process the pitfalls of current rules and regulations were discussed. Current practices of risk assessment were critically reviewed. The outline design of a case ship to be used in the subsequent study of this project was developed in **Chapter 5**. Methods and procedure used in the project were developed and discussed in **Chapter 6**, which also includes a description of an in-house computational tool named as IQRA (integrated quantitative risk assessment). **Chapter 7** presents the details of risk assessment methods, including various estimation and calculation formulae for consequence analysis used in the IQRA. **Chapters 8 through 11** contain a series of studies on specific aspects of LNG-fuelled ships which were thought to present significant hazards using the IQRA software. Specifically:

- **Chapter 8** covers on-board safety exclusion zone for LNG bunkering.
- **Chapter 9** discusses safety exclusion zone for LNG bunkering at the fuel-supplying point.
- **Chapter 10** carries out a quantitative risk assessment for fuel preparation room (FPR) having a high-pressure fuel gas supply (HP FGS) system.
- **Chapter 11** deals with quantitative risk assessment of medium-sized floating regasification unit.

**Chapter 12** discusses contributions, novelties, limitations of this research and recommendations for future works. Finally, **Chapter 13** summarizes the meaningful conclusions arrived at through this research work.

**Appendices A to C** provide supplementary information not included in the main text as follows:

- **Appendix A** deals with the validation works for the numerical methods applied in the software.

- **Appendix B** presents the results of FE analysis on fuel preparation room discussed in Chapter 10.
- **Appendix C** provides the list of LNG-fuelled ships.

## 2. PROJECT AIM AND OBJECTIVES

### 2.1. Aim and objectives

The overall aim of this project was to contribute to enhancing the safety of the LNG-fuelled ships and other LNG-associated vessels, investigating their potential risks systematically and complementing regulatory/practical gaps. More specifically the objectives are as follows:

- (1) To examine the risk areas of LNG-fuelled ships and make a survey of the relevant current regulations; to enhance understanding of LNG fuel system safety and make a critical review of the risk analysis methods and the current regulatory framework;
- (2) To improve the risk assessment methods to be used based on the critical review, in particular, for LNG fuel systems and bunkering systems.
- (3) To develop an integrated risk assessment computational tool.
- (4) To identify the key factors affecting the safety of LNG-fuelled ships and to investigate the manner in which they influence the safety; to enhance the general understanding of the safety of LNG-fuelled ships so that it can contribute towards formulating improved regulatory provisions.
- (5) To suggest future research work to put a step forward for enhancing the safety of LNG-fuelled ships. The research is to be guided to explore extended scopes while investigating uncertainties and limitations raised on this paper.

## 2.2. Tasks

In order to achieve the research aim and objectives above some tasks were to be performed as outlined in the diagram of Figure 2.1 and explained below.

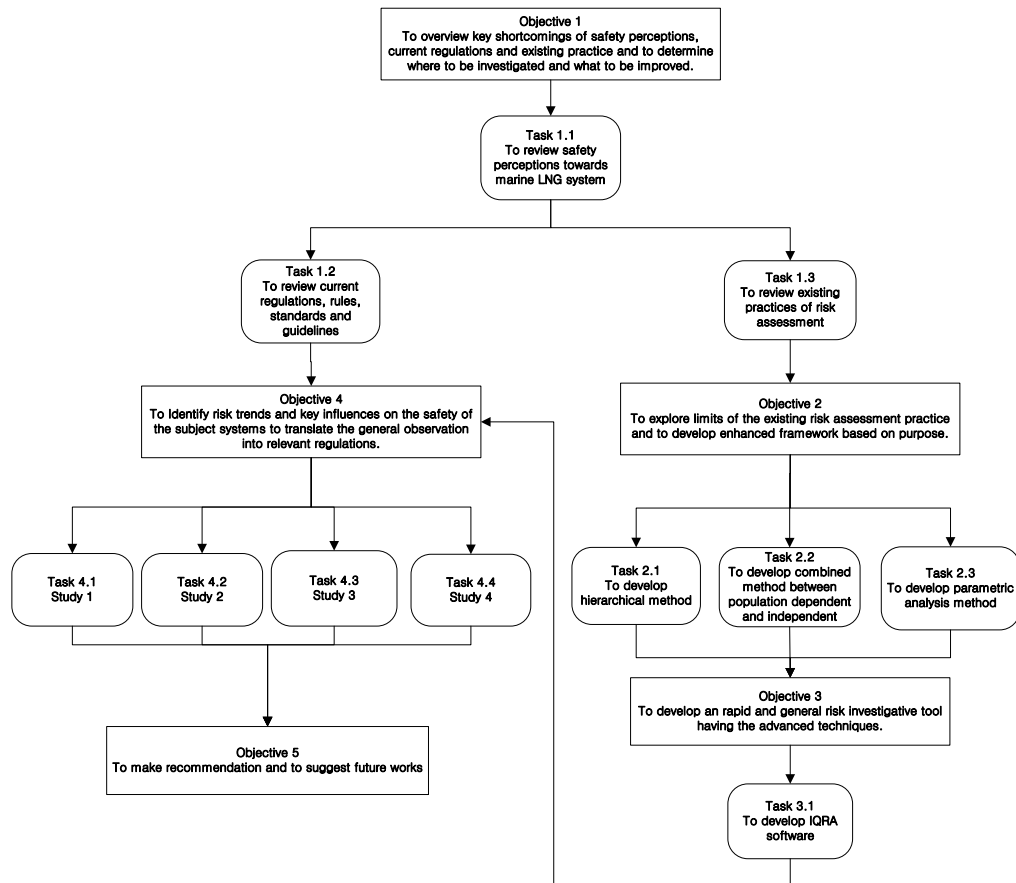


Figure 2.1. Outline flowchart for the research work.

### Task 1.1 Overview of safety of LNG-fuelled ships

The vulnerable points in the safety of LNG-fuelled ships were examined to identify what needs to be studied in greater detail.

### **Task 1.2/1.3 Literature review**

A thorough literature review was conducted based on the publications pertinent to safety of LNG-fuelled ships and risk assessment methods in general. More specifically, the current practice of assessing and ensuring safety of marine LNG systems was reviewed. The current status of regulatory framework associated with LNG-fuelled ships will be studied, and this would indicate the way forward.

### **Task 2.1 System modelling**

Lack of historical accident data can be one of the main hurdles in assessing the safety of novel and complex systems in a quantitative way. A hierarchical system modelling method was developed to overcome this problem.

### **Task 2.2 Enhanced fatality risk assessment process**

It appeared that the safety exclusion zones have so far been set based on the result of risk assessment quite independent of population distribution. However, it was believed that a more credible method should take into account the usual distribution of workers and other personnel throughout the affected site. The results from the population-independent and population-dependent analysis were compared, contrasted and combined in determining the required extent of the exclusion zones.

### **Task 2.3 Sensitivity/parametric analysis**

In order to gain some overall insight into the risk faced by LNG-fuelled ships and how to minimise it, it would be necessary to carry out some methodical parametric and sensitivity analyses. It was firstly to identify the key factors and parameters which influence the safety. This project may not be able to perform a comprehensive parametric/sensitivity study, but it would be shown how this



could be done and how the results could be introduced into the relevant regulations.

### **Task 3 Risk assessment software**

It was envisaged that a large number of risk assessment computation would be necessary to achieve the objectives, including the parametric/sensitivity analyses. It was decided, therefore, that a comprehensive computation tool was necessary. Having reviewed some existing software dealing with this type of problems, it was found that most of them dealt with frequency and consequence analyses quite separately leaving the users to do the most important task of combining the two together. It was also found that the programs still leave much laborious work to the users. Consequently, it was decided at an early stage of this project to write an integrated program which deals with the frequency and consequence analyses in one operation.

### **Tasks 4.1 and 4.2 Safety of LNG bunkering process (on-board bunkering and bunkering at fuel supplying point)**

The safety of the bunkering process was examined. Since bunkering is essentially a fuel transfer process, the two most vulnerable points will be at the receiving end (on-board bunkering station) and the supplying end. The required minimum extent of safety exclusion zones was studied and compared to the provisions of existing regulations and guidelines. A parametric analysis was carried out to identify the factors which influence the extent the most.

### **Task 4.3 Safety of high pressure fuel gas supply system (HP-FGS system)**

The fuel preparation room (FPR) of an LNG-fuelled ship deals with fuel gas and therefore its safety needs to be assessed. Especially, it may contain a high pressure system which may, when leaked, produce a condition conducive for

explosion. The consequence, therefore, needed to be studied with particular emphasis on structural impact of possible explosions.

#### **Task 4.4 Safety of floating regasification units (FRUs)**

Even though FRUs are not directly related to LNG-fuelled ships, they also handle the gas in various different forms. These contain highly sophisticated systems many of which are new to the industry. This was an ideal testing ground for the hierarchical modelling technique to be developed in this project.

#### **Task 5**

The work carried out in the project and the knowledge and insight gained through it was reviewed, with an emphasis on the application of the results to regulations and guidelines. Further work needed was identified and the way forward was suggested.

### 3. OVERVIEW OF SAFETY OF LNG-FUELLED SHIPS

The purpose of this chapter was to provide insights about the importance of the safety evaluation for the LNG-fuelled ships and to address the need for a special research outlined in this project. The focus of this chapter was placed on safety perception on LNG-fuelled ships, current rule, regulations, standards and guidelines. Opportunities to enhance their shortcomings and limits were, therefore, highlighted. In addition to this chapter, detailed investigations of current rules, regulations and practices were described through the conceptual design of an LNG-fuelled ship in the following chapter.

#### 3.1. System description in LNG-fuelled ships

The term, LNG-fuelled ships, refers to ships using LNG as fuel, and in general, whose propulsion systems are powered by either dual fuel engines<sup>2</sup> or multi-fuel engines<sup>3</sup> (IMO 2017). The fundamental idea of LNG-fuelled ships, therefore, was to obtain propulsion power from using LNG as a new source of marine fuel. To achieve this, it was essential for the vessels to have relevant LNG process systems on board. Figure 3.1 outlines the overall system of an LNG-fuelled ship that can be categorized into four main systems: bunkering system, LNG fuel tank system with extra spaces for appropriate piping (tank connection space), fuel gas supply system and dual fuel engine system.

---

<sup>2</sup> Engines that employ fuel covered by IGF Code and oil fuel. Oil fuels may include distillate and residual fuels.

<sup>3</sup> Engines that can use two or more different fuels that are separate from each other.

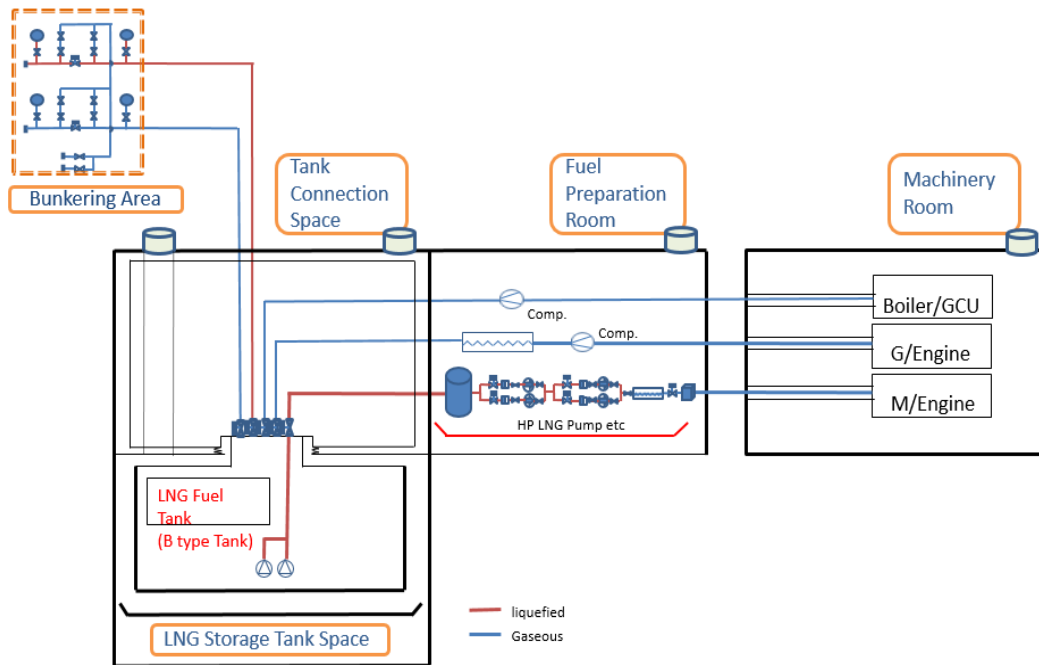


Figure 3.1. Outline of system arrangement of LNG-fuelled ship (KR 2016).

### 3.1.1. Bunkering system

In most cases bunkering is carried out when the ship visits a port for loading or unloading its cargo. In this regard LNG-fuelled ships, other than LNG carriers, have a slight problem, because many ports lack LNG bunkering infrastructure at present (Aymelek 2015). In order to overcome this problem, a number of transitional bunkering methods have been devised as shown in Figure 3.2.

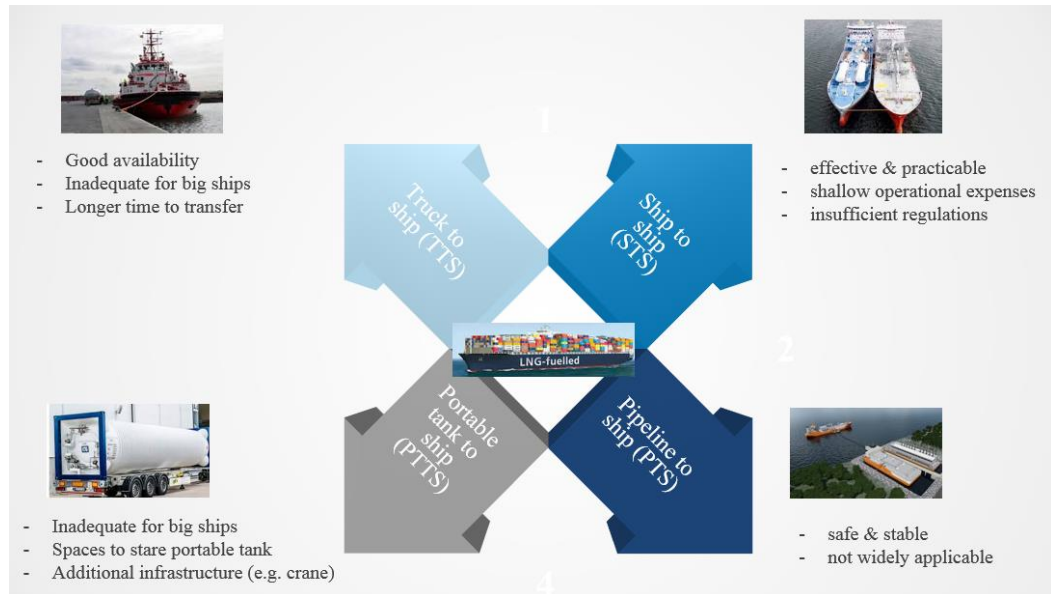


Figure 3.2. Standard LNG bunkering options (modified based on ISO 2015c).

LNG bunkering from terminal storage tanks to ship is the most familiar to most people as this closely resembles the long-established cargo operation procedures of LNG carriers. While this option is highly reliable and advantageous in transferring a large amount of LNG to the receiving ship at once, the number of ports equipped with necessary LNG bunkering facilities is very limited at present - only 117 LNG terminals are on-stream worldwide (IGU 2017) as of January 2017.

For small ships, using tank lorries to supply LNG to ships may be a feasible option. This is a mobile facility and, on arrival at the pre-arranged location, must be connected to the receiving ship moored at dockside through hoses. This option allows the ship to be bunkered virtually at any location, but the process does take LNG to be fuelled longer than other options and the amount of LNG that can be transferred at once is quite limited. Therefore, it will be difficult to use this method for large ships. The transport cost is also rather high.

The ship-to-ship transfer is a common practice for bunkering of traditional fuel oils. Its main strength is the high accessibility as a LNG feeder ship can come alongside the client ship while at its berth. It can be used for all LNG-fuelled ships of any size. However, safety concerns during LNG transfer

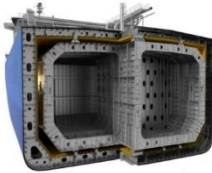



may be an issue, as the pipelines are vulnerable to fatigue possibly caused by relative motions between the feeder ship and LNG-fuelled client ship.

Pre-charged portable LNG tanks can be carried on board instead of bunkering. The empty tanks can be replaced with full ones in ports, in the similar way as an exhausted fuel tank for a portable gas fire is replaced by a full one at a shop. This method will reduce the bunkering time and potential hazards by simple and easy operational procedures. However, it requires additional spaces for portable tank storage on deck and it suffers from limited bunkering capacity.

### *3.1.2. LNG fuel tank*

LNG requires more care in the design of its storage tanks than the conventional liquid fuels, as LNG fuel tanks are subject to cryogenic environment (generally  $-163^{\circ}\text{C} \sim -150^{\circ}\text{C}$ ). There are four main types of LNG fuel tanks used on board at present: one is a membrane type and the other three are independent types A, B and C. Table 3.1 summarises the characteristics of each type.

Table 3.1 Standard LNG fuel tanks.

Type	Independent Type A	Independent Type B	Independent Type C	Membrane
				
Volume efficiency	good	good/normal	normal	good
Secondary barrier	complete secondary barrier	partial secondary barrier	unnecessary	complete secondary barrier
Application in LNGC	possible but maybe inefficient	Moss / SPB	compression type	GT No. 96, TZ Mark III, GTT CS-1
Application as LNG fuel tanks	possible but maybe inefficient	possible and efficient but no example so far	all LNG-fuelled ships use this type	possible and efficient but no example so far
Max. design pressure	0.07 MPa	0.07 MPa	-	0.07 MPa
Strengths/weaknesses	high costs	high reliability, problems with BOG treatment	high reliability, possible to store BOG	sloshing issue

While there is no record of using LNG tanks of membrane type and types A and B for smaller LNG-fuelled ships, such as ferries and OSVs, type C tanks are commonly used. This type of LNG tanks is available in a range of capacity up to 500 m<sup>3</sup>, with a maximum allowable working pressure of 20 bar.

As the energy density of LNG is approximately half that of traditional liquid fuels, twice tank capacities are required to store equivalent energy quantity. Type C tanks are usually designed in a cylindrical shape which is not desirable for the on-board space utilisation. Since additional space is

necessary to isolate the gas system in the event of a leak developing, the required volume for type C storage system on board would be three or four times that required for the conventional fuel system, which may lead to a significant loss of cargo space. For this reason, several alternative designs are currently under development for larger LNG-fuelled ships (WPCI 2015).

### 3.1.3. Fuel gas supply system (FGS system)

Although there are diverse designs a FGS system is basically designed to supply and boost LNG vaporized gas into engines. The type of gas-fueled engine types can be categorized based on whether supplied fuels are high pressure or low pressure. With high pressure engines, such as manufactured by MAN Diesel, the FGS system consists of a suction drum, boost pumps, HP pumps, HP vaporizer and train. The suction drum plays the role of a buffer for the stable LNG supply to the FGS system from the LNG fuel tanks. Therefore, the control of the suction drum level, pressure, and temperature is important. Booster pumps are installed to ensure the average effective suction head of the HP pumps but they can be omitted if the arrangement of fuel supply system satisfies the net positive suction head of the HP pumps. The main function of the HP systems is to increase fuel pressure to up to 350 bars before injection into the engines. The high pressure LNG generated by HP pumps is transported to the heater where it is converted back to its gaseous state. The vaporized natural gas is then regulated for pressure through the gas train and ready to be used as fuel (MAN Diesel 2015). General outline of FGS system is shown in Figure 3.3.

On the other hand, low pressure engines (mainly four stroke engines), such as those manufactured by Wärtsilä, use as low as 5-7 bar and therefore do not require HP pumps.



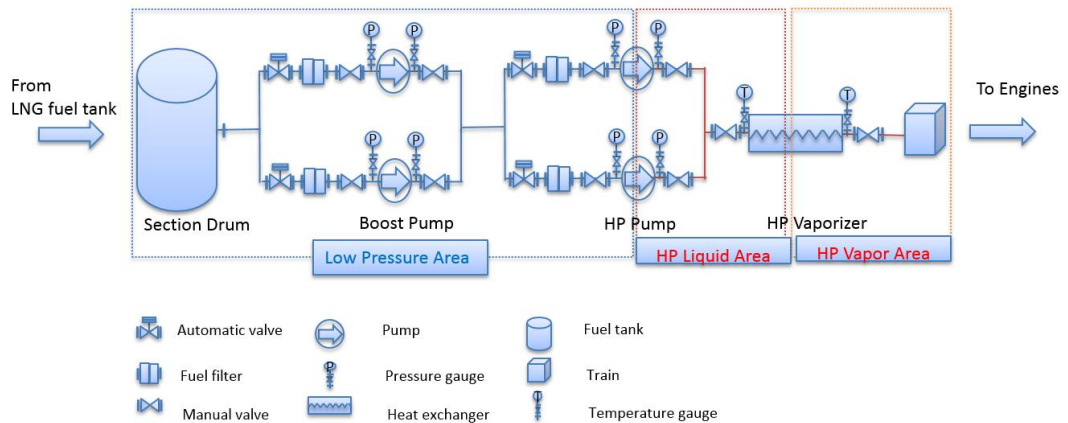


Figure 3.3. General outline of FGS system(modified based on (MAN Diesel 2015)).

### 3.1.4. Dual-fuel engine (or multi-fuel engine)

Conventionally, propulsion systems in the majority of LNG carriers use external combustion engines and use the boil-off gas (BOG) and liquid oils for fuel. The advantage of this mechanism is that the pressure in the LNG cargo tanks can be controlled by burning off the excessive BOG together with liquid fuel for propulsion. The LNG carriers have been forced to use the more inefficient external combustion engines because there is no on-board facility to deal with the BOG. However, with the introduction of dual fuel engines, BOG can be used to fire internal combustion engines too. With the increasing popularity of dual-fuel engines, LNG carriers as well as other types of ships are beginning to adopt this type of engines.

As described in the previous section, in dual fuel (or multi-fuel) engines can use either low pressure or high pressure gas injection. Usually two stroke engines adopt the high pressure system while low pressure systems are more suited for four stroke engines (MAN Diesel 2015).

## 3.2. Safety of LNG-fuelled ships

LNG is a liquid hydrocarbon mixture that is mainly used for the storage and transport of natural gas, and is mainly composed of colourless, non-toxic and non-corrosive methane (CH<sub>4</sub>) (ISO 2013). With the very low boiling temperature (about - 163 °C in the atmospheric condition), LNG must be stored and processed in cryogenically-insulated systems that keep the LNG temperature below the threshold level. An incident of LNG release from any part of these systems, therefore, will lead to the rapid vaporization of the liquid with the formation of the cold natural gas, known as BOG, which, when mixed with air, forms a flammable cloud. Such uncontrolled LNG release may present several potential threats, such as asphyxiation, cryogenic burns, structural embrittlement and fire and explosion. Moreover, the effect of LNG release is much more critical than the release in its gaseous state because the phase change from liquid to gas expands the volume of natural gas to about 600 times (ISO 2015b).

In this context the history of LNG accidents would be worth reviewing in order to get an insight into the safety of LNG-fuelled ships. The chemical industry has reported more than twenty LNG accidents and some of them resulted in severe casualties. The first LNG accident of an LNG tank failure claimed 124 lives and 200 ~ 400 injuries in Cleveland, Ohio, USA in 1944, which was followed by a series of critical accidents as described in Table 3.2 (Woodward and Pitbaldo 2010; Hamutuk 2008)

Table 3.2 Previous accidents involving LNG facilities.

Year	Location	Description	Fatalities	Injuries
1944	Cleveland, USA	Brittle rupture of three LNG tanks at a commercial LNG peak shaving plant. The leaked LNG was being vaporized and exploded.	124	200-400
1973	New York, USA	Tears of an LNG tank at an LNG peak shaving import terminal with membrane-lined tanks. The leaked LNG was vaporised and trapped between the membrane and the tank wall, which finally ignited and exploded.	37	0
1979	Lusby, USA	Inadequate tightening pump seal at an LNG import terminal. The leaked LNG was vaporized and ignited.	1	1
1985	Pinson, USA	Welding failure of a vessel at an LNG peak shaving facility. The leaked LNG was vaporized and ignited.	0	6
1987	Mercury, USA	Occurrence of static electricity during tests at the U.S. Department of Energy. The tested vapour cloud was ignited.	0	0
1989	Thurley, UK	Opened drain valve of LNG vaporizers at a peak shaving facility. LNG was released as a high pressure jet and the vapour cloud was ignited.	0	2
2004	Skikda, Algeria	Leak of a refrigerant line at an LNG liquefaction plant. The released vapour entered a steam boiler and a vapour-cloud explosion and fire was triggered.	27	80

Compared with the industrial LNG, the LNG carriers have had an excellent safety history over six decades of operation as there has never been an incident involving breach of cargo containment systems resulting in LNG spillage. IMO (2007) reported 182 incidents of LNG carriers between 1964 and 2005 and some issuable accidents are described in Table 3.3.

Table 3.3 Previous accidents involving LNG carriers.

Year	Ship name	Incident category	Description
1969	Polar Alaska (Methane Polar)	CCS	Violent sloshing of LNG in cargo tank caused cable tray to break loose which, in turn, slashed the thin membrane cargo tank wall, thereby LNG leaked into the inter-barrier space but no LNG was released from the secondary barrier.
1970	Arctic Tokyo	CCS	Heavy seas caused sloshing of cargo tanks, leading to local deformation of the primary barrier (invar membrane) and supporting insulation boxes. LNG leaked into the inter-barrier space but no LNG was released from the secondary barrier.
1978	Khannur	Col	Collision with a cargo ship Hong Hwa in the Straits of Singapore caused minor damage. No LNG released.
1979	El Paso Paul Kayser	Grd	Being stranded in the straits of Gibraltar caused deformation of cargo tanks. No LNG released.
1983	Norman Lady	EM	Being moved astern under its own power during cool-down of the cargo transfer arms. All cargo transfer arms sheared and LNG spilled, but no ignition involved.
1984	Melrose	FE	Fire in engine room but no structural damage involved.
1985	Annabella	EM	LNG being released from the tank or piping, but not ignited.
1985	Isabella	EM	Failure of cargo valve caused LNG overflow that led to deck fractures.
1990	Bachir Chihani	CCS	Structural cracks allegedly caused by stressing and fatigue in inner hull caused ingress of ballast water into the space behind the cargo hold insulation.
1998	LNG Bonny	EM	Black-out and drifted 90 miles off Miyakoshima. After repairs completed voyage was resumed.
2002	Norman Lady	Col	Collision with a U.S. submarine caused a leakage of seawater into the double bottom dry tank area.

CCS = Cargo Containment System; Col = Collision; Grd = Grounding; EM = Equipment or Machinery HW = Heavy Weather; Cnt = Contact; FE = Fire or Explosion

The excellent safety record of LNG carriers may bring about a false sense confidence with the safety of LNG-fuelled ships. It is important to note that LNG carriers only have to store and transport the cargo LNG with some additional facility to deal with BOG, while LNG-fuelled ships must be directly involved in

processing LNG like the chemical processing systems. If any accident happens the consequence will be more likely to be critical as discussed in the accidents in the chemical industry. In addition, Appendix D presents the summary of 186 LNG-fuelled ships both in service and on order, with which it can be perceived that as the number of LNG-fuelled ships rapidly increases, the frequency of LNG handling and accidents of LNG leakage may follow.

## 4. LITERATURE REVIEW

This project has set out to examine the safety of LNG-fuelled ships. In this context, this Chapter was to critically review the previous efforts on contributing to intensifying the safety of LNG-fuelled ships by evaluating the ideas and information in previous papers in order to identify what we already know on the subject and what is acquired from them. In addition to the work on potential hazards of LNG, growing interest of using the liquid gas as a marine fuel has led to several studies on the safety of LNG-fuelled ships.

This section was also designed to identify the limitations of previous research on the risk of the particularly identified two parts: LNG bunkering and HP FGS system. Therefore, it is to secure the opportunity to improve their safety throughout this research. Based on what were discussed throughout the previous chapters from Chapter 3 to 4, the publications relevant to this work can be broadly divided into those related to:

- physics of fire/explosion;
- current rule and regulations;
- safety of LNG-fuelled ships; and
- risk assessment methods.

### 4.1. Fire/explosion associated with LNG

People have been vaguely aware that LNG is a dangerous substance which can catch fire or explode given any opportunity. It is not surprising, therefore, that a number of experiments have been conducted to determine if the substance is really very dangerous and, if so, how dangerous. Table 4.1 summarises the LNG fire tests which have been reported in various publications.

Table 4.1 LNG fire tests (Woodward and Pitbaldo 2010; Zabetakis 2965; May and McQueen 1973)

Year	Place	Types	Flame length, L; pool diameter, D	Burn regression rate (m/s)	Mean emissive power (kW/m <sup>2</sup> )
------	-------	-------	--------------------------------------	-------------------------------	---

1962	Lake Charles, LA	On land	-	-	-
1969	Libya	On water	70 m L × 5 m D	$1.6 \times 10^{-4}$	92
1973	San Clemente, CA	On land	1.8 m D	$1.5 \times 10^{-4}$	100
			6.1 m D	$2.2 \times 10^{-4}$	$160 \pm 17$
1974-76	China Lake, CA	On water	8.5 to 15 m D 25 to 55 m L	$3.4 \times 10^{-4}$ to $9.6 \times 10^{-4}$	$210 \pm 20$
1976	Japan	On land	2m × 2 m square	-	58
1980	United Kingdom	On land	6.9 – 15.4 m D	-	-
1980	Maplin Sands, England	On land/ water	20 m D × 43 m L	$2.37 \times 10^{-4}$	$153 \pm 16$ (average), $219$ (maximum)
			30 m D × 80 m L		
1981	Japan	On land	2.5 m × 2.5 m square	-	-
1984	China Lake “Coyote Series”	On land	-	-	150-340
1987	Montoir, France	On land	35 m D × 77 m L	$3.1 \times 10^{-4}$	230 – 305
2009	Sante Fe, NM, USA	On water	-	-	-

It is worth noting that the emissive power observed in all the experiments far exceeds  $35 \text{ kW/m}^2$  which is normally taken to be the critical power causing 100 % death rate when a human is exposed to it.

Some notable tests of these are reviewed in more detail below:

### **LNG fire tests**

Chain Lake, 1978 (Schneider 1980; Raj et al. 1979): Sixteen tests with spill capacity of  $3\text{-}5.5 \text{ m}^3$  and rates between 0.02 and  $0.11 \text{ m}^3/\text{s}$  were carried out on water. The main aim of the tests was to measure the degree of thermal radiations from fires on water. Pool fires, delayed ignition tests, and flash fires were tested and their results were compared. Pool fires were observed with  $210 \pm 20 \text{ kW/m}^2$  of surface emissive powers and flash fire was  $220 \pm 30 \text{ kW/m}^2$ , whereas delayed ignition did not form visibly thick flame.

Maplin Sands, 1980 (Mizner and Eyre 1983 and 1982; Hirst and Eyre 1983): In order to investigate the behaviour of LNG dispersion and thermal radiation, 20 tests with  $5\text{-}20 \text{ m}^3$  capacity were carried out within the 300 m diameter dyke. The average surface emissive power for LNG pool fire was observed at  $203 \text{ kW/m}^2$  (with a range of  $178\text{-}248 \text{ kW/m}^2$ ). For flash fires, the average surface emissive power was measured at  $174 \text{ kW/m}^2$  with a range of  $137\text{-}225 \text{ kW/m}^2$ .

The test of LNG pool fires on land within a 20 m diameter dyke was also carried out by controlling the variables such as burning rate, fuel composition, wind speed, wind direction and humidity. The average emissive power was measured at  $153 \pm 16 \text{ kW/m}^2$  with a maximum of  $219 \text{ kW/m}^2$ .

Coyote, 1984 (Rodean et al. 1984): Four tests with various LNG spill amounts ranging from 14.6 to 28 m<sup>3</sup> with flow rates between 13.5 and 17.1 m<sup>3</sup>/min were performed. Various mixture ratios of fuels (methane, propane and ethane) were applied. Test conducted in the mildest atmospheric conditions produced the widest flash fire cloud up to the downwind distance of 210 m. For pool fire, the surface emissive power was measured in the range of 150-340 kW/m<sup>2</sup>.

Montoir, 1987 (Nedelka et al. 1989): Tests with 35 m diameter LNG pool fire were performed. Various factors were measured including the behaviour of flame, level of thermal radiation and average flame surface emissive power. The average surface emissive power was seen to lie within the range of 230-305 kW/m<sup>2</sup>.

### **LNG explosion tests**

Several experiments have been conducted to investigate LNG explosion:

China Lake, 1978 (Schneider et al. 1980): Methane-air and methane-propane mixtures were used for explosion tests in a detonation tube. Results revealed that the explosion of methane-air mixtures stopped at deflagration and did not lead to detonation while methane-propane mixtures did. It was also found that detonations occurred in the vapour mixture when propane concentrations were 6 % or greater, leading to the conclusion that the explosive impact of methane is relatively smaller than propane.

Vander Monlen and Nicholls, 1979 (Vander Molen and Nicholls 1979): Explosion tests for methane-ethane mixtures were performed. The concentration of ethane was controlled from 0 to 5.66 % by volume of the total methane-ethane-air mixture. A stable explosion was observed as a blast propagating with a constant velocity.



### **Modelling of LNG fire/explosion**

Based on the observations from the tests conducted, work has been carried out to model and simulate LNG fire and explosion. In some of the relevant publications, empirical and analytical models (see Chapter 8 for details) were used within conventional risk assessment framework.

Li and Huang (2012) have investigated the fire and explosion risk associated with LNG carrier ships based on analytical models, namely, the Dow method. The results obtained from Dow method, then, were compared with those from the conventional analytical models of boiling liquid expanding vapour explosion (BLEVE) and vapour cloud explosion (VCE) models. The risk models with Dow method resulted in relatively smaller impact levels than the conventional ones.

Aneziris et al. (2014) have integrated several risk assessment techniques to establish the appropriate level of safety zone during the LNG transferring operation against the risk of fire and explosion at offshore LNG terminals. They used historical accident frequency data for probability analysis and used an in-house computer code SOCRATES. The results indicated that offshore terminals could be more dangerous than onshore terminals due to the increase in the number and size of facilities.

Dan et al. (2014) have investigated the risk of fire and explosion on the topside LNG-liquefaction system of FLNG. Frequency analysis was carried out with historical accidental records combined with ETA while the consequence analysis was conducted with commercial software, PHAST. The results revealed that additional protection measures on the topside of the FLNG would be unnecessary as the risk of such LNG systems was seen to be within the tolerable level.

Hightower et al. (2004) have developed guidance on risk analysis for large LNG spill over water, providing general insights on the hazards of LNG spill. They also investigated the magnitude of associated risks, fire and explosion. They

addressed the theoretical and experimental gaps for the hazards of LNG spills on water.

Esteves and Parise (2013) have introduced a consequence model to predict the level of thermal radiation associated with potential pool fires in order to evaluate critical distance to protect the onshore LNG facility. By overviewing the experimental data and existing models on the velocity of LNG vaporization and burning rates when a pool fire occurs, their model was proven to be practical for predicting the impact level of pool fire.

Outside of the marine industry, Stefana et al. (2016) have assessed the risk of a dual fuel system applied to heavy-duty trucks in a qualitative way. They applied conventional frequency analysis models FTA and FMEA to investigate the risk of fires and explosions pertaining to the operation of dual fuel system on the trucks. The results showed there would be no significant difference in risk level between the dual fuel system and the conventional diesel system. However, this research exposed the limitation of qualitative risk assessment, implying the necessity of further study in a quantitative way.

### **Numerical simulation of LNG fire/explosion**

To improve the exactitude of consequence of LNG hazards, computational fluid dynamics (CFD) codes were widely applied to the problem. Notable studies include the following.

Gavelli et al. (2011) has evaluated the effect of vapour cloud explosion (VCE) for LNG carriers during cargo offloading. The study was focused largely on the consequence analysis by using the CFD software FLACS. They concluded that the effect of the explosion depends on the surrounding conditions, in particular, whether it is a partially confined or partially congested.

Dadashzadeh et al. (2013) have integrated two different CFD software, FDS and FLACS to model the fire and explosion scenario and quantify their consequences at an LNG processing plant. The results were plotted into a Probit model to quantify the level of human injuries and fatality. Results suggested that the

integration of different consequences, fire and explosion, would lead to more conservative results than those obtained from the individual assessment of those hazards.

Gupta and Chan (2016) have conducted a CFD-based explosion analysis in time-domain. It was claimed that the proposed approach improved the accuracy of the results. The results were combined with those of frequency analysis, and then plotted as exceedance curves to determine the tolerability of the explosion risk level.

Jin and Jang (2015) have addressed the shortcomings of existing FRA procedures for structural consequence analysis, i.e. unrealistic application of design accidental loads (DALs) to structural consequence analysis. To remedy this problem, they introduced new procedures with an extended structural consequence analysis by carrying out probabilistic safety assessment of topside structure of offshore units using CFD code KFX.

Qiao and Zhang (2010) have quantified the impact of vapour cloud explosions by means of CFD for onshore and offshore facilities. The work focused on the determining the cost-optimal design by balancing between the cost and the safety against the potential explosions. Research results concluded that leak rate, gas density and wind speed and ventilation conditions are the key parameters which affect the impact of explosion.

Dan et al. (2012) have compared the impact of vapour cloud explosion obtained from empirical model, phenomenological model and a CFD-model: TNT, PHAST and FLACS with hydrogen carbon mixtures. The results obtained from CFD model was far less severe than the results from the other two models.

The previous papers discussed in this section could be a good reference to provide stakeholders with general understanding/insight of the safety of LNG-fuelled ships.

## 4.2. Current regulations, rules, standards and guidelines

This section is to overview the current regulatory frameworks relevant to LNG-fuelled ships in three categories: international regulations, classification rules and standards & guidelines.

#### *4.2.1. International regulations*

IGC Code, adopted in 1986 by the IMO, has been uniformly applied to LNG carriers engaged in international voyage, providing an international standards for the safe transport of liquefied gases and certain other substances via sea route in bulk. On the other hand, there has been no international regulations for LNG-fuelled ships other than LNG carriers, and it became quite an urgent matter to develop one to prepare for the rapidly increasing number of ships using fuels with low flash point, particularly as a result of more stringent emissions requirements. As shown in Figure 4.1, the Marine Safety Committee (MSC) of IMO started work in 2004 to develop new regulations to improve the safety of LNG-fuelled ships. As a result, IMO Res.MSC.286 (85) - *Interim Guidelines on Safety for Natural Gas-fuelled Engine Installations in Ship* was adopted in 2009. The Resolution initially provides specific requirements for ships using LNG as a marine fuel. In addition, a Sub-Committee also agreed on a work plan for the next phase of development of the IGF Code, standing for *International Code of safety for ships using Gases or other low-flashpoint Fuels*, and adopted it in 2016. The principal purpose of the IGF Code is to set out mandatory provisions for the arrangement, installation, control and monitoring of machinery, equipment and systems for low flashpoint fuels - such as LNG - to minimize the potential risks towards the ship, its crewmembers and the environment. The mandatory regulation is applied to both new and existing ships with gross tonnage of 500 and above, including ships converting from the use of conventional oil fuel to the use of gases or other low-flashpoint fuels (IMO 2017; Ha 2017). Similarly, many other regulations, rules, standards and guidelines related to LNG-fuelled ships have been introduced by different organizations.

However, the current safety provisions for LNG fuel vessels are limited to design and operational guidelines but without quantified safety requirements.

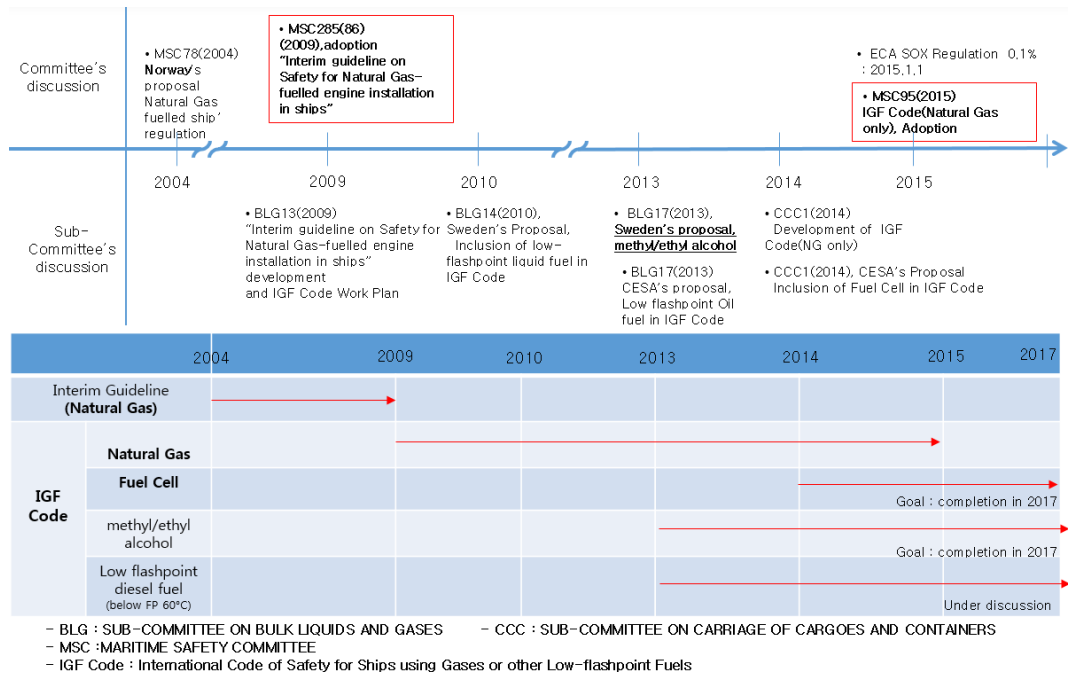


Figure 4.1. History of IMO regulatory work for safety of LNG-fuelled ship (Ha 2017).

#### 4.2.2. Class rules

Major classification Societies, such as DNV, LR, BV and ABS, have developed their own rules and guidelines for LNG-fuelled ships in 2011 and 2012:

- LR (2011) - 'Rules and Regulations for the Classification of Natural Gas Fuelled Ships';
- DNV (2011) - 'Part 6 Chapter 13, Gas Fuelled Ship Installations';
- BV (2012) - 'Safety Rules for Gas-Fuelled Engine Installations in Ships';
- ABS (2012) - 'ABS Guide for Propulsion and Auxiliary Systems for Gas Fuelled Ships'.

These class rules are largely in line with the IGF Code in providing safety requirements and guidelines for gas-fuelled systems as well as for arrangement and location of gas fuel tanks and auxiliary LNG systems. This has resulted in the class rules lacking quantified guidelines as in IGF Code.

#### 4.2.3. Other related standards and guidelines

International Organization for Standardization (ISO), a non-governmental organization composed of representatives from various national standardization organizations, has published a variety of guidelines on the safety of LNG terminals and LNG carriers. Of these a few standards can be useful in deriving the safety standard of LNG-fuelled ships. For example, ‘*Refrigerated light hydrocarbon - measurement of cargoes on board LNG carriers*’ (ISO 2012) and ‘*Characteristics of LNG influencing design and material selection*’ (ISO 2013) address the risk of maritime LNG transportation, providing a certain level of safety guidelines. ‘*Installation and Equipment for Liquefied Natural Gas - Ship to shore interface and Port Operations*’ (ISO 2010) was originally designed for conventional onshore LNG terminals and for safe operation of LNGCs engaged in international trade. Nevertheless, it is common practice to apply it for offshore LNG operations.

For the safety of LNG bunkering, ‘*Guidance on performing risk assessment in the design of onshore LNG installations including the ship/shore interface*’ (ISO 2015a) was developed to provide principal guidelines on the assessment of major safety hazards as part of planning, designing and operating LNG facilities onshore, using risk-based assessment methods.

Deciding that the past standards for the maritime LNG bunkering are insufficient, ISO has developed new guidelines for LNG transferring systems entitled ‘*Guidelines for systems and installations for supply of LNG as fuel to ships*’ (ISO 2015b). It points out the necessity of risk assessment although not providing any specific guidelines on the procedure of risk

assessment of LNG bunkering other than saying either deterministic or probabilistic approach is acceptable.

The Society of International Gas Tanker and Terminal Operators (SIGTTO), a non-profit organization established in Bermuda in 1978, has developed several safety guidelines for LNG handling as follows:

- *'Liquefied Gas handling principles on ships and in Terminals'* (SIGTTO 2000);
- *'LNG operations in Port Areas'* (SIGTTO 2003);
- *'Liquefied Gas Fire Hazard Management'* (SIGTTO 2004);
- *'ESD Arrangements & Linked Ship/ Shore Systems for Liquefied Gas Carriers'* (SIGTTO 2009).

These SIGTTO guidelines, however, are based on large-scale LNG transfers, and, therefore, cannot be directly applied to the bunkering system for LNG-fuelled ships. To remedy these shortcomings, SIGTTO developed a new guideline, *'Ship to Ship Transfer Guide for Petroleum, Chemicals and Liquefied Gases'* (SIGTTO 2013) for ship-to-ship bunkering method.

On the subject of LNG fire risks, National Fire Protection Association (NFPA), an international non-profit organization based in the US, provides some general regulations and standards, such as *'Standard for the Production, Storage and Handling of Liquefied Natural Gas (LNG), including for plant siting and layout for process equipment, stationary LNG storage, vaporizing facilities, components, operating, maintenance, training and the performance of risk assessment'* (NFPA 2009), *'Fire protection standard for pleasure and commercial motor craft including requirements for design and fire safety for boat less than 300 gross tons'* (NFPA 2015), and *'LNG Vehicular Fuel System Code'* (NFPA 2004).

European Committee for Standardization (CEN) has also developed a number of standards for the safety of LNG handling, such as *'Installations and equipment for liquefied natural gas — General characteristics of liquefied natural gas'* (BS EN 1997), *'Installation and equipment for*

*liquefied natural gas — Design of onshore installations*' (BS EN 2007), *'Installation and equipment for liquefied natural gas — Design and testing of marine transfer systems*' (BS EN 2008), *'Installations and equipment for liquefied natural gas — Design of onshore installations with a storage capacity between 5 t and 200 t*' (BS EN 2002) and *'Design and manufacture of site-built, vertical, cylindrical, flat-bottomed steel tanks for the storage of refrigerated, liquefied gases with operating temperatures between 0 to -165 °C*' (BS EN 2006). These standards can be used as references for the design, installation and arrangement for LNG systems on-board.

Various American societies have also developed Code of Federal Regulations (CFR) standards on different activities in the LNG supply chain.

As can be seen above, there are some guidelines and standards associated with the safety of transport of gas and gas fuel in general. They demand that risk assessment be carried out, but none gives specific provisions of risk assessment procedures and acceptable risks.

### 4.3. Safety challenges on LNG-fuelled ship

Typically, the design of LNG-fuelled ships is analogous to conventional LNG carriers in many aspects, such as the arrangement of LNG storage tanks and the loading/unloading systems and their operating procedures. However, there are also some new aspects in LNG-fuelled ships, in particular LNG bunkering and FGS system where are not provided with quantified safety guidelines from the current regulations.

#### 4.3.1. Risks associated with LNG bunkering

For ships using LNG as a fuel, LNG bunkering is an unavoidable process. The most established method of LNG bunkering is to transfer LNG from an LNG terminal to a receiving ship in a similar way of LNG carriers where



the cargo of LNG is loaded and unloaded into and out of on-board cargo tanks. However, the lack of terminal infrastructure has encouraged several alternative methods to emerge, such as using LNG tank lorries, LNG feeder ships or portable LNG tanks (ABS 2014; ISO 2015c). Since the world's first LNG-fuelled ship was put into service in 2000, a number of small to medium scale LNG bunkering has taken place using some of these alternative methods (DNVGL 2015). It is important to note that, compared to the conventional LNG cargo transfer, LNG bunkering will involve smaller but probably more numerous equipment.

LNG bunkering requires careful attention to safe operations as it entails potential risks pertaining directly to the cryogenic liquid transfer and vapour returns, much more than the conventional liquid fuel bunkering. According to a report of Norwegian Maritime Authority (Lasse 2015), four accidents associated with LNG spill have been reported – one of which led to an injury of a crew member on his hands and legs due to cryogenic burn. Moreover, in large scale LNG bunkering operations for large ocean going ships, significant uncertainties associated with massive accidental LNG release are present. In view of the possibly catastrophic consequence of such accidents, the risks associated with LNG bunkering merits careful studies.

Currently in Europe, for small LNG-fuelled ships, mainly ferries and OSVs, bunkering methods of terminal-to-ship and tank lorry-to-ship are being used. However, due to insufficient LNG bunkering infrastructures across the world, much of bunkering is done through bunkering ships. The idea portable LNG tanks is mooted as well, but so far has not been taken up. The selection of bunkering methods depends on the available infrastructure, ship's characteristics and operational profiles.

In line with this, it is essential that all LNG bunkering operations are undertaken with care so as to prevent leakage of LNG or its vapour and to control all sources of ignition, because LNG spill/leakage on deck can result in a rapidly evaporating pool that produces a vapour cloud driven by the wind. If any point of a vapour cloud of certain concentration reaches an ignition source, a flash fire will result. The ship-to-ship bunkering process

poses higher potential hazards than other methods as the connection between bunkering ship and LNG-fuelled ship is vulnerable to high amplitude relative motions between the two.

Although IMO and other local organizations have developed safety requirements such as watch keeper, ESD system and firefighting systems, the failure of these systems cannot be discounted. The current rules and regulations concerning the design and operation of LNG bunkering system are somewhat vague and lack specific quantified guidelines.

#### *Current regulations for LNG bunkering*

At the request of the IMO, the European Commission and the Baltic and International Maritime Council (BIMCO), ISO 20519:2017, *Ships and marine technology – Specification for bunkering of liquefied natural gas fuelled vessels*, introduced the safety requirements on the LNG bunkering transfer systems and equipment for LNG-fuelled ships. The standards provided the safety guidance on hardware, operational procedures, and documentary requirements for the LNG provider, training, qualifications of personnel and LNG facilities (ISO 2017). This new ISO standards may help operators select vessel fuel providers that meet defined safety and fuel quality standards. However, although this standard addressed the broad safety of LNG bunkering, it is still limited to linguistic guidelines that lacked the quantification of safety requirements. Moreover, no details are available to establish the safe exclusion zone in case of potential LNG hazards during bunkering.

ISO/TS 18683 (ISO 2015c) recommends establishing a safety exclusion zone around the LNG bunkering station access to which is to be restricted to all non-essential personnel during bunkering so as to minimise the probability of ignition and the threat to human lives in the event of an accident. Such a safety exclusion zone encompassing the supply point on the terminal side and the bunkering station on the ship is illustrated in Figure 4.2 **Error! Reference source not found.** This standard allows the extent of

the safety exclusion zone to be determined either deterministically based on the worst-case scenario or probabilistically using quantitative risk assessment.

In certain cases, safety exclusion zone determined through a deterministic method may turn out to be impracticably large, because such a method is usually based on an extreme event regardless of the probability of its occurrence. The determination of the ‘extreme’ event is somewhat arbitrary as well.

A few flag states specify the extent of safety exclusion zones for bunkering, but they appear to be rather arbitrary and it is highly doubtful if any these have resulted from systematic risk assessment. Moreover, siting of LNG bunkering point must be determined so as to minimise the risk to human lives.

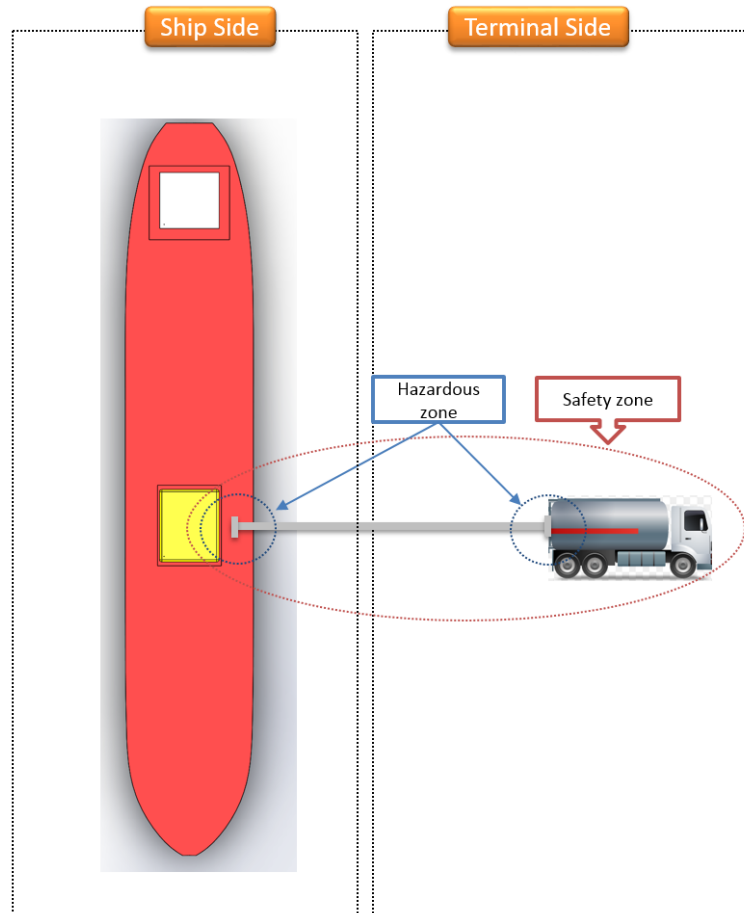


Figure 4.2. Illustration of a safety exclusion zone for LNG bunkering (ISO 2015c).

### Previous research for LNG bunkering

Germany and Norway (2012) have carried out hazard identification for ships using LNG as a marine fuel and their results were submitted as an information document to the IMO. In this study, potential LNG hazards affecting the crew and third parties were identified in a general way. Bunkering operation was identified as one of the most dangerous procedures. ABS (2014) summarized the current regulations and guidelines of LNG bunkering, highlighting the absence of direct regulations for LNG bunkering. However, it was acknowledged that several international bodies have conducted research on developing a robust regulatory framework with specific requirements applicable to various types of LNG bunkering. Nevertheless, these studies were largely limited in identifying potential risks

that could arise when handling on-board LNG using qualitative risk assessment. It has been recognized that reliability of analysis was low. They also lack guidelines to provide the safety requirements for LNG bunkering in a quantitative way.

Republic of Korea (2015) investigated the potential risk of explosion at on-board LNG bunkering stations, simulating the impact of explosion using a CFD code. The work showed that the impact of an instantaneous explosion of a massive concentration of LNG vapour was high enough to require proper safety measures. The study, however, was deterministic in nature considering only one extreme case. It concluded that a probabilistic approach must be used to investigate realistic cases and to derive effective regulations and guidelines.

To addition, various quantitative risk assessment studies have been carried out to determine the extent of safety exclusion zones on a case-by-case basis (DNV 2012a; Norway 2012; ADN 2014; DNVGL 2014a). For example, DNV (2012a) has conducted a site-specific quantitative risk assessment of LNG bunkering in an effort to determine a safe distance for passing ships at the Port of Rotterdam, whereas DNVGL (2014a) has carried out a case study for proposed LNG bunkering ports in USA, estimating safety exclusion zones for the LNG terminals. The limitations of those research in developing generally-applicable safety regulations were mainly placed on the fact that the results are relevant to given situations rather than to general ones.

DNVGL (2014b) has developed a guideline for LNG bunkering facilities, which recommend establishing a safety exclusion zone so that the probability of a critical accident is less than  $1.0E-6$  per bunkering on condition that the minimum zone should not be less than 10 m. A critical accident was defined as a flash fire which can cause the loss of any human lives other than the personnel essential for bunkering. However, the guideline has given rise to several issues. First of all, there are discrepancies between the ISO Standards and the DNVGL guideline: the ISO Standards require all possible consequences such as radiation and blast pressure caused by fire and explosion to be considered, whereas the guideline is concerned

with only the consequence of flash fire. Secondly, it is reasonable to assume that the frequency of bunkering will have a great bearing on risks, but it can be argued that the DNV GL guideline does not fully consider the frequency of LNG bunkering.

In general, the findings of previous studies were somewhat site-specific to be translated into general regulations directly. Most of case studies are also limited to small-to-medium sized ships. This has left the possibility of a massive accidental LNG release associated with large ocean going ships during bunkering. In this context, it is urgently required to develop a set of quantified guidelines for establishing the safety exclusion zone of LNG bunkering station.

#### *4.3.2. Low risk for low pressure FGS system*

The purpose of the marine fuel gas system is to fill, store and vaporise LNG and to supply natural gas to engines on a ship. The system is designed for minimum heat in leakage to guarantee maximum holding time. Different engine technologies (2-stroke, 4-stroke, Otto Diesel-process) requiring different gas supply systems. For 4-stroke engines with Otto cycle normally requires the low pressure of FGS system ranging from 4 bar to 16 bar.

Compared to high pressure FGS system, the risk of low pressure system is relatively low: bigger gas pipes, but with lower gas pressure/density, low risk of leakages, less expansion energy of gas in case of pipe-to-pipe connection rupture.

#### *4.3.3. High risk for high pressure FGS system*

It is advantageous for large LNG-fuelled ships to adopt HP FGS system because of its higher efficiency. But in this system the pressure of LNG goes up to 300 bar (g), and the IGF Code requires it to be installed within the fuel

preparation room (FPR), which is essentially a confined space. This can present the hazard of vapour cloud explosion (VCE) which can occur when a large flammable mass of hydrocarbon is released, vaporized and finally ignited in confined spaces (DNVGL 2014a; DNVGL 2014b).

FPR for many types of LNG-fuelled ships, such as bulk carriers, ferries and container ships are arranged below the load line. So, the explosion may result in deformation or breaking of wall which can lead to the breach of watertight integrity of the hull. Therefore, the hazards associated with the release of the high pressure LNG must be studied in order to enhance the safety of LNG-fuelled ship.

#### Current regulations for HP FGS system

The fundamental regulation of the IGF Code to which all ocean-going LNG-fuelled ships having gross tonnage of 500 and above are subjected, requires the impact of any explosion to be confined to the originating area only, not allowing it to cause disruption of the proper functioning of systems located in other spaces (IMO 2017). However, the Code and other related rules and standards have not been able to provide any specific guidelines on quantifying these risks and recommendations on designing and arranging the FPRs containing HP FGS system.

The first ocean-going LNG-fuelled container ship entered service in late 2015, and the FPR of this ship was arranged on the open deck between two LNG fuel storage tanks as illustrated in Figure 4.3 (Piellisch 2013). It is conceivable that an incident of explosion in the FPR can damage the storage tanks, and the accident can escalate as a consequence. It may be that such eventuality was examined and such risk dismissed to be negligible at the design stage. According to an email correspondence from the duty ship designer for this ship, working at DSEC, however, neither specific studies on the possibility of such accidents were undertaken nor the boundary structure of the FPR was strengthened against explosion for the simple reason that there is no specific requirement.

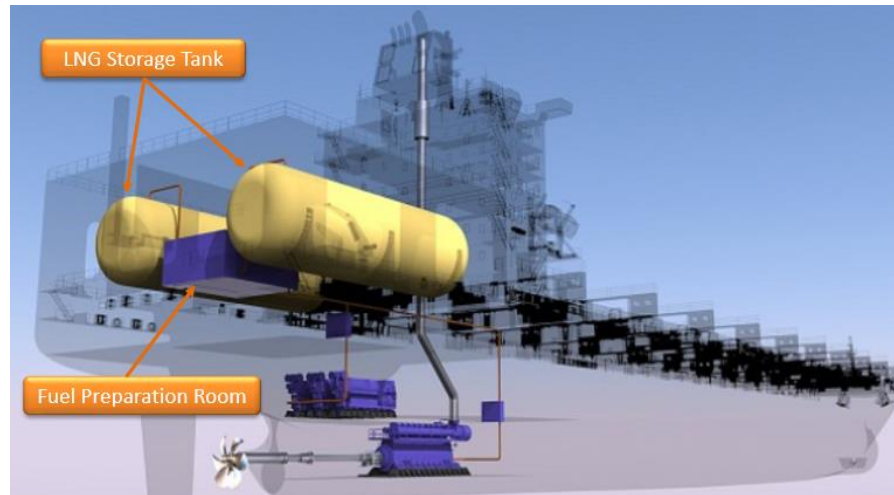


Figure 4.3 Diagrammatic representation of fuel system on an LNG-fuelled container ship (Piellisch 2013).

In larger LNG-fuelled ships, such as very large ore carriers (VLOCs) or container ships over 10,000 TEU, the risk is probably higher, as it is recommended that the FPR is to be arranged below the open deck due to limited on-deck spaces. In this case, an incident of explosion leading to rupture of the hull structure which can result in water ingress endangering the whole ship or affect the equipment in adjoining spaces.

#### Previous research for HP FGS system

In contrast to several studies on the LNG explosion in the chemical/offshore industries (Gavelli et al. 2011; Dan et al., 2014), equivalent sets of studies for LNG-fuelled ships, especially for FPR having HP FGS system have rarely been conducted. A few related studies can be discussed here.

Republic of Korea (2014) examined the potential risk of explosion in an FPR containing an HP-FGS system, concluding that the deterministic impact of an instantaneous explosion in the room would be significant. Although it was the first study addressing the safety of a key fuel gas system component, the analysis was too simplistic to determine whether any safety measures are necessary or not. Once again, probabilistic risk assessment will be required to assess the safety of FGS system properly.



Lee et al. (2015) compared the LNG fire risk of two different types of low pressure FGS system with working pressure of 10 bars: one was pump type FGS and the other was build-up type FGS. To evaluate the consequent level of fires affecting the structure of the fuel preparation room, the study adopted the process of probabilistic risk assessment by using a CFD code, KFX, for consequence analysis that was later integrated with frequency analysis carried out based on the historical records of accidents. In terms of fire incidents, the results revealed that the build-up type FGS was relatively safer than the pump type FGS overall.

The dearth of previous research on investigating the risk of HP FGS system in a systematic way, would be a stark reminder of a plenty of works to be studied. It was thought that the dearth of past studies addressing the potential risk of explosion in HP-FGS system has been due to the short history of LNG-fuelled ships and not because the subject is unimportant. Much of the effort described in this thesis, therefore, was directed to investigate the nature of risks associated with the FGS systems.

#### 4.4. Overview of risk assessment to investigate the safety of LNG-fuelled ship

The safety of ships against many and varied marine hazards has traditionally relied on IMO regulations and classification society rules, which are rarely based on risk assessment. Where there is no relevant regulations or inadequate provisions, goal-oriented approaches are necessary, and here risk assessment plays an important role, particularly in decisions involving uncertainty, novel systems, deviation from standard practice and risk trade-offs. Good examples of such practices can be found in offshore industry where many new systems, structures and arrangements are developed continuously. Likewise, In order to investigate the safety of LNG fuelled ships, this project adopts the technique of risk assessment.

IMO has introduced the formal safety assessment (FSA) as a proactive and systematic means of developing new safety regulations (IMO 2007). It consists mainly of five step processes: hazard identification, risk assessment, development of risk control options, cost-benefit assessment, and making recommendations for decision-making as illustrated in Figure 4.4.

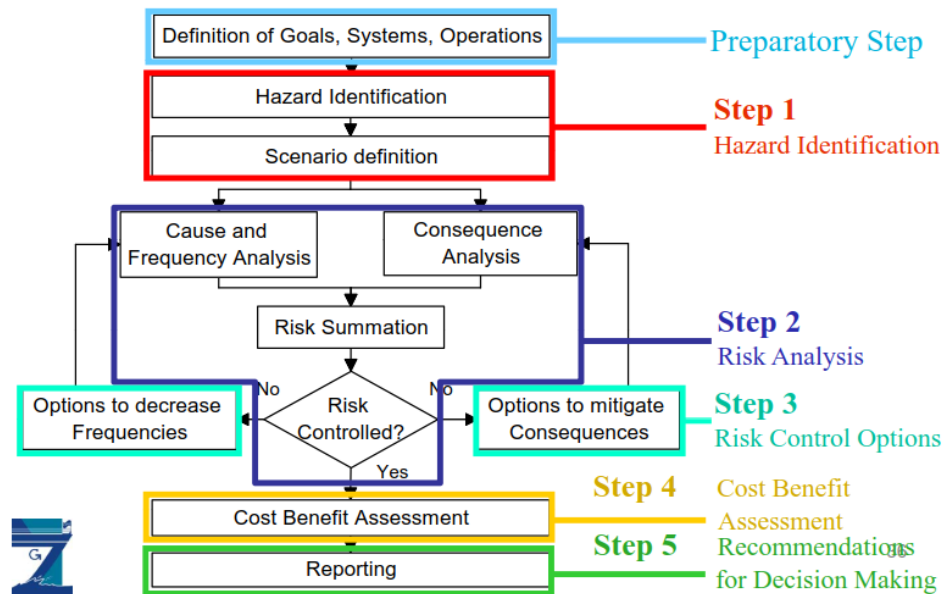


Figure 4.4. Formal safety assessment (IMO 1997).

#### 4.4.1. Hazard identification

Hazard identification (HAZID) is the process of identifying hazards, and forms the essential first step of a risk assessment. The aim of this process is to obtain a list of potential risks using either qualitative or quantitative risk assessment techniques.

Major methods for HAZID are as follows:

- HAZOP – Hazard and Operability Study
- FMECA – Failure Modes, Effects and Criticality Analysis
- SWIFT – Structured What-If Checklist Technique

A hazard and operability (HAZOP) study is a way of identifying the potential hazards associated with target systems. The team of experts from

different aspects systematically investigates each sub-system of the process, while generally reviewing the process and instrumentation diagrams (P&IDs). They adopt a standard list of guidewords which assist them to identify deviations from design intent. In overviewing each credible deviation, they analyse possible causes and consequences, and evaluate whether safeguards should be recommended. They record their conclusions in a standard format during the sessions. Guidance on HAZOP can be found in, to cite a few, Kletz (1997, 1999) DUNJÓ et al. (2010) and Goyal et al. (2012).

A failure modes, effects and criticality analysis (FMECA) (or its simpler form, FMEA) is a systematic approach to identify the failure modes of mechanical or electrical systems. This method aids safety evaluators to estimate a failure of each component and subsequent effects and criticality. The results can present failure modes with probability and severity of results and direct mitigation efforts if necessary (IEC 1985).

The structured what-if checklist (SWIFT) technique is a method to identify hazards based on the use of brainstorming. Like in HAZOP, SWIFT uses a team familiar with the installation, under the guidance of a specialist in the SWIFT technique (Witter 1992). The main differences, compared to a HAZOP can be summarized as below:

- The discussion proceeds systematically through the installation's modules or operations at the system and procedural level, not individual items or tasks.
- The method relies on brainstorming (creative thinking) and checklists, not an official list of guidewords.

#### 4.4.2. Risk analysis

In general, risk assessment can be carried out either qualitatively or quantitatively (Rausand and Høyland 2004). Qualitative methods are easier to apply, but will tend to produce less insight. Conversely, quantitative

methods are more challenging for a range of resources and skills, but provides potentially the most detailed understanding if significant spending is involved (HSE 2001). Some of the hazard identification techniques described in the previous section can focus on subsequent risk analysis.

### Qualitative methods

A qualitative risk matrix is often used to measure the levels of likelihood and severity of identified hazards thorough HAZID process. In all these methods the risk is determined by combining the severity of its impact with the likelihood of its occurrence (Rausand and Høyland, 2004).

An example of qualitative risk assessment process using HAZOP method is illustrated in Figure 4.5. It used a combination of HAZOP parameters (flow temperature, pressure and level) and guide words (no, less, more and reverse) to identify assorted hazards for a medium-sized floating regasification unit. The degree of frequency and consequence for the identified hazards was then assessed based on the experience and judgement of the expert panel (KR 2015b; Rausand and Høyland 2004).

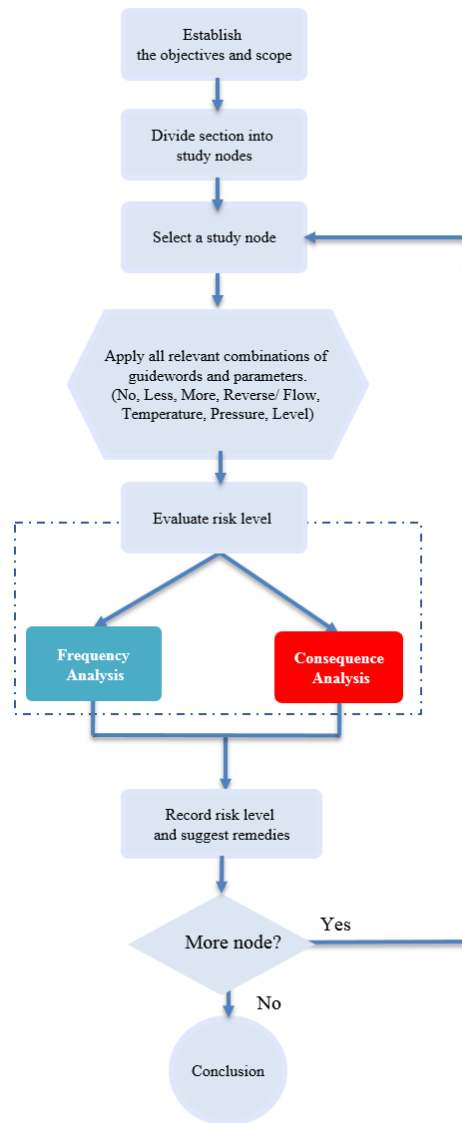


Figure 4.5 HAZOP framework (Lee 2016; Rausand and Høyland 2004).

The qualitative risk assessment method has been extensively applied to complex LNG technologies in a variety of marine/offshore industries. Tugnoli et al. (2010) performed the safety assessment of LNG regasification systems onshore and offshore. The potential hazards associated with the several types of LNG systems were investigated after identifying possible failure and consequence chains for each system. It concluded that advanced tools would be required for investigating the safety levels of LNG plants more systematically.

Paltrinieri et al. (2015) identified potential hazards associated with LNG regasification plants in a qualitative way. It cited new LNG technologies as challenging cases to identify potential hazards comprehensively and reliably, highlighting the lack of experience as the key limitation of the qualitative method. Giardina and Morale (2015) have carried out a qualitative risk assessment by combining an FMECA and HAZOP methods to investigate the safety of LNG regasification plant. Like other qualitative studies, the risk of the proposed plant had been determined based on expert judgment and experience. Although there is no denying that there are some advantages in using qualitative risk assessment methods, it could be problematic when assessing the risk of systems for which there is lack of knowledge and experience (Vinnem 2007).

Despite being broadly applicable, qualitative risk assessment has several inherent shortcomings:

- It will be difficult to make quantitative prediction with high credibility because the knowledge produced might not generalize to other people or other cases.
- It relies on the experts' decision over much. This may bring personal biases into the process, possibly leading to misjudgement (Rausand and Høyland 2004).

#### Quantitative methods

For more stringent safety investigations, a quantitative method through which frequency and consequence of unwanted events can be quantified based on reliable statistics and analytical/computer-aided calculations will be necessary (Rausand and Høyland, 2004).

Similar to qualitative approaches, quantitative risk assessment usually maintains a clear distinction between two important elements: frequency and consequence. For example, a hydrocarbon leak resulting in a fire or explosion is often considered the marine accident scenarios. This provides a clear distinction between the causes and likelihood of hydrocarbon leaks

(frequencies) and the effects of fires and explosions on people, property and the environment (consequences). For most hydrocarbon leaks, the estimation of leak frequencies can be largely independent of the modelling of fires/explosions (HSE 2001).

While the qualitative analysis uses coarse and somewhat arbitrary divisions of frequency and consequence, the quantitative analysis ‘computes’ the values based on historical data, logical reasoning, simulation and/or formulaic representation of physical phenomena.

On the other hand, for complex systems having a number of equipment working at different operating conditions, the industry often uses ‘selective’ quantitative risk assessment which examines only the risks associated with particular scenarios, operating conditions or sub-systems which are pre-identified as critical or hazardous through qualitative studies. Spouge (1999) and Vinnem (2007) have outlined general guidance of quantitative risk assessment applicable to offshore oil and gas units. Likewise, there are some example studies (Dan et al. 2014; ISO 2015) using this framework as illustrated in Figure 4.6. In this framework, qualitative risk assessment is preceded in order to identify critical parts of systems prior to ‘selective’ quantitative risk assessment.

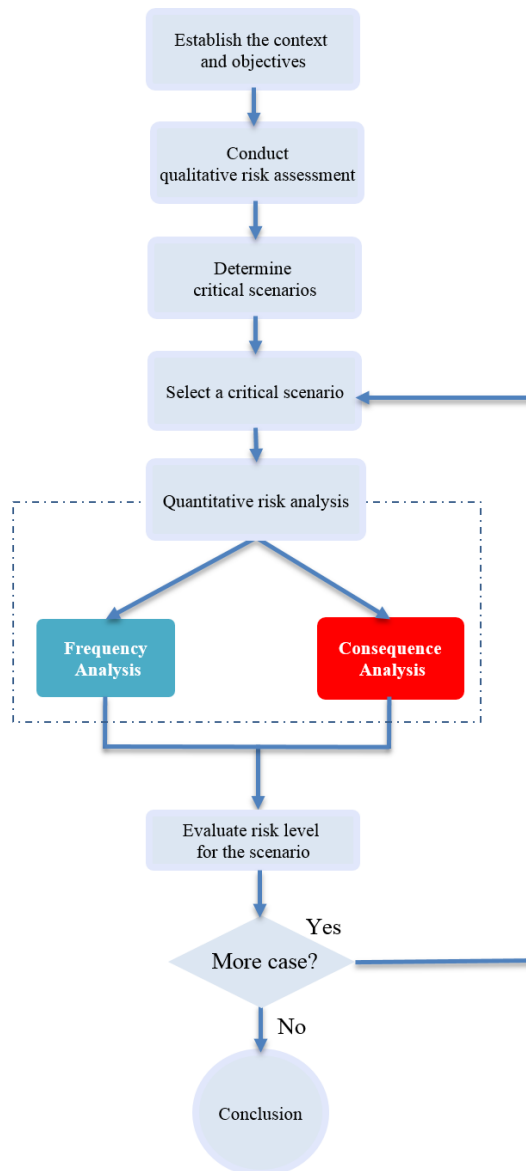


Figure 4.6. Selective quantitative risk assessment framework (Dan et al. 2014).

The selective quantitative risk assessment has also been extensively applied to complex LNG systems in a variety of marine/offshore industries. For example, Chae (2016) compared the risk impacts for different types of on-board LNG liquefaction systems. In addition, Park et al. (2017) have evaluated the safety of structure of LNG liquefaction process systems for FLNG against the potential explosion and Kim et al. (2016) carried out fire simulations to determine the optimal position of water deluge systems for an offshore unit through the selective quantitative risk assessment.



Martins et al. (2016) carried out risk analysis for an LNG regasification unit based on the selected hazardous scenarios. D'alessandro et al. (2016) developed a decision-making tool to select an LNG regasification plant site. In this study, the feasibility of the plant site was determined through a selective quantitative risk assessment where potential hazards were identified in a qualitative way.

As pointed out earlier, FSA was introduced to encourage the development of risk-based regulations, and has been applied to all types of ships (HSE 2001). However, no FSA procedures have been established for LNG-fuelled ships so far. Moreover, general guidelines on tools and techniques for hazard identification and risk assessment are given without realistic guidance on how to use these methods in an integrated way. Partly due to this, it is legitimate to question the effectiveness of the conventional quantitative risk assessment in investigating the safety of LNG-fuelled ships.

#### 4.5. Concluding remarks

Despite increasing popularity of LNG-fuelled ships, the current regulations and other regulatory provisions are inadequate to ensure their safety. There are a number of subsystems within the LNG-fuelled ships the safety of which has never received systematic studies. Of these, the systems which are open to the highest risk levels are thought to be bunkering system and high pressure fuel gas supply system. It has been seen that there are many risk assessment methods, and a number of studies have discussed the benefits and shortcomings of the current risk assessment methods applied to LNG systems. This thesis will, therefore, examine the safety of LNG-fuelled ships with particular emphasis on these two points, using quantitative risk assessment techniques.

Publications dealing with the safety of LNG systems and safety assessment methods in general pertinent to the current project were briefly reviewed and discussed in this chapter. Several past studies have studied the hazards of LNG in general, but their applicability to the safety of LNG-fuelled ships is still open to doubt. It is also clear that what regulations and guidelines there are for systems and subsystems associated with LNG-fuelled ships are far too vague to be of practical help in design and operation. It can be concluded, therefore, that systematic and thorough quantitative risk assessment studies are necessary for enhancing the relevant regulations.

Some limitations in risk assessment methods being currently employed have been identified and some new enhanced methods have been put forward to overcome this problem in this thesis.

## 5. CONCEPTUAL DESIGN OF A CASE SHIP

This chapter presents a conceptual design of an LNG-fuelled ship to examine the risks that it presents in detail. Since 2000 smaller LNG-fuelled ships have been designed with the LNG fuel tanks and other facilities on deck. For larger ships, however, the gas storage tanks and associated systems need to be much larger and it is no longer practically possible to place them on deck, leaving the only feasible location below the freeboard deck, possibly sacrificing some of the cargo spaces. The IGF Code appears to be much more stringent for below-deck storage tanks and, moreover, in this case the associated system will be much more complicated making the uncertainty of safety more pronounced.

For these reasons a 300,000 DWT VLOC, representing large modern ocean-going ships, was selected for this purpose. It was assumed that the ship, already in existence, was to be retrofitted with dual-fuel engines. Through the conceptual design process for converting this diesel ship into an LNG-fuelled ship, current compliances, rules, guidelines, and standards were overviewed and their shortcomings were explored. This conceptual design was carried out in collaboration with Korean Register and Polaris Shipping Co., Ltd.

Retrofitting a ship with LNG-fuelled engines involves some major tasks as follows:

- engine retrofitting;
- LNG fuel tank arrangement;
- fuel preparation room arrangement; and
- setting up bunkering stations.

These, of course, have to be carried out with considerations given to the structural characteristics of the subject ship along with operational conditions such as voyage profiles and fuel consumption. The process and decisions were to be made in compliance with the IGF Code, KR Class rules and the general practices. Table 5.1 summarizes general specifications and operational profiles of the case ship.

Table 5.1 General specifications of the case ship (by courtesy of Korean Resister)

300K DWT VLOC (Case Ship)	
	
<b>L x B x D</b>	328.0 m x 55.0 m x 29.0 m
<b>Main engine</b>	Hyundai MAN B&W 6G80ME-C9
<b>MCR/NCR<sup>4</sup></b>	20,680 kW x 65.8 rpm/17,578 kW x 62.3 rpm
<b>Cruising range</b>	Abt 25,000 miles per one return voyage from Brazil to East Asia

### 5.1. Arrangement of overall LNG fuel system

Considering the characteristics of cargo operation of VLOC, it seemed reasonable to place the LNG fuel storage tank below the freeboard deck to prevent any disturbance to cargo operations and possible damage from cargo operating machineries. For structural safety and convenience, it was decided that the most practicable location to place LNG fuel storage tank is within No.4 Cargo Hold (KR 2015a). The tank connection space and fuel preparation room would be located above the storage tank space within the same cargo hold to simplify the piping system. The piping from the fuel gas supply system to the engines in machinery room is arranged via the open deck, and therefore the pipes will have to be double-walled.

Figure 5.1 shows the conceptual arrangement of LNG fuel system for the case ship.

<sup>4</sup> Maximum continuous rating/nominal continuous rating (NCR is 85% of MCR)

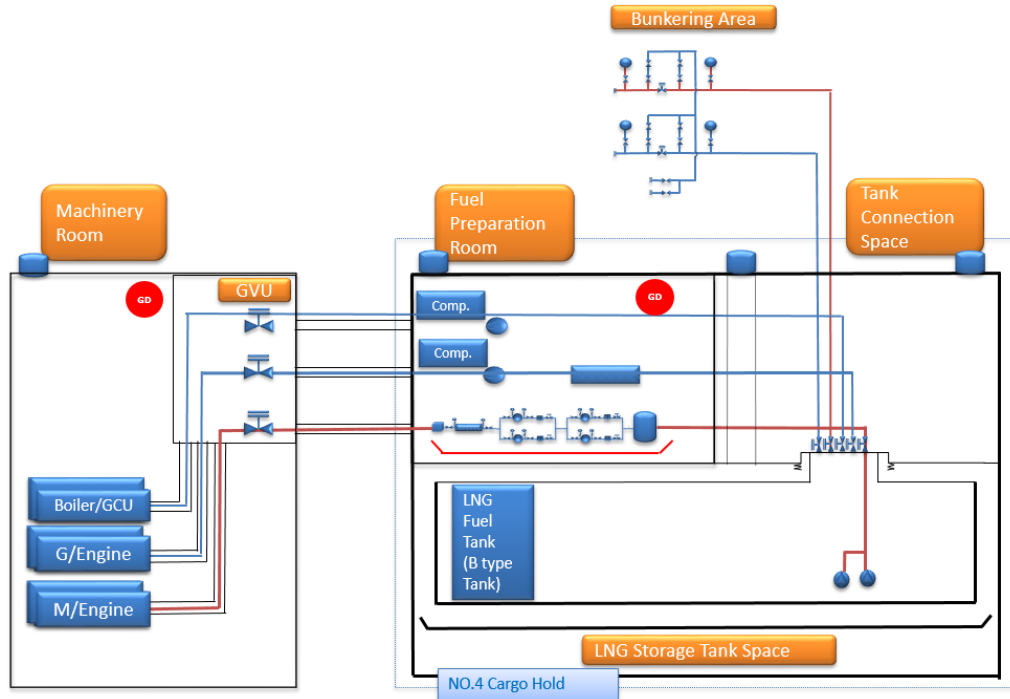


Figure 5.1. Outline of LNG fuel system.

### 5.1.1. LNG storage tank

To convert an existing diesel-fuelled ship into an LNG-fuelled ship, substantial retrofit works are involved. The case ship was originally equipped with Hyundai MAN B&W 6G80ME-C9 producing 20,680 kW at MCR. This has to be replaced with an appropriate dual fuel engine system. An engine selection software developed by MAN Diesel & Turbo was used to select an equivalent new dual-fuel engine, Hyundai MAN B&W 6G80ME-GI-C9 producing 20,680 kW at MCR.

Fuel consumption can be estimated for each fuel mode and engine load from Table 4.2. For example, at NCR the consumption is F.O 6.9 g/kWh in F.O. and 128.8 g/kWh (KR 2015) in gas for the gas mode. This is in contrast to the consumption figure in the heavy fuel mode of 158.7g/kWh. In the next step the estimated fuel consumption plays a key role in determining the capacity of LNG fuel storage tanks and bunkering intervals.

Since the power produced at NCR is 17,578 kW and the ship speed of 14.6 kts, the daily consumption of LNG is about 67 tonnes/day. The distance of return voyage is 25,000 NM, and therefore the tank capacity has to be at least 11,000 m<sup>3</sup>. Since this can be achieved comfortably using one tank and the characteristics of dual fuel engines do not necessarily require a redundancy in the gas fuel system, it was decided to use a single tank system. This has an additional advantage of simpler piping system.

The type of the fuel tank has to be determined next. IMO type A tank and membrane type tank were disregarded due to their high costs and complexity in retrofitting. From the point of view of optimal space utilisation, the rectangular IMO type B tank appears to be more attractive than the cylindrical type C tank.

IGF Code 5.3 requires the fuel storage tanks to be located in such a way that the outer vertical insulation of the tank is separated from the vertical shell plate of the ship by at least  $B/10$ , where  $B$  is the breadth of the ship. The code also stipulates that the bottom insulation has to be at least  $B/15$  above the bottom plate of the ship. There is sufficient room to locate the tank connection space and the fuel preparation room right above the tank, and the LNG bunkering stations are positioned on the freeboard deck.

For practical reasons, the tank connection space (defined by the IGF Code 2.2.15) is located adjoining LNG storage tank. Considering IGF Code 13.4.1, the tank connection space was designed as an enclosed space segregated from and the fuel storage hold space where the LNG storage tank is fitted. In case of the space being located below the freeboard deck, the effective mechanical ventilation system with a capacity of at least 30 air changes per hour are required.

### *5.1.2. Fuel preparation room*

The fuel preparation room is where fuel gas supply system is located. The requirements of the IGF Code for such a space are as follows:

- Fuel supply system is to have full redundancy and segregation all the way from the fuel tanks to the consumer, so that a leakage in one system does not lead to a loss of power.
- For single fuel installations, the fuel storage is to be divided between two or more tanks. The tanks are to be located in separate compartments.

Since the case ship is to have a dual fuel type engine, the second requirement is not relevant in our case. In order to prevent the unwanted accumulation of leaked gas, the IGF Code 13.6 requires fuel preparation rooms to be fitted with effective mechanical ventilation systems providing a ventilation capacity of at least 30 air changes per hour. It is not clear where this capacity figure of 30 changes per hour has been derived from. This may be sufficient for low pressure systems, but it is not known if it will be adequate for the new high pressure gas supply system. Indeed, the IGF Code is lacking in quantitative provisions for HP-FGS system altogether. Potential explosion due to a leak in the HP systems will be investigated in this study (see Chapter 10).

### *5.1.3. Bunkering system*

For a bunkering station located within an enclosed space, IGF Code 11.3.6 requires the space is to be separated by A-60 bulkheads from machinery spaces of category A, accommodation, control stations and high fire risk spaces. A-0 class divisions are to be used adjacent to tanks, voids and auxiliary machinery spaces of little or no fire risk. To avoid such complications and for simpler piping it was decided to place the bunkering stations on deck above the No.4 cargo hold as shown in Figure 5.2.

It is necessary to consider the operational profile of the case ship in designing the bunkering systems, as it is an important factor in determining bunkering capacity, flow rate, pipe size and position, allowable bunkering hours, bunkering methods, etc.

Although the details of bunkering systems may vary from ship to ship, they all have to meet the same safety requirements. For example, flow velocity is to be set no higher than 10 m/s as this is the maximum velocity for the hoses typically used by the industry (DNVGL 2014b). European design standard EN1472-2 states that the maximum allowable working pressure in an LNG transfer hose should be less than 10 bar.

Since an LNG leak during bunkering poses several hazards such as cryogenic burns, deck embrittlement, and even fires and explosion, it is necessary to limit the number of personnel exposed to such hazards. The simplest way of achieving this is by imposing a safety exclusion zone around the bunkering stations. However, as discussed in Chapter 3, there is still a lack of quantified guidelines in this regard.



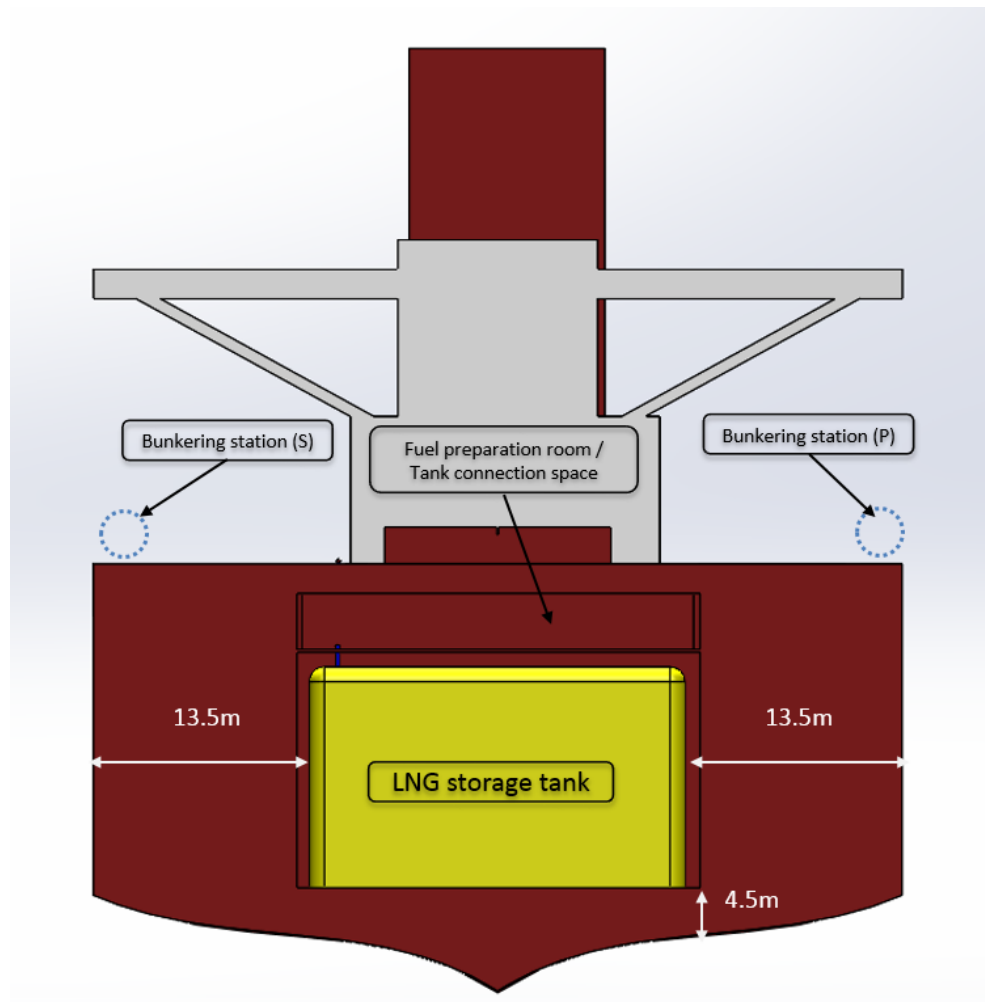


Figure 5.2. Arrangement of LNG storage tank for the case ship.

#### 5.1.4. Machinery room

The IGF Code deals with two types of machinery rooms: *Gas safe machinery spaces* and *ESD-protected machinery spaces* which are defined as follows:

- *Gas safe machinery spaces* where a single failure cannot lead to release of fuel gas into the machinery space. All fuel piping within machinery space boundaries is to be double walled.
- *ESD-protected machinery spaces* where a single failure may result in a gas release into the space. Venting has to be designed for a leakage scenario. Pressure relief devices and shutdown arrangements against

failures such as gas pipe ruptures or blowout of gaskets should be installed.

The machinery room for the case ship was designed as a *gas-safe machinery space*. Consequently, all the fuel pipelines fitted in the machinery room would be of double-wall type. In order to minimise the leak developing in the first place, the inner wall of the pipes should be made of 304L alloy, while the space between the concentric pipes is to have a ventilation facility with a capacity of at least 30 air changes per hour to minimise the consequence of a leak should any such occur. Likewise, ESD valves for each engine and boiler were fitted adjacent to the machinery room, which act automatically on detecting a gas leak or are manually operated.

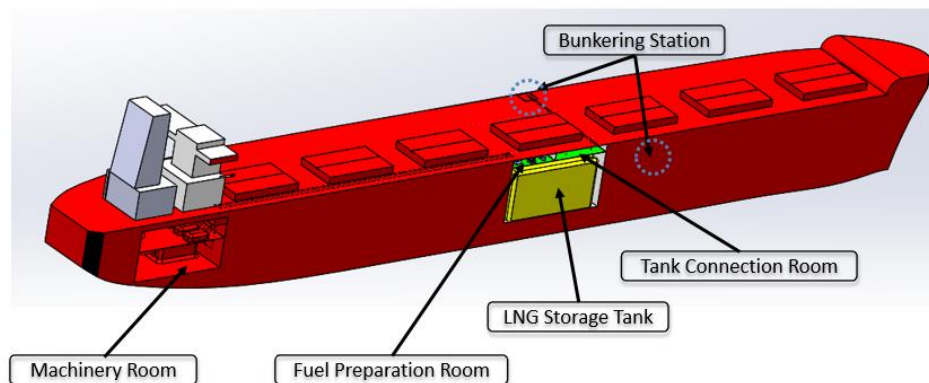


Figure 5.3. Conceptual design of LNG-fuelled ship.

Figure 5.3 shows the final conceptual design of the whole LNG systems for the case ship.

## 6. METHODOLOGY

The studies undertaken in this project are quite varied and complex. It will be, therefore, useful to expound the methods used in some detail before the actual studies are discussed. As pointed out already elsewhere in the thesis, risk assessment can usually be regarded as having two parts: frequency analysis and consequence analysis.

For frequency analysis historical data will be utilised where possible supported by fault tree analysis and event tree analysis. Complex systems with no historical records will be dealt with the hierarchical modelling method which will be described in more detail later in this chapter.

The consequence analysis to investigate the impact of jet, pool, flash fires and explosion are carried out using analytical methods for a variety of leak cases and operating conditions. In some cases, numerical computations (CFD and FEA) are used to investigate the impact.

Parametric investigations and sensitivity analyses were carried out where appropriate to obtain valuable insight into the nature and characteristics of risks commonly expected in these systems.

This methodology is then implemented into the IQRA software, which was developed to allow rapid outline assessment of risks, associated with fire and explosion in oil/gas process systems. The program was written in LabVIEW environment.

### 6.1. Introduction

The process of examining the safety is divided into three main stages: system modelling, risk assessment and decision-making based on the result. The major characteristics of each process are described in Figure 6.1.

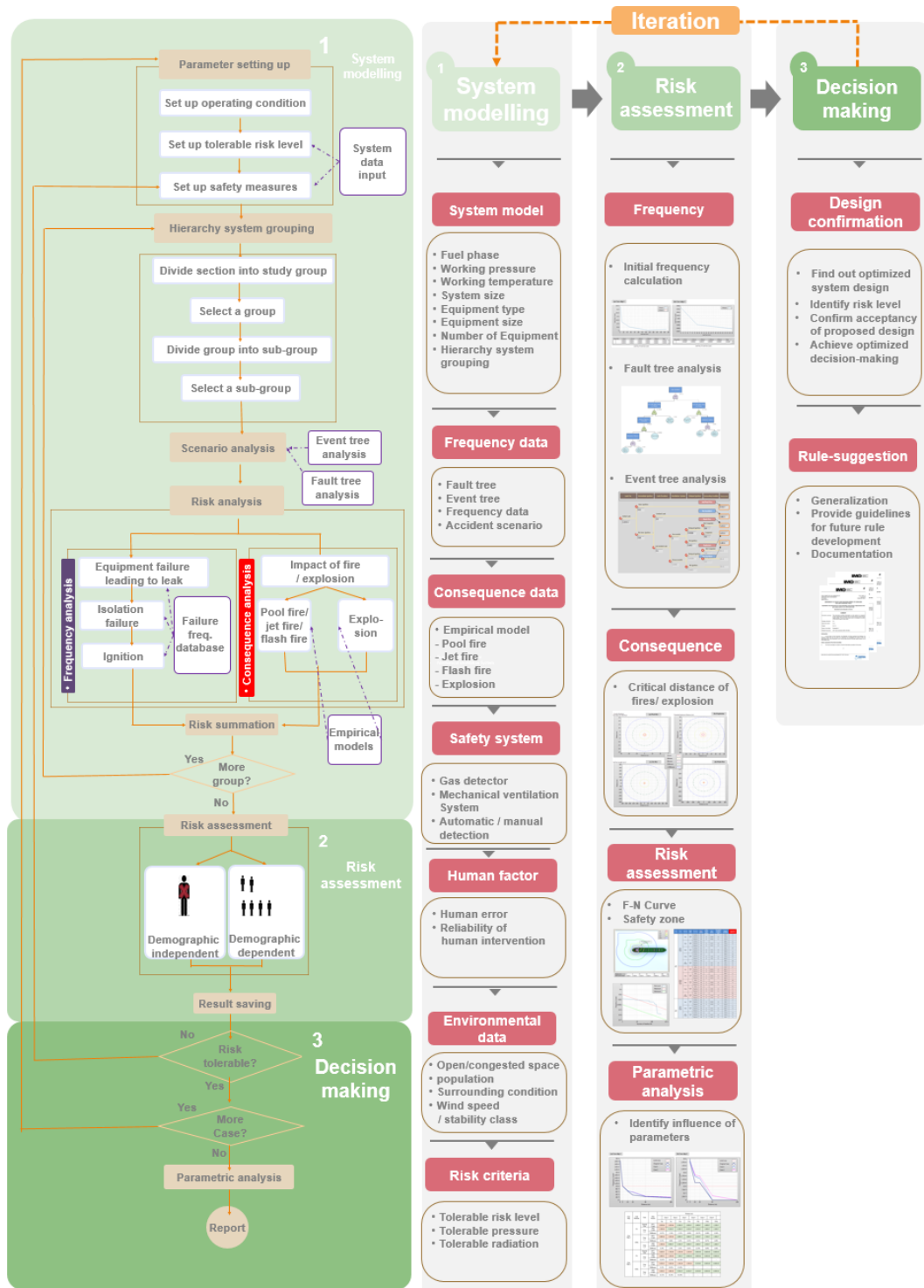


Figure 6.1. Outline flowchart risk assessment process.

### 6.1.1. System modelling

One key idea of this project is to develop a hierarchical system modelling method with which complex oil/gas processing systems with no direct historical data can be modelled more accurately. In this method the entire processing system is divided into primary groups according to certain chosen parameters, and these groups are then subdivided into secondary groups. This process is repeated until the complete system is broken down into elemental components which have historical accident data, such as pipes, valves, pumps, and so on (Figure 6.2).

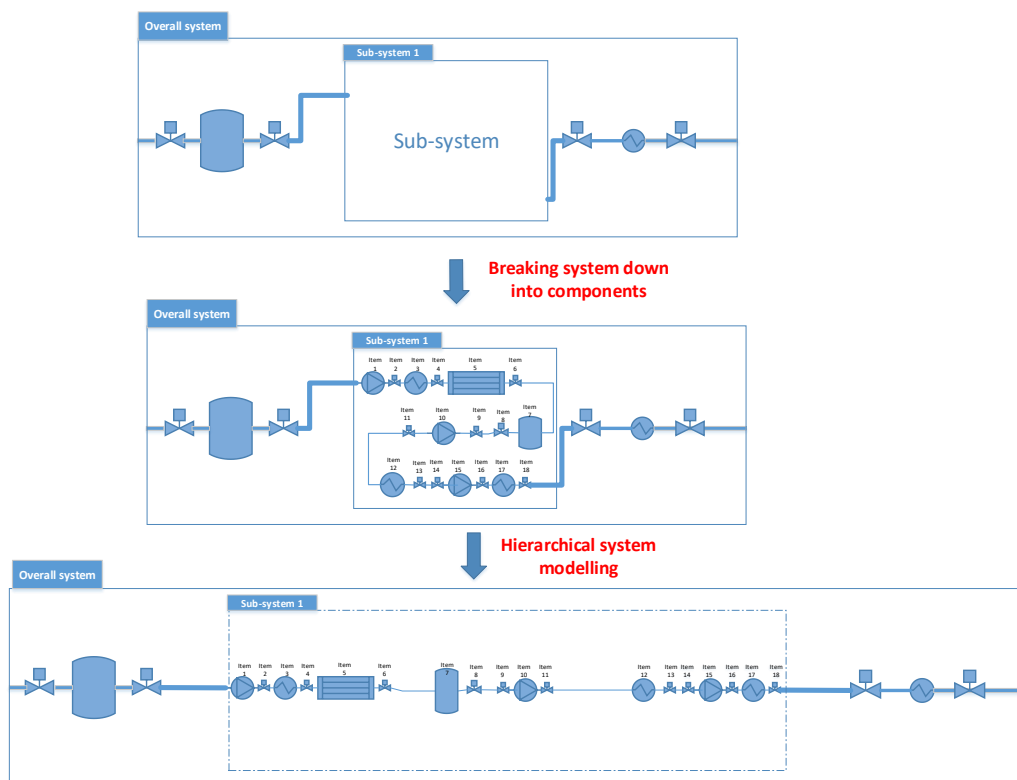


Figure 6.2. An example of hierarchical system modelling for a complex system.

#### Basic principle of hierarchal system modelling

To begin with, the question on whether each component should be assessed in a dependent manner or can be assessed independently was not newly brought by the hierarchical system modelling. The question has been inherited in every type of risk assessment for a long time.

In irrespective of hierarchical system modelling, Figure 6.2 represents a general LNG process system where each component in a complex system is linearly connected. One may perceive that the occurrence of fire/explosion initiated by the leak from Item 3 (pump) would lead to the damage to the neighbouring items such as Item 2 or 4 (valve), resulting in the secondary accident.

In this context, here is to explain why the risk of each component in a complex system was independently assessed and how the summation of the individual risk of each component can represent the overall risk of the complex system.

#### Common approaches to this issue

In case of the initial leak from Item 3, if the leak is successfully limited by safety measures (whether manually or automatically), it can be perceived that all the systems will be isolated; all valves may be shut-off in a credible manner to limit the leaks from the origin.

Even if the initial leak and the subsequent accident lead to the damage to any other parts of the system, which leads to additional leak, the system has been already isolated therefore the amount of the leak will be very limited. For a 50 mm diameter pipe with 10 m length, the contained LNG is merely 8.8 kg.

Moreover, such limited leak is less likely to damage to the LNG systems they are normally designed in the operation pressure at least 10 bar(s) up to 300 bar(g) they are totally higher than the impact of consequences. It was discussed the impact of LNG explosion would be less likely to be higher than 1 bar (g) in the literature review as the methane explosion would not form the detonation.

As shown in Figure 6.3 an accident of fire will take significant times to deteriorate the material of LNG system leading to the secondary accidents. Before it happens it is more likely for the system to be isolated thereby the

no fuel would be supplied. Otherwise, all personals will be spared sufficient time to evacuated.

Under this assumption, in the scenario of limited leak, the accident is commonly considered limited only to the leak part (this assumption is equivalent to treat the risk of component independently). In this regard, risk analysts commonly disregard the possibility of secondary accident.

However, there is still uncertainty whether the initial accident would possibly lead to secondary accidents. To consider it, in general, two approaches can be taken. One is the deterministic approach by designing the worst-case scenario in irrespective of probability. Second approach is to include the scenario of delayed leak isolation in the probabilistic analysis.

Given the impact of secondary accident is also determined by the leak amount involved in the accident, the scenario of delayed leak isolation would be designed that the sufficient leak time is given to investigate the worst-case scenarios (the leak time or amount from delayed isolation may be set equivalent to the condition that all systems are destructed by the initial accident).

For an example of this project, the delayed leak isolation was set up at 1,000 s (abtout 17 mins) (It is hardly imaged that the secondary accidents could be more critical than the 17 mins leaks and all the leaked LNG is calculated in estimating the impact of consequences.)

Therefore, the risk analysis can cover the uncertainty in the possible scenario of the secondary accident by taking a conservative stance in designing the scenario of delayed isolation.

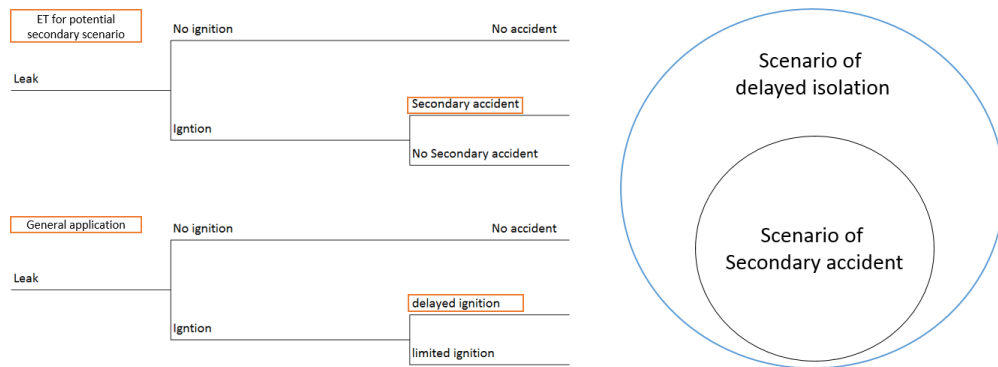


Figure 6.3. An example of ET for a LNG leak.

There are two types of ‘cross coupling’ between two or more components: one is the probability of the accidents occurring simultaneously; and the other is an accident in one component bringing about an accident in another component. We can ignore the first of these because the probability of this will be extremely low, although there is a small possibility that the simultaneous accident produces a more severe consequence than the sum of the two accidents. The second cross coupling refers to the possibility of one failure escalating into a larger incident involving more than the originator component. However, we have already taken into account this type of escalation in estimating the amount of fuel leaked and accumulated in constructing the accident scenarios. Therefore, it is not unreasonable to treat the components as separate isolated systems. We can, therefore, directly combine the risks of the individual sub-systems to obtain the overall risk of the entire system.



## 6.1.2. Approach to risk assessment

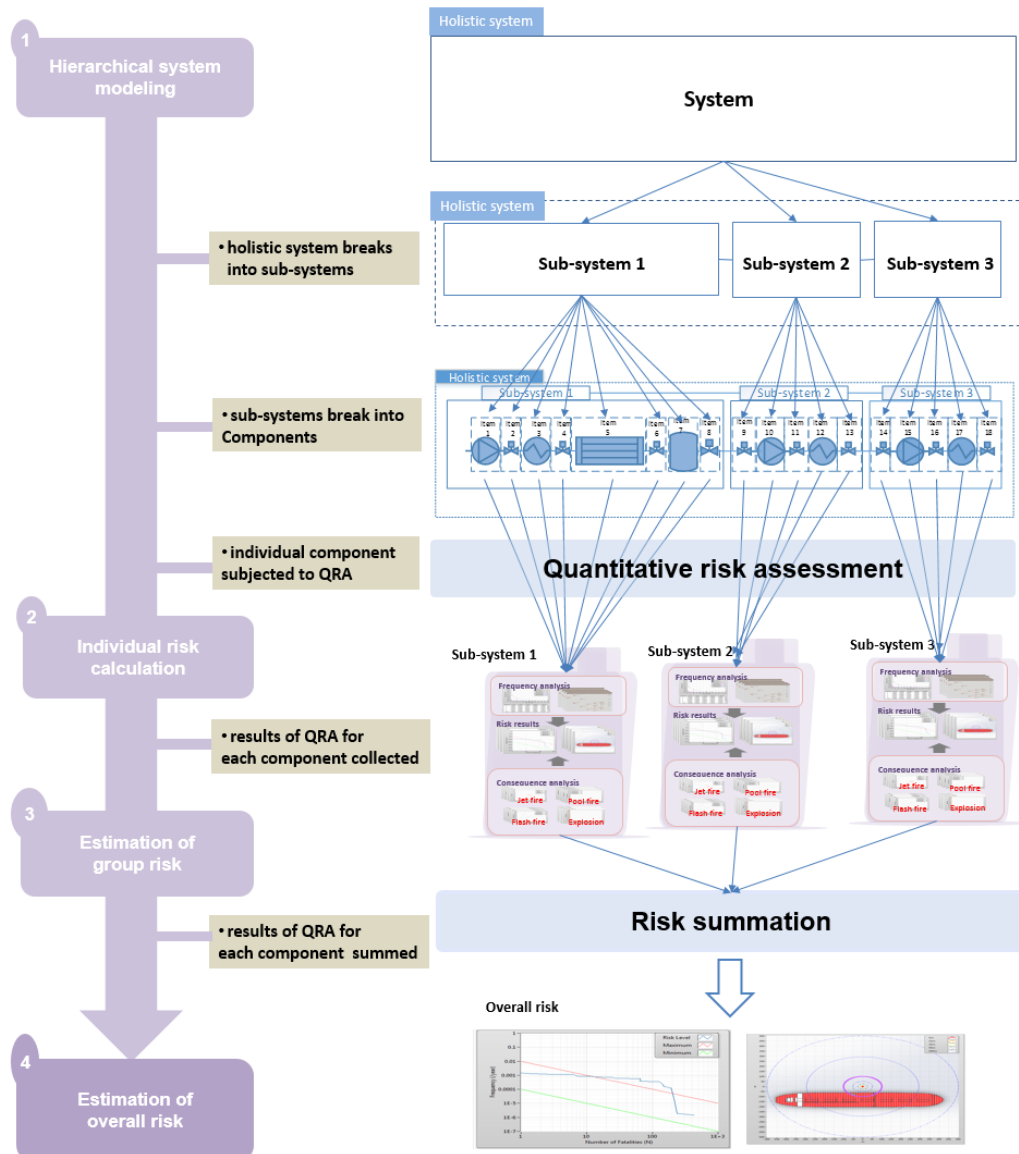


Figure 6.4. Risk assessment with hierarchical system modelling.

The risk of an individual component (or sub-system) can be obtained by combining the frequency of failure of the component with the impact of consequences (flash fire, jet fire, pool fire and explosion). The risk of a composite component can be assessed by summing the risks associated with the sub-components making up this component. In this way, the overall risk of the whole system, not just selective elements, can be estimated as shown in Figure 6.4.

The major consequences of fuel leak can be economical cost, environmental damage and human lives. Whilst recognising the importance of the first two types, it was decided to concentrate on the last, thus reckoning the risk in terms of probability of human lives lost in the form of F-N curves. It means the overall risk of the entire system is sensitive to the density and distribution of population exposed to the potential hazards. Thus it should be noted that the overall risk of the entire system is not a fixed value but can be changed by the density and distribution of population. The hierarchical modelling when applied to this type of risk assessment can be illustrated as in Figure 6.5.

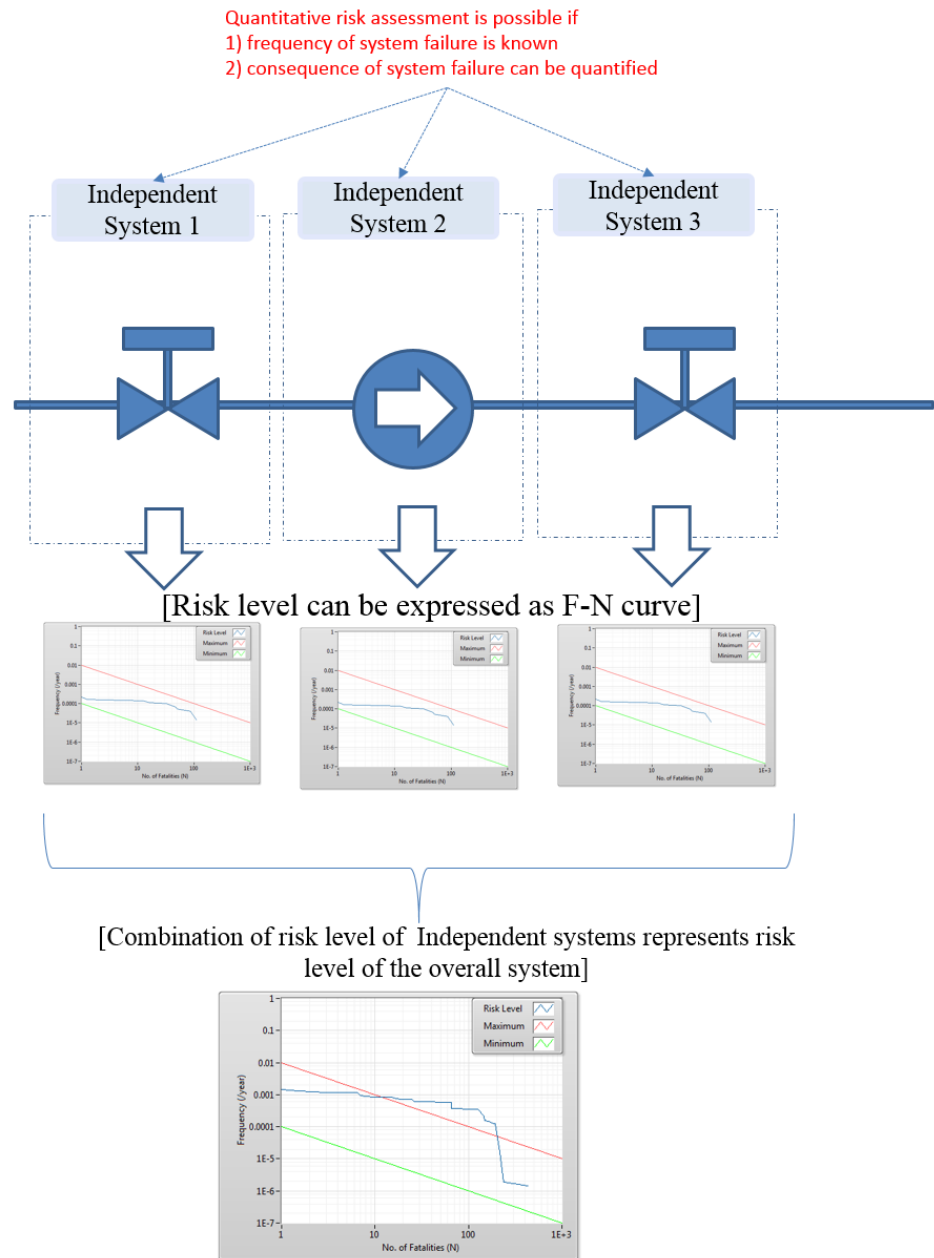


Figure 6.5. An example of quantitative risk assessment using hierarchical system modelling.

## 6.2. Methods adopted for risk assessment

The framework of the risk assessment carried out in this study was based on the authorized guidelines for risk assessment process (BS EN 1997), safety of machinery (BS EN 1991) and formal safety assessment (FSA) introduced by IMO (2002). The accident scenarios are identified from event tree analyses and

their likelihood is estimated. The consequence analysis is carried out based on the empirical and analytical models associated with fire and explosion.

### 6.2.1. Frequency analysis

Frequency analysis is a process of quantifying the probability of occurrence of unwanted events identified through the scenario analysis (Dan et al. 2014; ISO 2015c). Spilled LNG will undergo several physical processes simultaneously, such as pool formation, spread and boil-off. However, the final outcome can be diverse, depending on the nature of the leak and functioning of safety measures. Figure 6.6 shows a typical event tree (ET) of a series of accidental scenarios considered in the project.

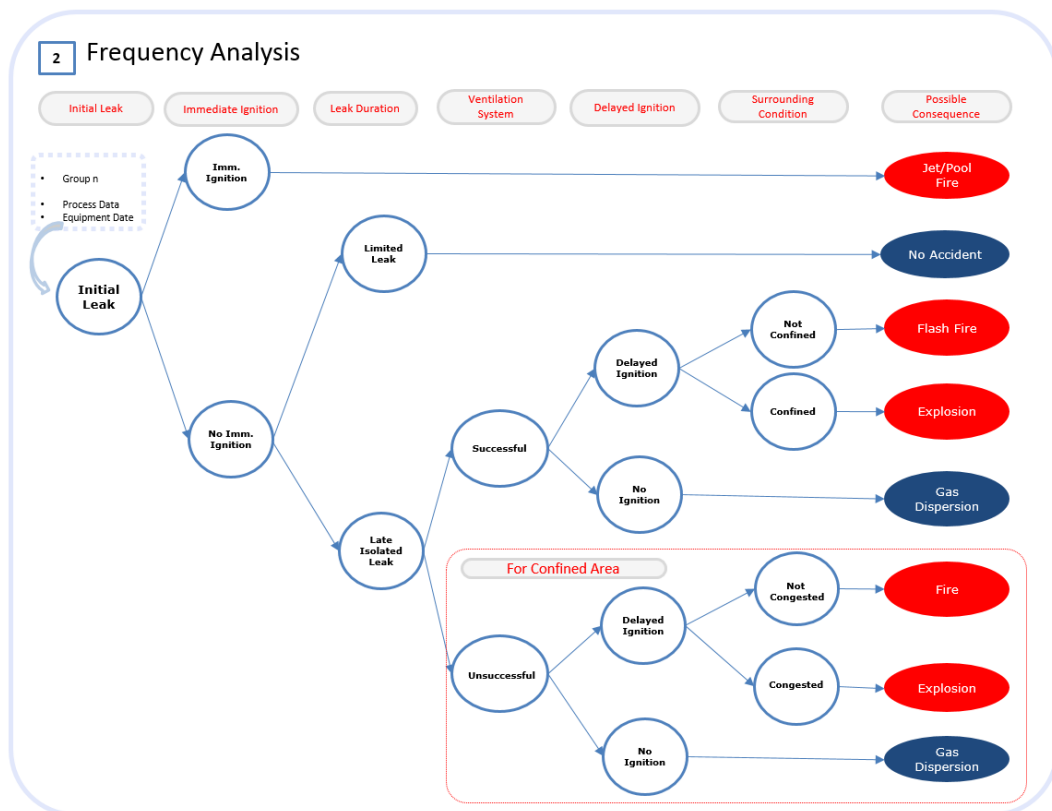


Figure 6.6. An example of event tree (Dan et al., 2014; ISO, 2015; Jeong et al. 2017a).

Immediate ignition is assumed to be associated with jet fire (for gas release) and pool fire (for liquid release), whereas delayed ignition leads to other types of outcome. A leak of liquid fuel forms a liquid pool, possibly leading to a pool

fire if ignited. Where the concentration of leaked material is between LFL and UFL (5 %~15 %), it is assumed that delayed ignition leads to a flash fire or an explosion if the gas is sufficiently enclosed. It is assumed that a pool fire (which is only associated with liquid leak) or flash fire may occur in open conditions (Dan et al. 2014). For open spaces, the frequency of each hazard is calculated as follows:

$$\blacksquare \quad F_{\text{Jet Fire}} = F_{\text{Initial Leak}} \cdot P_{\text{Imm. Ignition}} \quad (6.1)$$

$$\blacksquare \quad F_{\text{Pool Fire}} = F_{\text{Initial_Leak}} \cdot P_{\text{Imm. Ignition}} \quad (6.2)$$

$$\blacksquare \quad F_{\text{Flash Fire}} = F_{\text{Initial_Leak}} \cdot P_{\text{Late_Isolated_Leak}} \cdot P_{\text{Suc. Ven.}} \cdot P_{\text{Del. Ignition}} \cdot P_{\text{Not Congested}} \quad (6.3)$$

$$\blacksquare \quad F_{\text{Explosion}} = F_{\text{Initial_Leak}} \cdot P_{\text{Late_Isolated_Leak}} \cdot P_{\text{Suc. Ven.}} \cdot P_{\text{Del. Ignition}} \cdot P_{\text{Congested}} \quad (6.4)$$

Where,

F Frequency (/year)

P Probability

From the event tree the probability of the occurrence of the final outcomes can be quantified by adopting the recognized generic data and models which are widely accepted for investigating hydrocarbon releases including LNG. The contribution of escalating events leading to the final outcomes can also be modelled in this way, taking into account the reliability of safety measures and the working conditions. The frequency models used are described in more detail in Chapters 8 - 11.

### 6.2.2. Consequence analysis

The process of consequence analysis is outlined in Figure 6.7. It shows the consequence modelling methods including liquid and gas release rate, LNG pool spread and evaporation, and fire and explosion with respect to particular leak sizes. The details of consequence analysis methods, including various estimation and calculation formulae are discussed in the Appendix A.

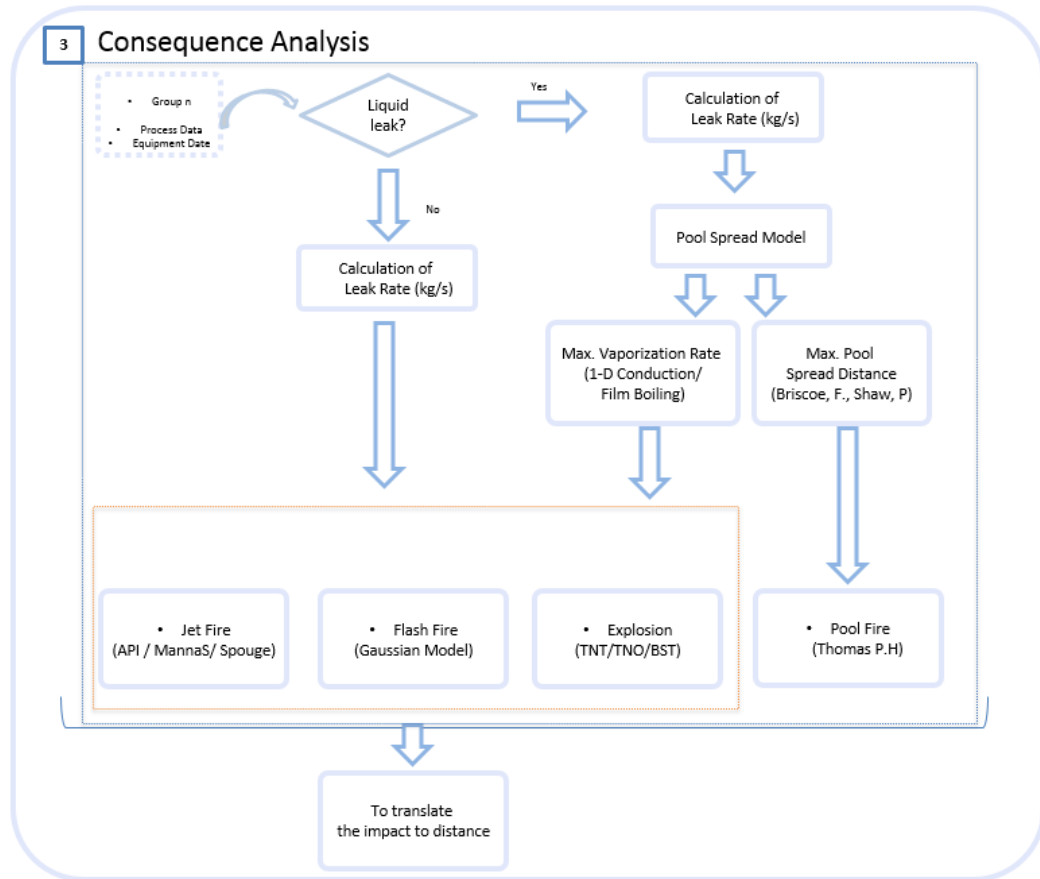


Figure 6.7. Process of consequence analysis.

For liquid leak model, the initial leak rate of LNG is calculated based on the classical work of Bernoulli's equation. For gas leak model, the mass rate for sonic or subsonic discharges from a leak hole is calculated by means of continuity equation and the law of ideal gases for an isentropic expansion (DNV 2012a).

The pool spread model by Briscoe and Shaw (1980) was used in conjunction with vaporization models of either 1-D conduction model of Carslaw and Jaeger (1962) based on Fourier's law or film boiling model of Klimenko (1981) based on Newton's law of cooling. Heat transfer by convection from ambient air or radiation is not included in this model, as this is assumed to be negligibly small.

The length of jet fires was calculated using several semi-empirical models: Cook model (Cook et al. 1990), Mannan model (Mannan 2005) or Spouge model (Spouge 1999), all of which are based on the fact that the

characteristics and impact of jet fires depend on the fuel composition, release conditions and release rate.

In order to estimate flash fire ranges, Gaussian gas dispersion models which predict dispersion effect and the gas concentration (Perkins 1974) were used.

The consequence of explosion was assessed with three simplified empirical models: TNT equivalence model (Woodward and Pitblado 2010), TNO multi-energy (Woodward and Pitblado; Frank 1980) models and Baker-Strehlow-Tang (BST) models (Woodward and Pitblado 2010; Baker 1973).

The average visible plume length in relation to the diameter of a fire is estimated by means of the flame model derived by Thomas (1965).

### *6.2.3. Risk assessment*

According to the published materials (ISO 2015c; DNV 2012b; DNV 2013; DNVGL 2014b; DNV 2015), the current common practice of determining the safety exclusion zones for LNG bunkering appears to be quantitative risk assessment conducted for population-independent conditions. However, the societal risk depends on population at and near the site, given that the consequence is usually expressed in terms of lives lost and injuries caused by accidents. Therefore, it is obvious that an accident will result in different societal risk levels in terms of harm to human life for different number of people present. In this context, it was necessary to develop a new framework to investigate the effect of population distribution to the extent of safety exclusion zones. The two approaches are outlined below.

#### *(a) Population-independent analysis*

It is clear that the probability of fatality is highest at the point of fire/explosion and gradually decreases as the distance from the spot increases. The critical distance can be defined as the distance at which

the probability of fatality becomes less than a given threshold value. This can be translated into a distance where thermal radiation or overpressure goes down to a critical level. This exercise can be conducted purely based on the estimated harm that thermal radiation and overpressure can cause without ever assuming any presence of humans.

Based on the critical distances estimated from consequence analysis, each incident outcome can be associated with a critical distance and its probability of occurrence. For each critical distance, the cumulative probability of occurrence can then be calculated by summing all the probability of the incident outcomes with less or equal critical distance. The required extent of the exclusion zone can then be determined by selecting the minimum critical distance which has probability of occurrence lower than the required value. For illustrative and comparison purposes the extent of exclusion zone can be divided into a number of arbitrary ranges, for example, Zone 1 (below 5m), Zone 2 (5-15m), Zone 3 (15-25m), Zone 4 (25-50m), Zone 5 (50-100m), and Zone 6 (100-200m).

It could be said that the purpose of using 'spatial zones' is related to the generalization of the present study. This will enable the rule-makers, for example, to specify a safety exclusion zone of radius at least so and so for such and such ships. The process of population-independent analysis is outlined in Figure 6.8.



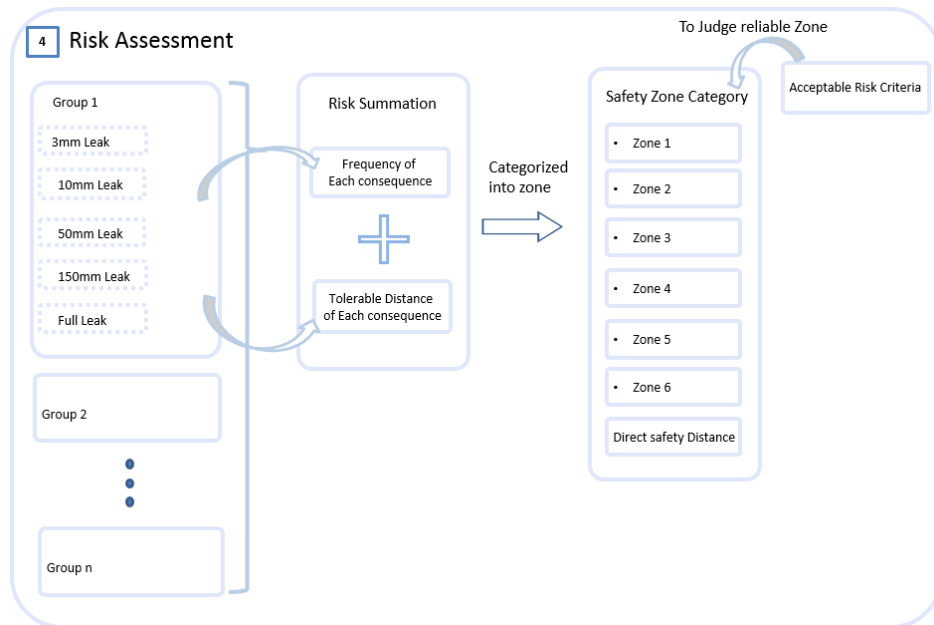


Figure 6.8 Layout for population-independent analysis (Jeong et al. 2017a).

*(b) Population-dependent analysis*

Despite the population-independent analysis discussed above, the true societal risk must depend on the density of population at site. Risk is usually expressed in terms of lives lost and injuries caused by accidents. To quantify the adverse impact of pool fire (by thermal radiation) and explosion (by overpressure), the probability of fatality ( $PR_F$ ) was estimated by probit models described in Equations (6.5) to (6.7) (Jafari et al. 2012; Zarei et al. 2013; Mohammadfam and Zarei 2015). Duration of exposure to thermal radiation ( $t_e$ ) was assumed to be 60 seconds, equivalent to the safety guidelines from the Centre for Chemical Process Safety (CCPS 1989).

$$PR_F = 0.5 \left[ 1 + \frac{PB_{PF} - 5}{|PB_{PF} - 5|} \operatorname{erf} \left( \frac{PB_{PF} - 5}{\sqrt{2}} \right) \right] \quad (6.5)$$

$$\text{For pool fire, } PB_{PF} = -14.9 + 2.56 \cdot \ln(q_{TR}^{4/3} \cdot t_e) \quad (6.6)$$

$$\text{For explosion, } PB_{PF} = -77 + 6.91 \cdot \ln(P_{BW}) \quad (6.7)$$

Where,

$PR_F$	Probability of fatalities
$PB_{PF}$	Probit corresponding to probability of fatalities
$q_{TR}$	Thermal radiation ( $W/m^2$ )
$t_e$	Exposed time (= 60 seconds)
$P_{BW}$	Overpressure of blast wave (Pa)

The number of fatalities is evaluated by multiplying the probability of fatalities with population distribution for each incident outcome and then summing these for all outcomes. Using the calculation results from Equations (6.5) to (6.7), the number of fatalities caused by pool fire and explosion are calculated by Equations (6.8) and (6.9) (Zarei et al. 2013; Mohammadfan and Zarei 2015).

$$NF_{PF} = \int_0^{A_C} PO_D \cdot PR_{F\_PF} dA = 2\pi \int_0^{r_C} PO_D \cdot PR_{F\_PF} dr \quad (6.8)$$

$$NF_{EX} = \int_0^{A_C} PO_D \cdot PR_{F\_EX} dA = 2\pi \int_0^{r_C} PO_D \cdot PR_{F\_EX} dr \quad (6.9)$$

Where,

$A_C$	Area concerned ( $m^2$ )
$NFPF$	Number of fatalities by pool fire (persons)
$NFEX$	Number of fatalities by explosion (persons)
$PO_D$	Population distribution (persons)
$PRF\_PF$	Probability of fatalities by pool fire
$PRF\_EX$	Probability of fatalities by explosion
$PO_D$	Population distribution (persons)
$r_C$	Radius of concerned area (m)

For pure methane, a gas concentration between lower flammable level (LFL: 5 %) and upper flammable level (UFL: 15 %) leads to a flash fire (Dan et al., 2014). In this context, the LFL of methane (5 % by volume)

is considered to be the criterion to determine the critical distance for the flash fire. Flash fires are directional due to wind (evenly distributed in, say, East, South, North and West). Therefore, a quarter of the population (25 %) within the critical zone can be regarded as fatalities as shown in Equation (6.10).

$$NF_{FF} = \int_0^{A_c} PO_D \cdot \frac{1}{4} dA = 2\pi \int_0^{r_c} PO_D \cdot \frac{1}{4} dr \quad (6.10)$$

Where,

$NF_{FF}$       Number of fatalities by flash fire (persons)

The emissive power of a jet fire ranges from 50 to 220 kW/m<sup>2</sup> and, since the rate of fatality is normally taken to be 100% when exposed to 37.5 kW/m<sup>2</sup>, the impact of fire radiation can be assumed to be critical on any personnel working within the predicted length of the fire (Tweeddale 2003). The direction of a jet fire depends on the positioning of the leak hole (say, up, down, left and right). The jet fires pointing up or down are less likely to come into contact with human bodies, and therefore only the left and right directions are regarded critical (probability of 0.5). For every critical jet fire, one quarter of the population (25 %) within the critical zone can be considered as fatalities as shown in Equation (6.11).

$$N_{JF} = \frac{1}{2} \int_0^{A_c} PO_D \cdot \frac{1}{4} dA = 2\pi \int_0^{r_c} PO_D \cdot \frac{1}{8} dr \quad (6.11)$$

Where,

$N_{JF}$       Number of fatalities by jet fire (persons)

Finally, the assessed risk is shown as F-N curves (frequency vs number of fatalities). The frequency of each accident is combined with its consequence (number of fatalities). Finally, the results are shown in F-N curves drawn as cumulative frequency against number of fatality. A simple example is shown in Figure 6.9.

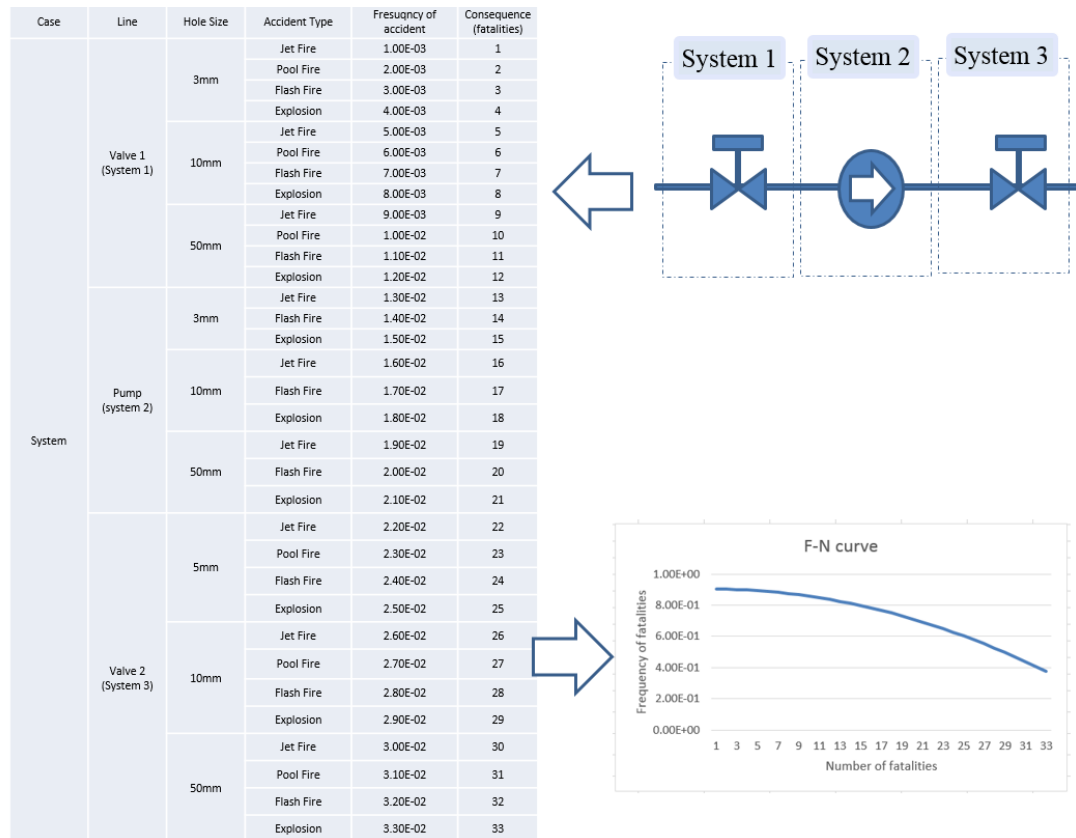


Figure 6.9. an example for estimating the F-N Curve from the complex system.

### 6.3. Software implementation

In order to accommodate highly complex and extensive risk assessment for a variety of systems and parameters, a computation tool was thought to be necessary.

Several quantitative risk assessment (QRA) software have been developed and widely used to the chemical and similar industries where the assessment of potential risks from unwanted events from chemical process systems is crucially important.

A focal point of such software centres around investigating the consequential effects initiated by chemical leaks. It may include modelling of pool spreading and evaporation, and flammable and toxic effects as well as calculating heat radiation from fire, over-pressures from explosions, toxic concentrations from dispersion, etc.

Some representative examples are ‘PHAST’ developed by DNVGL, ‘EFFECTS’ by TNO and RISKAN by R Albuquerque Consulting.

However, as a drawback of current software, the consequence results obtained from the software needs to be integrated with results of frequency analysis carried out from different calculation modules.

A new computer program was developed incorporating the key ideas and methodology discussed above. It was written in LabVIEW, a visual programming language developed by National Instruments. LabVIEW was chosen instead of more usual and more basic programming languages because of some excellent features of this language. Firstly, it is much easier to learn and use than, say C++. Secondly, the language provides a good facility for modular development of codes. Thirdly, it provides an excellent GUI facility and graphics mostly required for the present purpose. Fourthly, the debugging facility of this language is quite adequate for this work. The program was named IQRA software to emphasise the fact that it carries out frequency analysis and consequence analysis in an integrated manner.

Figure 6.10 shows how various functional components are organised within the program. It can be seen that the user interface can be divided into two parts: ‘Data input’ and ‘Analysis & result’. Note that the numbers in orange boxes correspond to the sample interface screenshots given in Figure 6.11.

The interface for data input is designed to accommodate hierarchical system modelling with selection of accident frequency database and consequence models. Optional safety measures, such as automatic gas detectors and emergency shutdown systems, can be selected. Some parameters associated with human factors can also be input at this stage.

Risk analysis is carried out for the given set of input data and the results are presented through the ‘Analysis & result’ interface. When the input data is modified, the analysis is performed automatically, so that users can explore the effect of altering the system variables with minimum effort.

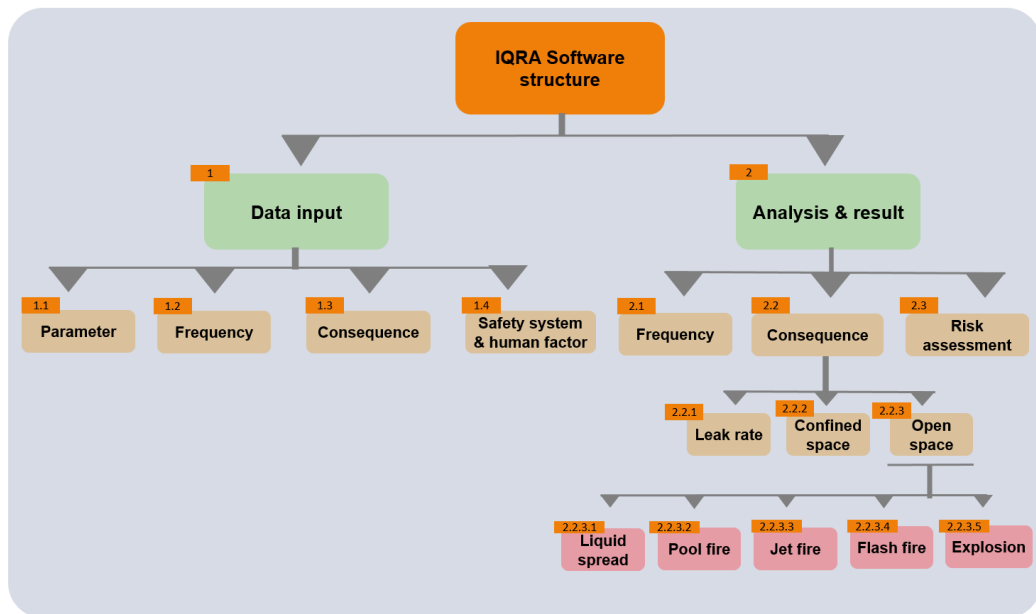


Figure 6.10. Organisation of main components of IQRA software.

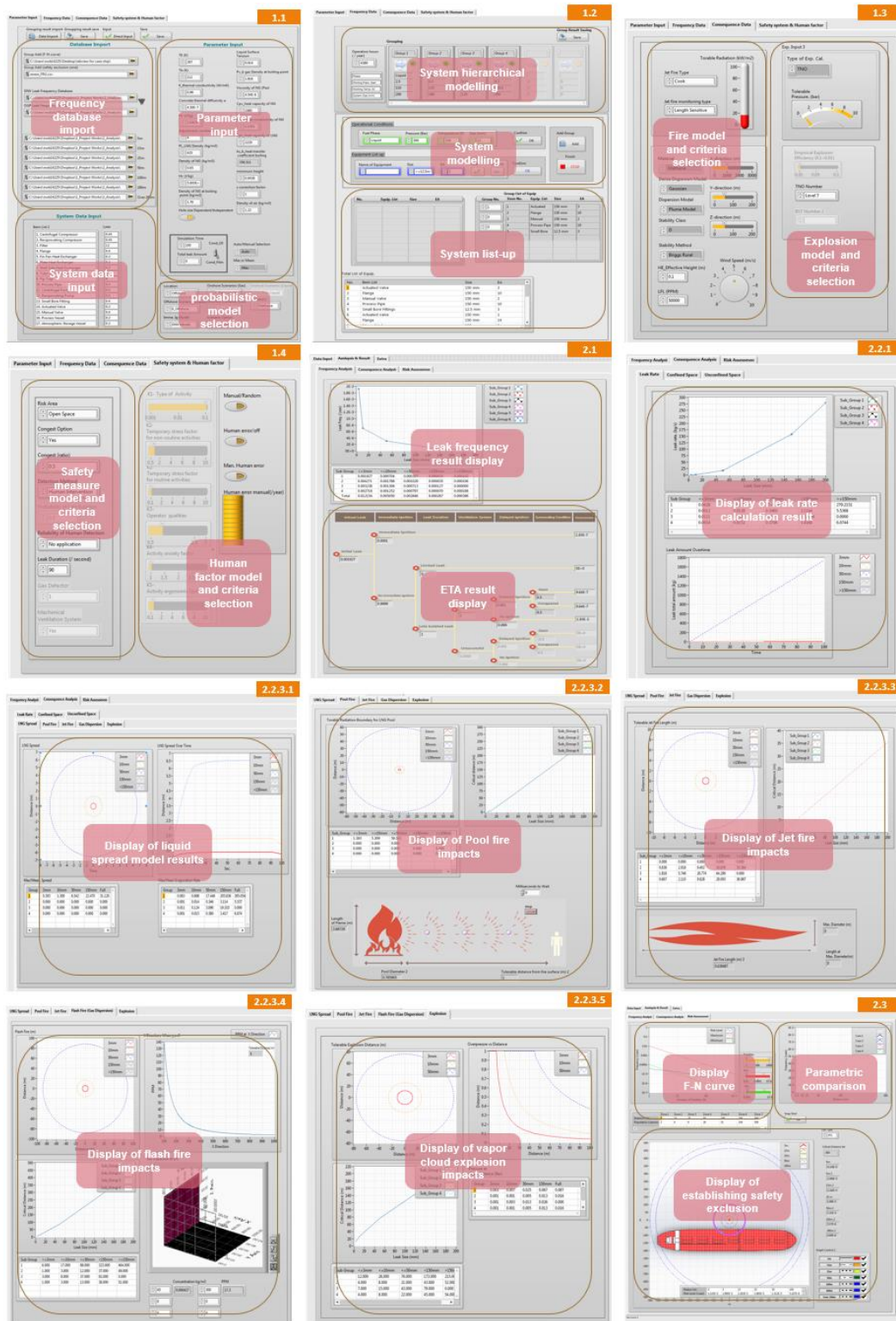


Figure 6.11. User interface of IQRA software.

The main strengths of the software are summarized in Figure 6.12. They can be summarised that it uses an integrated approach to the risk assessment with a built-in accident frequency calculator and a consequence estimator with which

the level of risk can be immediately calculated without any further processing outside the program. The results are produced in a quantitative way and can be readily translated into a form of F-N curve or safety exclusion zone. It is thought that this approach, together with the hierarchical modelling discussed above will facilitate the risk assessment during design stage, providing system designers rapid feedback regarding the safety levels of the system being designed. The flexibility of data entry helps the optimisation process by comparing the performance of various design alternatives from a safety standpoint. Time and effort can then be directed towards mitigating the highest risk factors.

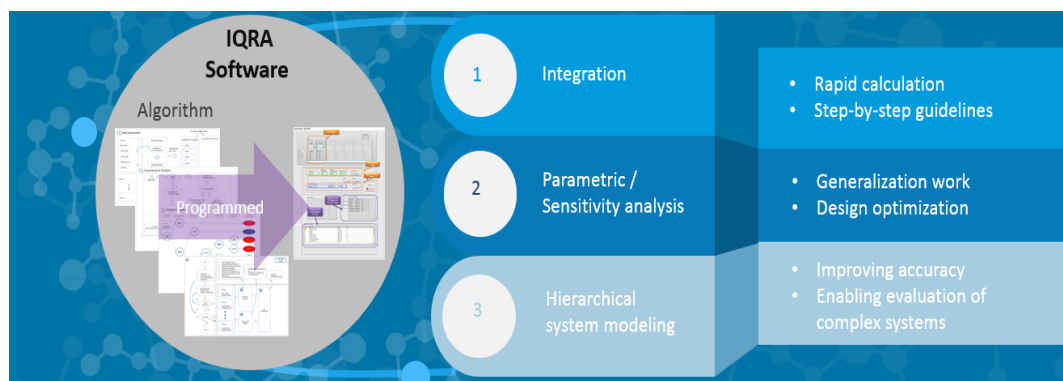


Figure 6.12. Main strengths of IQRA software.

In addition to these obvious benefits that designers can derive from this software, rule-makers can also benefit from parametric analysis using the software to identify the parameters which are influential in determining the system safety and the manner in which they affect the safety level. Different organizations and authorities often require different criteria for tolerable risk. These may be in the form of levels of overpressure and/or heat radiation due to explosion and fire. Since risk assessment commonly adopts data accumulated over many years of operational experience in offshore and chemical industries, the generic approach necessarily involved in rule development may cause some degree of uncertainty in the quantitative results of risk analysis. This is primarily due to the fact that different system modelling and fire/explosion modelling will result in different results even for the same system. In order to minimise such uncertainty, the software allows the users to carry out sensitivity analysis to determine how much



influence some factors have on the results. These include accident frequency databases and fire models. Environmental conditions and population distribution can also be set.

## 7. OVERVIEW OF CONSEQUENCE ANALYSIS

In this Chapter, the theoretical background of consequence models that have found widespread use in industry and academia for predicting pool spreading, vaporisation and the impact of fire/explosion is presented. The process of consequence analysis is outlined in Figure 6.7, showing the methods used in consequence modelling with several steps: calculation of liquid release rate, modelling of LNG pool spread and evaporation and evaluating the impact of fires and explosion in response to particular leak hole sizes.

### 7.1. Leak rate

Leak hole size as well as system conditions are used as the parameters to calculate the leak rate (kg/s) of the fluid. For liquid leak model, the initial leak rate of LNG is calculated based on the classical work of Bernoulli's equation in consideration of leak hole size as well as operating pressures. With the application of the discharge coefficient, a leak rate from an effective cross-sectional area of the leak outlet is calculated as shown in Equation (7.1).

$$Q_L = C_L \cdot A_L \cdot \sqrt{2\rho_L \cdot (P_s - P_a)} \quad (7.1)$$

Where

$A_L$  : cross-sectional area of leak [m<sup>2</sup>]

$C_L$  : discharge coefficient used for liquid (= 0.61)

$Q_L$  : leak rate for liquid [kg/s]

$\rho_L$  : LNG density [kg/m<sup>3</sup>]

$P_a$  : atmospheric pressure [Pa]

$P_s$  : absolute pressure inside pipe [Pa]

On the other hand, the gas leak rate is estimated for two specific flow regimes: sonic flow for high internal pressures and subsonic flow for low pressures. For

the gas leak model, Equation (7.2) defines the pressure at which the flow regimes change from sonic to subsonic (Yoon et al. 2008).

$$\left(\frac{P}{P_s}\right)_{CR} = \left(\frac{2}{\gamma+1}\right)^{\frac{\gamma}{\gamma-1}} \quad (7.2)$$

Equation (7.3) is used to calculate a gas leak rate at sonic flow condition:

$$Q_V = C_G \cdot A_L \cdot P_s \sqrt{\frac{\gamma \cdot MW}{RT_s} \left(\frac{2}{\gamma+1}\right)^{\frac{\gamma+1}{\gamma-1}}} \quad \text{for } \frac{P_a}{P_s} \leq \left(\frac{P}{P_s}\right)_{CR} \quad (7.3)$$

The gas leak rate at the subsonic velocity through the leak hole is calculated as shown in Equation (7.4) below:

$$Q_V = C_G \cdot A_L \cdot P_s \sqrt{\frac{\gamma \cdot g_c \cdot MW}{RT_s} \frac{\gamma}{\gamma-1} \left[ \left(\frac{P_a}{P_s}\right)^{\frac{2}{\gamma}} - \left(\frac{P_a}{P_s}\right)^{\frac{\gamma+1}{\gamma}} \right]} \quad \text{for } \frac{P_a}{P_s} > \left(\frac{P}{P_s}\right)_{CR} \quad (7.4)$$

Where

- $C_G$  discharge coefficient (=0.85)
- $g_c$  gas constant [1kg m/N·sec<sup>2</sup>]
- $MW$  molecular weight [kg/kmol]
- $Q_V$  leak rate for vapour [kg/s]
- $R$  gas constant, 8,314 [J/kmol K]
- $T_s$  storage temperature [K]

## 7.2. LNG spread/evaporation

In the event of an LNG leak, while the mass of the liquid accumulates on deck results in the formation of the pool, part of it vaporizes at the same time. The size of pool will progressively increase until the vaporization rate becomes higher than the spill rate.

### 7.2.1. LNG spread model

The proposed pool spread model is an integral model based on a set of equations that combine mass, momentum and energy balance expressed as an explicit function of time. The basic concept, known as ‘box model’, can be represented by Figure 7.1 as assuming that a circular pool of the leak liquid is formed with radius ( $r$ ) and radial liquid flow velocity and the liquid spreads on a flat, horizontal and solid surface.

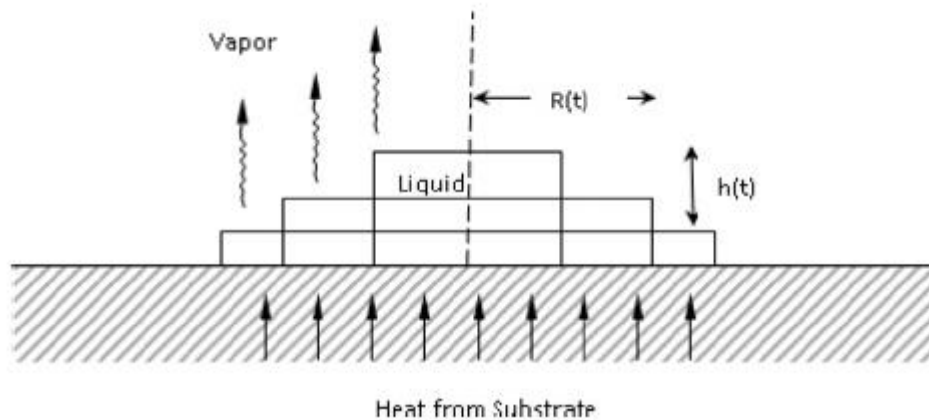


Figure 7.1. Box model used to indicate pool spreading behaviour.

(Omar et al. 2013; John and Pitblado 2010).

For LNG leak on the solid surface, a gravity-inertia is assumed to be the dominant momentum balance. The main driving force is gravity, which pushes the pool horizontally to spread the pool sideways and the friction resist the spread at the liquid bottom. This physical motion can be calculated by (Omar et al. 2013):

- Inertial forces = Gravitational forces - Friction

This can be written in an equation form as Equation (7.5).

$$\frac{\partial^2 r}{\partial t^2} = \frac{1}{\gamma} \cdot g \cdot \frac{h}{r} - C_F \quad (7.5)$$

Where

$R$  Pool radius

$\gamma$	Adjustment constant, 0.25 (Webber D.M, 1991)
$h$	Pool height, ( $= \frac{V}{\pi r^2}$ )
$C_F$	Friction
$T$	Time
$g$	Gravity (m/s <sup>2</sup> )

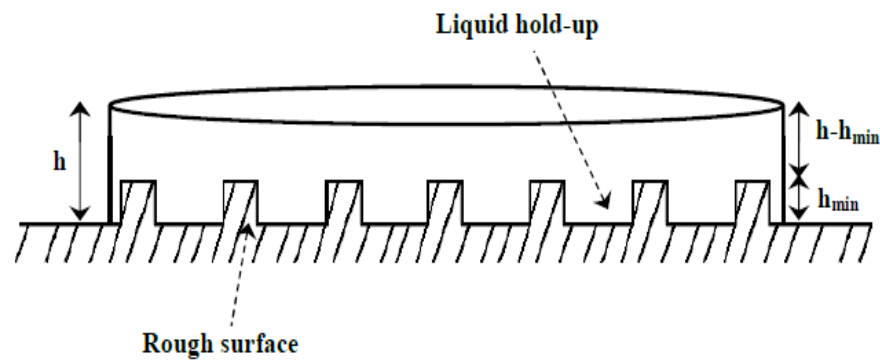


Figure 7.2. Schematic representation of a pool spreading on land.

The pool is modelled considering the minimum film of height,  $h_{min}$ , which is assumed to be equal to the average surface roughness length, as shown in Figure 7.2. Therefore, the pool spreading law is applied on the deck until the minimum height is reached as shown in Equation (7.6) (Briscoe and Shaw 1980);

$$\frac{dr}{dt} = \sqrt{\frac{1}{\gamma} \cdot g \cdot h - C_F \cdot t} \quad (7.6)$$

where

$$h = (h(t) - h_{min})$$

If  $h(t) < h_{min}$ , the pool shrinks and spreading law becomes :

$$\frac{dr}{dt} = -C_F \cdot t \quad (7.7)$$

The change in the radius and volume of the pool is calculated using the mass balance, which occupies the added LNG from the release source and

vaporized LNG at each time step. To update the pool volume,  $V$  and average pool height,  $h$ :

$$A_{pool} = \frac{m_{L\_leak}}{\rho_L \cdot h} \quad (7.8)$$

where

$m_{L\_leak}$  mass of leaked LNG

$$r_i = \sqrt{\frac{A_{pool\_i}}{\pi}} \quad (7.9)$$

$$r_i = r_{i-1} + \left(\frac{\partial r}{\partial t}\right) \cdot (t_i - t_{i-1}) \quad (7.10)$$

where

$r_i$  radius of LNG pool at time  $t_i$  (in m)

$r_{i-1}$  radius of LNG pool at time  $t_{i-1}$  (in m)

Therefore, the pool is calculated based on assumption that any case of the LNG pool height goes below the minimum height.

The mass of the LNG pool can be determined by adding the quantity leaked during a given time step while the evaporated mass in that time is subtracted. Therefore, the size of the LNG pool is determined by the interaction between two parameters: the quantity or the rate of LNG leak, and the rate of evaporation at any given time.

$$m_{L,i} = m_{L,i-1} + Q_{L\_leak} \cdot (t_i - t_{i-1}) - Q_{evp} \cdot (t_i - t_{i-1}) \quad (7.11)$$

where

$m_{L,i}$  : mass of LNG pool at time  $t_i$  (in kg)

$m_{L,i-1}$  : mass of LNG pool at time  $t_{i-1}$  (in kg)

### 7.2.2. Evaporation model

The vaporization rate of LNG is primarily related to the total heat transferred to the liquid. The spilled LNG forms a pool and the liquid is dominantly subjected to conductive heat transfer from the surface. Convection of surrounding air contributes to the vaporization of LNG to some degree as does solar radiation. However, heat transfer by convection from ambient air or radiation is not included in this analysis, as this is assumed negligibly small.

Conductive heat transfer with the surface is estimated to have the most significant contribution to the total heat transfer while the difference in temperature between the surface and the cryogenic liquid affects the heat conduction modes of film boiling or nucleate boiling.

#### (a) Heat conduction from solid substrate ( $Q_{cond\_1D}$ )

The heat transfer between the pool and the surface is modelled as a transient one-dimensional heat transfer process to estimate the physical behaviour of pool spreading and vaporising. The ground is assumed to be a semi-infinite solid in which the temperature will vary only in the vertical direction. Perfect thermal contact is assumed between the ground and the pool. Heat transfer from the deck surface to the cryogenic liquid pool can then be modelled using one-dimensional heat conduction (Carslaw et al. 1962; Basha et al. 2014).

For circular spreading pool, the heat flow rate in Watts is given by:

$$Q_{cond\_1D} = \frac{K_{deck} \cdot (T_{\infty} - T_b)}{\Delta H_v \cdot \sqrt{\pi \cdot \alpha_{deck} \cdot \Delta t}} \int_0^{r(t)} \frac{2\pi \cdot r' \cdot dr'}{(t - t')^{0.5}} \quad (7.12)$$

where

$Q_{cond\_1D}$	evaporation rate of the leaked LNG by conduction (in kg/s)
$K$	heat conductivity coefficient of deck (in J/mK)
$T_a$	temperature of surface material (in K)
$T_b$	temperature of LNG boiling point (in K)
$t$	current time (in s)

- $r'$  radius of the annular elements (in m)  
 $t'$  time of arrival of the pool at radius  $r'$  (in s)

This model also assumes that the temperature of ground surface is equal to that of the atmosphere.

Laboratory-scale experimental data obtained with LNG (Reid and Wang 1978) suggest that one-dimensional conduction equations can well represent heat transfer to diffusion pools for certain types of solids (Carslaw et al. 1962; Basha et al. 2013). However, the assumption of perfect contact between the two regimes limits the analysis of boiling behaviour of the LNG pool.

*(b) Heat Conduction from film boiling Method ( $Q_{cond\_film}$ )*

Due to the large temperature difference,  $\Delta T$ , between the liquid and the surface, it is more likely to lead to rapid boiling producing film or bubbles between the surface and the spilled LNG that hinders direct contact between the liquid and the solid surface creating thermal resistance. Depending on the temperature difference, the pool boiling can be classified into four different heat transfer regimes: convective, nucleate, transition, and film as shown in Figure 7.3.

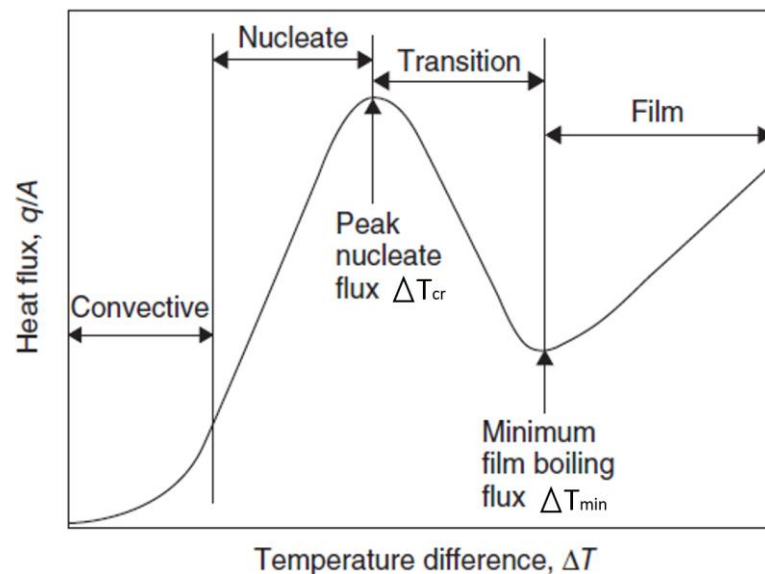




Figure 7.3. Heat flux versus excess temperature (Baumeister and Simon 1973; Basha et al. 2014)

- Nucleate boiling - two liquids are in direct contact and bubbles form at intervals
- Transitional boiling - part of the contact surface is in nucleate and part in film boiling
- Film boiling - two liquids are separated by a vapour film

Where

$\Delta T$  : temperature difference above the boiling point

$\Delta T_{cr}$  : temperature difference at peak nucleate flux

$\Delta T_{min}$  : temperature difference at minimum film boiling flux

Then, as illustrated in the figure, the heat flux increases as  $\Delta T$  increases if  $\Delta T < \Delta T_{cr}$ . The nucleate boiling is predicted to stop at a sufficiently high superheat temperature when the interaction of liquid and vapour prevents unrestricted supply of liquid to the heating surface. At this point, a maximum, or critical heat flux,  $q_{cr}$ , takes place at  $\Delta T_{cr}$ .

As the overheat further increases, the boiling becomes metastable and comes into a transient regime. At the point of  $\Delta T_{min}$ , the heat flux goes through minimum heat flux,  $q_{min}$ , which corresponds to the formation of a thin vapour film over the entire heating surface.  $q_{max}$  and  $q_{min}$  are given by Collier and Thome (1994).

$$q_{max} = q_{cr} = 0.16 \cdot \Delta H_v \cdot \rho_v^{\frac{1}{2}} \cdot [\sigma \cdot g \cdot (\rho_L - \rho_v)]^{\frac{1}{4}} \quad (7.13)$$

$$q_{min} = 0.18 \cdot K_v \cdot \Delta T_{min} \left[ \frac{g}{v_v \cdot \alpha_v} \left( \frac{\rho_L}{\rho_v} - 1 \right) \right]^{\frac{1}{3}} \quad (7.14)$$

Where

$v_v$  : specific volume of vapour

$\alpha_v$  : vapour thermal diffusivity

$K_v$  : vapour thermal conductivity

Correlations for the corresponding critical and minimum superheat,  $\Delta T_{min}$ , are provided by Klimenko (1981).

$$\Delta T_{cr} = 0.625(q_{max} \sigma \cdot T_L)^{\frac{1}{3}} \frac{\left[ \frac{10}{(\rho_w \cdot C_{pw} \cdot k_w)^{\frac{1}{2}}} + \sqrt{\frac{\nu}{k_L}} \right]^{\frac{2}{3}} \left[ 1 + 10 \left( \frac{\rho_L \cdot C_{pL} \cdot k_L}{\rho_w \cdot C_{pw} \cdot k_w} \right)^{\frac{1}{2}} \right]^{\frac{1}{3}}}{1 + 10 \left( \frac{\rho_{v,s}}{\rho_L - \rho_{v,s}} \right)^{\frac{2}{3}}} \quad (7.15)$$

Where

$\sigma$  interfacial tension (N/m<sup>2</sup>)

subscript  $L$  denotes LNG

subscript  $w$  denotes water

subscript  $s$  denotes surface

$$\Delta T_{Min} = (T_c - T_L) \cdot \left[ 0.16 + 0.24 \cdot \left( \frac{\rho_L \cdot C_{pL} \cdot k_L}{\rho_w \cdot C_{pw} \cdot k_w} \right)^{\frac{1}{4}} \right] \quad (7.16)$$

Where

$T_c$  Pseudo-critical temperature of LNG (190K)

These complicated phenomena make it difficult to predict the heat transfer process during boiling. However, considering the remarkably high temperature difference between the leaked LNG and the ground surface, the heat exchange is perceived dominantly taken place in the filming regime (above  $\Delta T_{min}$  in Figure 7.3) when a LNG leakage incident is encountered.

#### Heat transfer correlations for film boiling regime

Heat transfer correlations for film boiling as a function of a heat transfer coefficient for film boiling ( $h_{s\_film}$ ), the pool surface area and the temperature difference between the air ( $T_a$ ) and the pool ( $T_L$ ) are given by Klimenko (1981).

$$Q_{cond\_film} = \frac{h_{s\_film} \cdot A_{pool} \cdot (T_a - T_L)}{\Delta H_V} \quad (7.17)$$

Where

$Q_{cond\_film}$  : evaporation rate of the leaked LNG by film conduction

$h_{s\_film}$  : heat transfer coefficient for film boiling

$T_a$  : temperature of air

$T_L$  : temperature of LNG leak

In film region, the heat transfer coefficient of film boiling is expressed as a function of the Nusselt number,  $Nu_s$ , the thermal conductivity of the vapour film,  $\kappa_v$ , and the length-scale factor,  $L_c$ , as follows (Conrado and Vesovic 2000):

$$h_{s\_film} = \frac{N \cdot u_s \cdot \kappa_v}{L_c} \quad (7.18)$$

$$L_c = 2\pi \sqrt{\frac{\sigma}{g \cdot (\rho_L - \rho_v)}} \quad (7.19)$$

Where

in laminar region  $Ar < 10^8$ ,  $Nu_s = 0.19(Ar \cdot Pr)^{1/3} \cdot f_1$

in turbulent region  $Ar > 10^8$ ,  $Nu_s = 0.0086Ar^{1/2} \cdot Pr^{1/3} \cdot f_2$

$Ar$ : Archimedes number:  $(2\pi)^3 \frac{\sigma^{1.5} \cdot \rho_v}{\mu_v^2 \sqrt{g \cdot (\rho_L - \rho_v)}}$

$Pr$ : Prandtl number of vapour:  $\frac{C_{pv} \cdot \mu_v}{K_v}$

$f_1$  and  $f_2$  : dimensionless functions given by

$$\text{Laminar region: } \begin{cases} 1 & \text{for } \left( \frac{\Delta H_V}{C_{pL} \cdot \Delta T} \right) \leq 1.4 \\ 0.89 \cdot \left( \frac{\Delta H_V}{C_{pL} \cdot \Delta T} \right)^{\frac{1}{3}} & \text{for } \left( \frac{\Delta H_V}{C_{pL} \cdot \Delta T} \right) > 1.4 \end{cases}$$

$$\text{Turbulent region: } \begin{cases} 1 & \text{for } \left( \frac{\Delta H_V}{C_{pL} \cdot \Delta T} \right) \leq 2 \\ 0.71 \cdot \left( \frac{\Delta H_V}{C_{pL} \cdot \Delta T} \right)^{\frac{1}{2}} & \text{for } \left( \frac{\Delta H_V}{C_{pL} \cdot \Delta T} \right) > 2 \end{cases}$$

### Heat transfer correlations for transitional regime

The heat transfer coefficient in the transitional regime can be obtained by interpolating between the critical heat flux,  $q_{cr}$ , and the minimum heat flux,  $q_{min}$  as shown by Opschoor (1980).

$$h_{s\_trans} = \frac{[f \cdot q_{CHP} + (1-f) \cdot q_{min}]}{\Delta T} \quad (7.20)$$

The filter factor  $f$  is given by:

$$f = \left[ 1 - \frac{\Delta T - \Delta T_{cr}}{\Delta T_{min} - \Delta T_{cr}} \right]^7 \quad (7.21)$$

## 7.3. Jet fire model

The IQRA software calculates the length of jet fires using several semi-empirical models: Cook model (Cook et al. 1990), Mannan model (Lee 2012) and Spouge model (Spouge 1999), all of which are based on the fact that the characteristics and impact of jet fires depend on the fuel composition, release conditions and release rate. The studies carried out in this paper (as described in Chapters 8 to 11) have adopted the Cook model to estimate the impact of jet fire as it provides relatively conservative results than other models. The jet fire radius at each length point was calculated with API RP 521 flare model (Lee 2012). The emissive power of a jet fire ranges from 50 to 220kW/m<sup>2</sup> and the impact of fire radiation can be assumed to be critical on any personnel working within the predicted length of the fire (Tweeddale 1999).

According to the Cook model, the characteristics and impact of jet fires depends on the fuel composition and release rate.

$$L = 0.00326 \cdot [F_{dis} \cdot \Delta H_c]^{0.478} \quad (7.22)$$

Where

$F_{dis}$  : Mass discharge rate (kg/s)

$\Delta H_c$  : Heat of combustion (J/kg)

For alternative calculation, the Mannan model estimates flame length using the Equation (A.23).

$$L = 18.5 \cdot Q_{leak}^{0.41} \quad (7.23)$$

The Spouge model (Spouge 1999) uses the leak pressure and the diameter to calculate the jet fire length as described in the Equation (A.24).

$$L = 0.424 \cdot D_{mm}^{0.82} \cdot P_{bar}^{0.41} \quad (7.24)$$

Where

$D_{mm}$  : Leak diameter (mm)

$P_{bar}$  : Initial upstream pressure (bar)

A commonly accepted jet fire model is described below. This is based on the API RP 521 flare model. The relationships for jet fire length  $L$  and radius  $R_f$ , in meter, are

$$\left(\frac{R_f}{L}\right) = 0.0365 \cdot \left(\frac{s}{L}\right)^2 \cdot \ln\left(\frac{L}{s}\right) \quad (7.25)$$

Where

$s/L$  : Fractional distance along the plume length,  $0 \leq \left(\frac{L}{s}\right) \leq 1$

$R_f$  : Plume Radius (m)

## 7.4. Flash fire (dispersion model)

In order to estimate flash fire ranges, the IQRA software adopts Gaussian gas dispersion models by predicting dispersion effect and the gas concentration (Santamaria and Brana 1998). Regarding the selection of coefficients applying to the dispersion models, two different methods - Briggs coefficients (Briggs 1973) or Van Buijtenen coefficients (Santamaria and Brana 1998) - can be applied in this Software.

Gaussian models are used to predict downwind concentrations with a simple analytical expression that combines the release rate with atmospheric wind speed and graphically portrays sideways and vertical spread parameters that are determined by stability and downwind distance. In general form the Gaussian model can be expressed by the following simple equations:

### Plume Model

$$C(x,y,z;H_E)=\frac{Q_{\text{evp}}}{2\pi \cdot u_{\text{wind}} \cdot \sigma_y \cdot \sigma_z} \exp\left[-\frac{y^2}{2 \cdot \sigma_y^2}\right] \left\{ \exp\left[-\frac{(H_E-z)^2}{2 \cdot \sigma_z^2}\right] + \exp\left[-\frac{(H_E+z)^2}{2 \cdot \sigma_z^2}\right] \right\} \quad (7.26)$$

### Puff Model

$$C(x,y,z;t)=\frac{Q_{\text{evp}}^*}{\sqrt{2\pi^2} \sigma_x \cdot \sigma_y \cdot \sigma_z} \exp\left[-\frac{1}{2} \cdot \left(\frac{x-ut}{\sigma_x}\right)^2 + \frac{y^2}{\sigma_y^2}\right] \left\{ \exp\left[-\frac{(H_E-z)^2}{2 \cdot \sigma_z^2}\right] + \exp\left[-\frac{(H_E+z)^2}{2 \cdot \sigma_z^2}\right] \right\} \quad (7.27)$$

Where

$\sigma_y=ax^b$ ,  $\sigma_z=cx^d$  for Plume model

$\sigma_x=0.13x$ ,  $\sigma_y=0.5ax^b$ ,  $\sigma_z=cx^d$  for Puff model

The parameters  $\sigma_x$ ,  $\sigma_y$ ,  $\sigma_z$  can be obtained from semi-empirical formulae of Briggs and Van Buijtenen as shown in Table 7.1 and Table 7.2.

Table 7.1 Briggs sigmas.

Stability Class	$\sigma_y$	$\sigma_z$
A	$0.22 \cdot x \cdot (1+0.0001 \cdot x)^{-0.5}$	$0.20 \cdot x$
B	$0.16 \cdot x \cdot (1+0.0001 \cdot x)^{-0.5}$	$0.12 \cdot x$
C	$0.11 \cdot x \cdot (1+0.0001 \cdot x)^{-0.5}$	$0.08 \cdot x \cdot (1+0.0002 \cdot x)^{-0.5}$
D	$0.08 \cdot x \cdot (1+0.0001 \cdot x)^{-0.5}$	$0.06 \cdot x \cdot (1+0.0015 \cdot x)^{-0.5}$
E	$0.06 \cdot x \cdot (1+0.0001 \cdot x)^{-0.5}$	$0.03 \cdot x \cdot (1+0.0003 \cdot x)^{-1}$
F	$0.04 \cdot x \cdot (1+0.0001 \cdot x)^{-0.5}$	$0.016 \cdot x \cdot (1+0.0003 \cdot x)^{-1}$

Table 7.2 Van Buijtenen.

Stability Class	a	b	c	d
A	0.527	0.865	0.28	0.9
B	0.371	0.866	0.23	0.85
C	0.209	0.897	0.22	0.8
D	0.128	0.905	0.2	0.76
E	0.098	0.902	0.15	0.73
F	0.065	0.902	0.12	0.67

## 7.5. VCE model

The IQRA software estimates the magnitude of overpressure caused by explosion with three simplified empirical models: TNT equivalence model, TNO multi-energy, and Baker-Strehlow-Tang (BST) models

### 7.5.1. TNT equivalency explosion model

The TNT equivalency explosion model is the simplest method. With this model, the overpressure developed at specified distances can be calculated as shown in Equations (A.28 – A31) (Baker et al. 1973; Crowl and Louvar 2001). The total energy engaged in the VCE was initially converted into the equivalent mass of TNT by

$$m_{TNT} = \frac{m_{VEC} \cdot \eta \cdot \Delta H_{c\_mixture}}{\Delta H_{c(TNT)}} \quad (7.28)$$

where

$H_{c\_mixture}$	Heat of combustion for mixtures
$H$	Empirical explosion efficient (generally 1% ~ 10%)
$H_{c(gas)}$	Lower heat of combustion of gas (J/g)
$H_{c(TNT)}$	Heat of combustion of TNT (approx. 4,680 J/g)
$m_{TNT}$	Equivalent mass of TNT (kg)
$m_{VCE}$	Mass contributing to vapour cloud explosion (kg)

The total combustion energy of mixtures was calculated with

$$\Delta H_{c\_mixture} = \sum_{j=1}^K y_j \cdot h_j \quad (7.29)$$

Empirical explosion efficiency is generally set between 1 %~10 % based on experimental observations. The present study adopted 10 % in order to investigate the most stringent condition. The scaling parameter,  $Ze$ , can be calculated as

$$Ze = \frac{R_d}{m_{TNT}^{\frac{1}{3}}} \quad (7.30)$$

Where,

$R_d$  Distance from the ground zero point of VCE (m)

This parameter was then used to estimate the overpressure,  $P_s$

$$P_s = 573 \cdot Ze^{-1.685} \text{ (in KPa)} \quad (7.31)$$

Where,

$P_s$  Peak overpressure (Pa)



### 7.5.2. TNO multi-energy model

TNO multi-energy model is an alternative model and is simpler and more practical (Woodward and Pitbaldo 2010). Figure 7.4 shows ten curves that span the range of severities from mild deflagrations to detonations. Each curve is assigned an integer that indicates its severity. Thus, curve #1 represents mild deflagration and #10 stands for detonation. In most congested process plants, especially LNG liquefaction plants, TNO 7 is adopted. TNO 7 has a peak pressure of 1 bar(g).

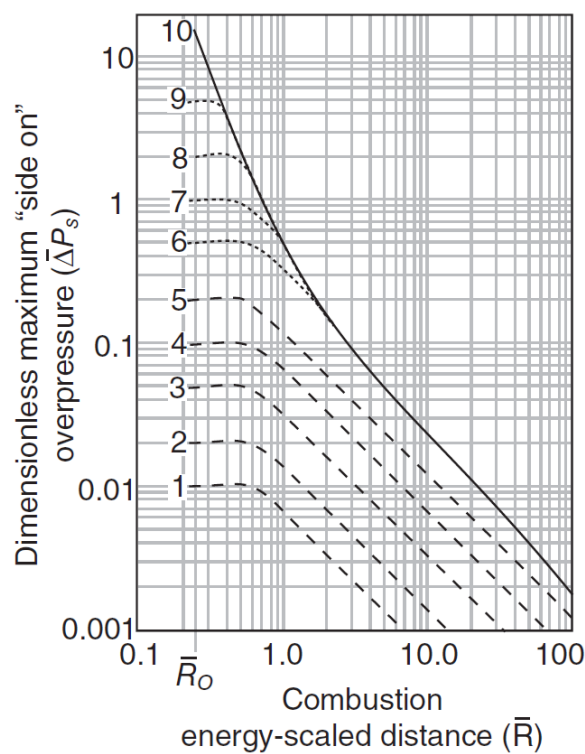


Figure 7.4. Normalised overpressure vs normalised distance for its use in TNO multi-energy model.

This model is increasingly acknowledged as a more reasonable alternative to TNT. The overpressure value can be calculated as (Alonso et al. 2006),

$$P_s = \bar{P}_s \cdot P_0 \quad (7.32)$$

Where,

$\bar{P}_s$  : non-dimensional peak overpressure

The non-dimensional peak pressure is obtained from

$$\bar{P}_s = \begin{cases} 1 & , 0.23 < \bar{R} < 0.5 \\ 4.06 \cdot 10^{-1} \bar{R}^{-1.2} & , 0.5 < \bar{R} < 100 \end{cases} \quad (7.33)$$

Here  $\bar{R}$  is the combustion energy scale distance, which is merely a convention to be readily converted to other forms of normalization.

$$\bar{R} = R_d \cdot \left( \frac{P_0}{E} \right)^{\frac{1}{3}} \quad (7.34)$$

### 7.5.3. Baker-Strehlow-Tang model (BST)

This model has some similarities with the TNO multi-energy model as it adopts the same equation (Equation 8.34) to obtain the combustion energy scale distance,  $\bar{R}$ . On the other hand, this method uses a function to construct the graphical relationship between dimensionless and combustion energy scaled distance.

The curves used in the BST model, shown in Figure 7.5, are based on numerical modelling of constant velocity flames and accelerating flames spreading through spherical vapour clouds.

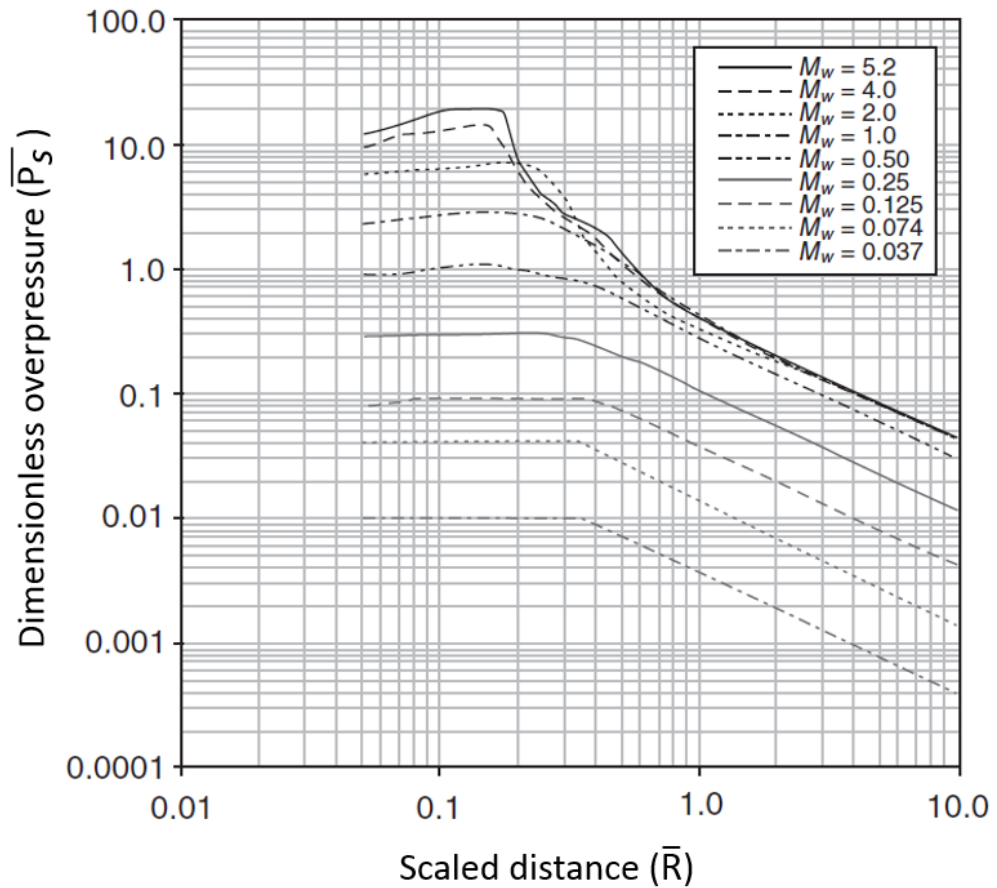


Figure 7.5. Dimensionless peak overpressure vs scaled distance for BST model (Melton and Marx 2009).

The ‘Mach number’,  $M_w$ , is determined by a combination of flame expansion dimension, fuel reactivity and obstacle density as shown in Table 7.3. Baker (Baker et al. 1994) suggested the fuel reactivity for methane to be categorised ‘low’ in Table 7.3. The recommended levels of obstacle density is given in the Table 7.5 (Melton and Marx 2009).

Table 7.3 Mach numbers (Mw) for BST model  
(Melton and Marx 2009).

Flame Expansion	Fuel Reactivity	Obstacle Density		
		Low	Medium	High
1 D	High	5.2	5.2	5.2
	Medium	1.03	1.77	2.27
	Low	0.294	1.03	2.27
2D	High	0.59	1.03	1.77
	Medium	0.47	0.66	1.6
	Low	0.079	0.47	0.66
2.5D	High	0.47	0.58	1.18
	Medium	0.29	0.55	1.0
	Low	0.053	0.35	<b>0.5</b>
3D	High	0.36	0.153	0.588
	Medium	0.11	0.44	0.5
	Low	0.026	0.23	0.34

Table 7.4 Fuel reactivity vs burning velocity (Melton and Marx 2009).

Fuel reactivity	Burning velocity	References
Low	$Sl \leq 0.4$ m/s	Methane
Medium	$0.4 \text{ m/s} < Sl < 0.75$ m/s	Propane
High	$Sl \geq 0.75$ m/s	Ethylene

Table 7.5 Obstacle density vs the volume blockage ratio (Melton and Marx 2009).

Obstacle density	volume blockage ratio (VBR)
Low	1.5%
Medium	4.3%
High	5.7%

## 7.6. Pool fire model

### (a) *Fire plume length ( $L_F$ )*

Based on the currently available experimental data and understanding of LNG pool fires, the following Equations 7.35 to 7.39 were accepted to

describe the LNG pool fire characteristics. The functional form used for this calculation is given below (Raj 2007):

$$\frac{L_F}{D} = A \cdot F^P \cdot (U^*)^q \quad (7.35)$$

Where,

$$F = \frac{G_b}{\rho_{air} \cdot \sqrt{g \cdot D}} = \text{Combustion Froude Number} = \text{Dimensionless burning rate}$$

$$U^* = \frac{U_{wind}}{\left[ \frac{G_b}{\rho_{air}} \cdot g \cdot D \right]^{\frac{1}{3}}} = \text{Dimensionless wind speed}$$

$L$  mean fire plume length of cylindrical shape fire column (in m)

$D$  equivalent diameter of the fire base (near circular) (in m)

$A$  constant obtained from test data

$P$  exponent (constant) on the Froude number developed from theory

$q$  exponent (constant) on the dimensionless wind, developed from theory

$G_b$  liquid mass burning flux (in kg/m<sup>2</sup>s)

$U_{wind}$  mean wind speed (in m/s)

$\rho_{air}$  density of air (in kg/m<sup>3</sup>s)

To estimate the burning flux, Equation (7.36), derived from the fire tests conducted by Mudan (1989), can be applied;

$$G_b = 10^{-3} \cdot \frac{\Delta H_c}{\Delta H_v^*} \quad (7.36)$$

Where,

$\Delta H_v^*$  modified heat of vaporization (in J/kg)

$\Delta H_C$  lower heat of combustion of the fuel (J/kg)

The equation uses the modified heat of vaporization,  $\Delta H_v^*$ , which represents the latent heat to warm the liquid to the boiling point plus the heat of evaporation.

$$\Delta H_v^* = \Delta H_v + \overline{C_{pL}} \cdot (T_b) \cdot \max\{0, T_b - T_L\} \quad (7.37)$$

Where,

$\overline{C_{pL}}$  average heat capacity of LNG (in J/kgK)

However, a mean value of 0.14 kg/m<sup>2</sup>s of burning flux is generally used (Nedelka et al. 1989) and this practice was adopted in this project. To estimate the average visible plume length with respect to the diameter of a fire using the Equations A.78 and A79.

$$\frac{L_F}{D} = 55 \cdot F^{2/3} \quad \text{for } U^* \leq 1 \quad (7.38)$$

$$\frac{L_F}{D} = 55 \cdot F^{2/3} \cdot (U^*)^{-0.21} \quad \text{for } U^* > 1 \quad (7.39)$$

(b) Soot mass yield (%)

The data for the mass fraction smoke yield ( $Y$  in %) versus fire diameter presented by these researchers can be correlated for crude oil fires as,

$$Y = 9.412 + 2.758 \cdot \log_{10}(D) \quad (7.40)$$

(c) Soot concentration

$$C_s = \rho_a \cdot Y \cdot \frac{1}{\left[ 1 + \frac{r}{\beta} + \frac{\Delta H_c}{C_a \cdot T_a} \right]} \quad (7.41)$$

Where

$\beta$  combustion efficiency factor (fraction of the mass of air entrained at any location that burns with its Stoichiometric equivalent mass of fuel) – assumed as a constant throughout the combustion zone -> 0.06 (Urbanski 2013)

$C_s$  mass concentration of smoke in the flame gases (in kg/m<sup>3</sup>)

$Y$  mass of smoke produced per unit mass of fuel burnt (in kg/kg)

$r$  stoichiometric air-to-fuel mass ratio for complete combustion, 17.17

(d) Soot production rate

$$Y = \frac{9.412 + 2.758 \cdot \log_{10}(D)}{100} \quad (7.42)$$

(e) Plume length of lower zone

$$\psi = \frac{L_c}{L} = 0.7 + 0.25 \cdot \log_{10}(F) \quad (7.43)$$

(f) Variation of emissive power

$$E_b = E_{\max} \cdot (1 - e^{-D/D_{opt}}), \quad \text{for } 0 \leq \frac{Z}{L} \leq \psi$$

$$E_s = E_b \cdot \left\{ p + (1 - p)e^{-(k_m C_s L_b)} \right\}, \quad \text{for } \psi \leq \frac{Z}{L} \leq 0 \quad (7.44)$$

Where

$D_{opt}$  optical Depth, 13.8m (Woodward and Pitblado, 2010)

$E_{\max}$  maximum emissive power (of the optically thick fire) (kW/m<sup>2</sup>)  
325kW/m<sup>2</sup> (Raj, 2007)

$E_b$  emissive power of the brightest part of the fire (near the base)

Only the case of  $0 \leq \frac{Z}{L} \leq \psi$  were considered in this project.

(g) Mean emissive power fraction

$$\frac{\bar{E}}{E_b} = \psi + \left\{ \frac{1 + 3 \cdot e^{-(k_m C_s L_b)}}{4} \right\} (1 - \psi) \quad (7.45)$$

*(h) Mean surface emissive power*

$$\bar{E} = E_b \cdot \left[ \psi + \left\{ \frac{1 + 3 \cdot e^{-(k_m C_s L_b)}}{4} \right\} (1 - \psi) \right] \quad (7.46)$$

Where,

$E_S$  emissive power of the smoke layer

$p(Z)$  probability of visibility of the inner fire at height Z,

$$p(\xi) = \left[ \frac{(1 - \xi)}{(1 - \psi)} \right]^3 \quad \text{for } \psi \leq \xi \leq 1$$

$k_m$  specific soot extinction area (assumed value 130) (m<sup>2</sup>/kg) (Mary Kay O'Connor Process Safety Center, 2008)

$L_b$  beam length, 0.63 D, for cylindrical fires (m)

$L_C$  axial length of the lower "bright" zone without smoke (m)

$\xi$  dimensionless length along fire plume axis = Z/L

*(i) Radiation effect*

Since a certain fraction of radiant energy towards the target point is absorbed by gases and droplets in the atmosphere, radiant heat is normally estimated using geometric view factors with weightings for emissivity. The radiant flux at the receiving point can be expressed as:

$$Q_{rad}(s) = E_{avg} \cdot F_{A_{fire} \rightarrow A_{obj}} \tau_{atm} \quad (7.47)$$

Where,

$Q_{rad}(s)$  radiant flux received on an object (kW/m<sup>2</sup>)

$E_{avg}$  mean SEP over the visible fire plume height (kW/m<sup>2</sup>)

$\tau_{atm}$  transmissivity of the atmosphere with RH (Relative Humidity)

$F_{A_{fire} \rightarrow A_{obj}}$  view factor

*(j) Atmospheric transmissivity*

At a distance of 100 m, the atmosphere can absorb or disperse about 20~40% of the radiated energy emitted by the fire. This is due to absorption by CO<sub>2</sub> and, above all, by the water vapour present in the atmosphere. The



atmospheric transmissivity is defined as the fraction of energy transmitted, and can be calculated approximately considering only the water vapour:

$$\tau_{\text{atm}} = 2.02 \cdot (P_{\text{w,sat}} s)^{-0.09} \quad (7.48)$$

where

$P_{\text{w,sat}}$  saturation vapour pressure of water (Pa)

$s$  the distance in meters between the emitting and receiving surfaces (m)

Also used in the above equation is a convenient approximation for the saturation vapour pressure of water with the air temperature in K and the vapour pressure in Pa.

$$P_{\text{w,sat}} = \exp \left[ 25.897 - \frac{5319.4}{T_a} \right] \quad (7.49)$$

#### (k) View factor

In the absence of absorption by the atmosphere, the radiation received by a surface outside the perimeter of a fire of known characteristics can be calculated once the geometric view factor  $F_{vg}$  is known. This can be done if the geometry of the fire and the receiving surface and their relative positions is known. Of special interest in this section are the view factors between a cylinder and the ground, summarised in Table 7.6 and Table 7.7 where the view factors for vertical and horizontal receiving surfaces, and the maximum radiation intensity, with an inclined surface are given (Hoftijzer 1979; Ramiro and Aisa 2012).

Table 7.6 View factor for a horizontal receiving surface (FH).

		a/b							
		0.1	0.2	0.5	1	2	5	10	20
c/b	1.1	0.132	0.242	0.332	0.354	0.36	0.362	0.363	0.363
	1.2	0.044	0.12	0.243	0.291	0.307	0.312	0.313	0.313
	1.5	0.005	0.024	0.097	0.17	0.212	0.228	0.231	0.232
	2	0.001	0.005	0.027	0.073	0.126	0.158	0.164	0.166
	4	0.000	0.000	0.001	0.007	0.022	0.057	0.073	0.078
	10	0.000	0.000	0.000	0.000	0.001	0.007	0.017	0.026
	20	0.000	0.000	0.000	0.000	0.000	0.001	0.003	0.008

Note:

a= pool fire flame height

b= radius of pool fire

c=distance between the centre of pool fire and receiving surface

Table 7.7 View factor for a vertical receiving surface (FV).

		a/b							
		0.1	0.2	0.5	1	2	5	10	20
c/b	1.1	0.33	0.415	0.449	0.453	0.454	0.454	0.454	0.454
	1.2	0.196	0.308	0.397	0.413	0.416	0.416	0.416	0.416
	1.5	0.071	0.135	0.253	0.312	0.329	0.333	0.333	0.333
	2	0.028	0.056	0.126	0.194	0.236	0.248	0.249	0.249
	4	0.005	0.01	0.024	0.047	0.08	0.115	0.123	0.124
	10	0.000	0.001	0.003	0.006	0.013	0.029	0.042	0.048
	20	0.000	0.000	0.000	0.001	0.003	0.007	0.014	0.02

## 8. ON-BOARD SAFETY EXCLUSION ZONE FOR LNG BUNKERING

### 8.1. Introduction

The purpose of this study was to identify the potential risks of LNG bunkering and to devise a statistical method for determining the safe exclusion zone around LNG bunkering station on board the ships with the help of IQRA software. A probabilistic risk assessment approach was adopted in this study to determine the safety exclusion zone for two case ships: one, a 300,000 DWT very large ore carrier (VLOC) and the other a 32,000 DWT bulk carrier. Only the population-independent assessment was carried out in this study, primarily because the personnel on board can be more easily controlled in such a way that all but the essential personnel can be kept out of the potential harm's way. The results can then be compared with those obtained by a deterministic approach.

### 8.2. Case ships

In order to investigate rational safety exclusion zones required for LNG bunkering, two cargo ships of contrasting sizes were selected: a 300,000 DWT VLOC (referred to as Case Ship 1 hereafter) and a 32,000 DWT bulk carrier (referred to as Case Ship 2). These ships are presently the subject of 'LNG-Ready Ships', a joint project of Korean Register (KR), Hyundai Heavy Industries Co. Ltd and Hyundai Mipo Heavy Industries Co. Ltd. The main engines were modified to use dual fuel and the LNG fuel system was designed in accordance with the IGF Code, class rules and other relevant guidelines currently in force in cooperation with KR. Table 8.1 summarises general specifications and operational profiles of the case ships.

Table 8.1 General specifications of the case ships (by courtesy of Korea Register of Shipping).

	Specifications	
	300K DWT VLOC (Case Ship 1)	32K DWT bulk carrier (Case Ship 2)
		
<b>L x B x D</b>	328.0 m x 55.0 m x 29.0 m	168.5 m x 28.4 m x 14.25 m
<b>Main engine</b>	Hyundai MAN B&W 6G80ME-GI-C9	MAN B&W 6S40ME-GI
<b>MCR/NCR<sup>5</sup></b>	20,680 kW x 65.8 rpm/17,578 kW x 62.3 rpm	6,480kW x 139 rpm/5,832 x 134.2 rpm
<b>LNG consumption</b>	Abt. 67 tonnes/day	Abt. 19.8 tonnes/day
<b>Cruising range</b>	Abt. 25,000 miles per one voyage from Brazil to East Asia	Abt. 600 miles per one voyage from Donghae to Gwangyang South Korea
<b>LNG fuel tank</b>	11,000 m <sup>3</sup> (IMO B type)	125 m <sup>3</sup> (IMO C type)

Case Ship 1 is a typical ocean-going cargo ship engaged in international service routes, such as between Brazil and East Asia. The proposed nominal continuous rating (NCR) of the engine is 17,578 kW during service and LNG consumption is expected to be about 67 metric tonnes daily. This corresponds to the specific gas consumption (SGC) at NCR of 128.8 g/kWh (KR 2015a). The return voyage of the ship on the intended route will take approximately 70 days. Therefore, bunkering needs to be carried out roughly every 70 days, making the LNG fuel storage tank capacity to be 11,000 m<sup>3</sup>.

Case Ship 2 is engaged in a domestic service between Donghae and Gwangyang in South Korea. The fuel consumption is estimated to be 19.8 metric tonnes daily corresponding to the SGC at NCR of 142.1 g/kWh (KR 2016). According to the voyage profile given, this ship has a voyage cycle of 102 hours spending about 42 hours at sea and about 60 hours in port. The capacity of the LNG fuel tank was proposed to be 125 m<sup>3</sup>, and therefore LNG bunkering needs to take place every voyage, approximately 84 times annually.

The Case Ships 1 and 2 represent generic large and small ships – they are realistic enough but do not represent case-specific ships. In this context, bunkering of

<sup>5</sup> Maximum continuous rating/nominal continuous rating (85% of MCR)

Case Ship 1 can be characterised as ‘infrequent large scale’, while Case Ship 2 can be said to require ‘frequent small scale’ bunkering.

### 8.3. Fuel system design

The basic features of the LNG fuel systems and LNG bunkering systems were designed in accordance with the engine maker’s specifications and the operational profile of the case ships.

#### 8.3.1. Case Ship 1

It was agreed by all parties concerned that the best arrangement was to transform No.4 Cargo Hold into a space for LNG fuel systems, comprising an LNG fuel storage tank, a tank connection space and a fuel preparation room.

As described in Chapter 4, the bunkering stations are arranged on freeboard deck between No.3 and the erstwhile No.4 Cargo Holds port and starboard. A ship-to-ship bunkering is considered to be the most likely for the time being.

Figure 8.1 shows an outline piping diagram of the LNG bunkering system designed for this study. Fundamentally it consists of three lines similar to LNG cargo transfer systems: main line for LNG bunkering, vapour return line and N<sub>2</sub> inert line. In compliance with the LNG bunkering guidelines, emergency shut-down (ESD) valves are to be fitted to both main line and vapour return line. In addition, emergency release couplings (ERC) are to be fitted to the flange connections on the feeder side (ISO 2015c).

The pipes of the system are designed to be 250 mm in diameter and the length of piping required on each side is estimated to be 30 m, taking into account the ship’s beam. In order to keep the vapour return to a manageable proportion the maximum fluid velocity was assumed to be 5 m/s. This gives

the time required to fill up an empty LNG storage tank (11,000 m<sup>3</sup>) of 13 hours. Since bunkering is required about 5 times a year, the total annual bunkering time will be 65 hours.

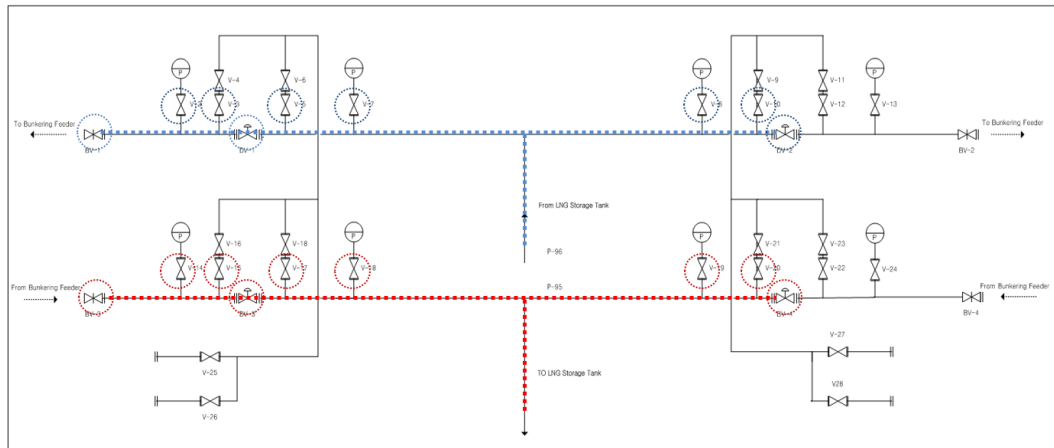


Figure 8.1. Outline bunkering system designed for Case Ship 1.

### 8.3.2. Case Ship 2

The conceptual LNG fuel piping system and its arrangement devised for the Case Ship 2 is outlined in Figure 8.2. The size of the storage tank is 125 m<sup>3</sup>, which makes it small enough to be installed on deck, in an open space behind the accommodation block. The bunkering system is placed port and starboard near the tank as shown in the illustration. Bunkering is likely to rely on tank lorries for the time being.

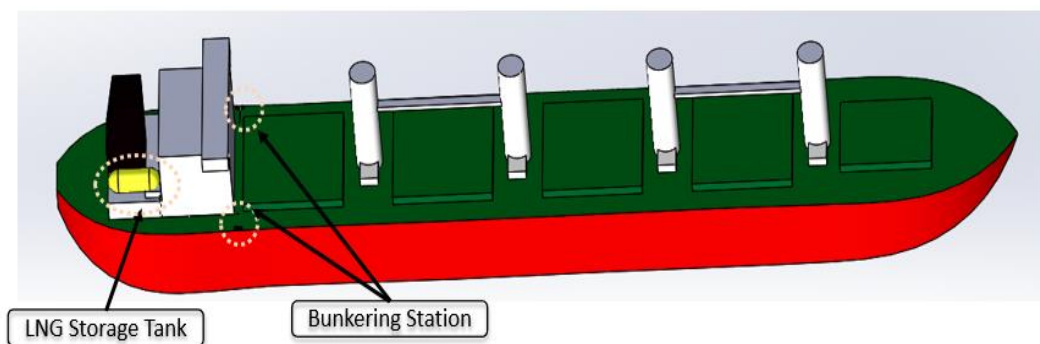


Figure 8.2. Arrangement of the LNG fuel systems for Case ship 2.

Figure 8.3 shows a piping diagram of the bunkering system designed for Case Ship 2. As for Case Ship 1, N<sub>2</sub> inert line is assumed to be provided on board. Since the bunkering method used is not ship-to-ship and the system size is small, ERC is not required, nor needed.

The proposed size of the pipes in the LNG bunkering system is 25 mm in diameter and the length of piping on each side is estimated to be 45 m. Since the IMO C type tank can contain the generated vapour inside the tank during bunkering, the vapour is not returned to the feeder side. For this reason, an appropriate fluid velocity of 8 m/s is assumed, making the time to fill up the initially empty storage tank about 9 hours each time and about 773 hours per year.

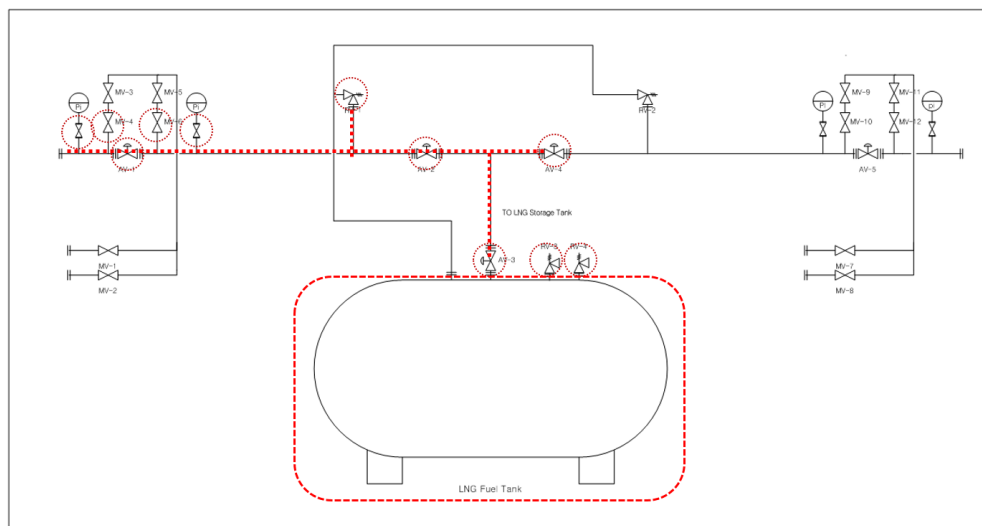


Figure 8.3. Outline design of bunkering system for Case ship 2.

The components included in the conceptual design of bunkering systems illustrated in Figure 8.1 and Figure 8.3 are listed in Table 8.2. The parts of Case Ship 1 located in a segregated space are excluded from this list. The equipment and the pipes involved in bunkering on each side are marked with dotted circles and lines in the figures.

Table 8.2 List of components in bunkering systems.

Case	No.	Equipment	Size	Quantity	
				Main liquid	Vapour return
Case ship 1	1	ESD valves	250mm	2	2
	2	ERC	250mm	1	1
	3	Flanges for main line	250mm	3	3
	4	Flanges for inert line	100mm	3	3
	5	Manual valves	250mm	2	2
	6	Pipes	250mm	30 m	30 m
	7	Pressure indicators	12.5mm	3	3
Case ship 2	1	ESD valve	25mm	1	Not applicable
	2	Flanges for main line	25mm	12	
	3	Flanges for inert line	12.5mm	2	
	4	LNG fuel tank	25mm	1	
	5	Manual valves	12.5mm	2	
	6	Pressure indicators	12.5mm	2	
	7	Pressure relief valves	25mm	3	
	8	Process pipes	25mm	45 m	
	9	Remote valves (excluding ESD valve)	25mm	3	

An accidental release of the fuel is the main danger associated with LNG bunkering. It is reasonable to consider that only the LNG main liquid line and the vapour return line are subject to risk of the fuel leak, since the N<sub>2</sub> inert line is not directly involved in LNG transfer. The two lines, however, are under different working conditions, and so they were separated into two groups in this study: one for main liquid system and the other for vapour return system. The working pressure for the main liquid line (hereafter referred to as Group 1) was assumed to be 3 bar(g) while that of the vapour return (hereafter referred to as Group 2) was assumed to be 1 bar(g) for both case ships. The working temperature of LNG flowing through the main line was assumed to be 112 K whereas that of the vapour return was set to be 123 K (DNV 2012b). It is reiterated here that Case Ship 2 does not require a vapour return line.



## 8.4. Risk assessment

### 8.4.1. Frequency analysis

Figure 8.4 illustrates the results obtained from IQRA. For Case Ship 1, Groups 1 and 2 are identical and consequently the initial fuel leak frequency is also the same. On the other hand, Case Ship 2 appears to have a higher leak frequency compared to Case Ship 1 due to the higher frequency of bunkering. It also shows that the occurrence of small leakage holes is more frequent than larger ones in both cases.

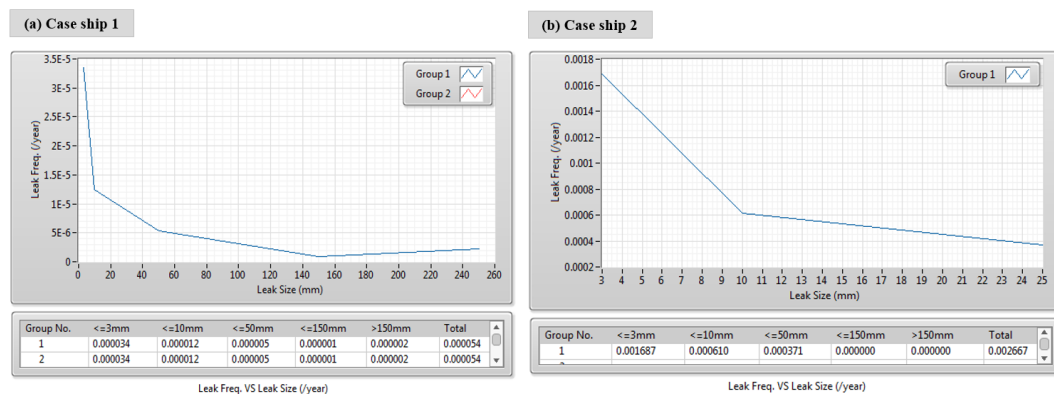


Figure 8.4. Leak frequency of proposed LNG bunkering systems.

A ‘late isolated leak’ scenario discussed in section 7.2.1 and Figure 7.5 was defined as an isolation action not taken immediately (with probability of 0.1) (Kletz 1991). In this study the maximum time to recognise and isolate the leak ‘immediately’ was taken to be 10 seconds, and thus a ‘limited leak’ with less than 10 seconds duration was assumed not to constitute an ‘accident’. DNVGL (DNV 2012a), for example, uses 30 seconds to define limited leaks, and therefore the 10 seconds criterion used in this study is much more conservative than that.

Safety measures are provided to ensure that, as long as they work effectively, all target accidents can be either prevented or contained with no serious consequence. For LNG bunkering in an open space, watch-keeping is the only practical safety measure that can be provided (since gas detectors will

be ineffectual in such circumstances), and therefore the scenario of ‘limited fuel leak’ represents the situation in which the watch-keeper takes an appropriate action immediately to stop the leak. This means that we can assume 90 % of initial liquid fuel leak does not lead to an ‘accident’ as the leak can be contained to a ‘limited leak’ which poses no danger associated with fire or explosion.

According to the IGF Code, Classification rules, ISO standards and other guidelines associated with LNG bunkering, in an unconfined space no mechanical ventilation is required. Therefore, there is no probability of the ventilation failing. In this particular instance, given the fact that on-board LNG bunkering stations are situated in an open deck, albeit with some structures in the vicinity, the space can be considered unconfined.

Surrounding condition, whether congested or open, is another important factor as it determines types of final accidents: fire or explosion. The usual structures near on-board bunkering stations include hatch coamings and covers, other pipes, cranes and so on with large variations between ships. However it is reasonable to consider that the surrounding conditions are generally closer to ‘open’ than ‘congested’. After some discussion with ship designers and a classification society (Korean Register), it was concluded that 20 % of occupancy ratio appears reasonable. Nevertheless, it was decided to investigate how much this factor affects the final outcome by using 10 % and 50 % in addition to the 20 % in a sensitivity analysis.

Figure 8.5 shows an event tree analysis (ETA) for a 3mm initial leak for Group 1 of the Case Ship 1 with the frequencies of the final outcomes.

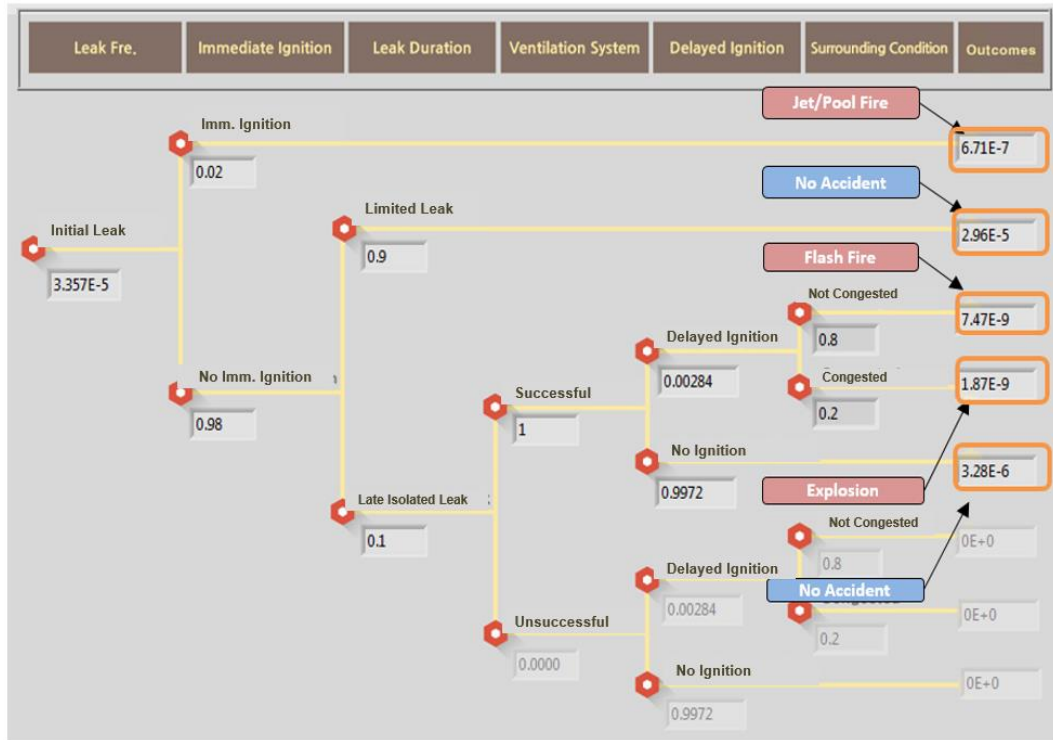


Figure 8.5. An event tree for 3mm leak hole from LNG bunkering main system for Case Ship 1.

Several models of ignition probability have so far been developed by various authors. For immediate ignition the Dutch model (DNV 2012b) was used, while for delayed ignition the Cox model (Cox et al. 1990) was used, as these models produce higher ignition probabilities than other models. The probability of immediate ignition according to the Dutch model is shown in Table 8.3 and the Cox model for delayed ignition is given by Equation (8.1).

Table 8.3 Probability of Immediate Ignition (DNV, 2012b).

Leak Rate ( $Q_{leak}$ )	Immediate ignition probability
< 10 kg/s	0.02
10 ~ 100 kg/s	0.04
> 100kg/s	0.09

$$PR_{DI} = 0.0158 \cdot Q_{LR}^{0.6415} \quad (8.1)$$

Where

$PR_{DI}$  the probability of delayed ignition

$Q_{LR}$  the leak rate (kg/s)

### 8.4.2. Consequence analysis

Using the methods discussed in Section 5.4.2, the leak rates with respect to various hole sizes are estimated in Table 8.4.

Table 8.4 Leak rates for various leak hole sizes (unit: kg/s).

Case	Group	Leak hole size				
		3mm	10mm	50mm	150mm	>150mm
Case Ship 1	1	0.0688	0.7647	19.1	172.0	477.9
	2	0.016	0.0177	0.442	3.978	11.05
Case Ship 2	1	0.688	0.7647	4.791	-	-

Fire/explosion is likely to generate a significant amount of thermal radiation or overpressure which poses danger to humans. The magnitude of radiation and overpressure is the highest at the ignition point and decreases as the distance from the origin increases. The safety guidelines from the Centre for Chemical Process Safety (CCPS) (Freeman 1990) define critical thermal radiation at  $37.5 \text{ kW/m}^2$  and critical overpressure at 1 bar(g), representing values exposure to which causes 100 % fatality to a person. Based on this, the case study analyses critical distances using the safety parameters of radiation and overpressure. The critical distance for jet fire and flash fire was determined as discussed in Section 7.2.3 (b) of this thesis. For producing a generic understanding, a neutral weather condition with a wind speed of 5 m/s was assumed (DNV 2012b). Note that less than 100 % fatality does not imply absolute safety. This point is discussed later in this paper.

An example of critical distance of each consequence with respect to each representative leak hole size is shown in Figure 8.6. These results confirm that the impact of consequences has a direct correlation with leak rate of the fuel, and that the critical distance determined purely by the impact of

accidents is, not surprisingly, much more extensive for a large scale LNG bunkering operation than a smaller one.

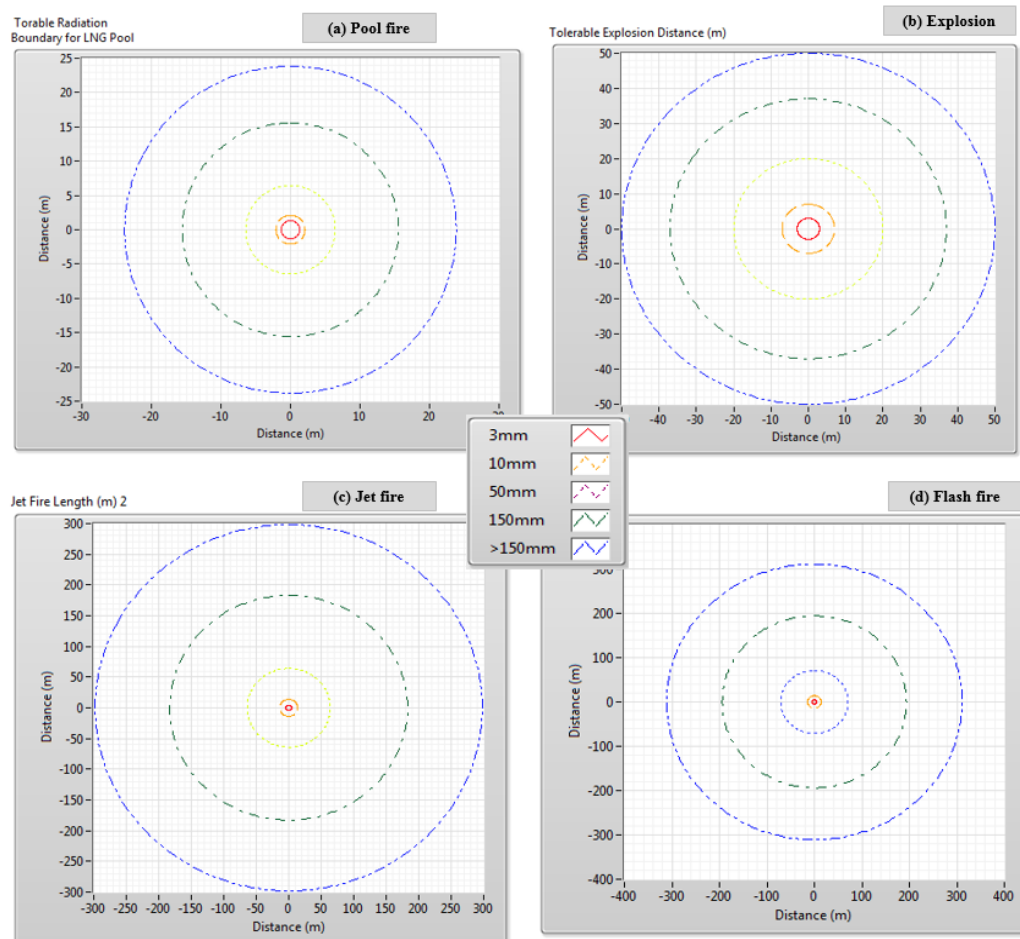


Figure 8.6. Example of critical distance for Group 1 for Case Ship 1.

### 8.4.3. Assessment results

Risk is defined as the product of the probability of occurrence of an accident and its consequence which is usually expressed in terms of lives lost and injuries caused or financial losses suffered. However, the current case is independent of demographical conditions, and another relevant factor has to be found for establishing the safety exclusion zone. In this study it was decided to use the risk acceptance criteria (acceptable accident rate) for this purpose. Since there is no agreed probabilistic risk criteria available for LNG bunkering at present, the most stringent criterion, i.e. the Dutch risk

criterion (DNV 2012b) (frequency limit of  $1.0E-6$ /year), was applied to estimate the ‘tolerably safe’ zones for LNG bunkering stations.

The numerical results of frequency and consequence analyses are brought together as listed in Table 8.5. The population-independent derivation of the critical distances and setting up of various zones have been discussed in 7.2.3 (a). From this, the critical distance furthest from the bunkering station with the frequency higher than the acceptable limit can be taken as the safety exclusion zone. The results are shown in Figure 8.7 for Case Ship 1 and Figure 8.8 for Case Ship 2. The minimum distances with less than the frequency limit are 6.4 m for Case Ship 1 and 36 m for Case Ship 2. Therefore, the minimum safety exclusion zone is Zone 2 (5-15 m) for Case Ship 1, and Zone 4 (25-50 m) for Case Ship 2. This result does imply that the size of safety zone appears to be more likely determined by bunkering frequency rather than the amount of LNG transferred.

It is to be noted that the safety exclusion zone for Case Ship 2 includes accommodation areas which must be protected from any hazards. Consequently, it may be necessary to rearrange the bunkering systems away from this area. Alternatively, the safety exclusion zone can be made smaller by enhancing the safety system, such as using double walled piping.

Table 8.5 Numerical result of frequency and consequence analysis.

Case	Line	Hole Size	Initial Leak Freq.	Fire Type	Imm. Ignition	Leak Duration (Late isolation)	Del. Ignition	Surrounding Condition (Congestion ratio)	Ignition Probability	Consequence (distance, m)	
Case Ship 1	Main Line - Group 1	3mm	3.36E-05	Pool Fire	0.02				6.71E-07	1.3	
				Flash Fire	0.98	0.1	0.00284	0.8	7.47E-09	5	
				Explosion	0.98	0.1	0.00284	0.2	1.87E-09	3	
		10mm	1.24E-05	Pool Fire	0.02					2.48E-07	2.1
				Flash Fire	0.98	0.1	0.0133	0.8	1.29E-08	14	
				Explosion	0.98	0.1	0.0133	0.2	3.24E-09	7	
		50mm	5.41E-06	Pool Fire	0.04					2.16E-07	6.4
				Flash Fire	0.96	0.1	0.105	0.8	4.36E-08	71	
				Explosion	0.96	0.1	0.105	0.2	1.09E-08	20	
		150mm	8.76E-07	Pool Fire	0.09					7.88E-08	15.6
				Flash Fire	0.91	0.1	0.429	0.8	2.73E-08	194	
				Explosion	0.91	0.1	0.429	0.2	6.84E-09	37	
	Full (250mm)	2.20E-06	Pool Fire	0.09					1.98E-07	23.8	
			Flash Fire	0.91	0.1	0.827	0.8	1.32E-07	311		
			Explosion	0.91	0.1	0.827	0.2	3.31E-08	50		
	Vapour Return Line - Group 2	3mm	3.36E-05	Jet Fire	0.02					6.71E-07	0.7
				Flash Fire	0.98	0.1	0.000253	0.8	6.66E-10	1	
				Explosion	0.98	0.1	0.000253	0.2	1.66E-10	1	
		10mm	1.24E-05	Jet Fire	0.02					2.48E-07	2.3
				Flash Fire	0.98	0.1	0.00119	0.8	1.16E-09	3	
				Explosion	0.98	0.1	0.00119	0.2	2.89E-10	3	
		50mm	5.41E-06	Jet Fire	0.02					1.08E-07	10.6
				Flash Fire	0.98	0.1	0.00936	0.8	3.97E-09	14	
				Explosion	0.98	0.1	0.00936	0.2	9.92E-10	7	
150mm		8.76E-07	Jet Fire	0.02					1.75E-08	30.2	
			Flash Fire	0.98	0.1	0.0383	0.8	2.63E-09	41		
			Explosion	0.98	0.1	0.0383	0.2	6.57E-10	14		
Full (250mm)	2.20E-06	Jet Fire	0.04					8.78E-08	49.2		
		Flash Fire	0.96	0.1	0.0738	0.8	1.24E-08	69			
		Explosion	0.96	0.1	0.0738	0.2	3.11E-09	19			
Case Ship 2	Main Line - Group 1	3mm	1.69E-03	Pool Fire	0.02				3.37E-05	1.3	
				Flash Fire	0.98	0.1	0.00284	0.8	3.76E-07	5	
				Explosion	0.98	0.1	0.00284	0.2	9.39E-08	3	
		10mm	6.10E-04	Pool Fire	0.02					1.22E-05	2.1
				Flash Fire	0.98	0.1	0.0133	0.8	6.36E-07	14	
				Explosion	0.98	0.1	0.0133	0.2	1.59E-07	7	
		Full (25mm)	3.71E-04	Pool Fire	0.02					7.41E-06	3.8
				Flash Fire	0.98	0.1	0.0431	0.8	1.25E-06	36	
				Explosion	0.98	0.1	0.0431	0.2	3.13E-07	13	

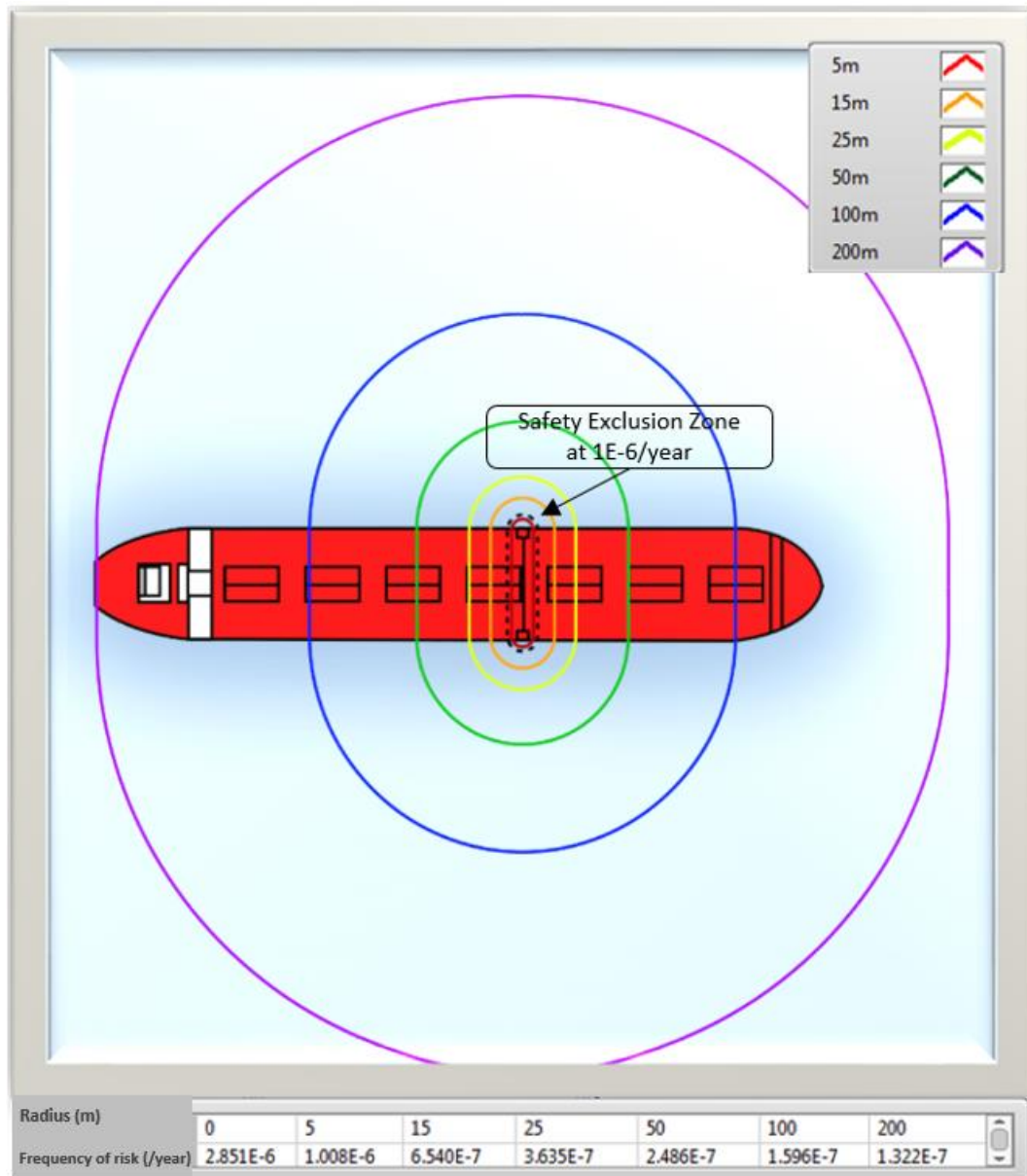


Figure 8.7 Risk level of safety exclusion zones for Case Ship 1.



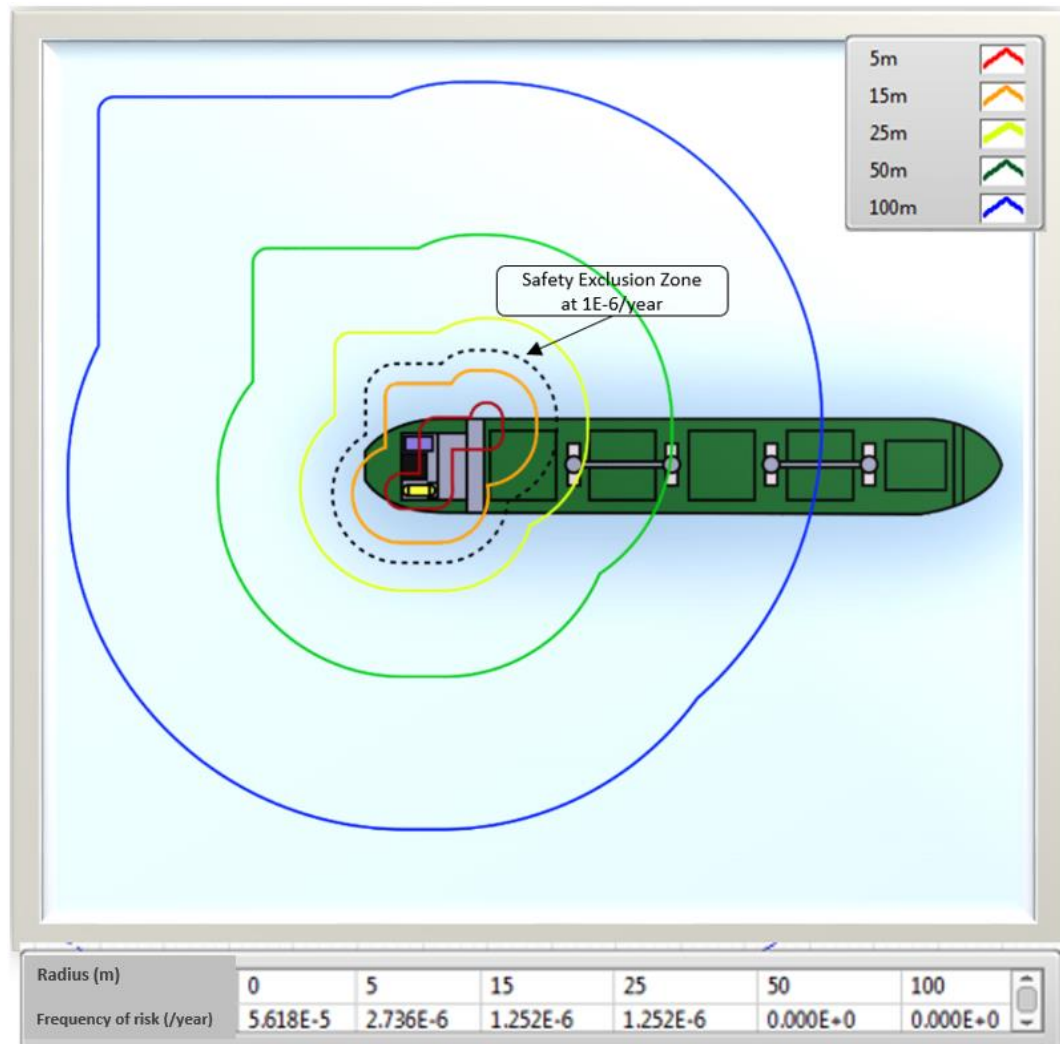


Figure 8.8 Risk level of safety exclusion zones for Case Ship 2.

In order to evaluate the critical distance for pool fire and explosion, the original study was conducted based on the degree of radiation and overpressure corresponding to 100% fatalities as the criterion. However, there still may be dangers outside the minimum safety exclusion zone with perhaps less than 100% fatality. For this reason, two additional cases of 50% fatality and 10% fatality as the criterion were also investigated. For radiation,  $12.5 \text{ kW/m}^2$  and  $5 \text{ kW/m}^2$ , and for overpressure, 0.3 bar(g) and 0.1 bar(g) are used for 50% and 10% fatalities, respectively (Freeman 1990; OGP 2010b).

Table 8.6 and Figure 8.9 show the analysis result of alternative cases. The regions shaded with red in the table refer to the safety exclusion zones while

the regions with green refer to the acceptable zones. In the figure, the horizontal line represents the limit of accident rate (1.0E-6/year) and the accident rates corresponding to each distance are drawn on the figure. It is observed that the application of the lower probability of fatalities resulted in the same safety exclusion zone despite slightly increased probability for both ships.

Table 8.6 Risk level of safety exclusion zones with respect to probability of fatalities (unit: /year).

Case Ship	Case	Distance (m)							
		Zone 1	Zone 2	Zone 3	Zone 4	Zone 5	Zone 6		
		0m	5m	15m	25m	50m	100m	200m	
Case Ship 1	Original Case (100% fatalities)	2.85E-06	1.01E-06	6.54E-07	3.63E-07	2.49E-07	1.60E-07	1.32E-07	
	Case 1	50% fatalities	2.85E-06	1.01E-06	6.59E-07	5.76E-07	2.66E-07	1.93E-07	1.32E-07
		Difference	0.00%	0.00%	0.76%	58.68%	6.83%	20.63%	0.00%
	Case 2	10% fatalities	2.85E-06	1.01E-06	6.61E-07	5.80E-07	2.70E-07	2.13E-07	1.72E-07
		Difference	0.00%	0.00%	1.07%	59.78%	8.43%	33.13%	30.30%
	Case Ship 2	Original Case (100% fatalities)	5.62E-05	2.74E-06	1.25E-06	1.25E-06	0.00E+00	0.00E+00	0.00E+00
Case 1		50% fatalities	5.62E-05	2.83E-06	1.72E-06	1.57E-06	0.00E+00	0.00E+00	0.00E+00
		Difference	0.00%	3.28%	37.60%	25.60%	-	-	-
Case 2		10% fatalities	5.62E-05	2.83E-06	1.82E-06	1.72E-06	3.13E-07	0.00E+00	0.00E+00
		Difference	0.00%	3.28%	45.60%	37.60%	-	-	-

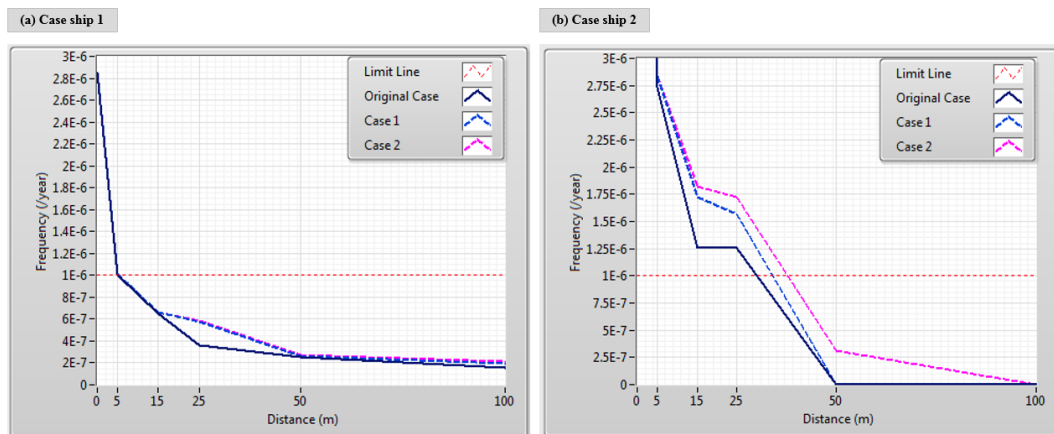


Figure 8.9 Risk level of safety exclusion zones with respect to probability of fatalities.

## 8.5. Sensitivity/parametric analysis

### 8.5.1. Sensitivity analysis for different data usage

Since the history of LNG-fuelled ships is too short for any meaningful statistics to be compiled, this case study has relied upon DNV equipment failure frequency database that contains appropriate generic data associated with LNG process equipment in offshore and chemical industries. This generic approach may cause some uncertainties in the results of frequency in a quantitative sense. In this context, a sensitivity analysis was carried out to investigate the effects of using a different data source. For this purpose, OGP hydrocarbon equipment failure frequency database (OGP 2010a) was used and the results are compared with the original results from using the DNV source.

In addition, throughout the quantitative risk assessment for LNG bunkering, several parameters were uncertain and/or assumed. One of them was leak duration and it was thought to be important to establish how this parameter would influence the overall results. For this purpose, another scenario of delayed recognition and isolation time of 1,000 seconds combined with the failure of proper watch-keeping added using the probability of delayed isolation proposed by Kletz (Kletz 1991). To analyse the alternative scenario, a modified event tree was constructed as shown in Figure 8.10.

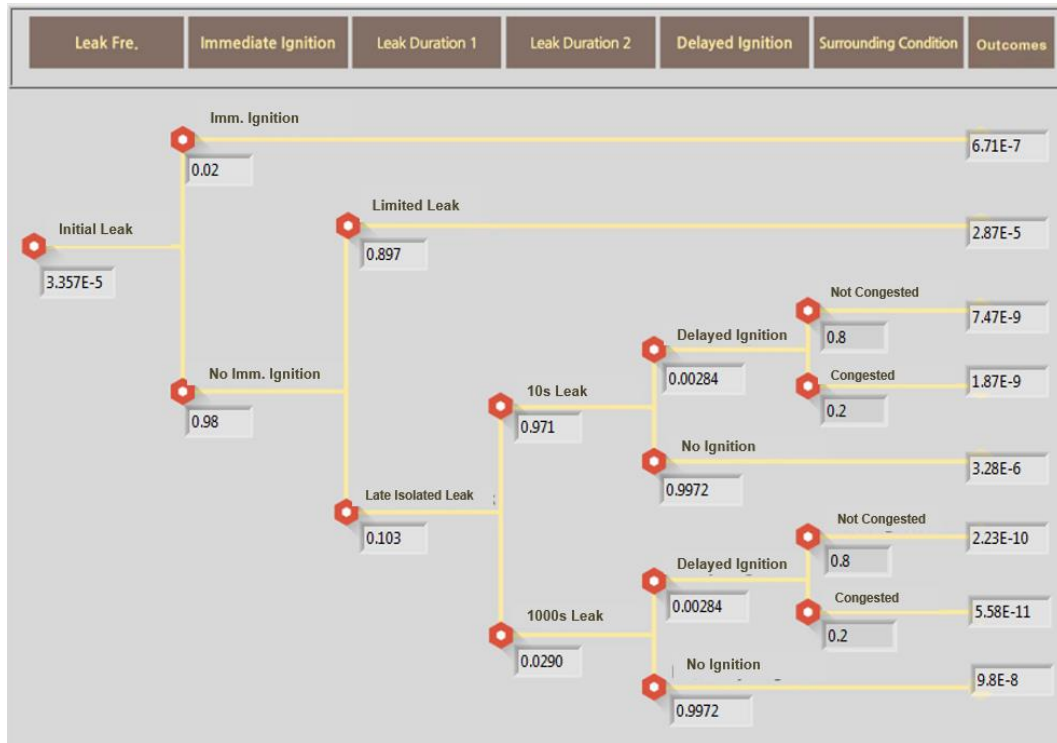


Figure 8.10. A modified event tree for 3mm leak hole from LNG bunkering main system for Case Ship 1.

Table 8.7 and Figure 8.11 show the result of the sensitivity analysis. In the case of 10-second leak duration for Case Ship 1, the OGP database reduces the minimum safety exclusion zone from Zone 2 to Zone 1 and the maximum difference of the accident rate in Zone 1 (below 5m) between DNV and OGP database is about 10 %. Nevertheless, the discrepancy is relatively insignificant.

On the other hand, adding the scenario of 1,000s leak duration made very little difference, albeit slightly higher, from the original scenario for 10s delay only. Similar trends were observed between DNV and OGP database, and the differences were also marginal.

The results of the sensitivity analysis for Case Ship 2 show relatively high differences between DNV and OGP database with over 50 % in Zone 1 for the 10 and 1,000 second leak duration. Again the DNV database produces higher frequencies than the OGP database. Based on the findings, it can be concluded that adding the prolonged leak duration up to 1,000 seconds into

the scenarios does not appear to influence the extent of safety exclusion zone very much while the selection of leak frequency database does; this can be explained by the fact that, although the impact of each consequence of 1,000 seconds leak would be significantly higher than 10 seconds leak, the probability of 1,000 seconds leak is far too small to make noticeable difference to the safety exclusion zones for the case ships.

Table 8.7 Risk level of safety exclusion zones with different scenarios and databases (unit: /year).

Case Ship	Leak Duration	Case	Data Source	Distance (m)								
				Zone 1	Zone 2	Zone 3	Zone 4	Zone 5	Zone 6			
				0m	5m	15m	25m	50m	100m	200m		
Case Ship 1	10s	Original Case	DNV (/year)	2.85E-06	1.01E-06	6.54E-07	3.63E-07	2.49E-07	1.60E-07	1.32E-07		
		Case 1_1	OGP (/year)	2.58E-06	9.54E-07	6.19E-07	3.41E-07	2.03E-07	1.49E-07	1.20E-07		
			Difference	-9.47%	-5.54%	-5.35%	-6.06%	-18.47%	-6.88%	-9.09%		
		Case 2_1	DNV (/year)	2.86E-06	1.02E-06	6.69E-07	3.86E-07	2.65E-07	1.74E-07	1.38E-07		
	1000s	Case 2_2	OGP (/year)	2.58E-06	9.69E-07	6.34E-07	3.64E-07	2.48E-07	1.63E-07	1.26E-07		
			Difference	0.19%	1.59%	2.42%	6.62%	22.39%	9.69%	4.68%		
		Case Ship 2	10s	Original Case	DNV (/year)	5.62E-05	2.74E-06	1.25E-06	1.25E-06	0.00E+00	0.00E+00	0.00E+00
				Case 1_1	OGP (/year)	2.66E-05	1.30E-06	7.10E-07	0.00E+00	0.00E+00	0.00E+00	0.00E+00
	Difference			-52.67%	-52.55%	-43.20%	-	-	-	-		
Case 2_1	DNV (/year)			5.63E-05	3.04E-06	1.54E-06	1.30E-06	9.35E-09	0.00E+00	0.00E+00		
1000s	Case 2_2		OGP (/year)	3.04E-05	1.86E-06	9.95E-07	8.43E-07	6.05E-09	0.00E+00	0.00E+00		
			Difference	14.13%	43.24%	40.18%	-	-	-	-		

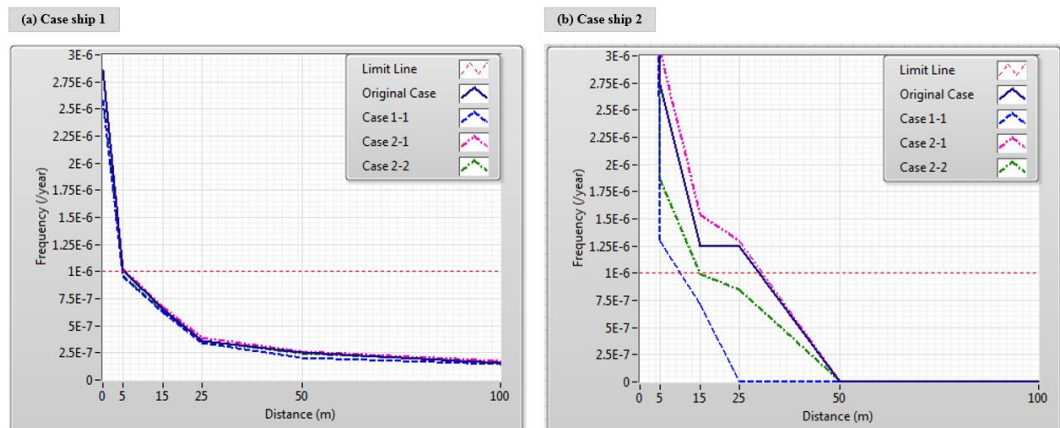


Figure 8.11 Risk level of safety exclusion zones with different scenarios and databases.

It may be recalled that the original study assumed the degree of congestion to be 20 %. In order to investigate the influence of this figure, two cases of 50 % and 10 % ‘congested’ conditions were investigated.

It is easy to conjecture that a higher congestion ratio increases the likelihood of explosion, but simultaneously reduces the likelihood of flash fire. Since the impact extent a of flash fire is wider than that of an explosion, a high congestion ratio must have lower overall risk as demonstrated by the results in Table 8.8 and Figure 8.12. For Case Ship 1, the congestion ratio is not significant while for Case Ship 2, high congestion ratio (50 %) reduced the minimum safety exclusion zone. Nevertheless, realistically, the congestion ratio is more likely to be far less than 50%. When a less congestion ratio of 10 % was applied, the difference was insignificant for both case ships.

Table 8.8 Risk level of safety exclusion zones with respect to congestion ratio (unit: /year).

Case Ship	Case	Distance (m)							
		Zone 1	Zone 2	Zone 3	Zone 4	Zone 5	Zone 6		
		0m	5m	15m	25m	50m	100m	200m	
Case Ship 1	Original Case (20% congested)	2.85E-06	1.01E-06	6.54E-07	3.63E-07	2.49E-07	1.60E-07	1.32E-07	
	Case 1	50% congested	2.85E-06	1.00E-06	6.53E-07	3.42E-07	2.17E-07	9.97E-08	8.26E-08
		Difference	0.00%	-0.99%	-0.15%	-5.79%	-12.85%	-37.69%	-37.42%
	Case 2	10% congested	2.85E-06	1.01E-06	6.54E-07	3.71E-07	2.59E-07	1.80E-07	1.49E-07
		Difference	0.00%	0.00%	0.00%	2.20%	4.02%	12.50%	12.88%
Case Ship 2	Original Case (20% congested)	5.62E-05	2.74E-06	1.25E-06	1.25E-06	0.00E+00	0.00E+00	0.00E+00	
	Case 1	50% congested	5.62E-05	2.60E-06	7.83E-07	7.83E-07	0.00E+00	0.00E+00	0.00E+00
		Difference	0.00%	-5.11%	-37.36%	-37.36%	-	-	-
	Case 2	10% congested	5.62E-05	2.78E-06	1.41E-06	1.41E-06	0.00E+00	0.00E+00	0.00E+00
		Difference	0.00%	1.46%	12.80%	12.80%	-	-	-

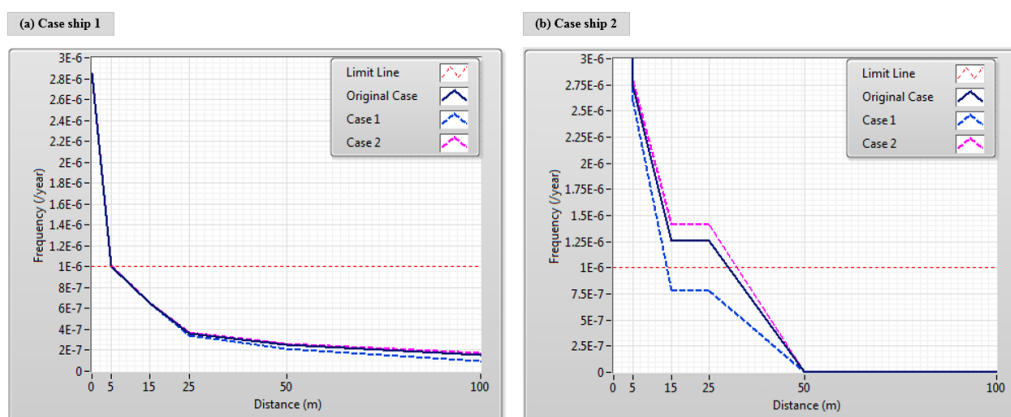


Figure 8.12 Risk level of safety exclusion zones with respect to congestion ratio.

### 8.5.2. Parametric analysis for flow rate

A flow rate is determined by the combination of the fluid velocity and the pipe size. Where the total amount of the fuel to be transferred is fixed, a higher transfer rate will guarantee the reduction in the total time required for bunkering. Given bunkering time is an important factor which affects the frequency of equipment failure leading to leak, a study was undertaken to investigate how sensitive the safety exclusion zone is to varying velocities and pipe sizes.

#### (a) Velocity

Based on the DNV Class guidelines (DNVGL 2014b), the velocity of LNG transfer should not exceed 10 m/s in order to prevent static electricity from being generated. Accordingly, four cases of differing velocities including the original one were compared: 3 m/s, 5 m/s, 8 m/s and 10 m/s. The amount of LNG fuel to be shipped was kept the same as the original case study, i.e. 10,000 m<sup>3</sup> and 125 m<sup>3</sup> for the Case Ships 1 and 2 respectively. The annual bunkering time with respect to different velocity rates are summarized in Table 8.9 which highlights significantly reduced annual bunkering times for higher velocities.

Table 8.9 Annual bunkering time for varying fluid velocity.

Case ship	Parameter	Flow Rate (m <sup>3</sup> /h)	Annual bunkering time (hours)
Case Ship 1	Case 1 (3m/s)	529.9	108
	Original Case (5m/s)	883.1	65
	Case 2 (8m/s)	1,413.0	41
	Case 3 (10m/s)	1,766.3	32
Case Ship 2	Case 1 (3m/s)	5.3	2,061
	Case 2 (5m/s)	8.8	1,288
	Original Case (8m/s)	14.1	773
	Case 3 (10m/s)	17.7	687

As previously stated, the frequency of initial leak is closely related to the annual bunkering time, since the increasing bunkering time leads to a higher probability of equipment failure. The findings of the parametric analysis are illustrated in Table 8.10 and Figure 8.13. It is observed that the Case 1 (3 m/s) with the highest annual bunkering times increases the frequency of the accident rate for both case ships in all zones. As a result, the safety exclusion zone for Case Ship 1 moves up to Zone 3, while Cases 2 (8 m/s) and 3 (10 m/s) move safety exclusion zone down to Zone 1. Similar effects can be observed for Case Ship 2 but the safety exclusion zones remain the same, because the critical impact of fire and explosions associated with Case Ship 2 does not reach Zone 4.

Table 8.10 Result of parametric analysis for velocity (unit: /year).

Case Ship	Case		Distance (m)							
			Zone 1	Zone 2	Zone 3	Zone 4	Zone 5	Zone 6		
			0m	5m	15m	25m	50m	100m	200m	
Case Ship 1	Original Case (5m/s)		2.85E-06	1.01E-06	6.54E-07	3.63E-07	2.49E-07	1.60E-07	1.32E-07	
	Case 1	3 m/s	4.74E-06	1.67E-06	1.09E-06	6.04E-07	3.58E-07	2.65E-07	2.20E-07	
		Difference	66.32%	65.35%	66.67%	66.39%	43.78%	65.63%	66.67%	
	Case 2	8 m/s	1.80E-06	6.36E-07	4.13E-07	2.29E-07	1.36E-07	1.01E-07	8.34E-08	
		Difference	-36.84%	-37.03%	-36.85%	-36.91%	-45.38%	-36.88%	-36.82%	
	Case 3	10 m/s	1.40E-06	4.96E-07	3.22E-07	1.79E-07	1.06E-07	7.86E-08	6.51E-08	
		Difference	-50.88%	-50.89%	-50.76%	-50.69%	-57.43%	-50.88%	-50.68%	
	Case Ship 2	Original Case (8m/s)		5.62E-05	2.74E-06	1.25E-06	1.25E-06	0.00E+00	0.00E+00	0.00E+00
Case 1		3 m/s	1.50E-04	7.29E-06	3.34E-06	3.34E-06	0.00E+00	0.00E+00	0.00E+00	
		Difference	166.90%	166.06%	167.20%	167.20%	-	-	-	
Case 2		5 m/s	9.36E-05	4.56E-06	2.09E-06	2.09E-06	0.00E+00	0.00E+00	0.00E+00	
		Difference	66.55%	66.42%	67.20%	67.20%	-	-	-	
Case 3		10 m/s	4.99E-05	2.43E-06	1.11E-06	1.11E-06	0.00E+00	0.00E+00	0.00E+00	
		Difference	-11.21%	-11.31%	-11.20%	-11.20%	-	-	-	



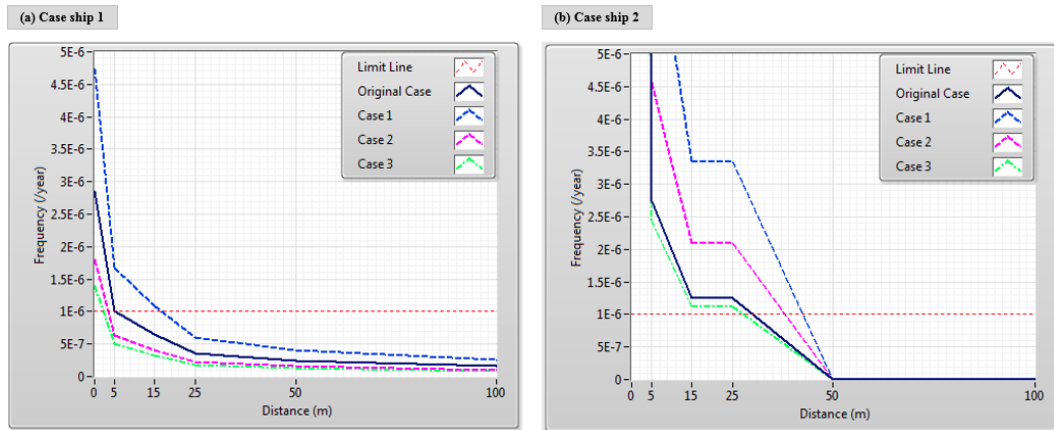


Figure 8.13 Result of parametric analysis for velocity.

(b) Pipe size

The pipe sizes of 250 mm and 25 mm for Case Ships 1 and 2 respectively were chosen during the design stage. However, from the result of parametric analysis with fluid velocity, it can be deduced that similar results will be obtained if the pipe sizes are varied. To verify this, another parametric analysis was conducted using 150 mm, 350 mm and 500 mm pipes for Case Ship 1, and 12.5 mm, 50 mm and 100 mm pipes for Case Ship 2. The flow velocities were kept the same as the original case study, and the consequent annual bunkering time is summarised in Table 8.11.

Table 8.11 Annual bunkering time for varying pipe size.

Case Ships	Parameter	Flow Rate (m <sup>3</sup> /h)	Annual bunkering time (hours)
Case Ship 1	Case 1 (150mm)	317.9	180
	Original Case (250mm)	883.1	65
	Case 2(350mm)	1,730.9	33
	Case 3 (500mm)	3,532.5	16
Case Ship 2	Case 1 (12.5mm)	3.5	3,092
	Original Case (25mm)	14.1	773
	Case 2(50mm)	56.5	258
	Case 3 (100mm)	226.1	86

The bunkering time will obviously affect the failure rate. But different system size will also have different failure rate in the database. The results of the parametric analysis are summarised in Table 8.12 and

Figure 8.14. As expected, they show a similar trend with the analysis results of velocity parameters. For Case Ship 1, the reduced system size of 150 mm (Case 1) leads to the safety exclusion zone moving up to Zone 4 while the increased system sizes of 350 mm (Case 2) and 500 mm (Case 3) result in Zone 2. Similar trend and results are observable for Case Ship 2.

Table 8.12 Result of parametric analysis for piping size (unit: /year).

Case Ship	Case		Distance (m)							
			Zone 1	Zone 2	Zone 3	Zone 4	Zone 5	Zone 6		
			0m	5m	15m	25m	50m	100m	200m	
Case Ship 1	Original Case (250mm)		2.85E-06	1.01E-06	6.54E-07	3.63E-07	2.49E-07	1.60E-07	1.32E-07	
	Case 1	150mm	7.77E-06	2.71E-06	1.75E-06	9.76E-07	6.69E-07	4.28E-07	3.56E-07	
		Difference	172.63%	168.32%	167.58%	168.87%	168.67%	167.50%	169.70%	
	Case 2	350mm	1.54E-06	5.46E-07	3.54E-07	1.96E-07	1.34E-07	8.61E-08	7.07E-08	
		Difference	-45.96%	-45.94%	-45.87%	-46.01%	-46.18%	-46.19%	-46.44%	
	Case 3	500mm	8.60E-07	3.09E-07	2.00E-07	1.11E-07	7.53E-08	4.85E-08	3.90E-08	
		Difference	-69.82%	-69.41%	-69.42%	-69.42%	-69.76%	-69.69%	-70.45%	
	Case Ship 2	Original Case (25mm)		5.62E-05	2.74E-06	1.25E-06	1.25E-06	0.00E+00	0.00E+00	0.00E+00
		Case 1	12.5mm	5.46E-04	1.72E-05	4.29E-06	0.00E+00	0.00E+00	0.00E+00	0.00E+00
Difference			871.53%	527.74%	243.20%	-100.00%	-	-	-	
Case 2		50mm	1.34E-05	4.55E-06	8.70E-07	6.96E-07	6.96E-07	0.00E+00	0.00E+00	
		Difference	-76.16%	66.06%	-30.40%	-44.32%	-	-	-	
Case 3		100mm	3.90E-06	1.51E-06	4.24E-07	3.96E-07	3.39E-07	2.26E-07	0.00E+00	
		Difference	-93.06%	-44.89%	-66.08%	-68.32%	-	-	-	

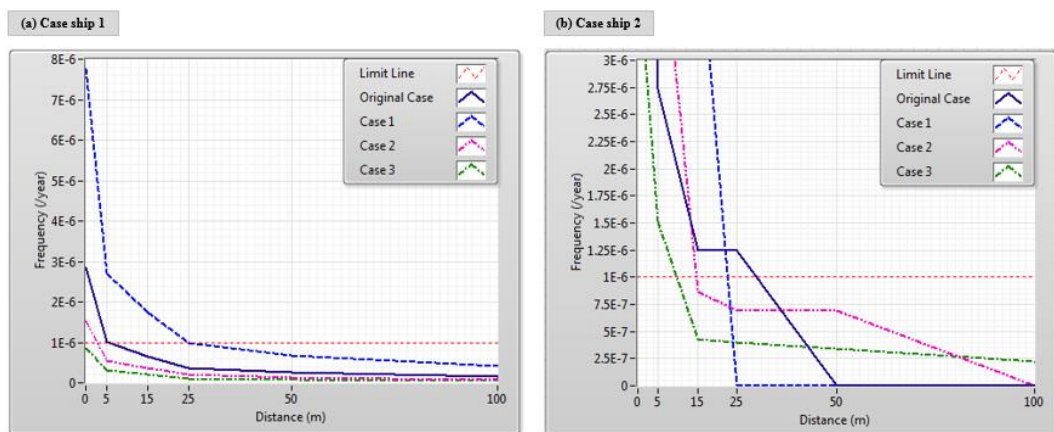


Figure 8.14. Result of parametric analysis for system size.

It may be thought that some velocities and system sizes used for the parametric analysis are unrealistic for the operational profiles of the

ships. Nevertheless, the findings of this parametric analysis with varying flow rate helped conclude that bunkering frequency and time taken for the bunkering operations are the key parameters in probabilistically determining the safety exclusion zone. The result indicates that the most important parameter is the total duration of the bunkering operations required. Larger pipes and higher fluid velocity enables higher volumes to be transferred, thereby reducing the bunkering time required.

### 8.5.3. Comparison with deterministic approach

The deterministic approach of estimating the extent of safety exclusion zone uses a representative risk scenario (worst-case scenario). For Case Ship 1, the highest leak rate when fully ruptured is determined to be 477.9 kg/s. As shown in Figure 8.15, the result of gas dispersion modelling with the software determines the safety exclusion zone at 514 m from the leak origin. This is longer than the ship's length, and is considerably larger than that obtained by the probabilistic approach.

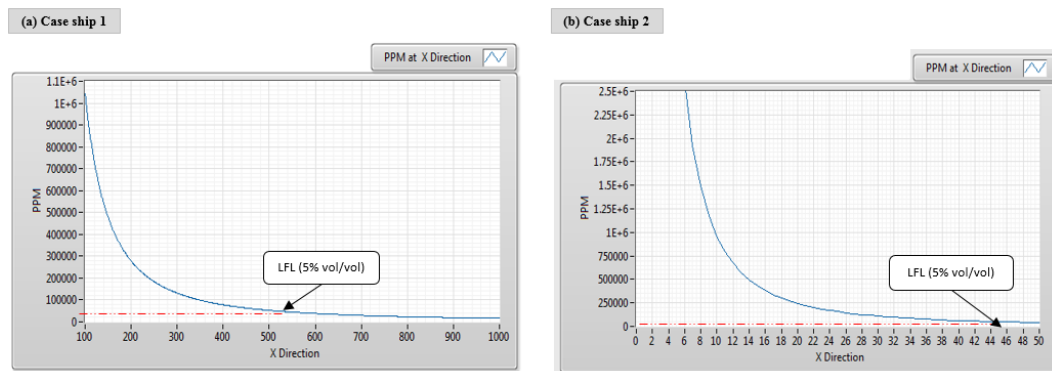


Figure 8.15. LFL boundary for deterministic approach – PPM over x direction.

On the other hand, the maximum leak rate when fully ruptured is about 4.779 kg/s for Case Ship 2. When the gas dispersion model was used, the safety distance became 45 m from the leak origin, which is reasonably close to the result obtained from the probabilistic approach.

It is interesting to note that the Port of Gothenburg (2014), which presently provides LNG bunkering services, established safety exclusion zones depending on the ship type: 15 m radius for container ships and bulk carriers, 25 m for other types of ships.

#### 8.5.4. Comparison with DNV GL risk criteria

The minimum safety exclusion zones were calculated with DNV GL risk criteria (1.0E-6 per bunkering) for comparison with the results obtained from the probabilistic approach of this study. Case Ship 1 has 13 hours of operation time for each bunkering while Case Ship 2 has 9 hours. DNV GL approach ignores the annual frequency of bunkering, and thus the unit of frequency is transformed from ‘per year’ to ‘per bunkering’. The analysis results are shown in Table 8.13 and Figure 8.16; for both case ships the overall accident rate is beneath the risk criteria even for no safety zone. DNV GL guideline, however, requires the safety exclusion zone of greater than 10 m radius for all ships. This result contrasts strikingly to the results from the probabilistic approach which suggested a safety zone of 36m radius for Case Ship 2.

Table 8.13 Analysis results based on DNV GL guideline (unit: /bunkering).

Case ship	Distance (m)						
	Zone 1	Zone 2	Zone 3	Zone 4	Zone 5	Zone 6	
	0m	5m	15m	25m	50m	100m	200m
Case Ship 1	5.70E-07	2.02E-07	1.31E-07	7.27E-08	4.97E-08	3.19E-08	2.64E-08
Case Ship 2	6.54E-07	3.19E-08	1.46E-08	1.46E-08	0.00E+00	0.00E+00	0.00E+00

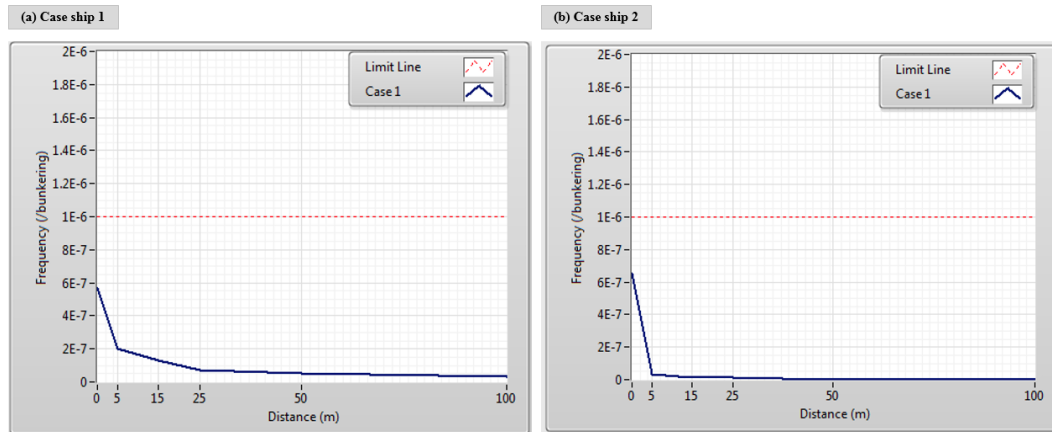


Figure 8.16. Analysis results based on DNV GL guideline.

## 8.6. Concluding remarks

This study investigated using the IQRA Software the potential risk of LNG bunkering and evaluated the extent of indicative safety exclusion zones for LNG bunkering station for two contrasting case ships - one has low frequency but high consequence of risk while the other has high frequency but low consequence of risk - based on the risk criteria of  $1.0E-6$  /year. The result of the study shows that the minimum safety exclusion zone is 6.4 m radius, or Zone 2, for Case Ship 1 (high consequence) while 36m radius, or Zone 4, for Case Ship 2 (high frequency).

This is contrary to what our common sense tells us, as it is, on the face of it, entirely credible to think that a large scale LNG bunkering (high consequence of risk) needs to have a more extensive safety exclusion zone, compared to small scale LNG bunkering (low consequence of risk). However, the result of this study clearly indicates that bunkering frequency and the total time taken for bunkering operations in a year are the key parameters in determining the risk level of LNG bunkering, and the consequence appears to be less important. Larger pipes and higher fluid velocity enables higher volumes to be transferred, thereby reducing the bunkering time required.

It is thought that there may be a case for making the relevant rules and regulations more explicit and more stringent. However, as shown through sensitivity and parametric analysis, the overall results of risk assessment for

LNG bunkering is influenced in some degree by parameters used in the analysis. It can be concluded, therefore, that the problem requires more extensive studies and discussion to draw a consensus on the standard database and scenarios to be used. It was also found that the safety exclusion zones set up through deterministic approaches may be over-extensive and impractical for large scale LNG bunkering. It is because the deterministic approach is based on the worst case scenario regardless of the likelihood. This problem appears to be overcome through using the probabilistic risk-based approach.

The current DNVGL guidelines specify safety exclusion zones based on risk per bunkering operation. However, the current study showed that this is incomplete as it does not take into account the total time the equipment and the system as a whole is used which governs the frequency of failure.

For a variety of reasons IMO member states have yet to develop their own explicit regulations concerning safety exclusion zones in LNG bunkering. The present study can therefore be viewed as a contribution towards safer uses of LNG as a marine fuel.

## 9. SAFETY EXCLUSION ZONE FOR LNG BUNKERING AT FUEL-SUPPLYING POINT

### 9.1. Introduction

The on-board risk and exclusion zone was treated in the previous chapter. This chapter describes a study conducted to identify potential risks associated with LNG bunkering at the fuel-supplying point. A series of parametric analyses was also carried out to obtain a more methodical understanding of how various parameters influence on the extent of recommended safety exclusion zones. Through the parametric analyses general relationships between the risk and various parameters could be established from which the importance of the selected parameters might be evaluated.

Both population-independent and population-dependent approaches were used for this study. Since there will be a distribution of humans around fuel supply point (e.g. bunkering terminal ashore), such as port personnel and residents nearby, a population-dependent approach was used. The results of both approaches were combined to determine the most appropriate safety exclusion zones for the conditions represented by the sets of parameters.

### 9.2. Description of study

#### *9.2.1. Identification of parameters*

Results of risk assessment for LNG bunkering may be sensitive to several parameters and some of them may be more influential than others. In order to investigate the degree of the parametric sensitivity on the risk of LNG bunkering at supplying point, four key parameters originally identified by a DNV GL report (DNVGL 2014b) were adopted as follows:

- Transfer flow rate (bunkering method): when flow velocity is fixed, transfer flow rate relies on piping system size which is determined by the type of bunkering method. A higher transfer flow rate shortens the time required for bunkering and, consequently, frequency of initial leak, but it does increase the probability of ignition.
- Bunkering volume: for a constant transfer flow rate and operating pressure (system size), higher bunkering volume requires longer bunkering duration, resulting in higher probability of occurrence of LNG leak from the bunkering system.
- Port population: port population is an important parameter in societal risk because exposing a larger population to risk increases the potential loss of life.
- Tolerable risk criterion: since there is no international consensus on the level of risk which is tolerable, the sensitivity of the extent of safety exclusion zones to this criterion needs to be investigated.

### *9.2.2. Bunkering case design*

To begin with, the bunkering cases were designed by selecting a set of parameters. These parameters were bunkering method (and bunkering system), bunkering volume and port population as shown in Figure 9.1.



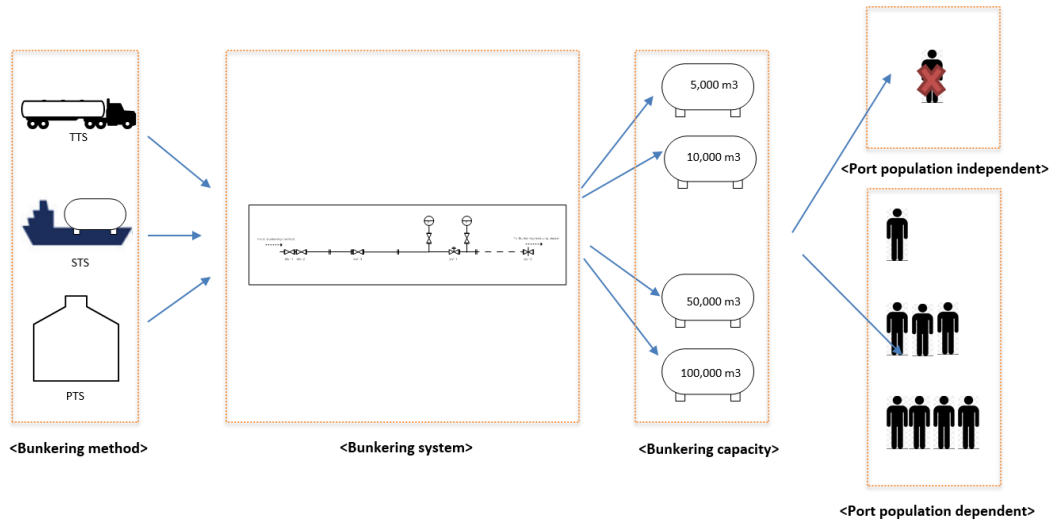


Figure 9.1. Concept of parametric risk analysis.

Three bunkering methods were considered - TTS, STS and PTS by which the composition of bunkering system was determined. TTS has a low transferring capacity up to 10,000 gallons/hour (about 39 m<sup>3</sup>/h), and STS is capable of supplying 40,000 gallons/hour (about 151 m<sup>3</sup>/h), while there is no specific limit for PTS (DNVGL 2014b). Based on this, this study assumed the equipment size of 25 mm for TTS, 100 mm for STS and 250 mm for PTS while the size of pressure indicators was uniformly 12.5 mm.

Table 9.1 shows the list of LNG bunkering equipment, and the present study assumed that all methods use the same equipment with only the length of pipeline being different. On the other hand, the vapour return line is not included in this case study as the consequence of the vapour leak from the return line is relatively minor compared to that of the main line.

Table 9.1 List of LNG bunkering equipment.

No.	Equipment	Quantity		
		TTS	STS	PTS
1	ESD Valve	1	1	1
2	ERC	1	1	1
3	Flange	12	12	12
4	Manual Valve	3	3	3
5	Pipe (per 1m)	20	10	100
6	Press. indicator	2	2	2
7	Flexible Hose	1	1	1

Four different cases of annual LNG bunkering volumes were studied: 5,000 m<sup>3</sup> (Case 1), 10,000 m<sup>3</sup> (Case 2), 50,000 m<sup>3</sup> (Case 3) and 100,000 m<sup>3</sup> (Case 4). Three cases of port population distribution were also studied and the details are given later in this section.

For the initial set up, the working pressure for the bunkering liquid line was assumed to be 3 bar(g), and the working temperature of LNG flowing through the main line was set to 112K (DNV 2012b). Recall that the pipe size used for the three bunkering methods in this study was 25 mm for TTS, 100 mm for STS and 250 mm for PTS. The total annual bunkering time needed for various volumes of LNG transfer for the fluid velocity of 5 m/s is determined based on the bunkering rates of each method: 0.1132 h/m<sup>3</sup> for TTS, 0.0071 h/m<sup>3</sup> for STS and 0.0011 h/m<sup>3</sup> for PTS. TTS with a small pipe has much higher annual bunkering time required than the other methods. Where bunkering time is too high, especially for the TTS method, multiple bunkering connections may be needed.

### 9.2.3. Approaches adopted

A flowchart of the methodology, which is based on the discussion in Chapter 7, is shown in Figure 9.2. Once the initial parameters are set up, the software follows a standard quantitative risk assessment process which consists of

scenario analysis, frequency analysis, consequence analysis and risk assessment (Jin and Jang 2015).

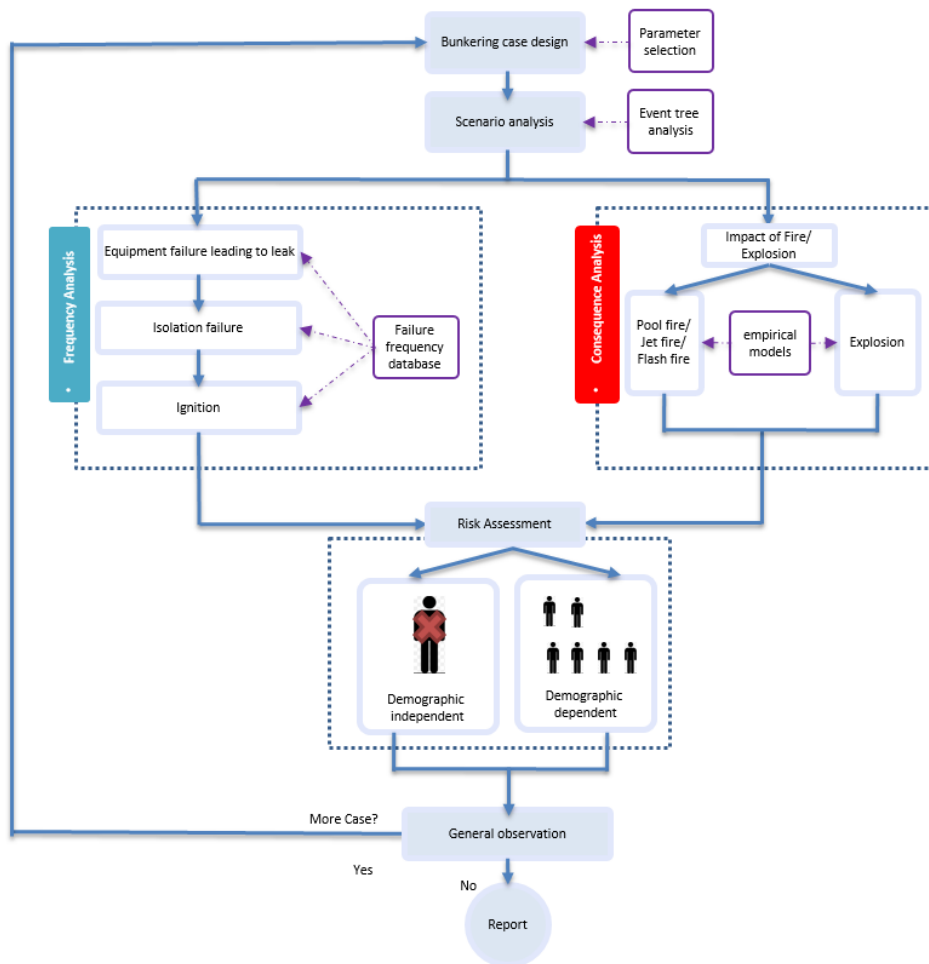


Figure 9.2. A flowchart of study based on IQRA software.

(a) Population-independent analysis

The present study regards the critical distance is where there is 50 % or higher probability of fatality. This translates into a distance where thermal radiation reaches down to 16.0 kW/m<sup>2</sup> and overpressure is reduced to 0.4 bar(g). In addition, the LFL of methane (5 % by volume) is considered to be the criterion to determine the critical distance for the flash fire.

Each consequence can then be classed into all the discrete zones up to and including the zone where its critical distance falls. The frequencies of all the consequences belonging to each zone are then summed to produce the total frequency of accidents reaching that zone. The safe exclusion zone is then determined to be the nearest zone from the accident point with less than the tolerable risk criterion.

(b) Population-dependent analysis

The societal risk depends on the density of population at site. Since the present study was focused on general observation rather than site-specific analysis, three different cases of port population (where P\_Case 1 – access is severely restricted, P\_Case 2 – access is moderately restricted, and P\_Case 3 – access is not restricted) were used for the population-dependent analysis as shown in Figure 9.3; the demographical data aggregated into seven zones was used and the population was assumed evenly distributed in the discrete zones as specified in Section 7.2.3 (b).

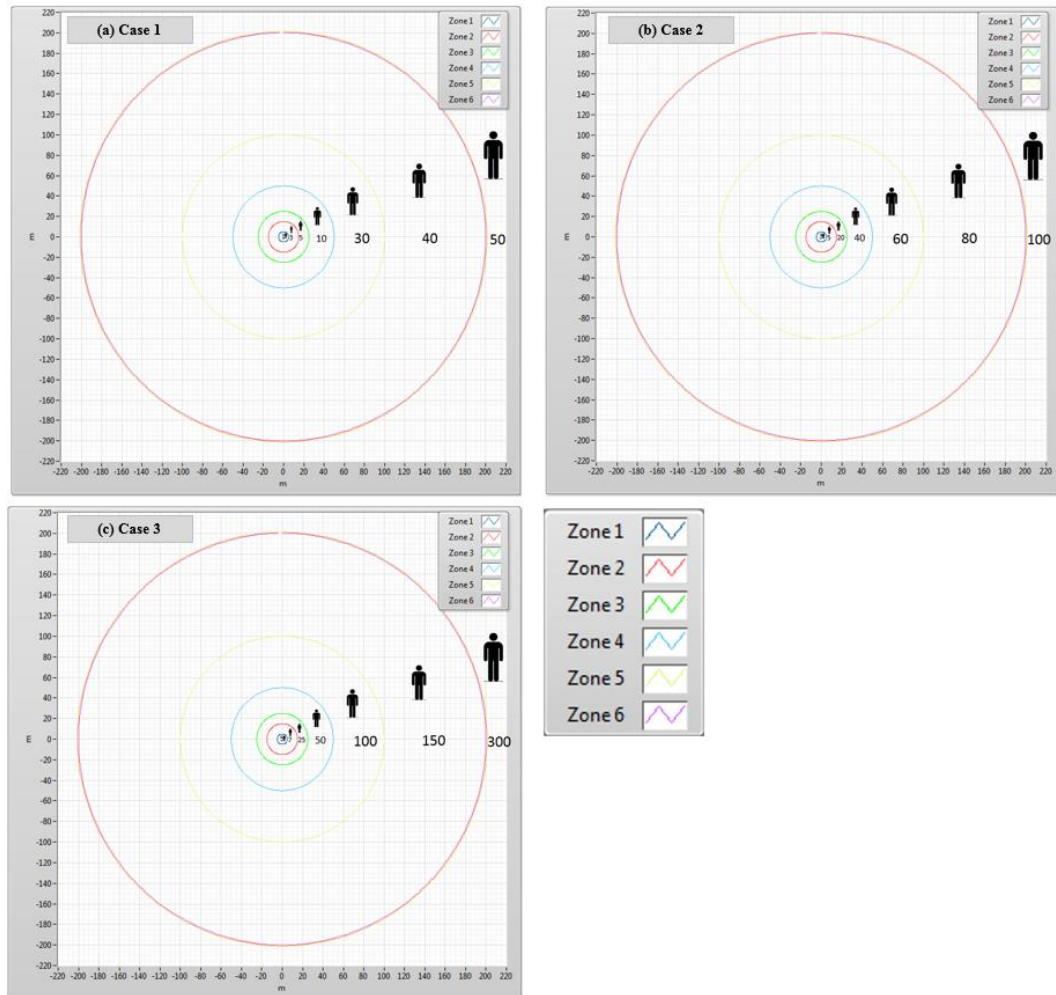


Figure 9.3. Assumed port population (unit: persons).

### 9.3. Risk assessment

#### 9.3.1. Frequency analysis

Estimation of the frequency of initial leak from failure of bunkering equipment was based on DNV Leak Frequency Datasheets (DNV 2012a). As in the on-board bunkering station study, the software adopts generic failure data associated with human errors from Kletz (Kletz 1991) and Dutch model for immediate ignition and Cox model for delayed ignition (DNV 2012b; Cox et al. 1990).

Figure 9.4 illustrates the calculated results of leak frequencies with respect to different leak hole sizes in the case of 5,000 m<sup>3</sup> annual transferring volume for each bunkering method, and the results of all cases (Cases 1- 4) are tabulated in Table 9.2: this was calculated with the list of equipment involved in the LNG bunkering in Table 1 based on the DNV guidelines.

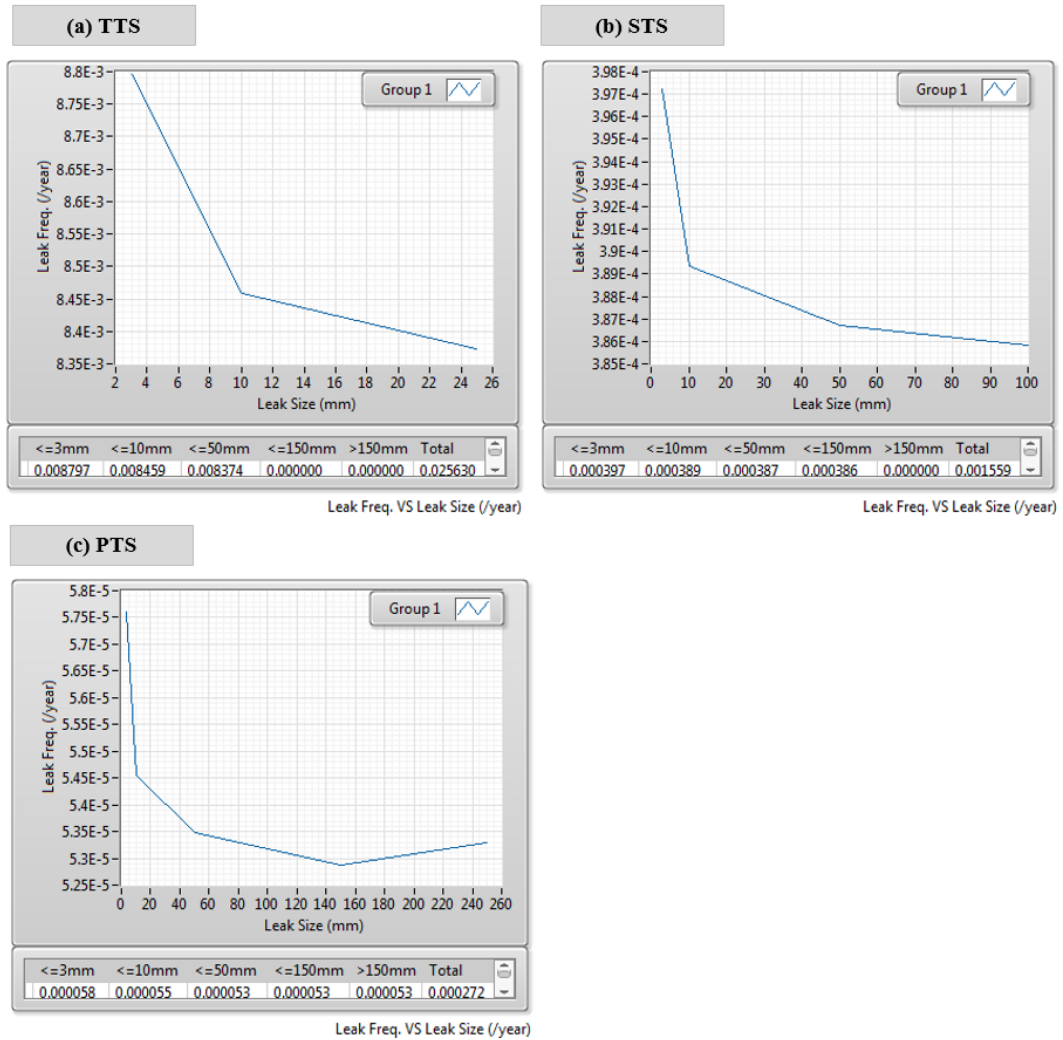


Figure 9.4. Leak frequency of various LNG bunkering systems (Case 1 – 5,000 m<sup>3</sup>).

Although the leak frequency is affected by the equipment used and system size, the analysis shows that the leak frequencies are directly proportional to the annual bunkering time required. As a result, TTS has very high leak frequencies, significantly higher than the other methods.

Table 9.2 Leak frequency of LNG bunkering systems with respect to capacity (unit:/year).

Method	Case	Leak hole size					Total
		<=3mm	<=10mm	<=50mm	<=150mm	>150mm	
TTS	Case 1 (5,000m <sup>3</sup> )	8.80E-03	8.46E-03	8.37E-03	0.00E+00	0.00E+00	2.56E-02
	Case 2 (10,000m <sup>3</sup> )	1.76E-02	1.69E-02	1.67E-02	0.00E+00	0.00E+00	5.13E-02
	Case 3 (50,000 m <sup>3</sup> )	8.80E-02	8.46E-02	8.38E-02	0.00E+00	0.00E+00	2.56E-01
	Case 4 (100,000 m <sup>3</sup> )	1.76E-01	1.69E-01	1.68E-01	0.00E+00	0.00E+00	5.13E-01
STS	Case 1 (5,000 m <sup>3</sup> )	3.97E-04	3.89E-04	3.87E-04	3.86E-04	0.00E+00	1.56E-03
	Case 2 (10,000 m <sup>3</sup> )	8.06E-04	7.90E-04	7.84E-04	7.83E-04	0.00E+00	3.16E-03
	Case 3 (50,000 m <sup>3</sup> )	4.02E-03	3.94E-03	3.91E-03	3.90E-03	0.00E+00	1.58E-02
	Case 4 (100,000 m <sup>3</sup> )	8.04E-03	7.88E-03	7.82E-03	7.80E-03	0.00E+00	3.15E-02
PTS	Case 1 (5,000 m <sup>3</sup> )	5.80E-05	5.50E-05	5.30E-05	5.30E-05	5.30E-05	2.72E-04
	Case 2 (10,000 m <sup>3</sup> )	1.06E-04	1.00E-04	9.80E-05	9.70E-05	9.80E-05	4.99E-04
	Case 3 (50,000 m <sup>3</sup> )	5.47E-04	5.18E-04	5.08E-04	5.02E-04	5.06E-04	2.58E-03
	Case 4 (100,000 m <sup>3</sup> )	1.09E-03	1.03E-03	1.01E-03	9.96E-04	1.00E-03	5.12E-03

According to a study on human errors (Kletz 1991), the probability of successful isolation of a leaking system without delay is 0.9 while the probability of a delay in isolation of at least 10 seconds is 0.1. The safety measures are basically designed that, as long as it works effectively, all target accidents can be either prevented or contained with no serious consequence. For LNG bunkering in an open space, watch-keeping is the only safety measure that can be provided (since gas detectors will be ineffectual in such circumstances) and the scenario of ‘limited fuel leak’ represents the situation in which the watch-keeper takes an appropriate action immediately to stop the leak. This means that it was assumed that 90 % of initial liquid fuel leak does not lead to an ‘accident’ as the leak can be contained to a ‘limited leak’ which was supposed to pose no danger.

The characteristics of the space around the leak site, i.e. if congested or open, is another important factor as it determines the type of final outcome (i.e. fire or explosion) of the accident. It is difficult to generalise the degree of congestion in the space, but it should be reasonable to consider that the





impact of fires and explosion with respect to particular leak sizes. Since the risk of asphyxiation is negligible in open spaces and cryogenic harm is limited to the spread area, this study is focused on the risk associated with fire and explosion.

In order to estimate consequences, methods described in Appendix A, i.e. Gaussian gas dispersion models for flash fire (Perkins 1974), TNO multi-energy model (TNO 7) for explosion (Woodward and Pitblado 2010; Frank 1980) and Thomas method (1965) for pool fire. The leak rates estimated are presented in Table 9.3.

Table 9.3 Leak rates for various leak hole sizes (unit: kg/s).

Case	Leak hole size				
	3mm	10mm	=<50mm	=<150mm	>150mm
<b>TTS</b>	0.0688	0.7647	4.7791	-	-
<b>STS</b>	0.0688	0.7647	19.1166	76.4662	-
<b>PTS</b>	0.0688	0.7647	19.1166	172.049	477.913

Using the analytical and empirical models described in Appendix A, the impact of each accident was evaluated. For flash fire, a natural weather condition with a wind speed of 5 m/s was assumed for general observation (DNV 2012b). The results reveal that the impact of consequence has a direct correlation with the leak rate: that is, the critical distances of accidents associated with a large scale LNG bunkering are much more extensive than those of a small one. This is illustrated in Figure 9.6.

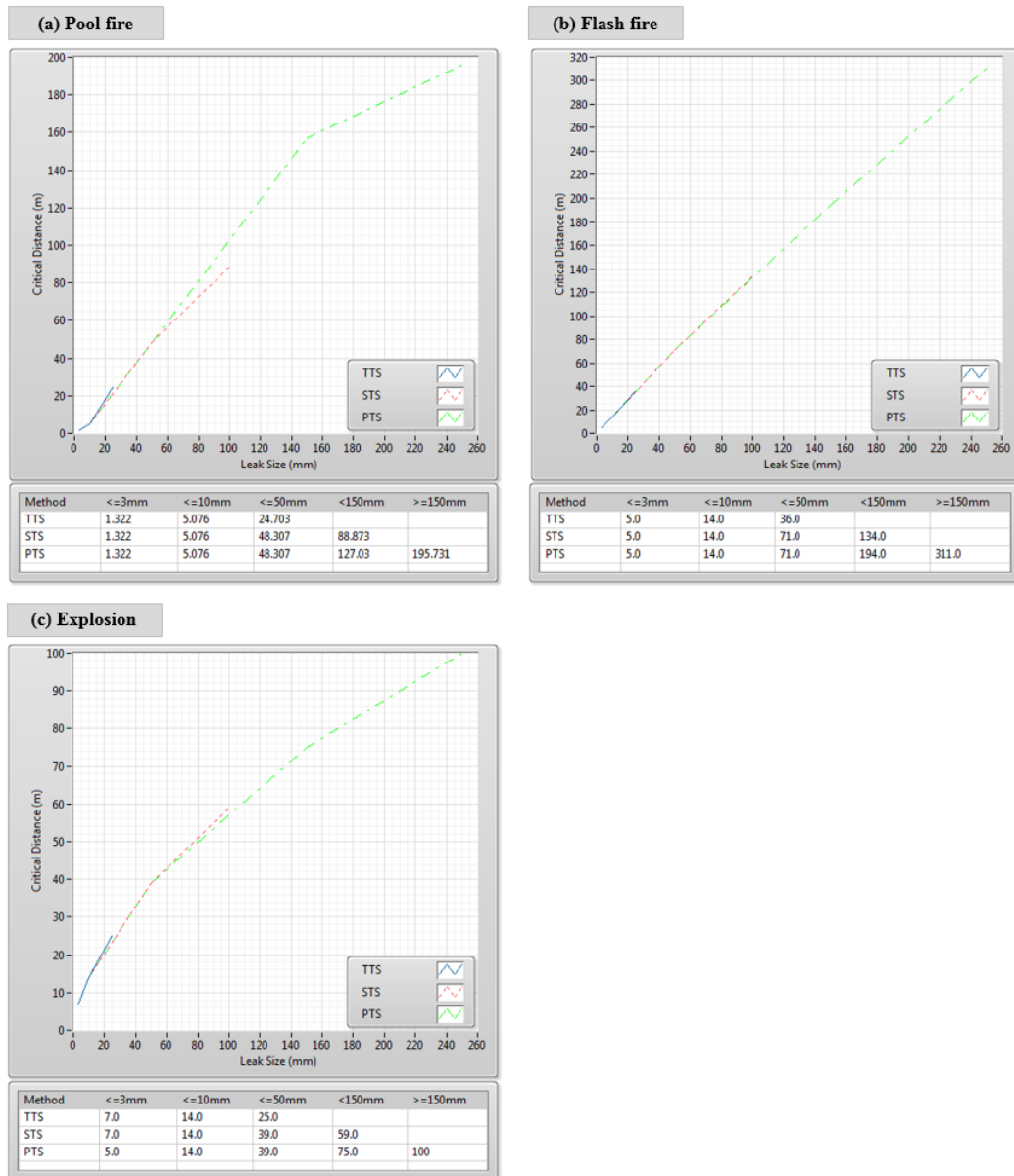


Figure 9.6. Critical distance from accidents with respect to bunkering method.

### 9.3.3. Assessment results

The numerical results of frequency and consequence analyses for various parameters are brought together in Table 9.4.

Table 9.4 Numerical result of frequency and consequence analysis.

Method	Hole Size	Initial Frequency				Scenario Leading to Undesirable Events				Frequency of Accident				Critical Distance, (m)		
		Case 1 5,000m <sup>3</sup>	Case 2 10,000 m <sup>3</sup>	Case 3 50,000 m <sup>3</sup>	Case 4 100,000 m <sup>3</sup>	Imm.Ignit ion	Leak Duration (Late Isolation)	Delayed Ignition	Surrounding Condition (Congestion Ratio)	Fire Type	Case 1 5,000m <sup>3</sup>	Case 2 10,000 m <sup>3</sup>	Case 3 50,000 m <sup>3</sup>		Case 4 100,000 m <sup>3</sup>	
TTS	3mm	8.80E-03	1.76E-02	8.80E-02	1.76E-01	0.02				Pool Fire	1.76E-04	3.52E-04	1.76E-03	3.52E-03	1.3	
						0.98	0.1	0.00284	0.8	Flash Fire	1.96E-06	3.92E-06	1.96E-05	3.92E-05	5	
						0.98	0.1	0.00284	0.2	Explosion	4.90E-07	9.79E-07	4.90E-06	9.80E-06	7	
	10mm	8.46E-03	1.69E-02	8.46E-02	1.69E-01	0.02				Pool Fire	1.69E-04	3.38E-04	1.69E-03	3.38E-03	5.1	
						0.98	0.1	0.0133	0.8	Flash Fire	8.82E-06	1.76E-05	8.82E-05	1.76E-04	14	
						0.98	0.1	0.0133	0.2	Explosion	2.21E-06	4.41E-06	2.21E-05	4.41E-05	14	
	<50mm	8.37E-03	1.67E-02	8.38E-02	1.68E-01	0.02				Pool Fire	1.67E-04	3.35E-04	1.68E-03	3.35E-03	24.7	
						0.98	0.1	0.0431	0.8	Flash Fire	2.83E-05	5.66E-05	2.83E-04	5.66E-04	36	
						0.98	0.1	0.0431	0.2	Explosion	7.07E-06	1.41E-05	7.08E-05	1.42E-04	25	
	STS	3mm	3.97E-04	8.06E-04	4.02E-03	8.02E-03	0.02				Pool Fire	7.94E-06	1.61E-05	8.03E-05	1.60E-04	1.3
							0.98	0.1	0.00284	0.8	Flash Fire	8.84E-08	1.79E-07	8.94E-07	1.79E-06	5
							0.98	0.1	0.00284	0.2	Explosion	2.21E-08	4.49E-08	2.24E-07	4.47E-07	7
10mm		3.89E-04	7.90E-04	3.94E-03	7.86E-03	0.02				Pool Fire	7.78E-06	1.58E-05	7.88E-05	1.57E-04	5.1	
						0.98	0.1	0.0133	0.8	Flash Fire	4.06E-07	8.24E-07	4.11E-06	8.20E-06	14	
						0.98	0.1	0.0133	0.2	Explosion	1.01E-07	2.06E-07	1.03E-06	2.05E-06	7	
50mm		3.87E-04	7.84E-04	3.91E-03	7.81E-03	0.04				Pool Fire	1.55E-05	3.14E-05	1.56E-04	3.12E-04	48.3	
						0.96	0.1	0.105	0.8	Flash Fire	3.12E-06	6.32E-06	3.15E-05	6.30E-05	71	
						0.96	0.1	0.105	0.2	Explosion	7.80E-07	1.58E-06	7.88E-06	1.57E-05	39	
<150mm		3.86E-04	7.83E-04	3.90E-03	7.79E-03	0.04				Pool Fire	1.54E-05	3.13E-05	1.56E-04	3.12E-04	88.9	
						0.96	0.1	0.255	0.8	Flash Fire	7.56E-06	1.53E-05	7.64E-05	1.53E-04	134	
						0.96	0.1	0.255	0.2	Explosion	1.89E-06	3.83E-06	1.91E-05	3.82E-05	59	
PTS	3mm	5.80E-05	1.06E-04	5.47E-04	1.09E-03	0.02				Pool Fire	1.16E-06	2.12E-06	1.09E-05	2.17E-05	1.3	
						0.98	0.1	0.00284	0.8	Flash Fire	1.29E-08	2.36E-08	1.22E-07	2.42E-07	5	
						0.98	0.1	0.00284	0.2	Explosion	3.23E-09	5.90E-09	3.04E-08	6.04E-08	7	
	10mm	5.50E-05	1.00E-04	5.18E-04	1.03E-03	0.02				Pool Fire	1.10E-06	2.00E-06	1.04E-05	2.05E-05	5.1	
						0.98	0.1	0.0133	0.8	Flash Fire	5.73E-08	1.04E-07	5.40E-07	1.07E-06	14	
						0.98	0.1	0.0133	0.2	Explosion	1.43E-08	2.61E-08	1.35E-07	2.68E-07	14	
	50mm	5.30E-05	9.80E-05	5.08E-04	1.01E-03	0.04				Pool Fire	2.12E-06	3.92E-06	2.03E-05	4.03E-05	48.3	
						0.96	0.1	0.105	0.8	Flash Fire	4.27E-07	7.90E-07	4.10E-06	8.12E-06	71	
						0.96	0.1	0.105	0.2	Explosion	1.07E-07	1.98E-07	1.02E-06	2.03E-06	39	
	150mm	5.30E-05	9.70E-05	5.02E-04	9.96E-04	0.09				Pool Fire	4.77E-06	8.73E-06	4.52E-05	8.96E-05	127.0	
						0.91	0.1	0.429	0.8	Flash Fire	1.66E-06	3.03E-06	1.57E-05	3.11E-05	194	
						0.91	0.1	0.429	0.2	Explosion	4.14E-07	7.57E-07	3.92E-06	7.78E-06	75	
>150mm	5.30E-05	9.80E-05	5.06E-04	1.00E-03	0.09				Pool Fire	4.77E-06	8.82E-06	4.55E-05	9.04E-05	195.7		
					0.91	0.1	0.827	0.8	Flash Fire	3.19E-06	5.90E-06	3.05E-05	6.04E-05	311		
					0.91	0.1	0.827	0.2	Explosion	7.98E-07	1.48E-06	7.62E-06	1.51E-05	100		

(a) Population-independent analysis

Population-independent analyses were carried out in a similar manner as discussed in Chapter 8. The graphs in Figure 9.7 show the frequency of the relevant distance to lie within the critical distance. From this the frequency of the critical distance to fall within each safety zone can be evaluated.

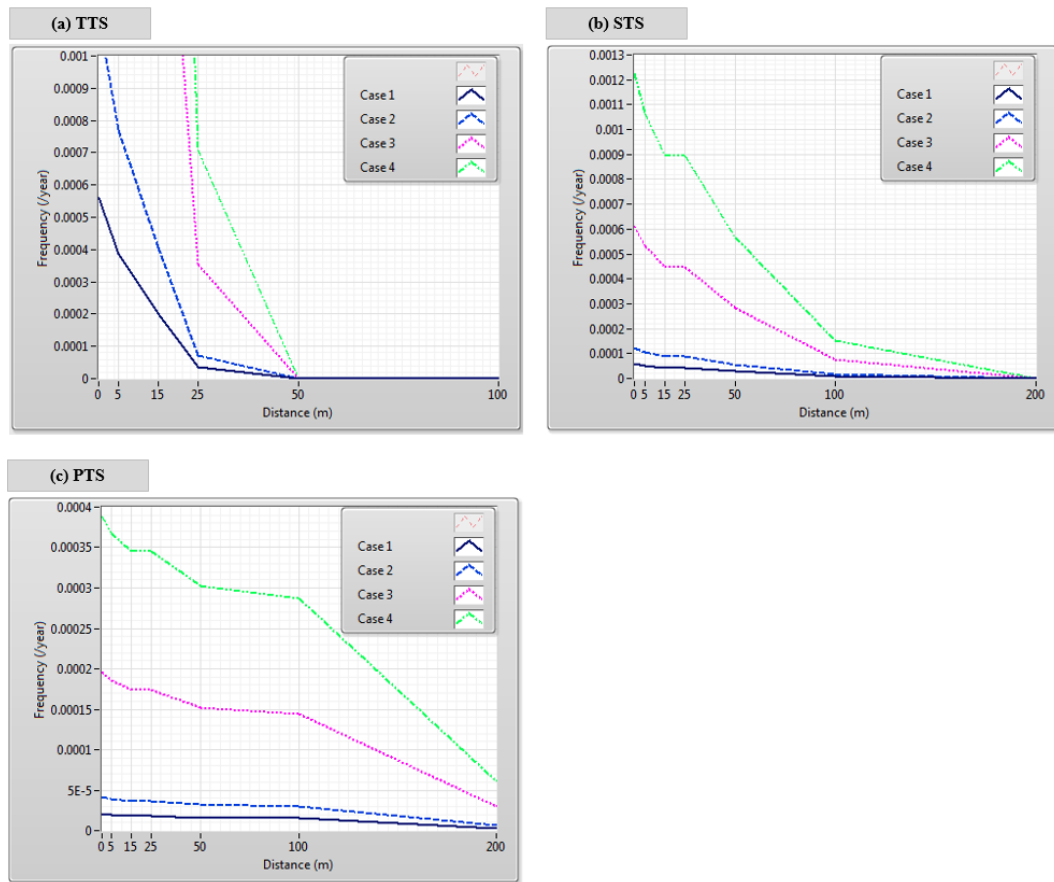


Figure 9.7. Risk frequency for critical distances.

As different flag states and terminal authorities may have different level of risk criteria associated with LNG bunkering, it is clear that there is no consensus on the risk level as yet. In this context, the present study adopted several tolerable risk levels (1.0E-3, 1.0E-4 and 1.0E-5/year) to investigate how this would affect the extent of safety exclusion zone (DNVGL 2014b). The results are summarised in Table 9.5.

Table 9.5 Zones with less than tolerable risks.

Case	Method	Tolerable Risk Level		
		1.0E-5 / year	1.0E-4 / year	1.0E-3 / year
Case 1 (5000m <sup>3</sup> )	TTS	36m (Zone 4)	24.7m (Zone 4)	1.3m (Zone 1)
	STS	88.7m (Zone 5)	No critical zone	No critical zone
	PTS	127m (Zone 6)	No critical zone	No critical zone
Case 2 (10,000m <sup>3</sup> )	TTS	36m (Zone 4)	24.7m (Zone 4)	1.3m (Zone 1)
	STS	134m (Zone 6)	5.07m (Zone 2)	No critical zone
	PTS	195.7m (Zone 6)	No critical zone	No critical zone
Case 3 (50,000m <sup>3</sup> )	TTS	36m (Zone 4)	36m (Zone 4)	24.7m (Zone 4)
	STS	134m (Zone 6)	88.8m (Zone 5)	No critical zone
	PTS	311m (Zone 7)	127m (Zone 6)	No critical zone
Case 4 (100,000m <sup>3</sup> )	TTS	36m (Zone 4)	36m (Zone 4)	24.7m (Zone 4)
	STS	134m (Zone 6)	134m (Zone 6)	5.07m (Zone 2)
	PTS	311m (Zone 7)	195.7m (Zone 6)	No critical zone

It appears that the PTS requires generally more extensive exclusion zones than other bunkering methods in nearly all cases. It is also clearly shown that the tolerable risk level influences the extent of safety exclusion zone to a great extent. As expected, more stringent criterion is seen to extend the zones. For example, Zone 4 is the minimum for 1.0E-5/year while all zones are tolerable when 1.0E-3/year is applied.

The transferring volume also influences the extent of safety zone, primarily because higher volume requires longer time duration of bunkering operation, thereby increasing the probability of leakage occurring. As expected, higher volume requires the more extensive safety exclusion zone.

*(b) Population-dependent analysis*

The probability of fatalities occurring can be presented in an F-N curve as shown in Figure 9.8. It is a common practice to show the upper and lower limits of tolerable risk on the same graph (Norway 2000; Vanem et al. 2008; Wang 2001), so that it is possible to see whether the risk of the system being examined is tolerable or not. IMO MSC circular 72/16 gives the upper tolerable level as a straight line connecting 1.0E-2/year for a single loss and with 1.0E-5/year for 1,000 losses, while the lower

tolerable level is defined as a straight line connecting  $1.0E-4$ /year for a single loss and  $1.0E-7$ /year for 1,000 losses. Results obtained from the population-dependent risk assessment for three different port population cases described in Figure 9.3 are shown in Figure 9.8 to Figure 9.10.

The results consistently show that higher bunkering volumes lead to higher overall risk levels. In the population condition 1 shown in Figure 9.8, the risk level of TTS method dealing with  $100,000 \text{ m}^3$  exceeds tolerable limits while STS and PTS remain within the tolerable level for all cases.

For the population condition 2 shown in Figure 9.9, the risk tends to be higher than the first condition with the risk level of TTS method for  $50,000 \text{ m}^3$  exceeding tolerable limits; and all methods exceed the tolerable level for  $100,000 \text{ m}^3$ .

Population condition 3 shown in Figure 9.10 is the worst case where all three methods exceed tolerable risk for both  $50,000$  and  $100,000 \text{ m}^3$ .

This is as expected, as exposing a larger population to an accident obviously increases the number of potential fatalities. The result confirms that the density of port population is an important parameter in determining the extent of safety exclusion zone.

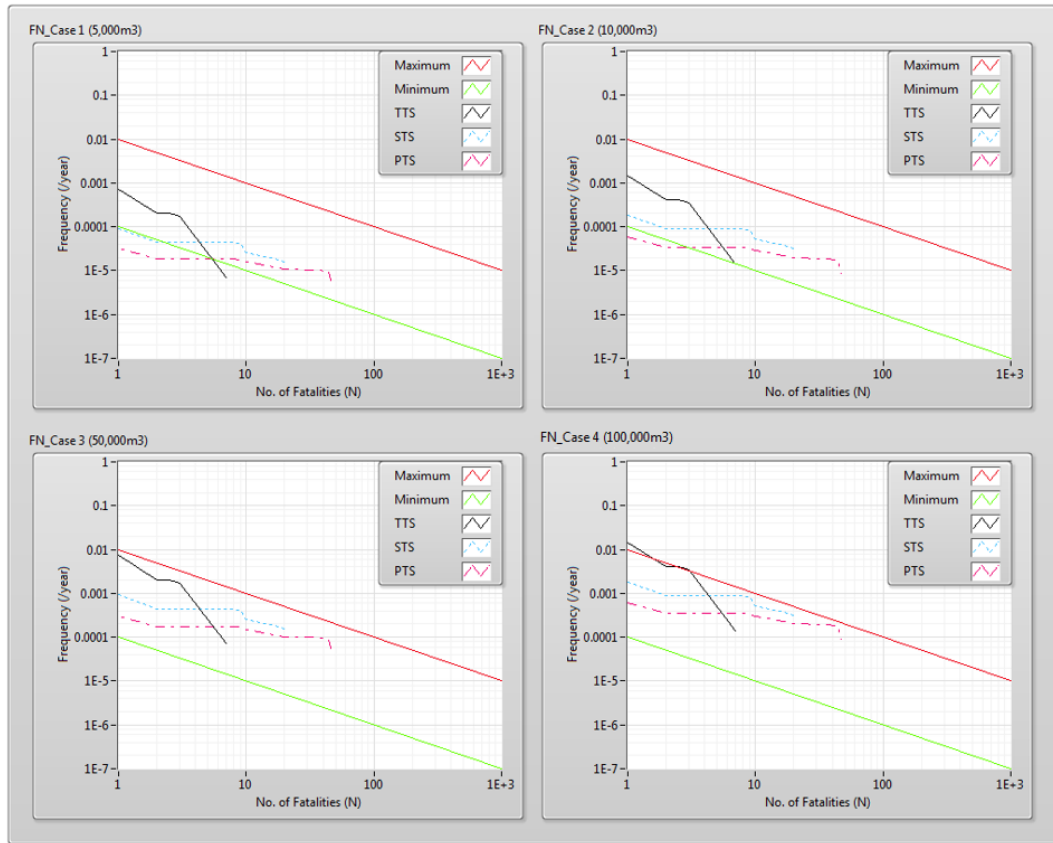


Figure 9.8. F-N curves for port population 1 (P\_Case 1).

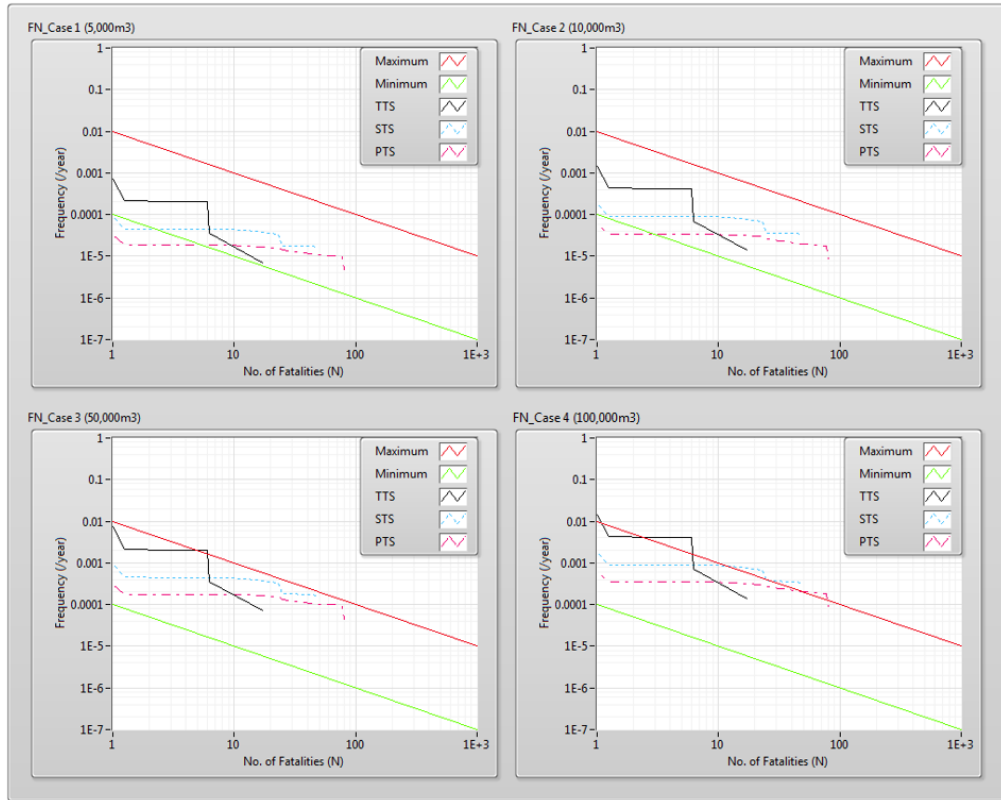


Figure 9.9. F-N curves for port population 2 (P\_Case 2).

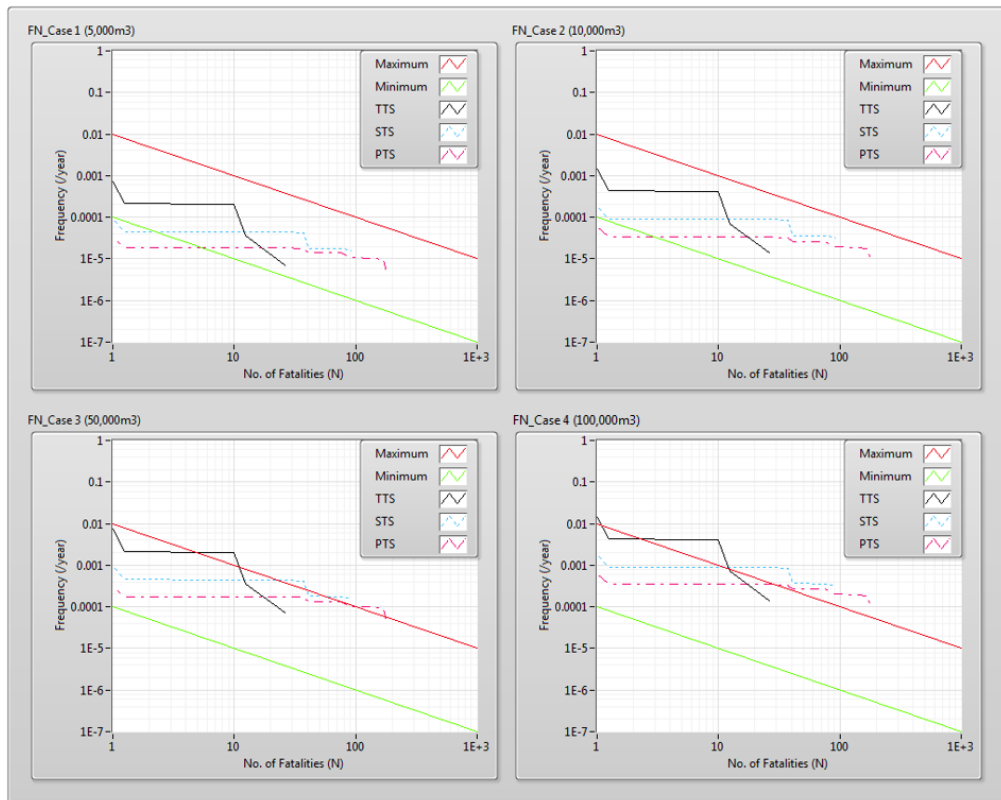


Figure 9.10. F-N curves for port population 3 (P\_Case 3).



The overall result of population-dependent analysis is summarized in Table 9.6. All bunkering methods are acceptable in Cases 1 and 2 for all port population conditions, whereas no bunkering method is tolerable for Cases 3 and 4 for population condition 3. This would suggest that additional safety measures are needed to improve the safety of LNG bunkering for high volume in high density population cases. The simplest way of achieving this appears to be restricting people’s access to the area in a manner discussed below.

Table 9.6 Summary of risk levels for various cases.

Case	Method	P_Case 1	P_Case 2	P_Case 3
Case 1 (5000m <sup>3</sup> )	TTS	Acceptable	Acceptable	Acceptable
	STS	Acceptable	Acceptable	Acceptable
	PTS	Acceptable	Acceptable	Acceptable
Case 2 (10,000m <sup>3</sup> )	TTS	Acceptable	Acceptable	Acceptable
	STS	Acceptable	Acceptable	Acceptable
	PTS	Acceptable	Acceptable	Acceptable
Case 3 (50,000m <sup>3</sup> )	TTS	Acceptable	No Acceptable	No Acceptable
	STS	Acceptable	Acceptable	No Acceptable
	PTS	Acceptable	Acceptable	No Acceptable
Case 4 (100,000m <sup>3</sup> )	TTS	No Acceptable	No Acceptable	No Acceptable
	STS	Acceptable	No Acceptable	No Acceptable
	PTS	Acceptable	No Acceptable	No Acceptable

*(c) Combination of the two approaches*

The results from both population-independent and population-dependent analyses were considered in determining the exclusion zone. Any case with the risks from the population-dependent analysis lower than the upper tolerable limit was considered to have no critical zone. For the cases where critical zones do exist, the critical distance evaluated from population-independent analysis can be used as the safety exclusion zone within which the access of human is strictly limited, so that within this zone, the population is minimized to the same level of P\_Case 1.

Table 9.7 shows the results of each case with modified populations. The risk criterion of 1.0E-3/year zone was not considered, because it is far too lenient. Figure 9.11 represents the F-N graph for modified population.

Table 9.7 Modified population (unit: persons).

Case	Risk criterion (1.0E-4/year)							Risk criterion (1.0E-5/year)						
	Zone 1	Zone 2	Zone 3	Zone 4	Zone 5	Zone 6	Zone 7	Zone 1	Zone 2	Zone 3	Zone 4	Zone 5	Zone 6	Zone 7
(a)	1	3	5	10	30	40	50	1	3	5	10	30	40	50
(b)	1	3	5	10	60	80	100	1	3	5	10	60	80	100
(c)	1	3	5	10	60	80	100	1	3	5	10	60	80	100
(d)	1	3	5	10	30	40	100	1	3	5	10	30	40	100
(e)	1	3	5	10	30	40	100	1	3	5	10	30	40	50
(f)	1	3	5	10	100	150	300	1	3	5	10	100	150	300
(g)	1	3	5	10	30	150	300	1	3	5	10	30	40	300
(h)	1	3	5	10	30	40	300	1	3	5	10	30	40	50
(i)	1	3	5	10	100	150	300	1	3	5	10	100	150	300
(j)	1	3	5	10	30	40	300	1	3	5	10	30	40	300
(k)	1	3	5	10	30	40	300	1	3	5	10	30	40	50

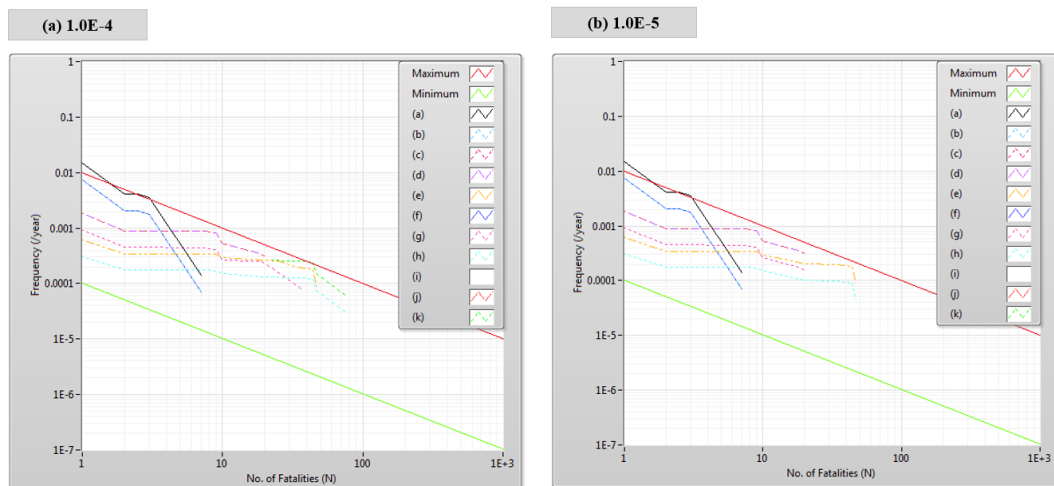


Figure 9.11. F-N curves for modified port population.

From this study it seems entirely reasonable to state that a safety exclusion zone is not necessary for the cases where the risk level is below the upper tolerable limit, provided all the safety procedures are strictly adhered to. It is also reasonably clear that the TTS is not appropriate for high volume transferring cases (Cases 3 and 4).

## 9.4. Concluding remarks

This study carried out quantitative risk assessment of LNG bunkering in relation to several parametric variables: bunkering method (transfer flow rate), bunkering volume, port population and tolerable risk criteria. Population-independent analysis was performed to determine critical distances, while the societal risks of LNG bunkering were investigated through population-dependent analysis.

As shown through parametric analysis, the overall results of risk assessment for LNG bunkering are influenced to some degree by parameters used in the analysis.

It was found that the total annual time required for bunkering is one of the most critical factors in determining the probability of occurrence of leaks. This is the most critical reason why the TTS method is unsuitable for high volume LNG bunkering from the safety point of view. Associated with this main parameter are other parameters, including pipe size, bunkering method, flow rate, bunkering capacity and population distribution. It was also found that the human presence should be strictly limited within safety exclusion zone so that the population condition 1 is achieved.

The population-independent analysis as recommended by ISO standards, class rules and other common practice guidelines can result in safety exclusion zones too extensive for practical application. It was found that a population-dependent analysis produces much more realistic safety exclusion zones by controlling the number of personnel near the bunkering area. A method of combining the two approaches in establishing acceptable safety exclusion zones has been demonstrated through this study.

It is thought that there may be a case for making the relevant rules and regulations more explicit and providing clear procedural guidance to assess the extent of the safety exclusion zone for LNG bunkering. However, it may require more extensive studies and discussion to draw a consensus on the standard database and scenarios

## 10. QUANTITATIVE RISK ASSESSMENT OF FPR WITH HP FGS SYSTEM

### 10.1. Introduction

As identified in Chapter 3, one of the potentially hazardous areas in LNG-fuelled ships is the fuel gas supply system in fuel preparation room. However, not much is known about the safety of this system, particularly HP FGS systems which can be found in large dual-fuel engines. Consequently, the safety of fuel preparation room containing high pressure fuel gas supply systems was systematically investigated in order to identify shortcomings and practical gaps of the current regulations.

A very large ore carrier of 300,000 DWT described Chapter 4 was taken as an example and the LNG fuel system was designed for it. Along with a fault tree and event tree analysis models, generic failure data from various sources were used to estimate frequency of potential explosion. For the consequence analysis computational fluid dynamics and finite element analysis software were used to estimate the impact of explosions on the boundary structure of the fuel preparation room.

### 10.2. Description of study

#### 10.2.1. *Ship information*

Even though the ship was described in fair details, the information is repeated here for the sake of completeness. This ship is the subject of ‘LNG-Ready Ships<sup>6</sup>’, a joint project between Korean Register (KR) and Hyundai

---

<sup>6</sup> Ships which can be easily retrofitted to use liquefied natural gas (LNG) bunkers.

Heavy Industries Co. Ltd. General specifications of the ship including operational profiles are summarised in Table 9.1.

The main engine was to be modified to a dual fuel engine and the LNG fuel system was designed for this ship in outline in accordance with the IGF Code, class rules and other relevant guidelines in cooperation with KR.

Table 10.1 General specifications of the case ship (KR 2015a).

Items	Specifications
L x B x D	328.0 m x 55.0 m x 29.0 m
Main Engine	Hyundai MAN B&W 6G80ME-C9 (before retrofit)
MCR/NCR	20,680 kW x 65.8 rpm/17,578 kW x 62.3 rpm
Speed	14.6 knots at sea trial
F.O. Consumption	abt. 67 tons/day
Cruising range	abt. 25,000 miles per one voyage from Brazil to East Asia
Cruising day	300 days per year at NCR

It was agreed by all parties concerned by that project that the best arrangement of the LNG fuel system was as represented in Figure 10.1. The proposed concept involves transforming No.4 cargo hold into the space for LNG fuel systems, placing the LNG fuel storage tank (IMO Type B Tank), the tank connection space and the FPR inside the same hold (KR 2015a). The load balance on the overall ship's structure and minimum interference to cargo operations were taken into consideration in the decision process. The ship's owner required the capacity of the LNG fuel storage tank to be at least 10,000 m<sup>3</sup>. The fuel supply to the engine room is through double wall pipes lying on the freeboard deck.

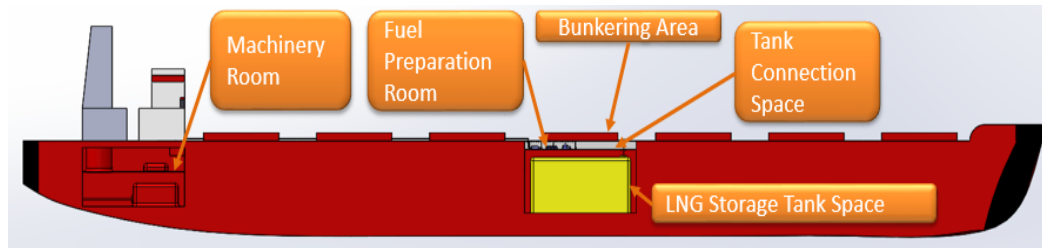


Figure 10.1. A proposed general arrangement of the LNG fuel system.

The FPR is 17 m long, 6 m wide and 2.5 m high. Originally the boundary walls of the FPR were designed with no special consideration given to the possible explosion inside. Instead, the general practice of ship structural design in similar cases of withstanding vibration and machinery loads was followed. However, three enhanced designs were also investigated in the consequence analysis.

The LNG supplied through the bunkering system is stored in the LNG storage tank from where two sets of submersible fuel supply pumps transfer the liquid fuel to FGS systems in the FPR. Since IGF Code requires the machinery room to be ‘gas-safe’, where any single failure is not to lead to fire/explosion, the fuel pipes inside the machinery room are made fully double-walled. On the other hand, if there are two engine rooms, the spaces are regarded as ‘ESD-protected’. In this case, if a gas leak is detected, the affected engine room is isolated by ESD system, leaving only the other one operational. For such arrangement double-walled pipes are not necessary. In addition, all confined spaces are fitted with exhaust type mechanical ventilation systems having a minimum capacity of 30 times per hour (IMO 2017; ABS 2015).

The concept design of the FGS systems was conducted in accordance with the engine maker’s specifications and the operational profile of the case ship, as these play a key role in determining the capacity of the FGS system, flow rate, pipe size, position, etc. The diameter of fuel supply line was determined to be 12.5 mm to meet the required fuel mass flow rate of 2,727.69 kg/h for the main engine (MAN Diesel and Turbo). It is to be noted, however, that the pipes of the FGS system are not double walled.

Detailed piping of the FGS system is given in Figure 10.2 and the specifications are summarised in Table 10.2. The FGS system for the main engine consists of a suction drum, HP pumps and a vaporizer. On the other hand, the FGS system for generator engines and auxiliary boiler has a boil-off gas (BOG) heater and compressors in order to adjust the temperature and pressure of the gas fed from the tank before being fed to the combustion systems.

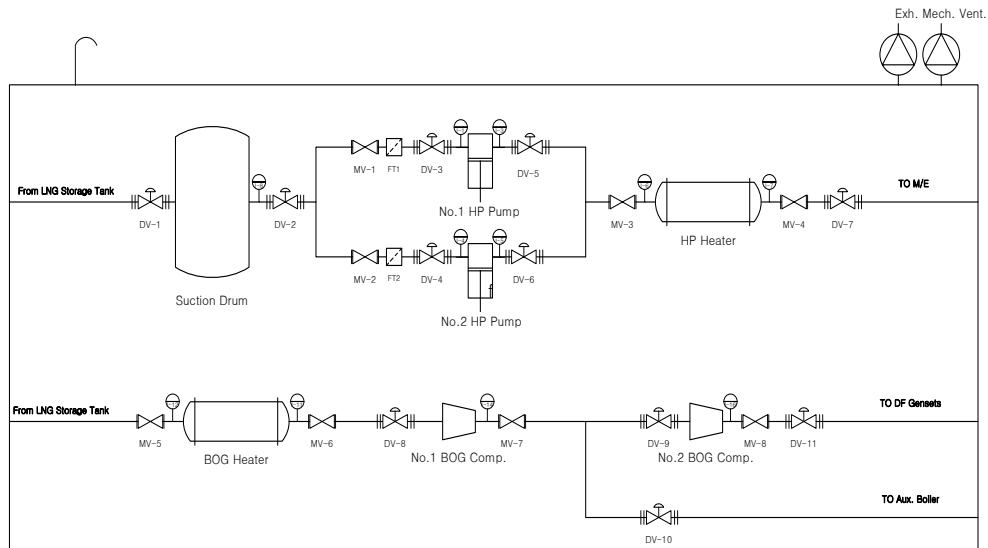


Figure 10.2. Concept design of the FGS system for the case ship.

Table 10.2 Specifications of the FGS system.

Items	Specifications
Mass flow rate for M/E	2,727.69 kg/h
Diameter of fuel supply line	12.5 mm
Working pressure	LPL for 5 bar , HPL for 300 bar
Working temperature	Liquid for 112K, Gas for 318K

The phase and condition of the fuel vary throughout this process, and, as a result, same size leak holes can cause different leak rates depending on their locations. In view of this, the FGS system for the main engine was grouped

into three sections: low pressure liquid (LPL), high pressure liquid (HPL) and high pressure vapour (HPV) sections. The FGS system for generator engines and auxiliary boiler was classified as low pressure vapour (LPV). The working pressure used in this study was 5 bars for low-pressure sections and 300 bars for high-pressure sections. The temperature of liquid section is 112K while vapour section is 318K (Republic of Korea 2014).

### *10.2.2. Approach adopted*

The IQRA software was utilized for frequency analysis where event tree analysis (ETA) was carried out for the fuel system to identify events that may cause vapour cloud explosion. General frequency data incorporated in the software from various sources was used and fault tree analysis (FTA) was applied where general fault data cannot be applied directly.

Unlike other case studies, some external numerical analysis programs were used in addition to IQRA software for consequence analysis. A CFD program was used to evaluate the effect of explosion while an FEA was employed for estimating the structural integrity against the impact of explosion. The research findings have shown that special attention needs to be paid to the structural design of FPR. It was also concluded from this study that the current rules are inadequate and urgently require clarification and updating (Versteeg and Malalasekera 2007).

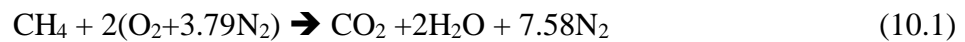
Consequence analysis consists of two parts: explosion analysis and structural analysis. In the explosion analysis the explosion is simulated using a CFD program and the magnitude of the consequent load on the FPR structure is determined, while in the structural analysis the effect of the load on the structure of the boundary wall of the FPR is assessed by means of an FEA software.

The impact of explosion on structures is a function of the ratio of fuel/air mixture and the distance from the ignition point (Versteeg and Malalasekera 2007). However, since the location of the ignition point will be



unpredictable and the ratio of fuel/air mixture is determined by various factors such as leak duration, the effectiveness of ventilation system and the time of ignition, it is hard to predict the properties of the explosion precisely. In this context a conservative model to investigate the worst-case will be safer than probabilistic models. Consequently, the explosion was modelled based on complete combustion of the ideal stoichiometric air/fuel ratio equivalent to 17.255 kg air for each kg of fuel (Versteeg and Malalasekera 2007).

The ignition point was assumed to be 1.0 m above the floor. This height was selected so as to apply a higher explosion impact load on the floor structure (room height is 2.5 m). Since LNG is primarily methane (CH<sub>4</sub>) with a small mixture of other hydrocarbons, the composition of the liquid fuel was assumed to be pure methane and the complete combustion equation for this study is given in Equation (10.1) (ISO 2013; Versteeg and Malalasekera 2007).



Risk is defined as the product of the probability of occurrence of an accident and its consequence. The consequence is usually expressed in terms of lives lost and injuries caused or financial losses sustained. In the current case, however, there is no direct danger to lives, since the FPR and the areas around it are normally unmanned. The damage to property is difficult to quantify, as it will be case-specific.

For these reasons, it was decided to examine the probability of occurrence of explosion as an item to be compared to the tolerable probability normally accepted by the industry. The consequence can also be examined by studying the stresses that the structure is likely to experience in the event of an explosion and comparing them to the allowable stresses of the material.

## 10.3. Risk assessment

### 10.3.1. Frequency analysis

In this step the frequency of initial leak, probability of safety system failures and probability of immediate/delayed ignition are estimated.

#### (a) Initial Leak Frequency

Since the FGS system is not categorized as a seriously risky section and consequently the pipes are not made double walled, the likelihood of initial leak from the pipes is much higher than in the engine room. The frequency of an initial leak from each equipment described in the conceptual design of FGS system was analysed with respect to three different leak hole sizes: 3 mm, 10 mm and full (12.5 mm) based on the DNV Leak Frequency Datasheets (DNV 2012a), and the results are summarised in Table 10.3.

Table 10.3 Frequency of initial leak with respect to leak size.

Section	Equipment List	No. of Equipment	Frequency of Leak (/year)		
			3mm leak	10mm leak	Full leak
LPL	Actuated valves	4	2.19E-03	6.89E-04	3.12E-04
	Filters	2	3.71E-03	1.83E-03	1.50E-03
	Flange	12	4.38E-04	1.59E-04	1.52E-04
	Manual valves	2	1.06E-04	4.60E-05	3.04E-05
	Pipe	14	1.33E-02	4.69E-03	2.17E-03
	Suction drum	1	9.46E-04	5.49E-04	8.57E-04
	Small gauge fittings	3	9.32E-04	4.08E-04	2.59E-04
	Total		2.16E-02	8.37E-03	5.28E-03
HPL	Actuate valves	2	1.10E-03	3.45E-04	1.56E-04
	HP pumps	2	7.37E-02	3.02E-02	1.66E-02
	Flange	6	2.19E-04	7.96E-05	7.61E-05
	Pipe	3	2.85E-03	1.00E-03	4.65E-04
	Small gauge fittings	3	9.32E-04	4.08E-04	2.59E-04
	Total		7.88E-02	3.21E-02	1.76E-02
HPV	Actuate valves	1	5.48E-04	1.72E-04	7.80E-05
	Flange	6	2.19E-04	7.96E-05	7.61E-05
	Heater	1	1.64E-03	7.71E-04	6.26E-04
	Pipe	3	2.85E-03	1.00E-03	4.65E-04
	Small gauge fittings	1	3.11E-04	1.36E-04	8.64E-05
	Total		5.56E-03	2.16E-03	1.33E-03
LPV	Actuated valves	4	2.19E-03	6.89E-04	3.12E-04
	BOG compressor	2	7.37E-02	3.02E-02	1.66E-02
	Flange	16	5.85E-04	2.12E-04	2.03E-04
	Heater	1	1.64E-03	7.71E-04	6.26E-04
	Manual valves	4	2.11E-04	9.20E-05	6.09E-05
	Pipe	20	1.90E-02	6.69E-03	3.10E-03
	Small gauge fittings	4	1.24E-03	5.43E-04	3.45E-04
	Total		9.85E-02	3.92E-02	2.13E-02

*(b) Probability of full leak/ventilation failure*

The final outcome of a fuel leak can be diverse, depending on the nature of the leak and functioning of the safety systems. The IGF Code has a mandatory requirement for all FPRs to be equipped with a gas detecting system. In addition, an exhaust type mechanical ventilation system with the capacity of 30 times air change each hour is required to blow the flammable gases out of the space continuously (IMO 2017; ABS 2015).

All fuel leak may not necessarily lead to a damaging outcome as long as both safety systems function effectively. However, there is a probability of the safety systems malfunctioning.

From this analysis the types of potential damaging outcomes were identified as fire and explosion. Asphyxiation is another accident outcome, but this was ignored, as it requires presence of a person in the FPR, which is unlikely as the FGS system is remotely controlled and a duty engineer is not normally exposed to a leak event in the room directly.

The gas detector triggers the alarm at 20 % of low explosive level (LEL) of fuel-air mixture, and activate the fuel change-over at 40 % of LEL, shutting down the gas inlet by activating the automatic cut-off valve fitted to the outside of the room and effecting change-over of the fuel system. Therefore, a failure of the gas detector can increase the fuel content in the room to higher than the LEL, leading to a late isolated sceanrio. On the other hand, even when the ventilation is working effectively, a high enough leak rate can lead to explosion scenarios (IMO 2017).

The probability of full leak scenario identified in the ETA is related to the failure of both manual and automatic isolation. The failure of manual isolation is caused by the failure of the gas detector or the alarm system, or the operator not taking or being able to take appropriate action when the alarm sounds, and this leads to the cut-off valve failing to close in time. Where automatic isolation is used, a failure of either leak detector or cut-off valve leads to the failure of the automatic shut-down. In both cases of failure the isolation of the leak is at least prolonged possibly for some time. Since there is no duty engineer constantly present, it is reseasonable to assume that the initial leak is to be detected by a gas detector rather than by a crew member.

The leaked liquid or gas fuel from a part of the FGS system may vaporize, disperse and be accumulated in the room. The proper operation of the ventilation system can remove the fuel gas from the

room or at least reduce the concentration level in the room. A failure of the ventilation system at the time of a leak will make this safety device useless.

The probability of safety system failure is obtained from various sources as shown in Table 10.4. The failure rate per year,  $\lambda$ , was calculated from the upper failure rates shown in the references given in the table.

Table 10.4 Reliability data for safety systems.

No.	Safety system list	$\lambda$	Reliability R(t)	Unreliability (1-R(t))	Reference
1	Gas detector	3.67E-01	0.6930	0.3070	(OREDA 2009)
2	Alarm	2.50E-04	0.99975	0.00025	(EPRI 1995)
3	Operator to obey alarm	-	0.97	0.03	(KletzT 1991)
4	Cut-off V/V	1.86E-02	0.9816	0.0184	(CCPS 1989)
5	Motor-driven fan	2.16E-01	0.805	0.195	
6	Change-over system	6.50E-03	0.99352	0.00648	

The failure rate per year,  $\lambda$ , was calculated from the upper failure rates given by the named sources. The reliability of each equipment was then estimated using Equation (10.2) (Santamaría and Brana 1998).

$$R(t) = e^{-\lambda t} \tag{10.2}$$

A fault tree analysis based on the reliability data showed that the probability of delayed isolation for one gas detector system was 0.113 as in Figure 10.3, while that of ventilation failure was 0.00126 as shown in Figure 10.4.

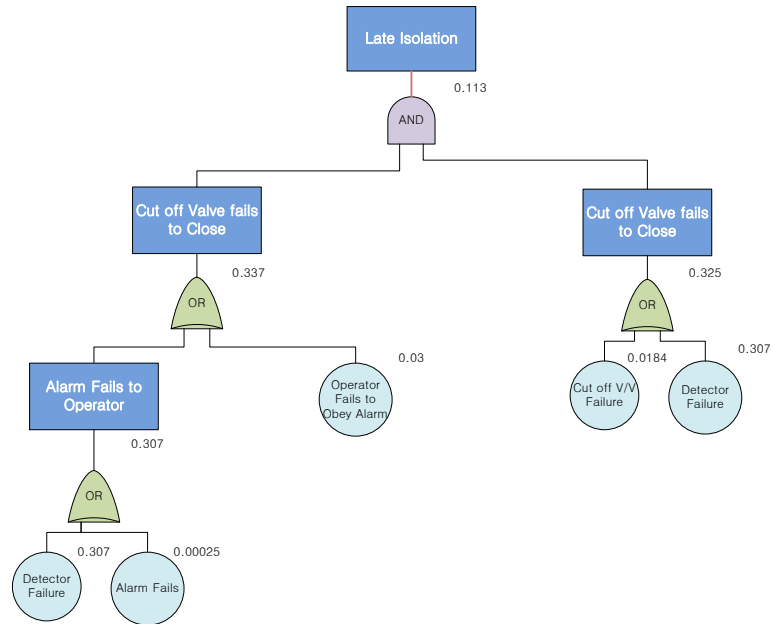


Figure 10.3. FT for late isolation with one gas detector system.

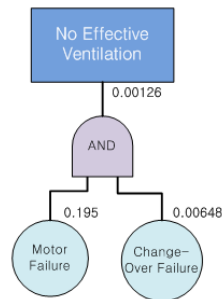


Figure 10.4. FTA for ventilation failure.

*(c) Probability of Immediate Ignition and Delayed Ignition*

Several models have been developed by the chemical industry to estimate the probability of ignition, but this study adopts DNV model (DNV 2013) for the probability of immediate ignition and OGP models as shown in Table 10.5 and Table 10.6.

Table 10.5 Probability of immediate ignition (DNV 2013).

Release rate (kg/s)		Immediate ignition probability
Gas	Liquid	
Less than 1	Less than 1.2	0.0001
1-10	1.2-25	0.001
Over 10	Over 25	0.01

Table 10.6 Probability of delayed ignition (OGP 2010c).

Release rate(kg/s)	Ignition condition		
	Gas (open deck)	Gas (congested)	Liquid
0.1	0.001	0.001	0.001
0.2	0.0011	0.0023	0.0014
0.5	0.0011	0.0066	0.0022
1	0.0012	0.015	0.003
2	0.0022	0.0174	0.0042
5	0.005	0.0213	0.0066
10	0.0091	0.0247	0.0092
20	0.0168	0.0287	0.0129
50	0.025	0.035	0.02
100	0.025	0.04	0.028
200	0.025	0.04	0.028
500	0.025	0.04	0.028
1000	0.025	0.04	0.028

### 10.3.2. Consequence analysis

The impact of an explosion can damage the structure of the FPR in any direction, possibly leading to subsequent spread of the accident to other compartments. As shown in Figure 10.5, the adjoining spaces of the FPR are a ballast tank, LNG storage tank space, tank connection room, a void space and No.3 and No.5 cargo holds. Although any damage to all the adjoining spaces matters, the LNG fuel storage tank space directly below the FPR is particularly vulnerable. Any breach of the storage tank can lead to a far more serious consequence. For this reason the consequence analysis of this study was focussed on the explosion impact on the bottom wall structure only.

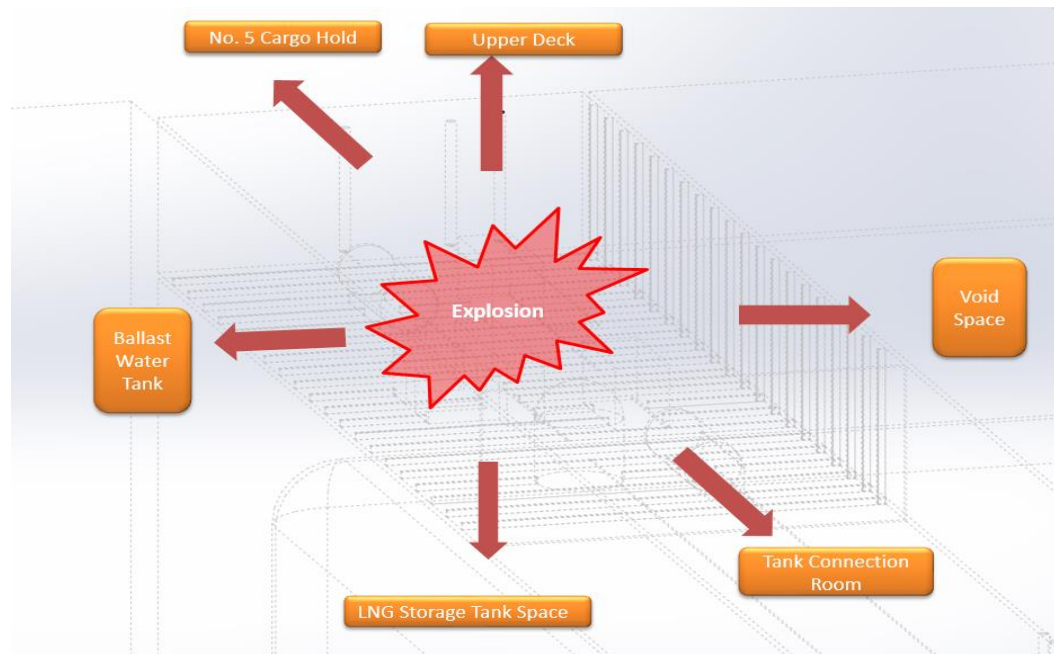


Figure 10.5. Possible directions of explosion impact.

*(a) Impact of Overpressure*

A series of test simulations was carried out to set up the explosion models. The benchmark used was the results of explosion simulations using FLACS described in an information document submitted to the CCC Sub-committee of IMO (Republic of Korea 2014). This document was the first study addressing the safety of a key fuel gas system component by examining the potential risk of explosion in an FPR containing an HP-FGS system. It concluded that the deterministic impact of an instantaneous explosion in the room would be significant.

Many combustion models are proposed. There is a big list of such models in literature but due to simplicity “The eddy break-up (EBU) model” proposed by Spalding and later modified by Magnussen and Hjertager (EDM - Eddy Dissipation Model) became one among the most popular models. It is based on the assumption that the reaction rate is controlled by turbulent mixing because of the dependence of reaction rate on the mixing of the turbulent eddies.



The same explosion conditions with the past IMO document were set up for this simulation. In order to predict the impact of explosion under the condition of complete combustion, this study employed STAR-CCM+, a CFD Code, using the premixed eddy break-up (PEBU) model which solves individual transport equations for mean species on the computational grid, tracking a fuel mass fraction on the grid through the equations. The PEBU model is widely used in combustion engineering, which interprets that rate of combustion is controlled rate of mixing.

The mean species concentrations are obtained as functions of the mean fuel mass fraction and a one-step global reaction scheme, which is internally calculated based on the unburnt gas composition (CD-adapco 2014). Since the flow is expected to be turbulent, it uses the Reynolds-averaged Navier-Stokes function with the  $k-\epsilon$  turbulence model which is compatible with the combustion model (Republic of Korea 2014).

In the document, with a gas leak of 5.353 kg the FLACS simulations predicted a maximum overpressure of 0.27 bars to the nearest wall at 0.75 m distance from the ignition point, and 3.7 bars for a 41.0 kg leak. For the test simulations with STAR-CCM+ the geometry of the FPR was built with a transverse 2D axisymmetric formulation. Mass ratios of fuel/air mixture equivalent to the condition used in the FLACS simulations were used. The results of 2D simulations were very close to the FLACS results with deviations of just over 10 % for 5.353 kg leak and less than 0.3 % for 41.0 kg leak as summarised in Table 10.7.

Table 10.7 Model verification tests.

Case	Scenario		Max. pressure		Deviation
	Leak Quantity	Mass Ratio Fuel/Air	FLACS (Republic of Korea 2014)	STAR-CCM+	
Case 1	5.353 kg	1:32.3	0.27 Bar	0.3Bar	0.03 Bar
Case 2	41.0 kg	1:4	3.7 Bar	3.71Bar	0.01 Bar

Figure 10.6 shows a 3D model of the conceptual FPR created in SolidWorks, a 3D modelling software, which was then transformed into a 2D axisymmetric model for CFD simulations as illustrated in Figure 10.7 and Table 10.8.

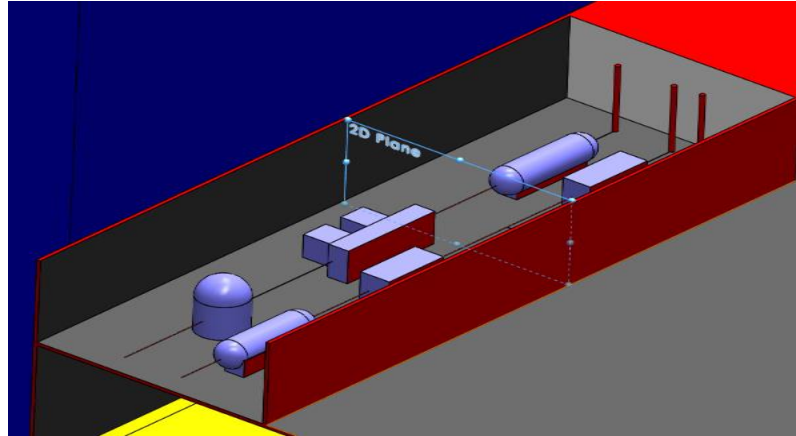


Figure 10.6. A 3D model of the FPR.

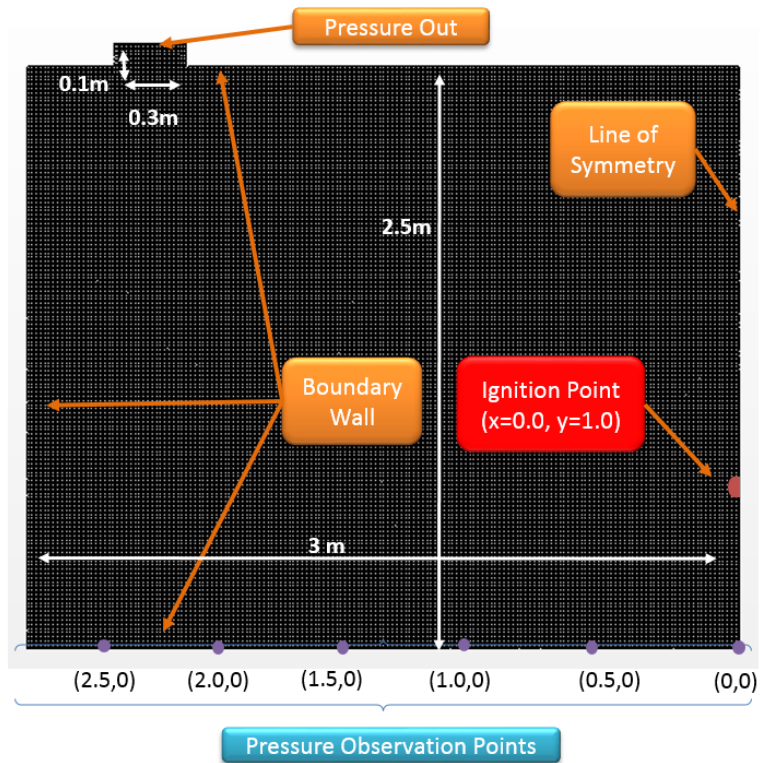


Figure 10.7. A 2D Model of the FPR.

Table 10.8 CFD simulation conditions.

Parameters	Value
2D Geometry	3.0m x 2.5m
Number of mesh cells	75,294
Initial temperature	293K
Initial pressure	101.3 kPa
Mass fractions of CH <sub>4</sub> , O <sub>2</sub> , N <sub>2</sub> (fuel-air ratio by mass 1:17.3)	0.0545, 0.2203, 0.7252

Since the explosion takes place within a very short time duration, the leak of the fuel during the process of explosion was ignored. The initial atmospheric pressure and temperature of the FPR were assumed to be 101.3 kPa and 293 K, respectively, and it was also assumed that there was no initial movement of air in the room. In order to investigate the maximum damage of the bottom structure rather than the equipment in the room, the pipes and equipment, which are normally situated below the potential explosion point, were not modelled. Numerically, the blast wave is driven by the initial conditions defined in the ignition point at (0.0, 1.0), focusing on the magnitude of overpressure imposed on the bottom wall structure which forms a boundary with the LNG storage tank space. The explosion was modelled as a complete combustion with the ideal stoichiometric fuel/air ratio equivalent to 1:17.3 in an attempt to investigate the maximum impact of explosion (Versteeg and Malalasekera 2007). The maximum overpressure is observed on the bottom wall at every 0.5 m. For the simulation, an implicit unsteady model was adopted with a very small time step of 1E-7 and the second order accuracy was used for both space and time.

*(b) Structural Analysis*

To assess the structural strength of the FPR with respect to the load produced by a gas explosion, ANSYS 15 was used. The floor of the FPR is a simple stiffened plate as shown in Figure 10.8. The primary stiffeners are transverse girders at 3,400 mm spacing and the deck longitudinals are spaced at 750 mm.

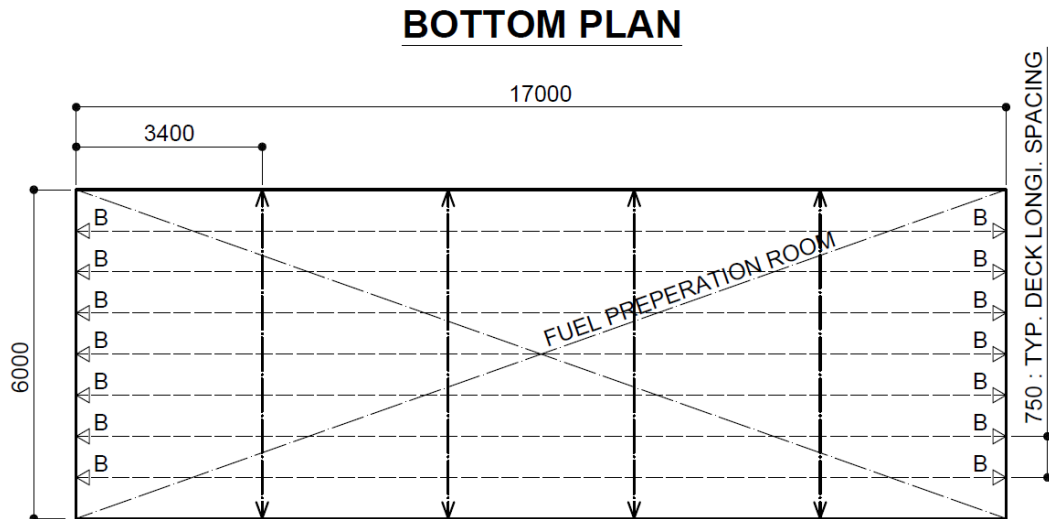


Figure 10.8. Details of the FPR floor structure.

In order to identify the minimum scantlings which can withstand the explosion load obtained from the simulation four different cases were studied using various sizes of primary supporting members, secondary members and the thickness of the base plate. These cases are summarised in Table 10.9. The girders were designed according to general shipyard practices, where the depth of the web is usually made three times the width of the face plate. It was assumed that all the structural members are made of normal structural steel, as defined by classification rules (DNV 2015), with the yield strength of 235 N/mm<sup>2</sup>. An example modelling of Case 1 is shown in Figure 10.9. For the FE analysis, the mesh size was kept at 50 mm throughout.

Table 10.9 Stiffened designs for each case.

	Case 1	Case 2	Case 3	Case 4
<b>Primary supporting member</b>	500x12+100x15 (T) <sup>7</sup>	700x12+100x15 (T)	900x15+200x18 (T)	1,100x15+200x18 (T)
<b>Secondary member</b>	100x75x10/14 A <sup>8</sup>	200x90x10/14 A	300x90x11/16 A	400x100x13/18 A
<b>Thickness of base plate</b>	10 mm	12 mm	14 mm	16 mm

<sup>7</sup> (web depth x web thickness + face plate breadth x face plate thickness)

<sup>8</sup> (web depth x flange breadth x web thickness/flange thickness)

<b>Total number of elements (for simulation)</b>	56,080	62,760	68,760	77,080
--	--------	--------	--------	--------

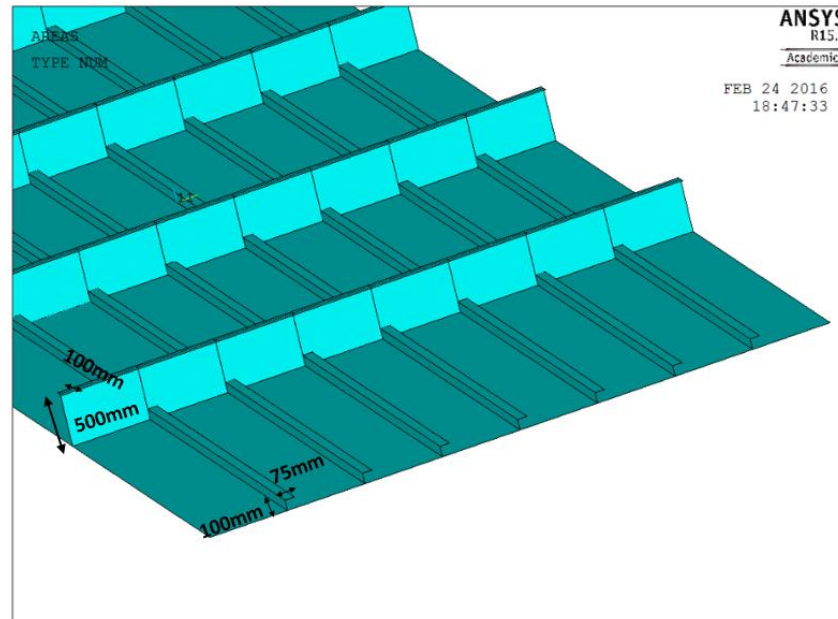


Figure 10.9. The stiffened bottom panel of the FPR for Case 1.

### 10.3.3. Assessment results

#### (a) Results of Frequency Analysis

From the frequency analysis using the ETA, the frequency of potential explosion for each case was estimated as shown in Table 10.10. The overall frequency of explosion is obtained by summing all the cases as illustrated in an FTA of Figure 10.10.

Table 10.10 Result of ETA for various cases.

Section	Case (Hole Size)	Leak Rate (kg/s)	Initial Frequency (/year)	Immediate Ignition	Leak Duration (Full Leak)		Ventilation System		Del. Ignition		Accident Equation (/year)	Accident Type
					Limited Leak	0.8902	Eff. Vent.	0.9987				
LPL Section	Case1_1 (3mm Leak)	0.0888	2.16E-02	0.0001	-	-	-	-	-	-	2.16E-06	Pool Fire
				0.9999	Limited Leak	0.8902	Eff. Vent.	0.9987			1.92E-02	No ignition
							No Eff. Vent.	0.0013	Delayed Ignition	0.001	2.42E-08	Flash/pool Fire
							No Ignition	0.999		0.999	2.42E-05	Gas Dispersion
					Late Isolated Leak	0.1098	Eff. Vent.	0.9987	Delayed Ignition	0.001	2.37E-06	Explosion
							No Ignition	0.999		0.999	2.37E-03	Gas Dispersion
						0.0013	Delayed Ignition	0.001	2.99E-09	Explosion		

							No Eff. Vent		No Ignition	0.999	2.98E-06	Flammable gas confined							
	Case1_2 (10mm Leak)	0.9870	8.37E-03	0.0001	-	-	-	-	-	-	8.37E-07	Pool Fire							
				0.9999	Limited Leak	0.8902	Eff. Vent.	0.9987	-	-	7.44E-03	No ignition							
							No Eff. Vent	0.0013	Delayed Ignition	0.015	1.41E-07	Flash/pool Fire							
				0.9999	Limited Leak	0.8902	Eff. Vent.	0.9987	Delayed Ignition	0.015	1.38E-05	Explosion	No Ignition	0.985	9.25E-06	Gas Dispersion			
													No Ignition	0.985	9.04E-04	Gas Dispersion			
				0.9999	Late Isolated Leak	0.1098	Eff. Vent.	0.9987	Delayed Ignition	0.015	1.74E-08	Explosion	No Ignition	0.985	1.14E-06	Flammable gas confined			
	No Ignition	0.985	1.14E-06										Flammable gas confined						
	Case1_3 (Full Leak)	1.54	5.28E-03	0.0010	-	-	-	-	-	-	-	5.28E-06	Pool Fire						
				0.9990	Limited Leak	0.8902	Eff. Vent.	0.9987	-	-	4.69E-03	No ignition							
							No Eff. Vent	0.0013	Delayed Ignition	0.0174	1.03E-07	Flash/pool Fire							
				0.9990	Limited Leak	0.8902	Eff. Vent.	0.9987	Delayed Ignition	0.0174	1.01E-05	Explosion	No Ignition	0.9826	5.82E-06	Gas Dispersion			
													No Ignition	0.9826	5.68E-04	Gas Dispersion			
0.9990				Late Isolated Leak	0.1098	Eff. Vent.	0.9987	Delayed Ignition	0.0174	1.27E-08	Explosion	No Ignition	0.9826	7.17E-07	Flammable gas confined				
	No Ignition	0.9826	7.17E-07									Flammable gas confined							
HPL Section	Case2_1 (3mm Leak)	0.6890	7.88E-02	0.0001	-	-	-	-	-	-	7.88E-06	Pool Fire							
				0.9999	Limited Leak	0.8902	Eff. Vent.	0.9987	-	-	7.01E-02	No ignition							
							No Eff. Vent	0.0013	Delayed Ignition	0.0150	1.33E-06	Flash/pool Fire							
				0.9999	Limited Leak	0.8902	Eff. Vent.	0.9987	Delayed Ignition	0.015	1.30E-04	Explosion	No Ignition	0.985	8.71E-05	Gas Dispersion			
													No Ignition	0.985	8.51E-03	Gas Dispersion			
				0.9999	Late Isolated Leak	0.1098	Eff. Vent.	0.9987	Delayed Ignition	0.015	1.63E-07	Explosion	No Ignition	0.985	1.07E-05	Flammable gas confined			
													No Ignition	0.985	1.07E-05	Flammable gas confined			
				Case2_2 (10mm Leak)	7.6600	3.21E-02	0.0010	-	-	-	-	-	-	-	3.21E-05	Pool Fire			
							0.9990	Limited Leak	0.8902	Eff. Vent.	0.9987	-	-	2.85E-02	No ignition				
										No Eff. Vent	0.0013	Delayed Ignition	0.0247	8.88E-07	Flash/pool Fire				
							0.9990	Limited Leak	0.8902	Eff. Vent.	0.9987	Delayed Ignition	0.0247	8.68E-05	Explosion	No Ignition	0.9753	3.51E-05	Gas Dispersion
																No Ignition	0.9753	3.43E-03	Gas Dispersion
	0.9990	Late Isolated Leak	0.1098				Eff. Vent.	0.9987	Delayed Ignition	0.0247	1.09E-07	Explosion	No Ignition	0.9753	4.32E-06	Flammable gas confined			
				No Ignition	0.9753	4.32E-06							Flammable gas confined						
	Case2_3 (Full Leak)	12.00	1.76E-02	0.0010	-	-	-	-	-	-	-	1.76E-05	Pool Fire						
				0.9990	Limited Leak	0.8902	Eff. Vent.	0.9987	-	-	1.56E-02	No ignition							
							No Eff. Vent	0.0013	Delayed Ignition	0.0287	5.66E-07	Flash/pool Fire							
				0.9990	Limited Leak	0.8902	Eff. Vent.	0.9987	Delayed Ignition	0.0287	5.53E-05	Explosion	No Ignition	0.9713	1.92E-05	Gas Dispersion			
													No Ignition	0.9713	1.87E-03	Gas Dispersion			
				0.9990	Late Isolated Leak	0.1098	Eff. Vent.	0.9987	Delayed Ignition	0.0287	6.98E-08	Explosion	No Ignition	0.9713	2.36E-06	Flammable gas confined			
													No Ignition	0.9713	2.36E-06	Flammable gas confined			

HPV Section	Case3_1 (3mm Leak)	0.3290	5.56E-03	0.0001	-	-	-	-	5.56E-07	Jet Fire		
				0.9999	Limited Leak	0.8902	Eff. Vent.	0.9987	-	-	4.95E-03	No ignition
							No Eff. Vent.	0.0013	Delayed Ignition	0.0066	4.12E-08	Flash/pool Fire
							No Ignition		0.9934	6.20E-06	Gas Dispersion	
					Late Isolated Leak	0.1098	Eff. Vent.	0.9987	Delayed Ignition	0.0066	4.02E-06	Explosion
							No Ignition		0.9934	6.06E-04	Gas Dispersion	
				No Eff. Vent.	0.0013	Delayed Ignition	0.0066	5.08E-09	Explosion			
				No Ignition		0.9934	7.64E-07	Flammable gas confined				
	Case3_2 (10mm Leak)	3.6500	2.16E-03	0.0010	-	-	-	-	2.16E-06	Jet Fire		
				0.9990	Limited Leak	0.8902	Eff. Vent.	0.9987	-	-	1.92E-03	No ignition
							No Eff. Vent.	0.0013	Delayed Ignition	0.0213	5.16E-08	Flash/pool Fire
							No Ignition		0.9787	2.37E-06	Gas Dispersion	
					Late Isolated Leak	0.1098	Eff. Vent.	0.9987	Delayed Ignition	0.0213	5.04E-06	Explosion
							No Ignition		0.9787	2.32E-04	Gas Dispersion	
				No Eff. Vent.	0.0013	Delayed Ignition	0.0213	6.37E-09	Explosion			
			No Ignition		0.9787	2.93E-07	Flammable gas confined					
Case3_3 (Full Leak)	5.70	1.33E-03	0.0010	-	-	-	-	1.33E-06	Jet Fire			
			0.9990	Limited Leak	0.8902	Eff. Vent.	0.9987	-	-	1.18E-03	No ignition	
						No Eff. Vent.	0.0013	Delayed Ignition	0.0247	3.69E-08	Flash/pool Fire	
						No Ignition		0.9753	1.46E-06	Gas Dispersion		
				Late Isolated Leak	0.1098	Eff. Vent.	0.9987	Delayed Ignition	0.0247	3.60E-06	Explosion	
						No Ignition		0.9753	1.42E-04	Gas Dispersion		
			No Eff. Vent.	0.0013	Delayed Ignition	0.0247	4.55E-09	Explosion				
			No Ignition		0.9753	1.80E-07	Flammable gas confined					
LPV Section	Case4_1 (3mm Leak)	0.0055	9.85E-02	0.0001	-	-	-	-	9.85E-06	Jet Fire		
				0.9999	Limited Leak	0.8902	Eff. Vent.	0.9987	-	-	8.76E-02	No ignition
							No Eff. Vent.	0.0013	Delayed Ignition	0.0010	1.11E-07	Flash/pool Fire
							No Ignition		0.999	1.10E-04	Gas Dispersion	
					Late Isolated Leak	0.1098	Eff. Vent.	0.9987	Delayed Ignition	0.001	1.08E-05	Explosion
							No Ignition		0.999	1.08E-02	Gas Dispersion	
				No Eff. Vent.	0.0013	Delayed Ignition	0.001	1.36E-08	Explosion			
				No Ignition		0.999	1.36E-05	Flammable gas confined				
	Case4_2 (10mm Leak)	0.0606	3.92E-02	0.0001	-	-	-	-	3.92E-06	Jet Fire		
				0.9999	Limited Leak	0.8902	Eff. Vent.	0.9987	-	-	3.49E-02	No ignition
							No Eff. Vent.	0.0013	Delayed Ignition	0.0010	4.40E-08	Flash/pool Fire
							No Ignition		0.999	4.40E-05	Gas Dispersion	
					Late Isolated Leak	0.1098	Eff. Vent.	0.9987	Delayed Ignition	0.001	4.30E-06	Explosion
							No Ignition		0.999	4.30E-03	Gas Dispersion	
				No Eff. Vent.	0.0013	Delayed Ignition	0.001	5.43E-09	Explosion			
			No Ignition		0.999	5.42E-06	Flammable gas confined					
Case4_3 (Full Leak)	5.70	2.13E-02	0.0001	-	-	-	-	2.13E-06	Jet Fire			
			0.9999	Limited Leak	0.8902	Eff. Vent.	0.9987	-	-	1.89E-02	No ignition	

						No Eff. Vent	0.0013	Delayed Ignition	0.0010	2.39E-08	Flash/pool Fire
								No Ignition	0.999	2.39E-05	Gas Dispersion
				Late Isolated Leak	0.1098	Eff. Vent.	0.9987	Delayed Ignition	0.001	2.33E-06	Explosion
								No Ignition	0.999	2.33E-03	Gas Dispersion
						No Eff. Vent	0.0013	Delayed Ignition	0.001	2.95E-09	Explosion
								No Ignition	0.999	2.94E-06	Flammable gas confined
Sum of Explosion Frequency									3.14E-04		/year

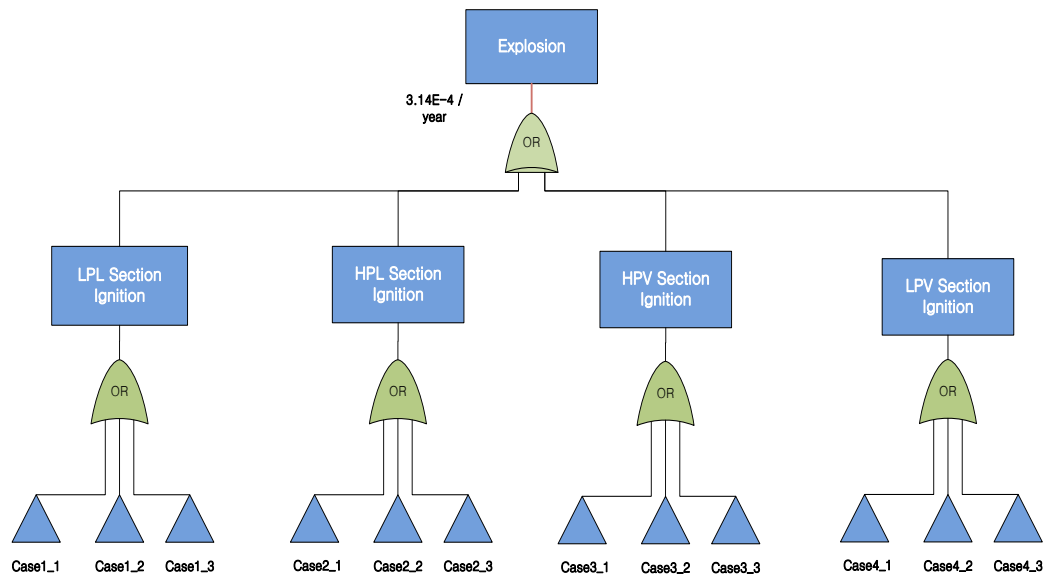


Figure 10.10. FTA showing the overall frequency of explosion.

The minimum leak rate which can lead to the fuel-air mixture equivalent to the LEL for the given size of the room and the ventilation devices was identified through a simple ventilation simulation. From this study it was determined that the explosion scenarios associated with 3 mm and 10 mm leak in LPV section, where leak rate is less than 0.07 kg/s, has little possibility of explosion as long as the ventilation system is effectively working. Therefore, the explosion frequencies associated with these scenarios were set to nil. The overall frequency of explosion was estimated to be 3.14E-4 /year.

Since there are no explicit guidelines for regulating risk levels for LNG-fuelled ships, the impairment frequency limit of 1.00E-4 /year suggested by NORSOKZ-013 was used to judge the acceptability of the



explosion frequency (NORSOK 2001). It is clear that the overall frequency exceeds this limit by a large margin, and the cases associated with the HPL section contributes to this frequency the most.

#### 10.4. Results of consequence analysis

The spread of overpressure as the explosion progresses can be observed in the flame contours of Figure 10.11. The result of the simulation found that the pressure at the ignition point immediately after ignition was 8.4 bars.

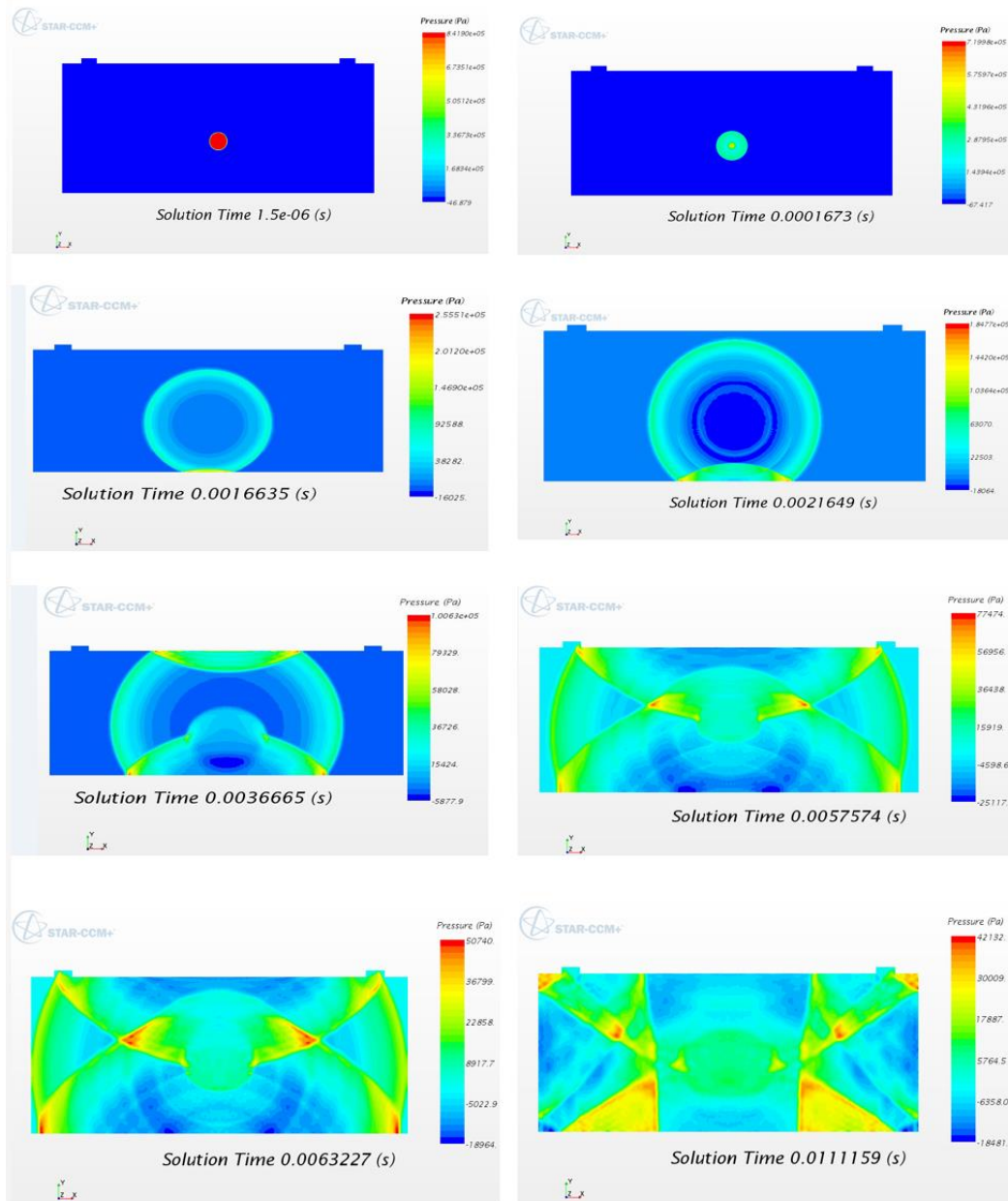


Figure 10.11. Progress of explosion.

The maximum overpressure on the floor at various transverse distances away from the ignition point obtained from the explosion simulation is summarised in Figure 10.12. It can be seen that the maximum overpressure at the centre of the floor is 291 kPa and it decreases as it proceeds away from the centre.

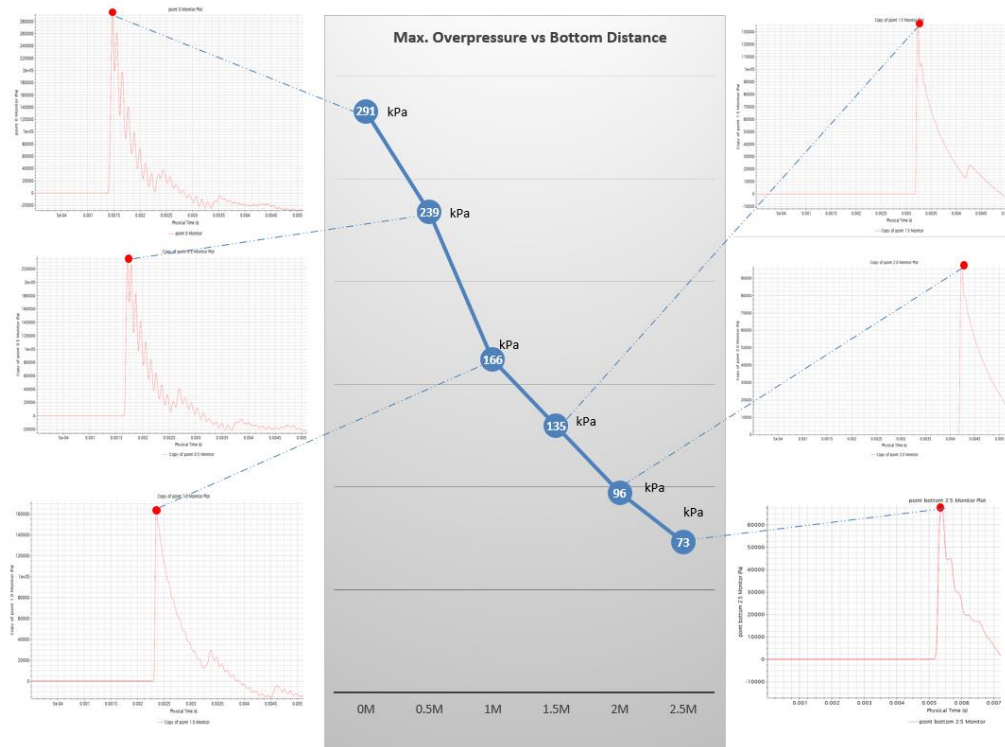


Figure 10.12. Maximum pressure on the floor at various distances from the ignition point.

Accordingly the pressure load as shown in Figure 10.13 was applied in the structural analysis: 291 KPa from the centre to the 0.5m radius, 239 KPa between 0.5 m and 1.0 m radius, 166 KPa between 1.0 m and 1.5 m radius, 135 KPa between 1.5 m and 2.0 m radius, 96 KPa between 2.0 m and 2.5 m radius and 73 KPa between 2.5 m and 3.0 m radius.

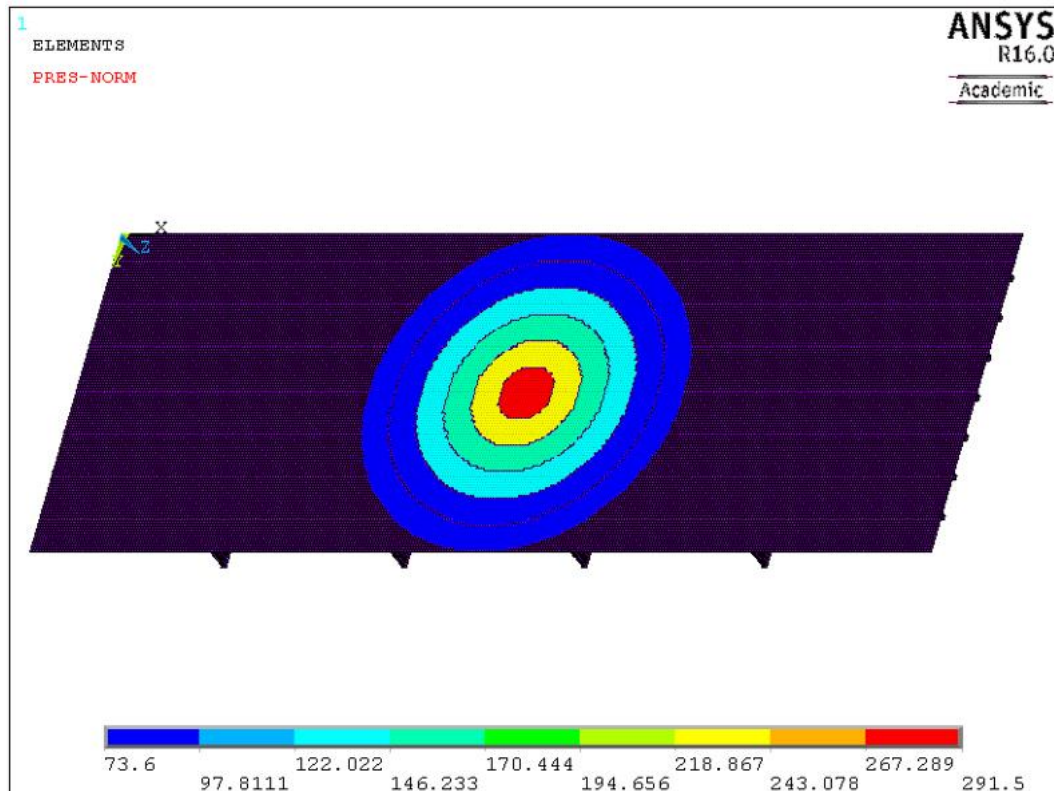


Figure 10.13. Pressure load applied in FE analysis.

The results of the FEA are presented in Figure 10.14 to Figure 10.16 in the form of shear stress, bending stress and equivalent stress for the four cases.

The maximum stresses to be experienced by the floor of the FPR in the event of an explosion are compared with the allowable stresses specified by the DNV GL Rule (DNV 2015) as shown in Table 10.11. It can be seen that all but Case 4 with the highest scantlings fails. This demonstrates that the boundary walls of the FPR must be strengthened considerably if the effects of any potential explosion are to be contained within it.

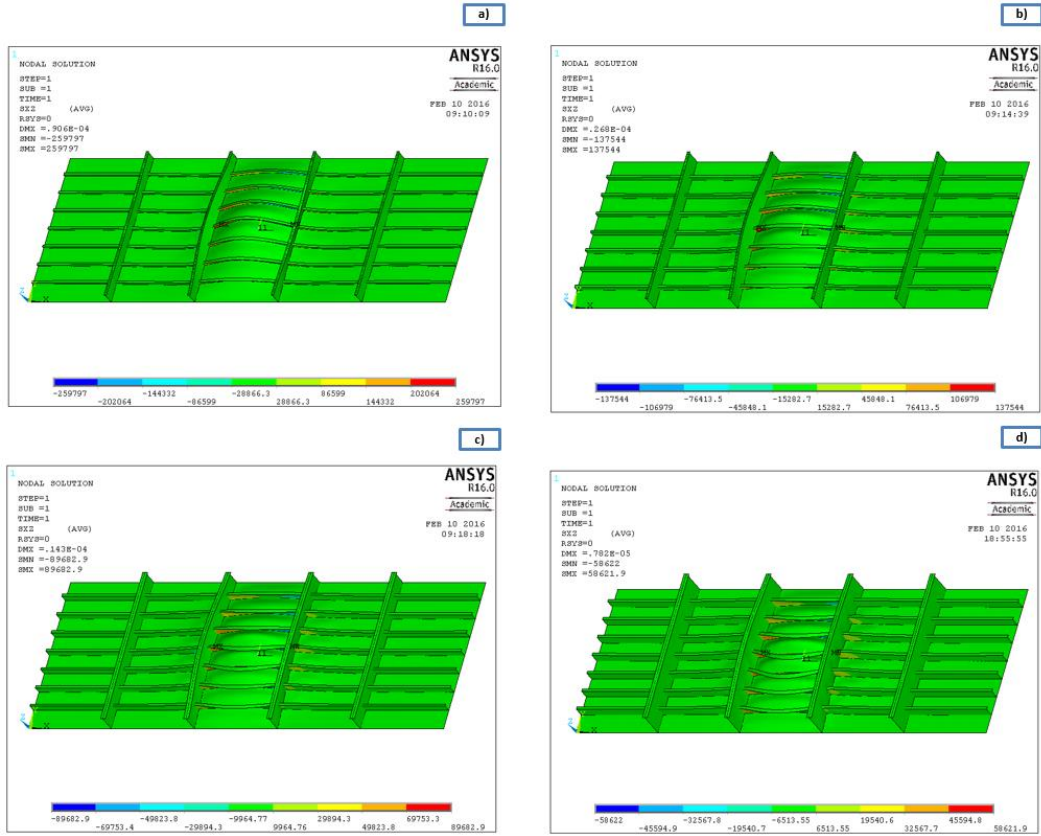


Figure 10.14. Shear stress on the floor: (a) Case 1; (b) Case 2; (c) Case 3; (d) Case 4.

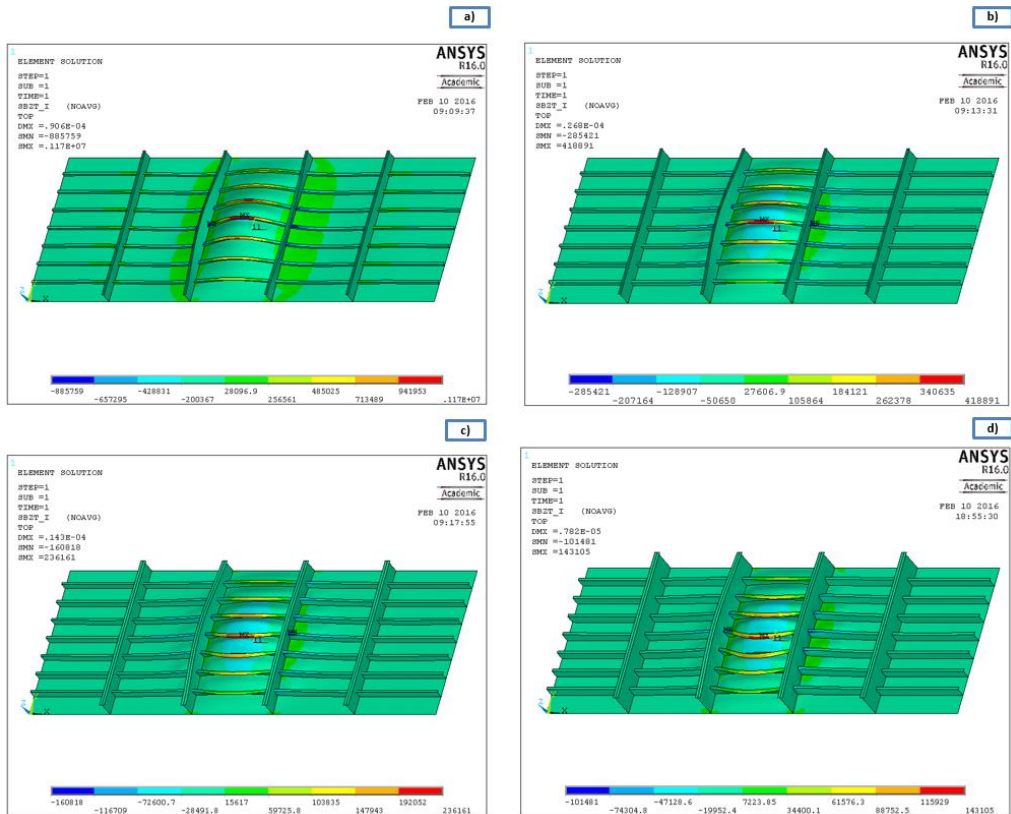


Figure 10.15. Bending stress on the floor: (a) Case 1; (b) Case 2; (c) Case 3; (d) Case 4.

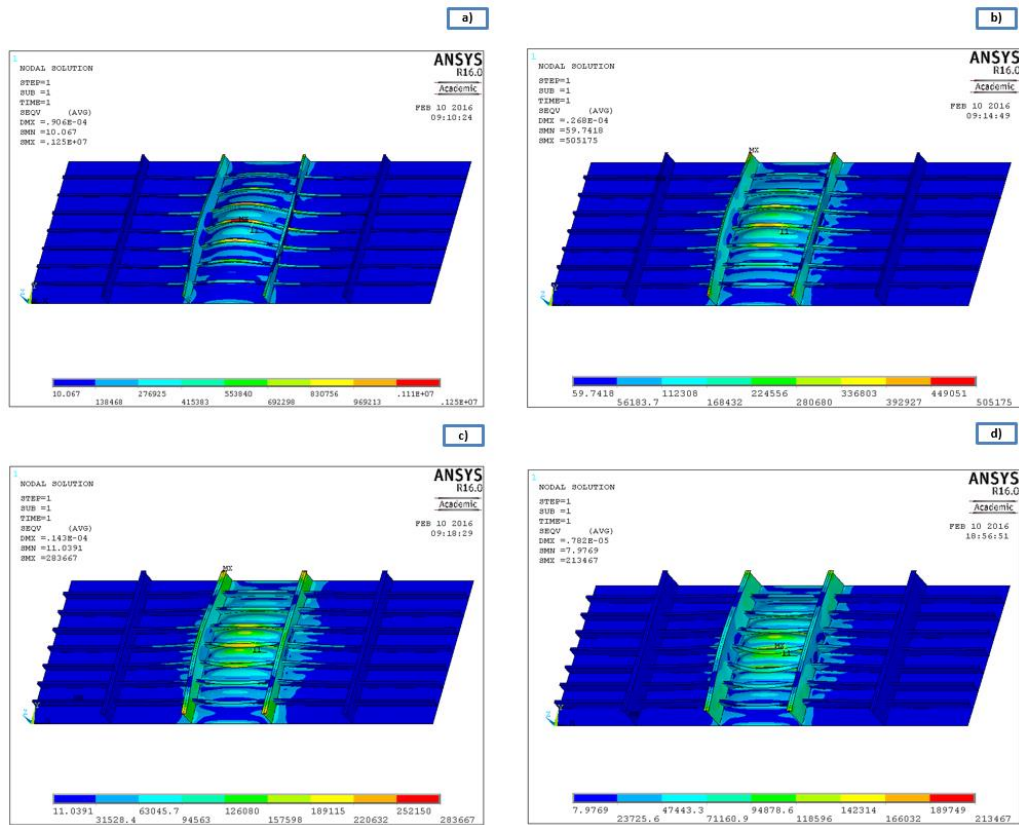


Figure 10.16. Equivalent stress on the floor: (a) Case 1; (b) Case 2; (c) Case 3; (d) Case 4.

Table 10.11 Summary of stresses for various scantlings.

Type of Stress	Allowable Stress (N/mm <sup>2</sup> )	Maximum Actual Stress (N/mm <sup>2</sup> )			
		Case1	Case 2	Case 3	Case 4
Shear stress	90.0	259.7	137.5	89.6	58.6
Bending stress	160.0	1170.0	440.1	243.2	143.1
Equivalent stress	245.0	1250.0	505.1	283.6	213.4

### 10.5. Sensitivity analysis

This study chose an arbitrary ignition point to investigate the risk of FPR associated with explosion. Given the fact that the explosion impact much depends on the distance from the ignition point, this generic approach may cause some uncertainties in the results of consequence in a quantitative sense. In addition, the assumption of complete combustion may have resulted in overestimation of explosion impact for some cases. In this context, a sensitivity

analysis was carried out to study the impact for various points of ignition with several cases of methane compositions – about 5 % (air-rich) shown in Equation (10.3), 10 % (near complete combustion) and about 15 % (fuel-rich) vol/vol shown in Equation (10.4) (Versteeg and Malalasekera 2007). The results are presented in Figure 10.17.

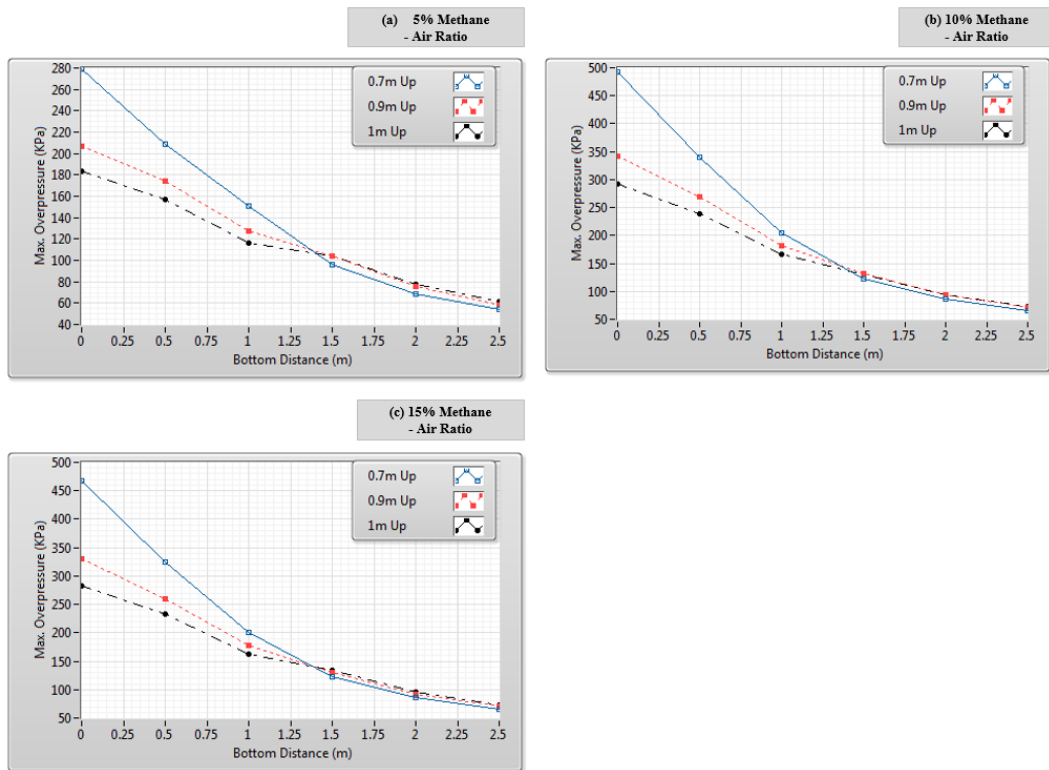
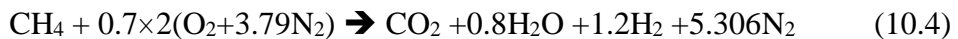
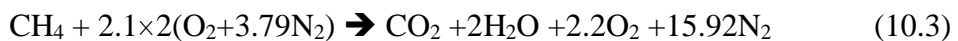


Figure 10.17. Maximum pressure on the floor at various distances from the ignition points and methane compositions.

Using the results of CFD analysis associated with alternative explosion scenarios, FE analysis was carried out. The results are shown in Table 10.12 where the regions shaded with red refer to unacceptably high stresses. As expected, the closer the ignition point from the floor, the higher the stress on the bottom structure of FPR was. The near-perfect combustion condition (about 10 % of methane-air ratio) led to higher impact of explosion. In addition, the fuel-rich condition (about 15 % of methane-air ratio) tended to have higher consequences than the fuel-scarce condition (about 5 % of methane-air ratio).



The results of this sensitivity study indicate that these parameters significantly affect the impact of potential explosion, implying that the impact of explosion can be mitigated by controlling ignition points and methane-air ratio.



Table 10.12 Summary of stresses associated with alternative scenarios for various scantlings.

Stress Type	Allowable Stress (N/mm <sup>2</sup> )	Methane-Air Ratio	Ignition Point (vertical distance from floor)	Maximum Actual Stress (N/mm <sup>2</sup> )			
				Case 1	Case 2	Case 3	Case 4
Shear Stress	90	5 %	0.7 m	214.2	120.8	80.6	57.6
			0.9 m	174.4	97.1	64.6	46.1
			1 m	156.8	87.1	57.9	41.3
		10 %	0.7 m	339.3	194.9	130.6	93.9
			0.9 m	267.6	150.9	100.6	72.0
			1 m	259.7	137.5	89.6	58.6
		15 %	0.7 m	326.2	186.9	125.1	90.0
			0.9 m	259.7	146.3	97.5	69.8
			1 m	230.7	129.3	86.1	61.6
Bending Stress	160	5 %	0.7 m	1000.0	376.0	213.8	141.9
			0.9 m	785.2	292.7	167.3	111.0
			1 m	695.6	259.7	149.1	98.9
		10 %	0.7 m	1680.0	634.5	360.9	239.7
			0.9 m	1250.0	468.9	267.1	177.2
			1 m	1170.0	440.1	243.2	143.1
		15 %	0.7 m	1600.0	605.0	344.1	288.5
			0.9 m	1121.0	453.6	258.4	171.5
			1 m	1060.0	395.1	225.9	149.8
Equivalent Stress	245	5 %	0.7 m	1070.0	400.5	227.7	200.0
			0.9 m	833.1	376.1	213.7	151.5
			1 m	738.1	361.2	205.3	134.3
		10 %	0.7 m	1780.0	666.6	373.0	352.9
			0.9 m	1330.0	517.8	294.3	248.9
			1 m	1250.0	505.1	283.6	213.4
		15 %	0.7 m	1700.0	635.6	355.5	334.5
			0.9 m	1129.0	507.2	288.3	240.4
			1 m	1120.0	485.5	275.9	207.3

### 10.6. Additional reference

To identify the minimum leak rate which can lead to LEL of fuel-air mixture, a simple ventilation analysis was conducted by using STAR-CCM+. Under effective ventilation condition with capacity of 2.57 kg/s equivalent to 30 times air change each hour for the FPR (17m x 6m x 2.5m), it was found that the continuous leak with 0.07kg/s converged to the volume fraction of CH<sub>4</sub> of 5%

(same as methane LEL). Therefore, the probability of explosion for small leak rate of less than 0.07 kg/s was ignored (see Figure 10.18 to Figure 10.20).

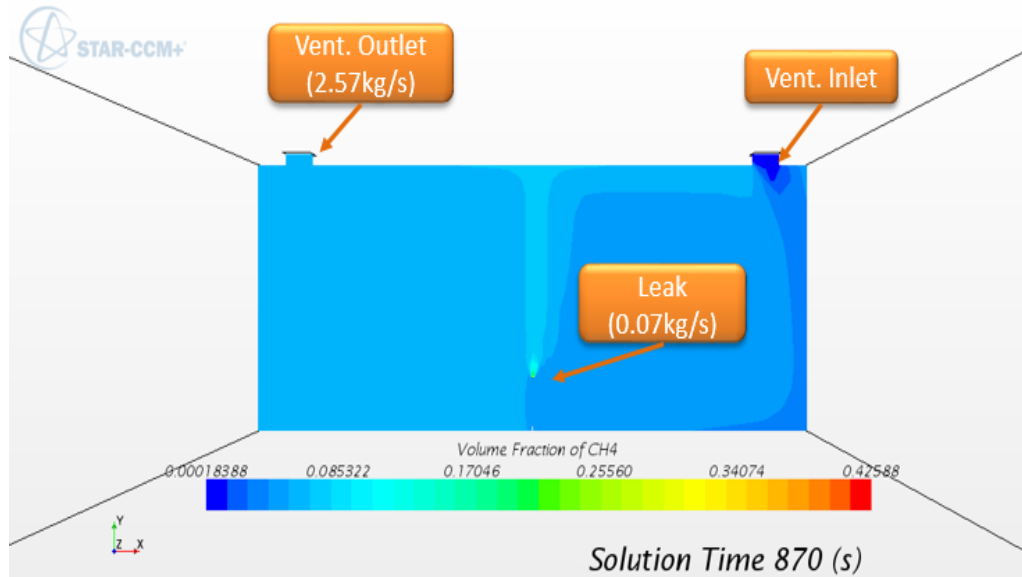


Figure 10.18. Ventilation analysis of FPR at 0.07 kg/s leak.

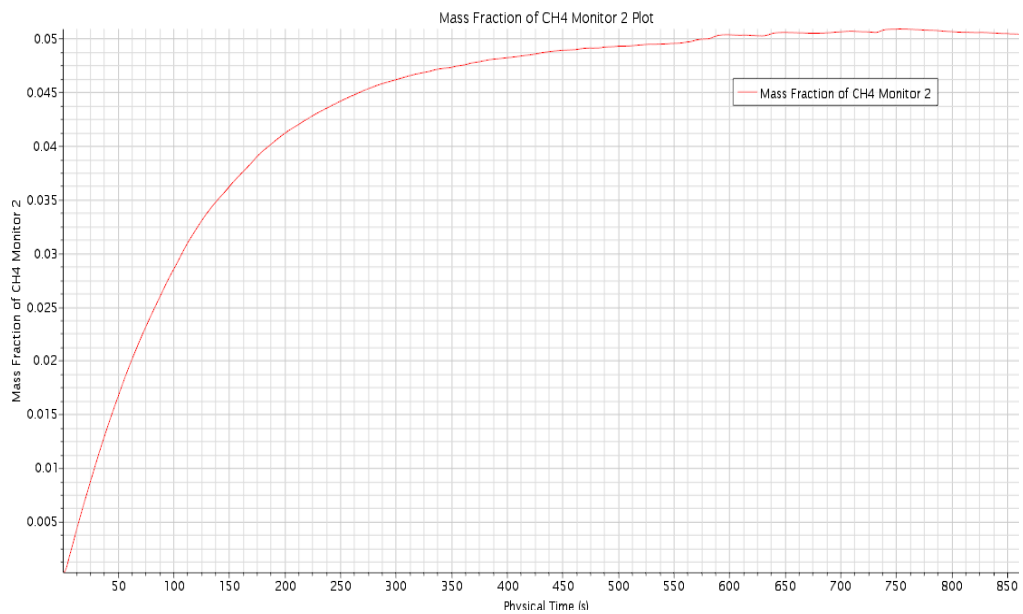


Figure 10.19. Mass fraction of CH<sub>4</sub> over time at 0.07 kg/s leak.

In order to verify the mesh independence in the explosion analysis, a mesh convergence test was conducted with three different base mesh sets (0.02m,

0.015m and 0.01m). Figure 10.20 shows the result. It can be seen that the finer two mesh systems produce more or less identical results with deviations well within the acceptable level.

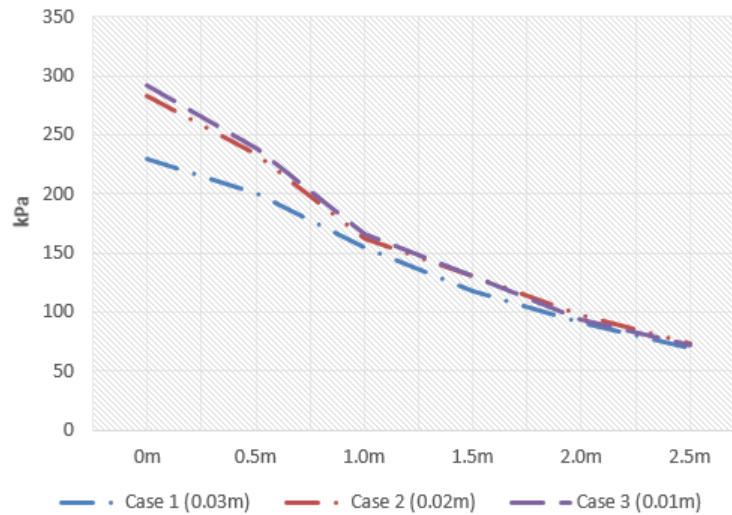


Figure 10.20. Mesh convergence test.

## 10.7. Concluding remarks

This study set out to investigate if the current rules, guidelines and design practices of LNG-fuelled ships are adequate. In the process an exemplary practical procedure for investigating the explosion risk of high pressure FPR was developed and demonstrated by studying the safety of FPRs of a case ship having high pressure FGS system. The findings from the study suggests that FPRs are subject to unacceptably high probability ( $3.14\text{E-}04$  per year) of explosion. The consequence analysis also revealed that the impact of explosion is severe enough to jeopardise the integrity of the boundary wall structure. From this it can be concluded that the risk is unacceptably high, and thus obviating the necessity for the procedure to evaluate the risk combining the probability and the severity.

Unacceptably high levels of both frequency and consequence of the potential explosion suggest that, at least, either the probability of occurrence of potential explosion is to be reduced by enhancing safety measures in FPR or the structural designs of an FPR is to be substantially enhanced.

Given the fact that the current IGF Code does not specify any safety requirement against the risk of explosion in an LNG-fuelled ship causing damage to other spaces in the ship, it is, therefore, thought that the current study can become a basis for a template for this type of risk analysis.

However, the sensitivity analysis showed that the ignition point and fuel composition significantly influence the degree of explosion impact on the structures, which implies that controlling of ignition points and fuel-air ratio can be a good safety means to mitigate the impact of explosion.

Lastly, it may be right to point out that the present study set out to show the gaps in the current regulatory provisions, especially with regard to addressing the necessity of higher safety level for high-pressure FPRs. It is believed this study has achieved this, or at least made a start on it. Therefore, it is expected that this work will be of some interest to the rule- and standard-makers who may well believe that developing more explicit and quantified guidelines is an urgent task.

## 11. QUANTITATIVE RISK ASSESSMENT OF MEDIUM-SIZED FLOATING REGASIFICATION UNIT

### 11.1. Introduction

Floating regasification units are likely to become more popular in the near future, but currently there are no sufficiently detailed and specific regulations and guidelines related to their safety. Therefore, their safety needs to be examined in a matter of urgency. Although they are not related or similar to LNG-fuelled ships, their safety may be worthy of investigating here as they are equipped with similar LNG process systems on-board. In addition, it will be a good study example to demonstrate the effectiveness of hierarchical system modelling applicable to complex systems.

During the design of the world's first medium-sized FRU a qualitative risk assessment was carried out. Although the results are useful, they cannot be used for developing rules and regulations directly. For such purposes some detailed quantitative studies are essential. This chapter introduces a study using a hierarchical system modelling method implemented in IQRA (integrated quantitative risk assessment) software to overcome the problem of the lack of direct statistical accident data of novel systems. The safety of the FRU mentioned above was assessed using this software and the results were compared against the results obtained from conventional approaches for qualitative and 'selective' quantitative risk assessment.

## 11.2. Description of study

### 11.2.1. Ship information

The JSK FRU operating in Port of Benoa, Indonesia (Figure 11.1) was selected for a case study. It supplies onshore power plants with natural gas after processing it using the on-board LNG regasification plants and its principal dimensions are 46.0 m long, 12.0 m broad and 5.0 m deep. It has an LNG loading system and an LNG storage tank fitted on open space while the regasification units are placed in a partially-confined room, designated as the ‘regasification unit space’. Two sides (starboard and aft) of the space are blocked by the wall structures while the other sides (forward and port) are open.



Figure 11.1. Case ship – JSK FRU (by courtesy of JSK Shipping Co., Ltd).

The FRU was designed in such a way that LNG supplied by LNG carriers is stored in an LNG storage tank (IMO C type 400m<sup>3</sup> tank). The storage tank help stabilize the pressure and the flow of the liquid fuel before the regasification process. The feed pumps transfer the stored LNG to the vaporizers where the liquid fuel is transformed into a gaseous form through heat exchange. During the regasification process, the excessive BOG (boil-off gas), naturally occurring inside the storage tank, flows by pressure difference to the BOG process system where the gas is heated by a preheater,

before being compressed by compressors. The regasification process is illustrated in Figure 11.2.

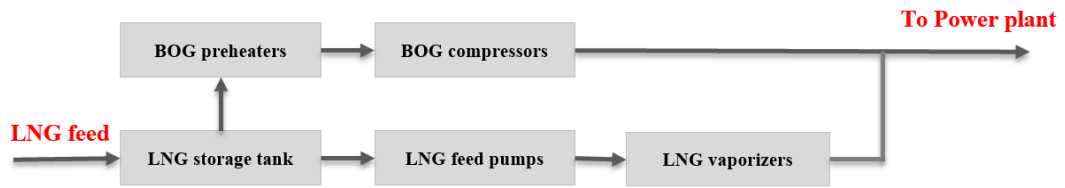


Figure 11.2. Regasification process.

### 11.2.2. Hierarchical system modelling

Due to the short operational history of FRUs the statistical accident data is in very short supply. For such circumstances a hierarchical system modelling, a method to derive the probability of failure from known historical data, was developed. In essence, it breaks down the plant to be studied into components for which the historical data exist. The data for the overall system can then be built up by combining the component data. Not only does this method allow the use of existing data on individual components of the system, but it also enables the safety of the whole system be studied instead of concentrating on critical hazards only. A more detailed explanation of this modelling was given in Chapter 7.

In this study, it was found that three-level hierarchy was sufficient to model the LNG regasification plant of the FRU. The risk of each group was individually assessed, and the risk of each sub-system was evaluated by integrating the risk of all its groups. The overall risk was then obtained by integrating the risk of all the sub-systems (Figure 11.3).

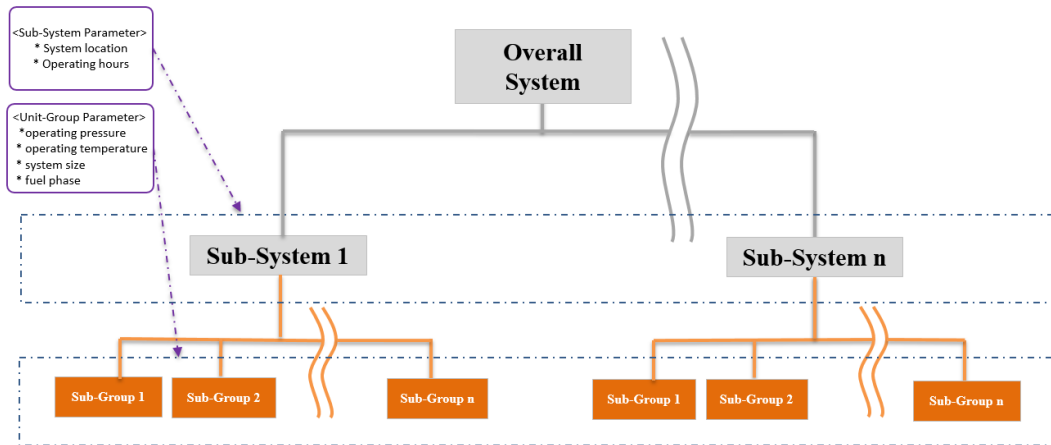


Figure 11.3. Proposed process of evaluating the overall risk using the hierarchical modelling.

If the estimated risk for the entire system is unacceptably high, safety measures must be applied (such as gas detectors with automatic isolation function). The overall risk is reassessed with the new measures added, and the process continues until the overall risk becomes tolerable.

Figure 11.4 shows a simplified piping system diagram of the FRU topside process classified into hierarchical groups. The whole system was separated into two sub-systems. The systems placed in open spaces were allocated to Sub-System 1 while the others located in partially-confined spaces were put into Sub-System 2.



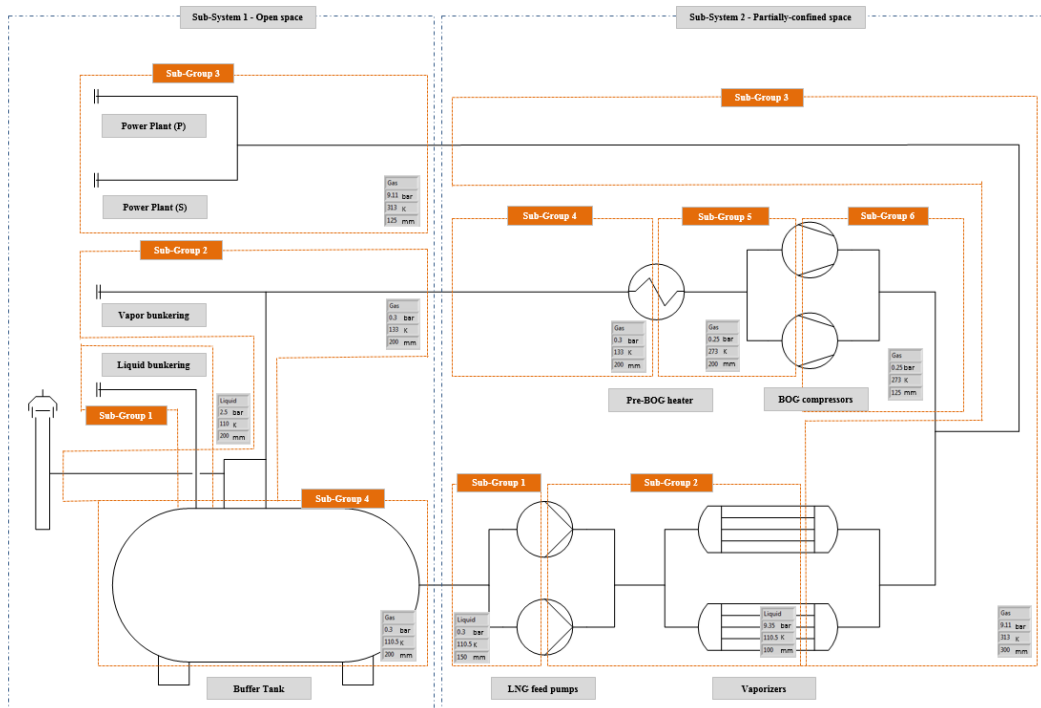


Figure 11.4. Simplified diagram of LNG regasification plant.

These were then divided into several sub-groups. Figure 11.5 summarises the characteristics of each sub-system and sub-group.

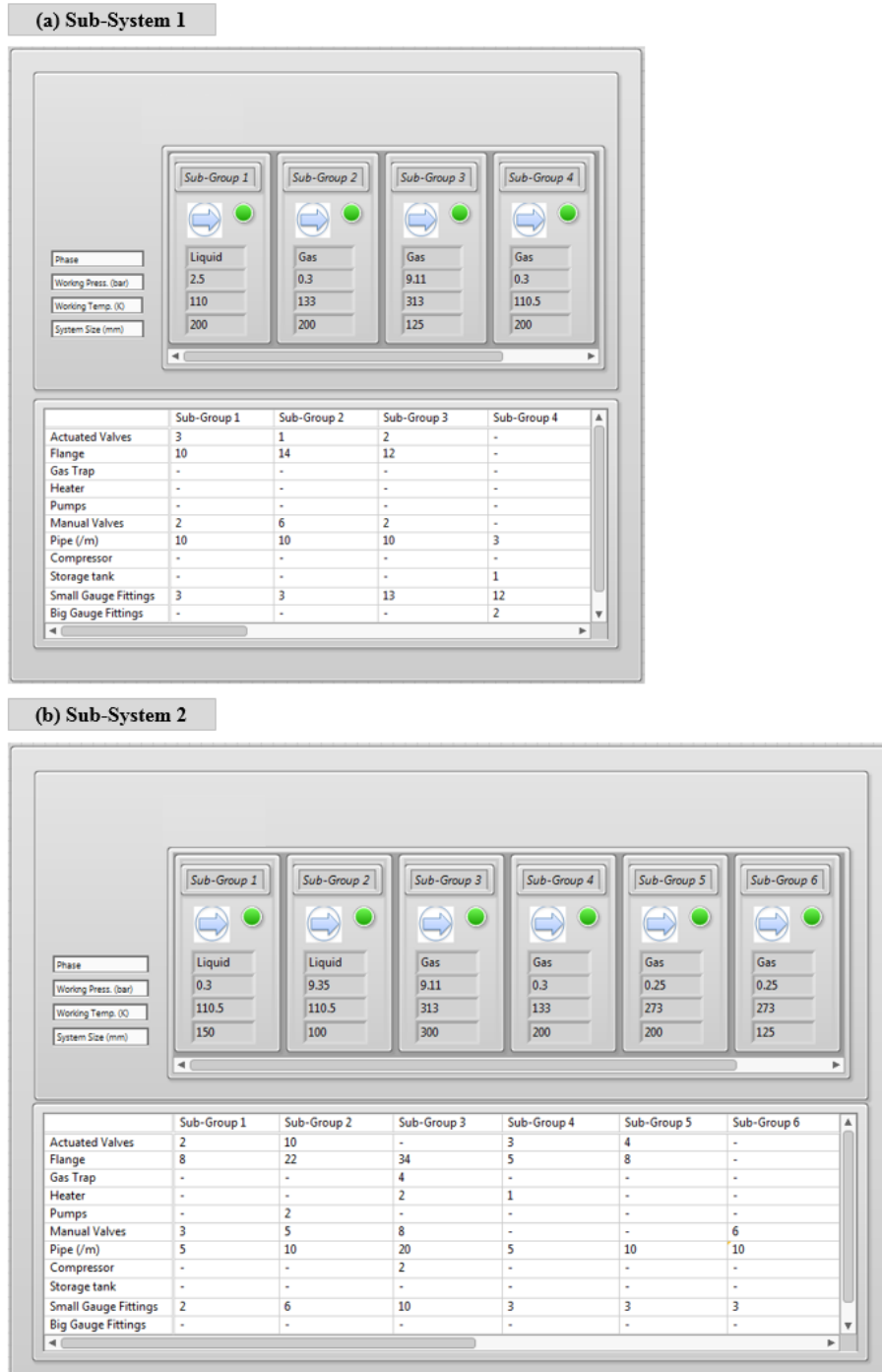


Figure 11.5. Hierarchical system modelling.

### 11.3. Risk assessment

#### 11.3.1. Frequency analysis

Five leak hole sizes were used for each sub-group, making the total number of cases 20 for Sub-System 1 with its four sub-groups and 30 for Sub-System 2 with its six sub-groups. Figure 11.6 shows the frequencies estimated, indicating that the probability of initial leak depends on the equipment involved and their size.

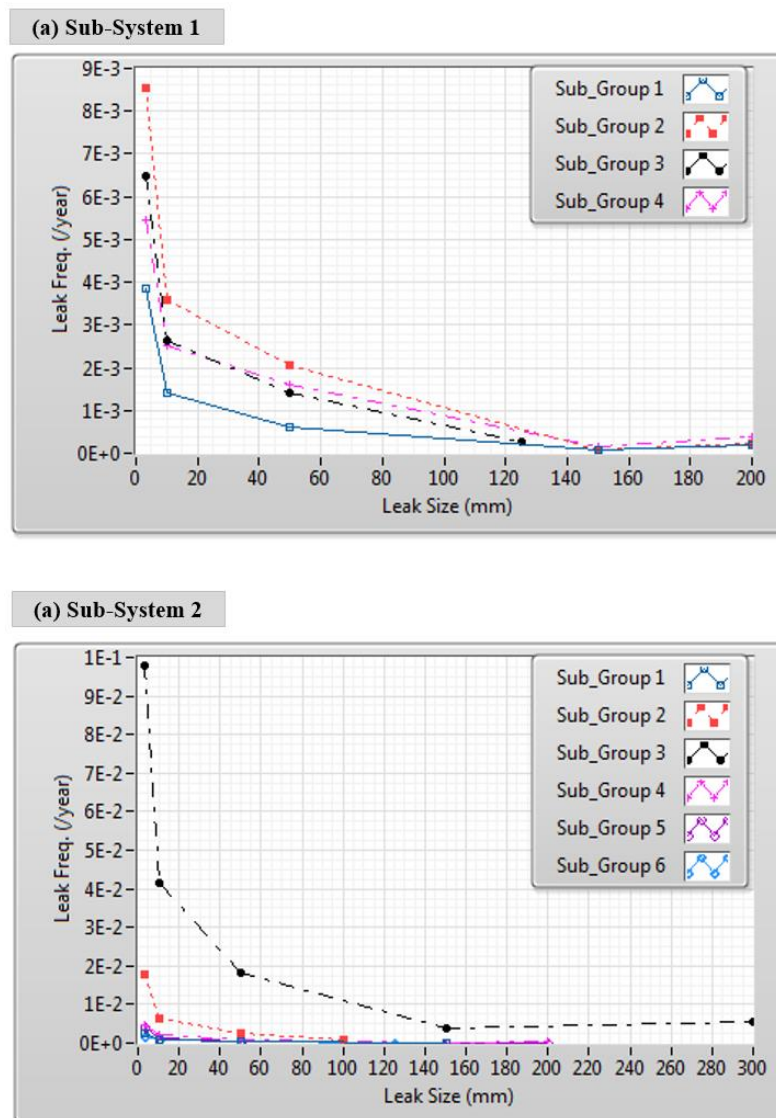


Figure 11.6. Estimated leak frequency.

In order to estimate the frequency of the final outcomes, each case of initial leak was subjected to ETA as discussed in Section 7.2.1. The scenario of limited fuel leak represents a situation where a safety system is immediately activated to isolate the leaky part of the system in the event of a fuel leak occurring. However, since the FRU as it stands does not have gas detectors or any other relevant safety measures, the first iteration did not consider any safety measures, and therefore the leak duration led to the late isolation scenario. In addition, to ensure that the worst case scenario was followed sufficient leak duration was allowed: thus, the leak recognition and isolation were assumed to be delayed by up to 10 minutes (Dan et al., 2014).

The case ship was designed in such a way as to make natural ventilation always effective for both open deck and the regasification unit space, thus obviating the necessity of a mechanical ventilation system. Therefore, the probability of ventilation system failure was disregarded. On the other hand, the congestion ratio was assumed to be 25 % for Sub-System 1 (as one out of four directions was blocked) and 50 % for Sub-System 2 (as two out of four directions were blocked).

An example of ET (3mm leak hole of Sub-Group 1 for Sub-System 1) is shown in Figure 11.7. The other cases for both Sub-Systems 1 and 2 also used the same process of ETA.

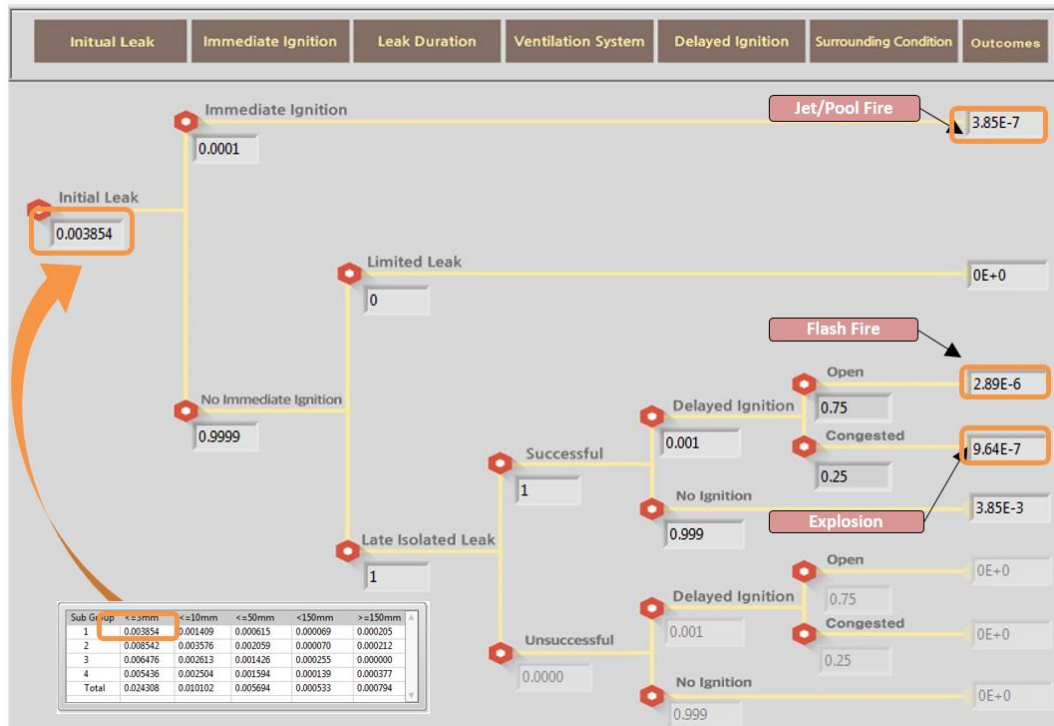


Figure 11.7. ET for 3mm leak hole for Sub-Group 1 of Sub-System 1.

The frequency of an initial leak from process equipment is analysed with respect to several representative leak hole sizes: 3 mm, 10 mm and 50 mm and 100 mm and full rupture size based on the DNV Leak Frequency Datasheets (DNV 2012a). The software also estimates the probability of ignition which is commonly determined by fuel phase and release rate; and a DNV model (DNV 2013) for immediate ignition as presented in Table 10.5 and OGP models (OGP 2010c) for delayed ignition described in Table 10.6.

### 11.3.2. Consequence analysis

The results show that the main factors determining the rates are leak hole size, leak pressure and fuel phase. Estimated leak rates are plotted in Figure 11.8.

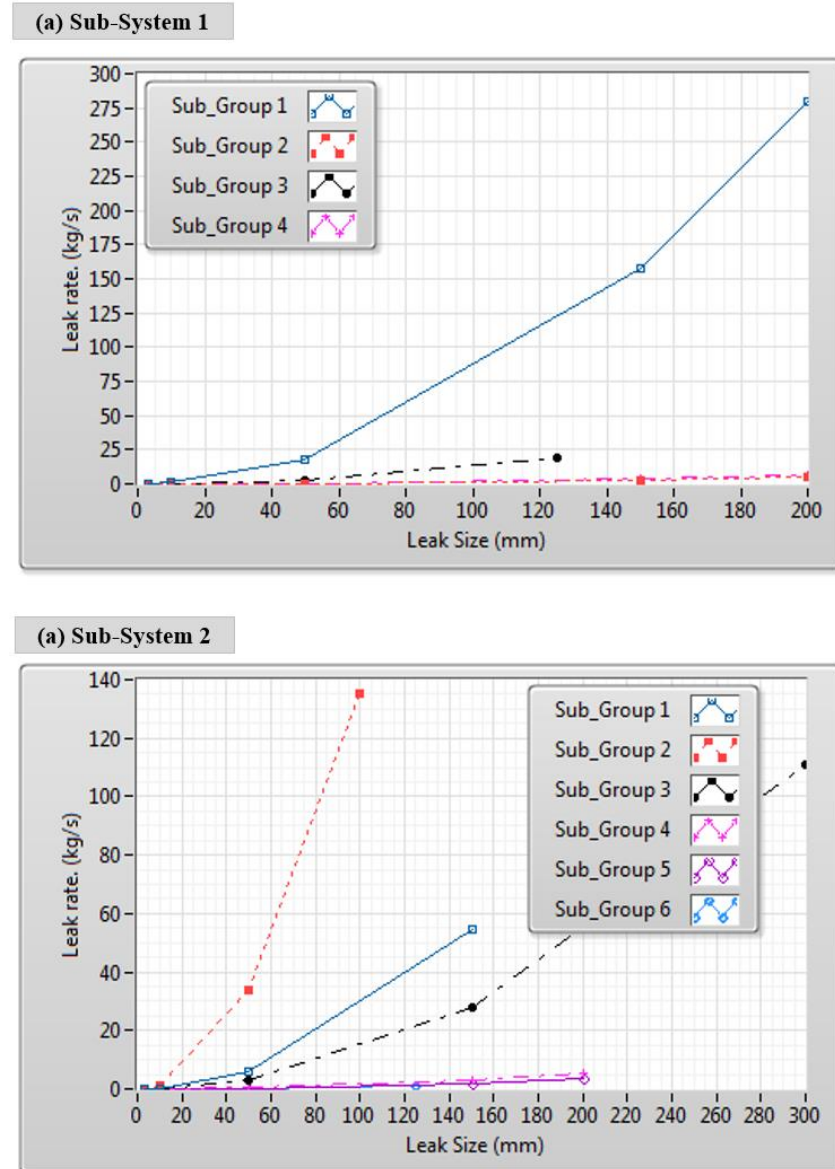


Figure 11.8. Estimated leak rates.

Using analytical and empirical models described in Appendix A, the impact of each accident was evaluated. For estimating flash fire, a neutral weather condition with a wind speed of 5 m/s was assumed in accordance with the prevalent annual weather records of Kuta/Bali, Indonesia (Windfinder 2016).

### 11.3.3. Assessment results

The discrete zones were peopled based on the actual data at the site as shown in Figure 11.9. It was assumed that the population was evenly distributed within each zone.

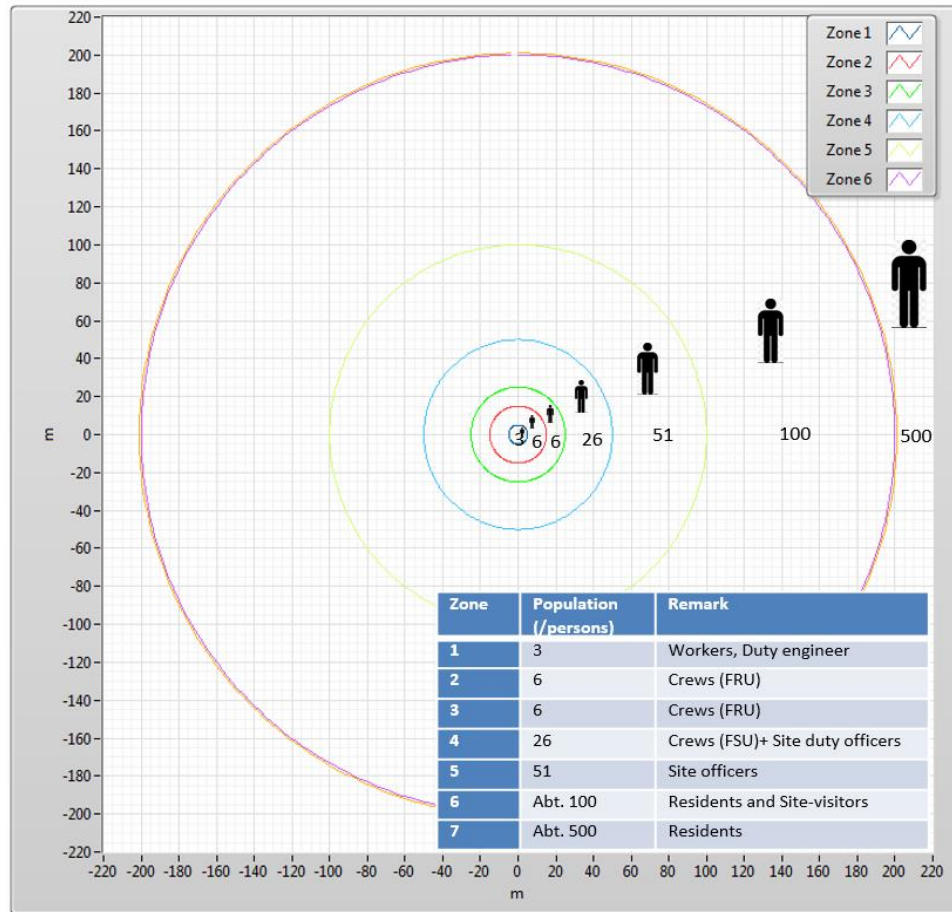


Figure 11.9. Population in the terminal (by courtesy of JSK Shipping Co., Ltd).

The results are presented as F-N graphs as shown in Figure 11.10. The risk of the whole system (summation of Sub-Systems 1 and 2) is also shown in that figure. It is a common practice to show the upper and lower limits of tolerable risk on the same graph (Norway 2000; Vanem et al. 2008), to allow judgement of tolerability of the risk. The range of tolerable level was taken from the IMO MSC Circular 72/16.

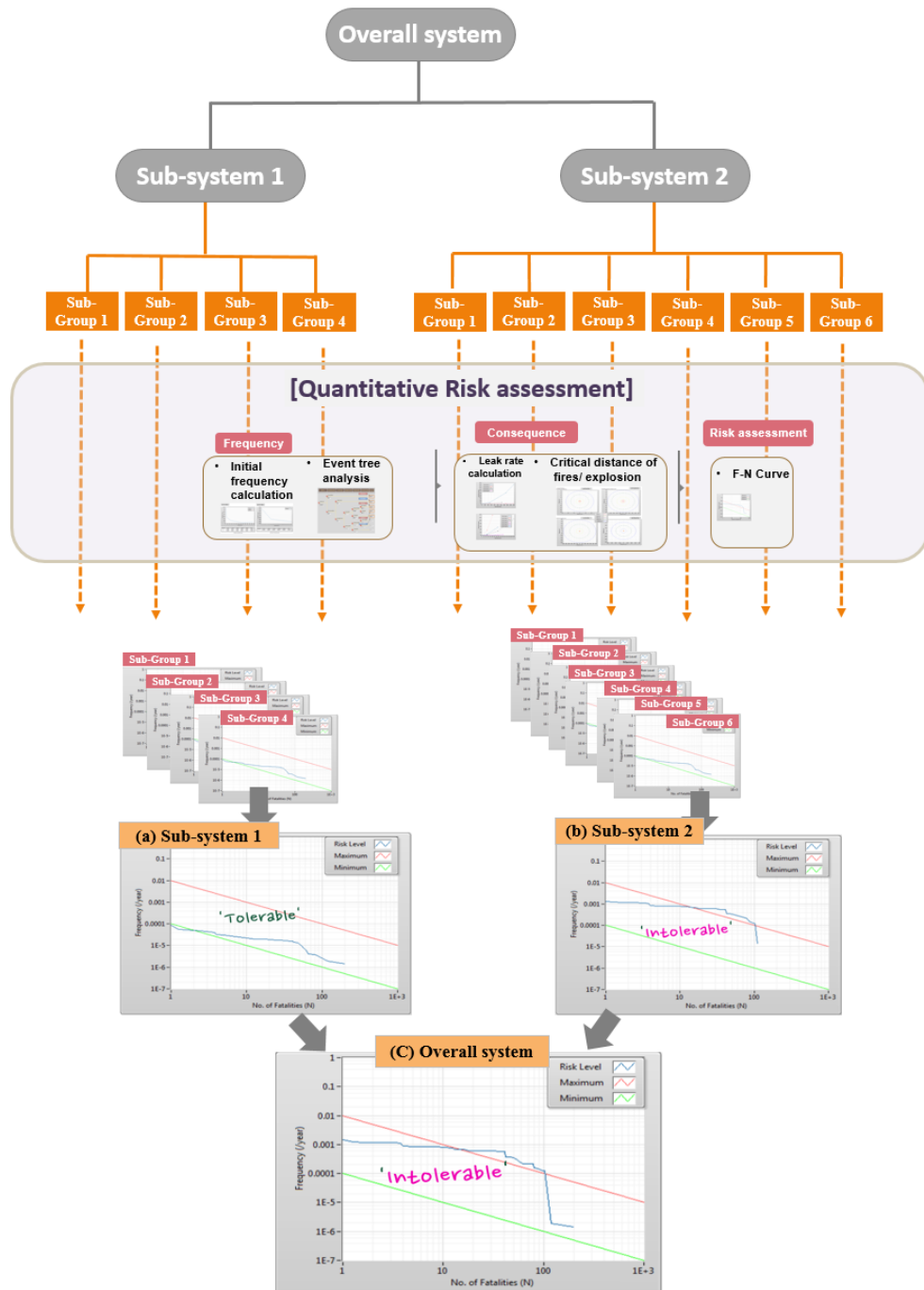


Figure 11.10. Risk F-N graphs.

The assessment results show that, although the risk of Sub-System 1 is well within the tolerable limit, the risk level of Sub-System 2 exceeds the limit, making the overall risk intolerably high. It was decided, therefore, that some safety measures had to be introduced to improve the safety.



## 11.4. Parametric analysis (application of safety measures)

### 11.4.1. *Modification of frequency analysis*

A safety system including an automatic gas detector was selected as the safety measure for this iteration. Such a system detects the presence of hydrocarbon in spaces where it is not normally expected and an alarm can be triggered when the concentration exceeds a threshold value. An emergency shut-off system is then activated automatically to isolate the leak. The isolation can also be effected manually if the automatic isolation malfunctions.

Taking into account these mitigation measures, a modified ET was developed as previously shown in Section 7.2.1. The limited leak scenario represents the case where the safety measures prevent an initial leak from developing into unfavourable outcomes. On the other hand, the late isolated leak scenario unfolds when both automatic and manual isolation processes fail.

In order to examine the probability of the late isolated leak scenario, the present study adopted fault tree analysis (FTA) method using the generic data about safety system failure from various sources. The failure rate per year,  $\lambda$ , was calculated from the upper failure rates given by the named sources. The reliability of each equipment was then estimated using Equation (10.2) (Santamaria and Brana 1998) as described in Chapter 10.

when one gas detector was used for the safety system (referred to as Case 1 hereafter) the result of FTA is equivalent to Figure 10.3 shown in the previous chapter while Figure 11.11 is for two gas detectors used (referred to as Case 2 hereafter). It was found that the probability of the late isolation associated with Case 2 was 0.014, far less than Case 1 that was 0.113. Examples of modified ETs for Cases 1 and 2 are shown in Figure 11.12.

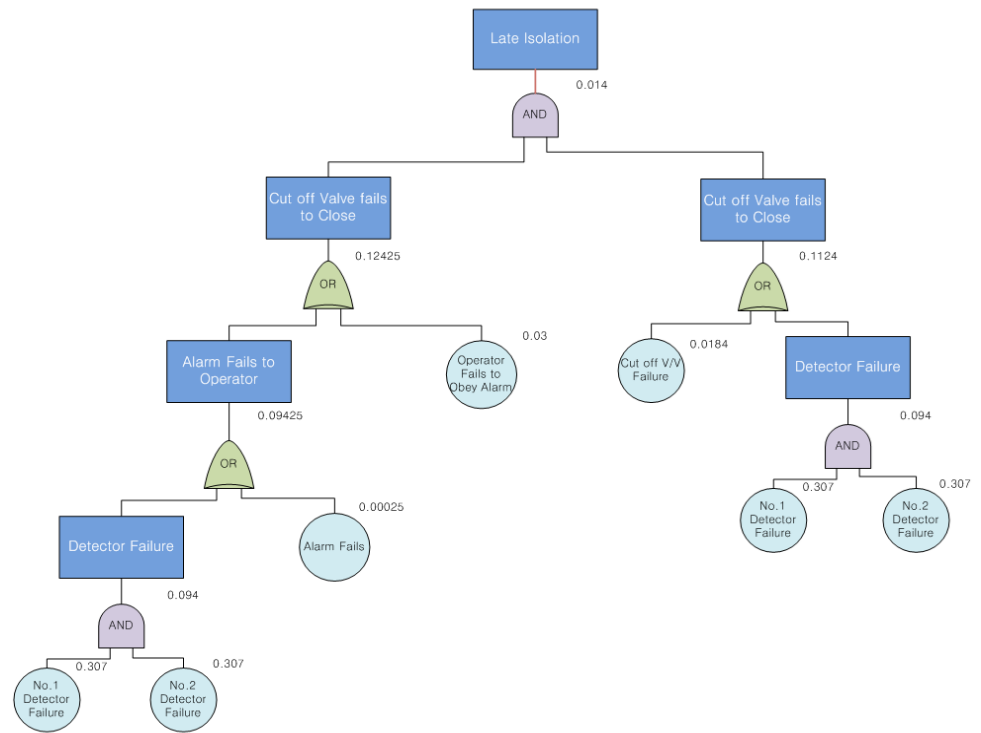


Figure 11.11. FT for late isolation with two gas detectors.

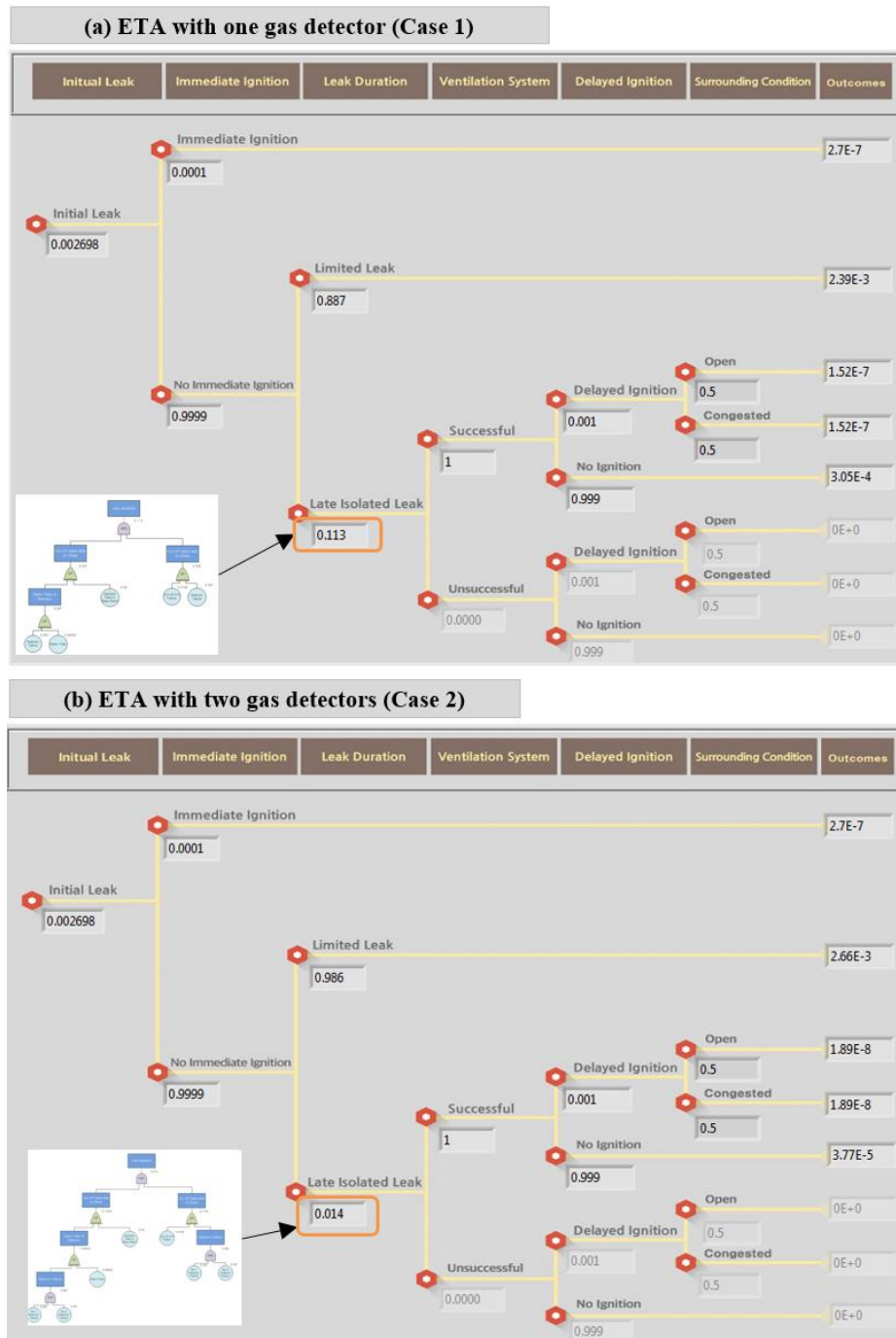


Figure 11.12. Modified ETs for 3mm leak hole for Sub-Group 1 of Sub-System 2.

11.4.2. Assessment results

(a) Safety measures applied to Sub-System 1

Figure 11.13 shows the assessment results when the safety measures (both Cases 1 and 2) were applied to Sub-System 1. It is plain that this use of the safety measures did nothing to reduce the overall risk of the entire system because the risk of Sub-System 2 was not affected. This results indicate that one of the safety recommendations from the original HAZOP study (i.e. installation of gas detectors with automatic isolation system at the LNG storage tank) would have been ineffective.

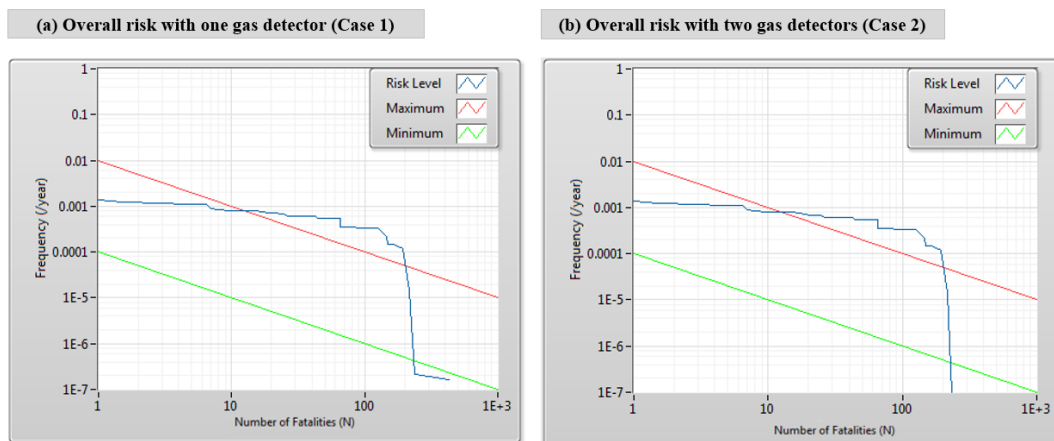


Figure 11.13. F-N graphs of risk with safety measures incorporated in Sub-System 1.

*(b) Safety measures applied to Sub-System 2*

Figure 11.14 shows the outcomes of the gas detectors incorporated in Sub-System 2, suggesting that this addition to Sub-System 2 will be effective. A single gas detector is seen to be sufficient to lower the overall risk level to within the tolerable limit, while two detectors lower the risk further. Given this, it can be concluded that at least one gas detector applied to Sub-System 2 can constitute ‘the appropriate number of gas detectors’ as mentioned in the original HAZOP recommendations.

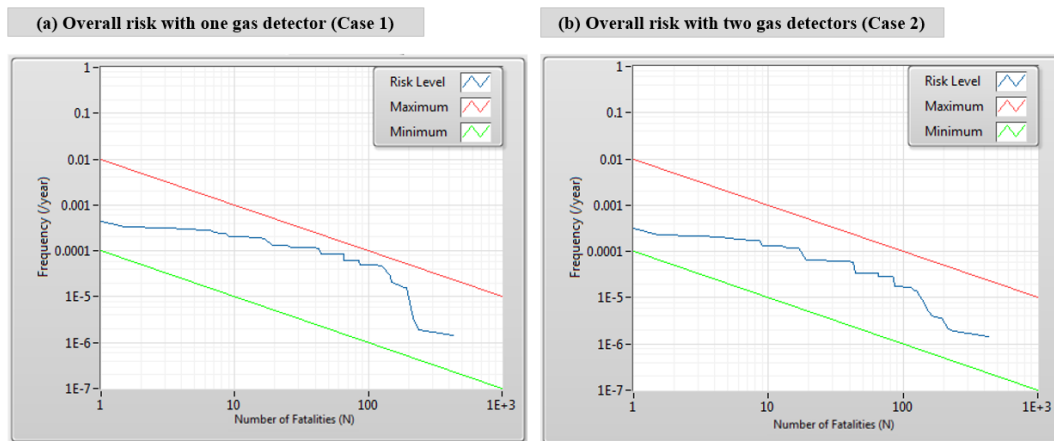


Figure 11.14. F-N graphs of risk with safety measures incorporated in Sub-System 2.

#### *11.4.3. Comparison with selective quantitative risk assessment*

In order to investigate the effectiveness of the hierarchical quantitative method, the same system was studied using the selective quantitative analysis for comparison. Three accidental scenarios identified through the HAZOP study were used for this selective quantitative risk assessment (KR 2015b).

- Scenario 1 - Liquid leak between LNG feed pump and regasification unit
- Scenario 2 - Vapour leak from BOG processing unit
- Scenario 3 - Liquid leak from LNG storage tank

A leak from manual valves and pipes attached to the systems were reckoned as the most probable case through the HAZOP study. For a stringent analysis, the leak was assumed to take place at the parts subjected to the highest pressure and the biggest piping system. In this context, the list of equipment involved in Scenario 1 is identical to Sub-Group 2 of Sub-System 2 while those of Scenarios 2 and 3 are the same as Sub-Group 4 of Sub-System 2 and Sub-Group 4 of Sub-System 1 respectively. The analysis results are summarized in Figure 11.15 and Table 11.1. As can be seen, the risks of all scenarios are within the tolerable zones in the F-N graphs, implying that enhancing the safety of FRU is unnecessary.

This conclusion is somewhat at odds with the conclusions of the HAZOP study and the hierarchical quantitative assessment. It is to be noted that the risk levels obtained from the selective quantitative assessment are far lower than the results obtained from the current study. This suggests that the selective assessment can underestimate the risks of safety-critical complex systems, sometimes to an unacceptable level.

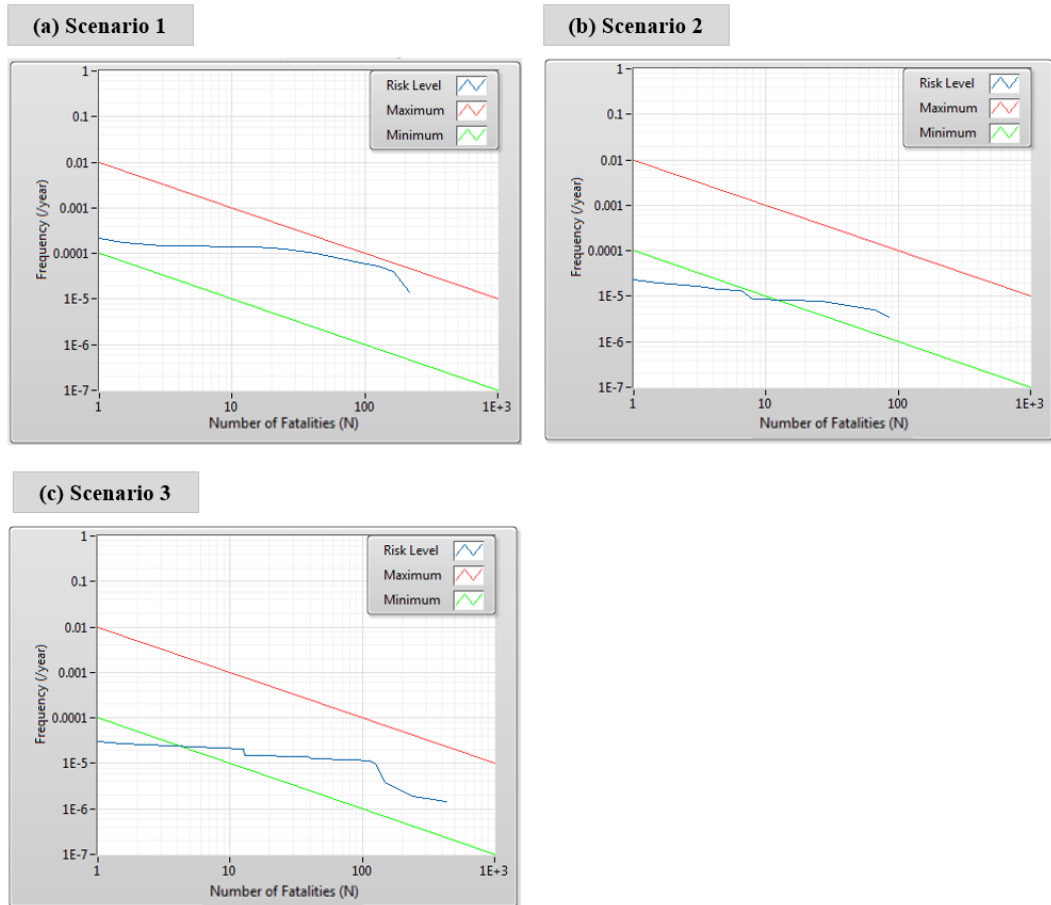


Figure 11.15. F-N graphs of risk from selective quantitative risk assessment.

Table 11.1 Results of selective quantitative risk assessment.

	Scenario 1	Scenario 2	Scenario 3
Frequency of outcomes	1.75E-4/year	1.21E-5/year	2.75E-5/year
Consequence of outcomes	Multiple fatalities	Multiple fatalities	Multiple fatalities
Safety system	Unnecessary	Unnecessary	Unnecessary

## 11.5. Concluding Remarks

This case study investigated the safety of the floating regasification unit (FRU) by applying a hierarchical system modelling method and parametric analysis. The value of this application has been brought to light by comparing existing methods of qualitative and quantitative risk assessment to this case study. It was clearly demonstrated too that the lack of direct statistical data in the new system was overcome.

The results of the comparison study are summarised in Table 11.2.

Table 11.2 Summary of study results.

Analysis	Qualitative risk assessment (HAZOP)	Selective quantitative risk assessment	Proposed quantitative risk assessment (with system hierarchy)
Frequency analysis	Up to once a year	1.75E-4/year (Scenario 1)	2.14E-3/year
Consequence analysis	Multiple major injuries or single fatality	Multiple fatalities (All cases)	Multiple fatalities
Safety measures	Appropriate number of gas detectors is to be fitted to; 1) Regasification unit 2) BOG processing unit 3) LNG storage tank	Not necessary (All cases)	Minimum one gas detector unit is to be fitted to regasification unit space (Group 2)

The initial HAZOP study identified fire/explosion caused by leak from pipe and valves as the most intolerable scenario, which may occur between once a year and once in ten years, causing multiple major injuries or a single fatality. It was recommended that the safety measures be independently applied to regasification plant, BOG processing unit and LNG storage tank.



## 12. DISCUSSION

### 12.1. Novelty of research

The novelty of the work done in this project lies in establishing and demonstrating the way that existing risk assessment techniques can be used to investigate the safety of a variety of novel LNG plants. It is thought that the idea and methods developed here can also be applied to systems other than those directly related to LNG. Above all else, it was clearly shown that the existing regulations may be insufficient to ensure satisfactory level of safety in LNG-fuelled ships.

It is important to point out here that efforts were made to keep the project as a generic and non-case-specific study. For example, an attempt was made to discover if the current practice of safety or risk assessment is adequate and can be relied upon to identify high risks. As such, the investigation concentrated on typical situations to improve our understanding of where the risks are in LNG-fuelled ships and how to minimise them so that the information generated can be used as a basis for future improvement of rules and standards.

The framework and methodology developed in this thesis provide structured guidelines to conduct quantitative risk assessment associated with LNG-fuelled ships as well as LNG process systems in terms of fire and explosion. It is thought that the sensitivity/parametric analyses performed during the project have improved our understanding of contributing factors to risks and methods of mitigating them as well as points to note during quantitative risk assessment.

The principle of the hierarchical system modelling method is a process of analysing and synthesising: the system is ‘analysed’ to the component level and the frequency of the system is then ‘synthesised’ from the failure frequencies of the basic components. It is believed that this principle can be applied to any situation where the overall risk consists of multiple hazard factors such as collision, excessive ship motions, harsh weather conditions and human failure.

Algorithms programmed in IQRA software have proven to be useful for helping the analysis results smoothly translated into future regulations and for decision-making when optimising process system designs.

### 12.1.1. *As a tool for early design stages*

In the early stages of developing a new process system or product, designers will wish to explore several ideas and concept designs, and perhaps shortlist some likely options before finalising a design and moving to the detailed design phase of development. In order for as many alternative designs to be assessed in as short a time as possible, effective and efficient evaluation tools are essential.

Figure 12.1 shows the importance of successful decision-making in early design stages, illustrating why it is desirable to bring forward the product knowledge as much as possible. If the early design decision is erroneous and modifications have to be introduced in later stages, considerable downstream costs may be incurred (Koch and Castillo 2017; Schmitz 2017; Giassi et al. 2004).

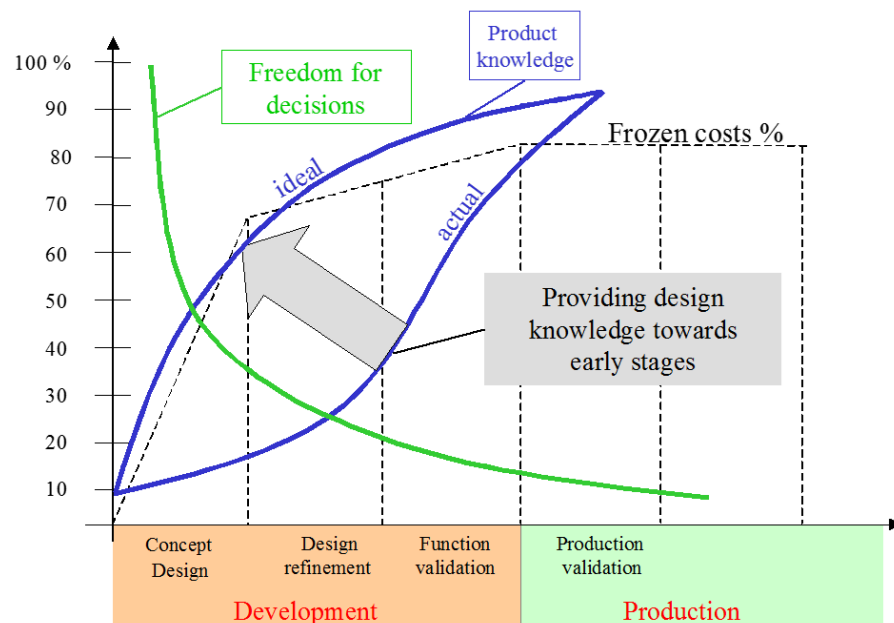


Figure 12.1. Design process, decision and knowledge availability (Koch and Castillo, 2017).

In order to avoid the costly modifications to the design to comply with relevant safety regulations and requirements at a later stage, the designers must be able to assess the level of risks associated with the design options as early as possible.

Figure 12.2 (a) represents the general process of safety evaluation for a hazardous system. In this process, the safety of the initial design is verified by an authorized safety organization (KR 2015b). If the risk is estimated to be intolerably high, the designer is required to modify the system and/or introduce safety measures. This process is repeated until the design is deemed to have lower-than-acceptable level of risk. It is apparent from this description that the roles of the designer and the safety assessors are complementary but distinct. Even though there may be some degree of communication between the two parties, such a process can be complex and protracted.

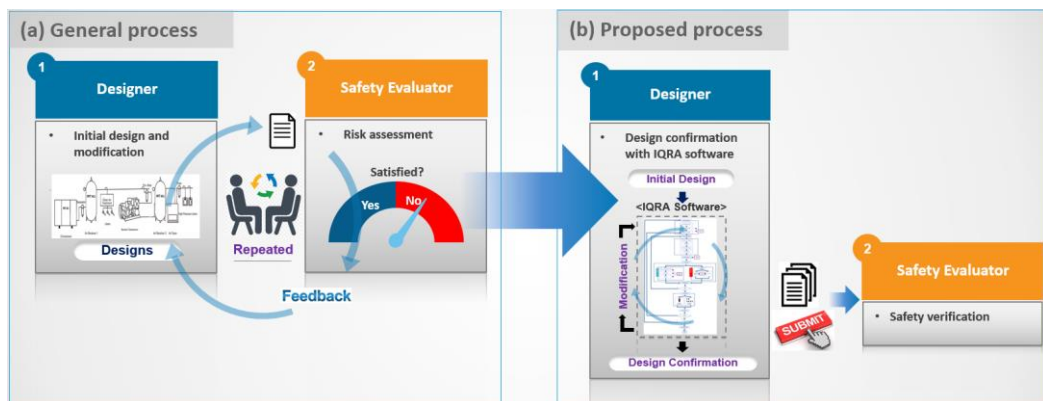


Figure 12.2. Traditional and ideal processes of safety evaluation for hazardous process systems.

One way of improving the design process, therefore, is to empower the designers to evaluate the safety of the systems that they are designing as quickly as possible even with less than complete knowledge of safety assessment methods. The IQRA software or other similar software can be used to bridge the skill gaps between the various parties involved by using representations of the risk model and analysis results that are easy to comprehend. It can be used as a tool by the designers to produce designs which comply with the safety requirements in principle, so that the approval process can be made shorter and the probability of final approval from the

authority higher. This proposed safety assessment process is depicted in the same Figure 12.2 (b).

### 12.1.2. *As a tool for rule-developing*

The speed with which technical development takes place and new process systems appear makes existing regulations, rules, guidelines and standards rapidly outdated. It is important for the regulations to keep pace with these developments. However, some types of oil/gas processing systems are so new that the regulations are non-existent or inadequate. In these circumstances the risk assessment methods based on first principles are very useful to ensure their safety.

As discussed in the previous chapters, there have been reports of a number of software for evaluating the risk of such new process systems in specific conditions. Not only are these therefore case-specific, but also they only perform the frequency calculations leaving the users to carry out highly time-consuming and error-prone consequence estimation.

Likewise, much of the risk assessment work published to date appears to be on a case-by-case basis, making the results useful only for the individual circumstances (Jeong et al. 2017a; Republic of Korea 2016). Despite these case-specific studies, lack of general observation of risk characteristics of processing systems and their trends hampers the rule-makers in updating appropriate regulations.

In view of this, the proposed software is designed to assess a wide range of fire and explosion scenarios for oil/gas systems, and the results of a systematic investigation can be used to identify key risk factors and to understand how various parameters affect risk levels. In developing a new regulation, generalization is an essential process through which common characteristics are identified so that a set of safety requirements can be developed for as many situations as possible. Figure 12.3 shows the

extensive range of work which can be done with the IQRA software compared to the existing case-specific software.

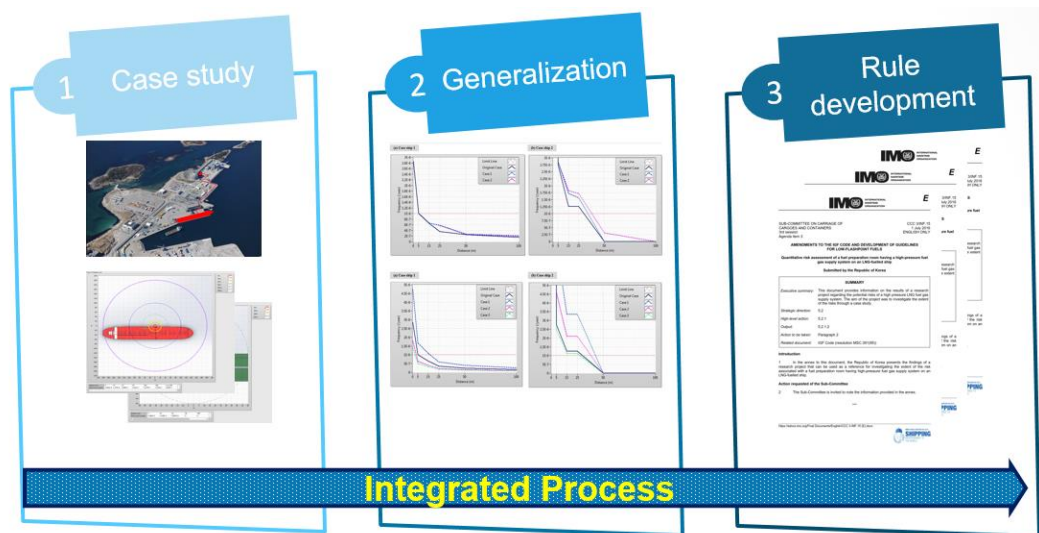


Figure 12.3. Integrated process contributing to rule-development.

## 12.2. Contributions to industries

At present, using LNG as a marine fuel is one of the top issues in the global shipping industry. Needless to say, the safety of people and ships in using and/or processing LNG is paramount. If it is agreed that enhancing the current regulations is an urgent task, it is expected that the results of the studies carried out in this thesis can make some contributions to decision-making and further regulatory framework for port authorities and rule-makers.

Several reports have been submitted as information documents to the CCC Subcommittee of IMO through the Korean delegate and it was very encouraging to learn that they were discussed by IMO member states from the viewpoint of enhancing current international regulations in London.

Summary of studies carried out on the safety of on-board bunkering and their contribution to the industry is presented in Figure 12.4.

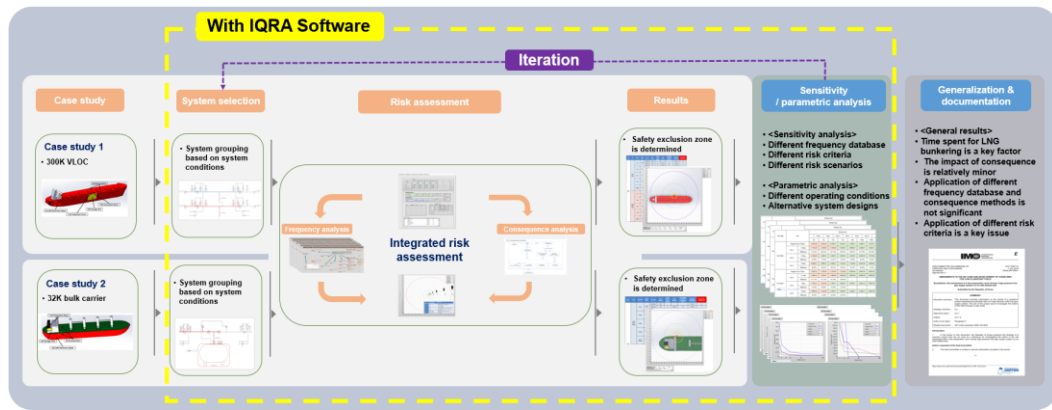


Figure 12.4. Summary of study on safety of on-board LNG bunkering.

The investigation on the safety of LNG bunkering from the point of view of fuel supplying end is summarised in Figure 12.5. The highlight of this study is the combined approach of population-independent and population-dependent analysis.

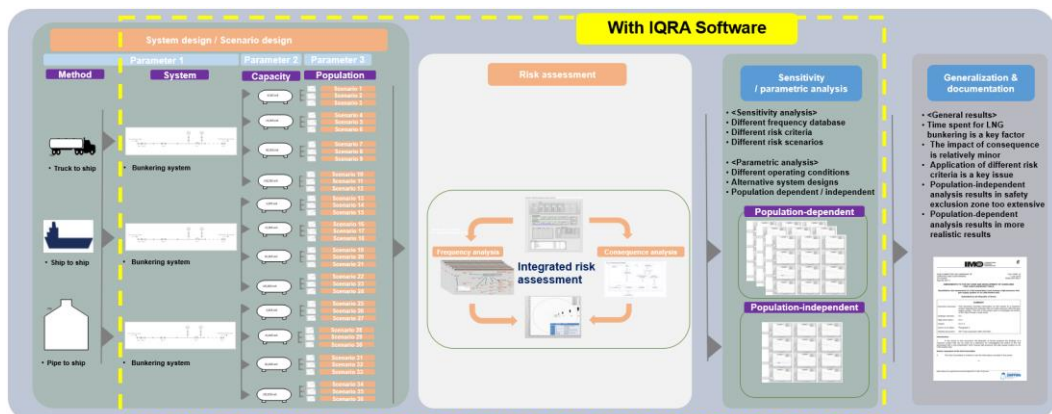


Figure 12.5. Summary of study of safety of LNG bunkering at supplying ends

A study on the risk of fuel preparation room (FPR) with a high pressure FGS system showed the practical limitations of the current international regulations. Taking a very large ore carrier of 300,000 tonne carrying capacity as a sample ship, the natural gas fuelling system was conceptually designed. The research findings have shown that special attention needs to be paid to the structural design of FPR. It was also concluded from this study that the current rules are inadequate and urgently require clarification and updating. The whole process of the case study is shown in Figure 12.6.

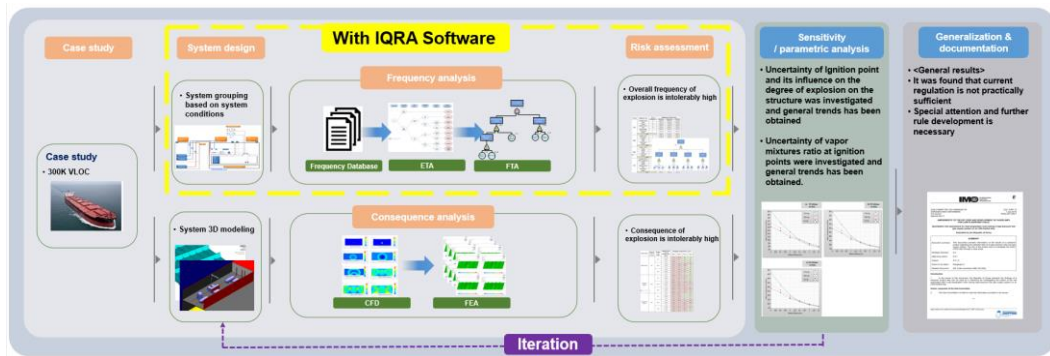


Figure 12.6. Summary of study on the safety of FPR.

An extra study was carried out to investigate the safety of floating regasification units the summary of which is given in Figure 12.7. It highlighted the shortcomings of some of the existing qualitative and quantitative risk analysis methods.

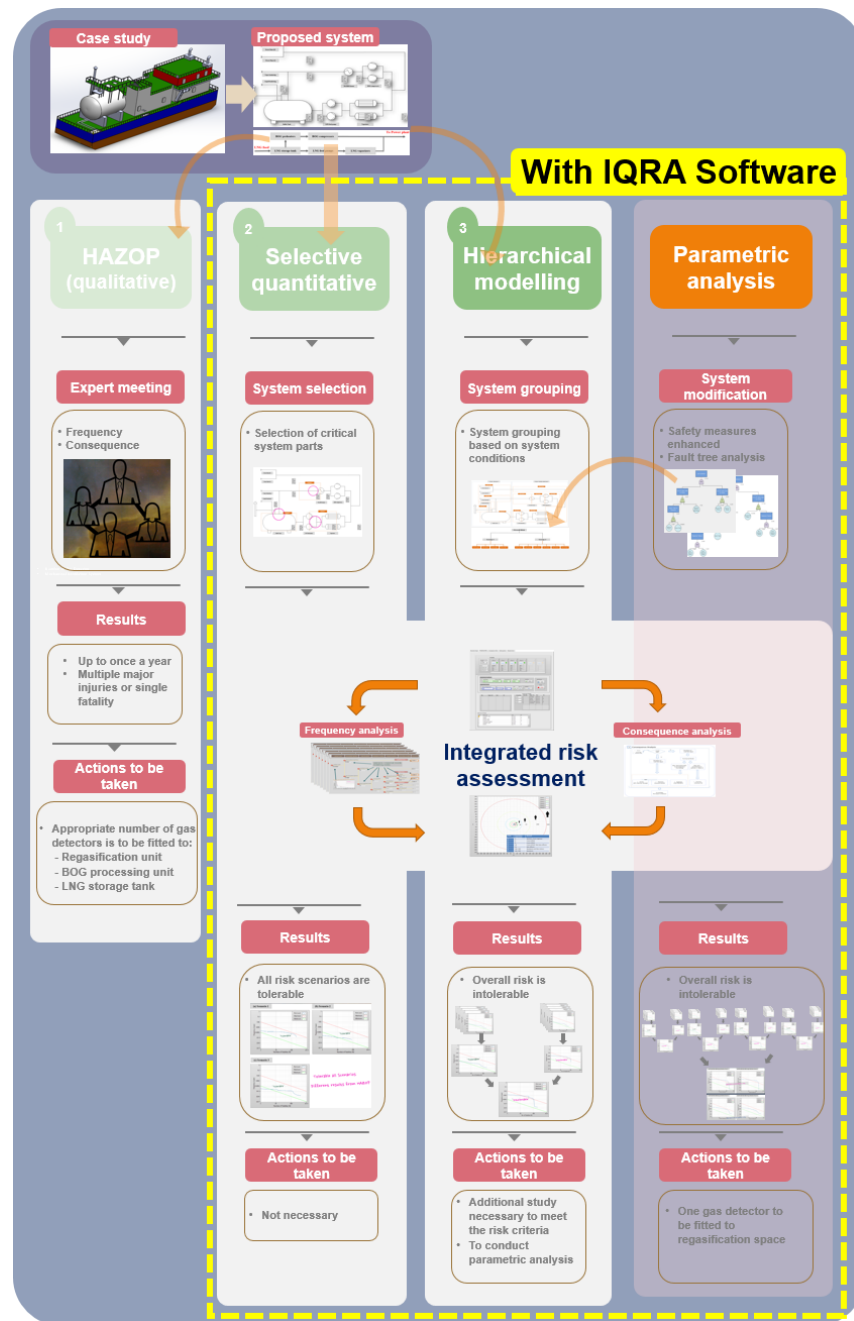


Figure 12.7. Summary of study on the safety of FRU.



### 12.3. Limitations and suggestions for future works

#### 12.3.1. *Software development*

The IQRA software has a limited scope in that, as it stands, it only deals with risks associated with fire and explosion from oil and gas process systems. It is thought that extension to other types of risks is a relatively minor task. In addition, the frequency analysis can be improved by incorporating a variety of techniques, such as fuzzy logic and Monte Carlo simulation, to take into account the uncertainty inherent in the risk data.

It can be argued that the analytical and empirical models for the consequence analysis implemented in this software are not state-of-the-art, but case studies have shown that this tool is excellent for use in preliminary investigation and general observation of the potential risk of process systems. It is true that the state-of-the-art numerical analysis software offers many advantages for specific conditions, but the case studies have shown it is possible to use these tools in conjunction with IQRA software. It may be that the areas which need to be rigorously investigated using the numerical analysis programs can be identified through IQRA.

#### 12.3.2. *Further research*

In general, the methane content in LNG is about 87~99% depending on the geographical location of production and the processing methods used. The LNG used in this study was assumed to be pure methane, and this will have introduced slight uncertainty in the results. However, the pure methane case was chosen as the representative case, as it was important for this study to address general situations. In any case the level of this uncertainty is not thought to be high enough to impair the general conclusions derived from the study and our understanding gained from it. Nevertheless, the sensitivity of LNG compositions on explosion impact needs to be investigated more thoroughly in the future.

The history of FRUs is very short indeed, and consequently there is no accumulated historical failure data available. The frequency analysis presented in this paper had to rely on available generic data compiled for investigating the safety of LNG process equipment in offshore and chemical industries. It is inevitable, therefore, that some of the quantitative results obtained from this study may not reflect reality. This may have to be carefully examined in the future, but effort has been made to be realistic using available data by breaking down the system to component level for which such data exist. It is thought that the hierarchical method goes considerable way towards generating realistic frequency data.

Whilst it is accepted that the LNG leaks during bunkering can occur due to external events, such as collision, excessive (relative) ship motions, extreme and unforeseen weather conditions and human error, they are difficult to take into account in formulating generic safety rules. That was why this study focussed on potential accidents associated with equipment failure only. With more experience with LNG bunkering in the future, a more accurate estimation of these factors may become possible in due course, but at the present time there is no data, primarily due to the brevity of LNG bunkering history.

It is important to note that the present study on bunkering was conducted to investigate the extent of safety exclusion zone required in general cases and the influence of some parameters on the exclusion zone. With this in mind the study was conducted in a site-independent manner as much as was possible. However, it is true that the impact of fire and explosion will be affected by geometry or meteorological conditions of the sites. For more site-specific assessment, therefore, it is recommended that the micro-scale meteorological/geometrical models of the LNG bunkering area be used for CFD or other numerical tools.

An attempt was made to generate additional information and aid general understanding of risks involved in LNG bunkering by carrying our rudimentary parametric analysis. For more comprehensive parametric analysis, however, it may be necessary to carry out the parametric analysis

for many more values of the parameters, including congestion ratio, wind speed, tolerable risk, critical fatality ratio and so on. Nevertheless, the studies were useful in that it was possible to identify some important parameters from them.

In the CFD simulation study of explosions in FPRs, all obstacles (e.g., heater, pipe, et al) in the room were omitted in the numerical models. In fact, obstacles may play an important role in the overpressure profiles. However, the main purpose of studying the safety of FPRs was to enhance the generic understanding of risks associated with this relatively new process and to determine the adequacy of the current provisions in this regard. In real situations, different ships have different arrangements of fuel gas supply systems fitted to FPRs and it is difficult to generalise them in a study such as ours. Moreover, specification of these location-specific parameters, being regarded as subjective variables, is not possible in rules and standards which have to cater for all kinds of situations. In this regard, it was more desirable to take the generic assumption of unrestricted spaces as these will produce more conservative results. On the other hand, as a recommendation for future studies where more specific analysis is required, it will be necessary to conduct case-by-case simulation with actual fuel-air ratio in the subject room by predicting exact leak duration and ignition timing for each case.

---

## 13. CONCLUSIONS

Based on the research work discussed in this thesis, the following conclusions can be drawn:

- 1) There is an urgent need for systematic investigation of the safety of LNG-fuelled ships and supporting systems. The main areas of concern in such ships include LNG bunkering systems and high pressure fuel gas supply system.
- 2) A hierarchical modelling method was applied to a complex novel system of floating regasification plant and it was found to be highly flexible and useful tool for dealing with systems with little or no operational data.
- 3) The safety of LNG bunkering system was examined for both on-board bunkering point and supplying point. The current guidelines for the safety exclusion zones in such circumstances are based on population-independent analysis. However, it was shown that the extent of the safety exclusion zone determined from such an analysis was too excessive and thus impractical to implement. Population-dependent analysis was thought to be more logical and indeed it produced a more readily acceptable exclusion zone. However, in this project a method was developed to combine the results from both approaches to ensure maximum effectiveness of the exclusion zone.
- 4) Quantitative risk analyses of fuel preparation room with high pressure fuel gas supply system have shown that the current designs can be structurally vulnerable to possible explosive accidents. It was concluded that explicit regulations and design guidelines of the fuel preparation room structure are necessary.
- 5) The various risk assessment methods have been integrated and implemented in a computer program called IQRA. It has been demonstrated that the use of this software reduces much of time-consuming, repetitive work in risk assessment allowing rapid outline assessment of risks associated with fire and explosion in oil/gas process systems. The parametric analyses and sensitivity studies carried out in this project were only possible by using this software.

The fact that the program can deal with risk assessment from system modelling to the final outcome proved to be a tremendous asset to the project.

- 6) As expected, qualitative risk analyses, such as HAZOP, appears to produce somewhat arbitrary results, for example, requiring additional safety measures far in excess of those found to require by a more objective quantitative analysis.
- 7) With the introduction of hierarchical modelling and powerful software such as IQRA, there is no reason why ‘selective’ quantitative risk analysis should be used in preference to a more comprehensive approach.
- 8) Through this project general understanding of the nature and scale of the risk associated with LNG-fuelled ships has been enhanced. It is important to carry out more extensive and systematic studies on the safety of gas-fuelled ships for developing regulations and guidelines, combined with and supported by case-specific example studies. Based on the current understanding a thorough discussion on how to progress with the regulatory work needs to take place between all stakeholders.

---

## REFERENCES

- ABS 2012. ABS Guide for Propulsion and Auxiliary Systems for Gas Fuelled Ships.
- ABS 2014. Bunkering of Liquefied Natural Gas-fueled Marine Vessels in North America. Houston Texas USA: ABS.
- ABS 2015. Guide for Propulsion and Auxiliary Systems For Gas Fuelled Ships. Houston Texas: ABS.
- LINDE ET AL 2010. LNG ship to ship bunkering procedure. Swedish Marine Technology Forum, devalla.
- ALONSO, F. D., FERRADÁ S, E. G., PÉREZ, J. F. S., AZNAR, A. M., GIMENO, J. R. & ALONSO, J. M. 2006. Characteristic overpressure–impulse–distance curves for vapour cloud explosions using the TNO Multi-Energy model. *Journal of hazardous materials*, 137, 734-741.
- ANEZIRIS, O., PAPAZOGLU, I., KONSTANTINIDOU, M. & NIVOLIANITOU, Z. 2014. Integrated risk assessment for LNG terminals. *Journal of Loss Prevention in the Process Industries*, 28, 23-35.
- ARNSDORF, B. 2013. Shell, GE to build nation's first LNG fueling stations for cargo ships [Online]. Bloomberg News. Available: <http://fuelfix.com/blog/2013/12/04/shell-ge-to-build-nations-first-lng-fueling-stations-for-cargo-ships/> 25.09.2017].
- AYMELEK, M., BOULOUGOURIS, E., TURAN, O. & KONOVESSIS, D. 2014. Challenges and opportunities for LNG as a ship fuel source and an application to bunkering network optimisation.
- BAKER, Q., TANG, M., SCHEIER, E. & SILVA, G. 1994. Vapor Cloud Explosion Analysis AIChE Loss Prevention Symposium. *Atlanta, Georgia, USA*.
- BAKER, W. E. 1973. *Explosions in air*, University of Texas Press.
- BALLAND, Ø. P. A. O. 2015. Machinery selection to comply with future sulphur emission regulations. *Maritiem Technology and Engineering*, 2014, Pages 787–795.
- BASHA, O., OLEWSKI, T., VÉCHOT, L., CASTIER, M. & MANNAN, S. 2014. Modeling of pool spreading of LNG on land. *Journal of Loss Prevention in the Process Industries*, 30, 307-314.
- BAUMEISTER, K. & SIMON, F. 1973. Leidenfrost temperature- Its correlation for liquid metals, cryogenes, hydrocarbons, and water. (*American Society of Mechanical Engineers, 1973.*) *ASME, Transactions, Series C- Journal of Heat Transfer*, 95, 166-173.
- BRIGGS, G. 1973. Diffusion estimation for small emissions, Atmospheric Turbulence and Diffusion Laboratory Contribution. Technical Report 79, National Oceanic and Atmospheric Administration, Oak Ridge.
- BRISCOE, F. & SHAW, P. 1980. Spread and evaporation of liquid. *Progress in Energy and Combustion Science*, 6, 127-140.
- BS EN 1991. EN292-1:1991 Safety of machinery — Basic concepts, general principles for design — Part 1 : Basci terminology, methodology.
- BS EN 1997. BS EN1050:1997 Safety of machinery - Principles for risk assessment. . *In: BS (ed.). BS*.
- BS EN 1997. EN1160: Installations and equipment for liquefied natural gas — General characteristics of liquefied natural gas.

- BS EN 2002. EN 13645: Installations and equipment for liquefied natural gas — Design of onshore installations with a storage capacity between 5 t and 200 t.
- BS EN 2006. EN 14620: Design and manufacture of site built, vertical, cylindrical, flat-bottomed steel tanks for the storage of refrigerated, liquefied gases with operating temperatures between 0 to -165 °C.
- BS EN 2007. EN1473: Installation and equipment for liquefied natural gas — Design of onshore installations.
- BS EN 2008. EN 1474-1,2,3: Installation and equipment for liquefied natural gas — Design and testing of marine transfer systems.
- BV 2012. Safety Rules for Gas-Fuelled Engine Installations in Ships.
- CARSLAW, H. S., JAEGER, J. C. & FESHBACH, H. 1962. Conduction of heat in solids. *Physics Today*, 15, 74-76.
- CCPS 1989. *Guidelines for Process Equipment Reliability Data with Data Tables*, New York, USA, CCPS.
- CD-ADAPCO 2014. User Guide: STAR-CCM+ Version 9.02.
- Chae, M. 2016. *Effect of liquefaction process selection on explosion risk of LNG-FPSO*. Seoul National University.
- COLLIER, J. G. & THOME, J. R. 1994. *Convective boiling and condensation*, Clarendon Press.
- COMMITTEE, A. A. 2014. Proposed text of a derogation regarding the use of LNG. Geneva Switzerland.
- CONRADO, C. & VESOVIC, V. 2000. The influence of chemical composition on vaporisation of LNG and LPG on unconfined water surfaces. *Chemical Engineering Science*, 55, 4549-4562.
- COOK, J., BAHRAMI, Z. & WHITEHOUSE, R. 1990. A comprehensive program for calculation of flame radiation levels. *Journal of loss prevention in the process industries*, 3, 150-155.
- COX, A. W., LEES, F. P. & ANG, M. L. 1990. *Classification of hazardous locations*, IChemE.
- CROWL, D. A. & LOUVAR, J. F. 2001. *Chemical process safety: fundamentals with applications*, Pearson Education.
- DADASHZADEH, M., KHAN, F., HAWBOLDT, K. & AMYOTTE, P. 2013. An integrated approach for fire and explosion consequence modelling. *Fire Safety Journal*, 61, 324-337.
- D'ALESSANDRO, A., IZURIETA, E. & TONELLI, S. 2016. Decision-making tools for a LNG regasification plant siting. *Journal of Loss Prevention in the Process Industries*, 43, 255-262.
- DAN, S., LEE, C. J., PARK, J., SHIN, D. & YOON, E. S. 2014. Quantitative risk analysis of fire and explosion on the top-side LNG-liquefaction process of LNG-FPSO. *Process Safety and Environmental Protection*, 92, 430-441.
- DNV 2011. Part 6 Chapter 13, Gas Fuelled Ship Installations. Oslo: DNV.
- DNV 2012a. Failure frequency guidance: Process Equipment Leak Frequency Data for use in QRA. Oslo Norway.
- DNV 2012b. Port toolkit risk profile LNG bunkering - Port of Rotterdam, Ministry of Infrastructure & Environment - Port of Antwerp, Port of Amsterdam and Zeeland Seaport. Oslo Norway.
- DNV 2013. Report for Skangass AS, Appendix A – Assumptions Register. DNV.
- DNV 2015. DNV Rules for Classification of Ships, Part 3 Chapter 1 Hull structural design - Ships with length 100 metres and above.
- DNVGL 2014a. PP087423-4, Rev 3: Liquefied Natural Gas (LNG) Bunkering Study. Oslo Norway: DNVGL.

- DNVGL 2014b. Recommended practice – DNVGL-RP-0006:2014-01: Development and operation of liquefied natural gas bunkering facilities. Oslo: DNVGL.
- DNVGL 2015. INFOCUS-LNG AS SHIP FUEL. *Latest developments and projects in the LNG industry*. Hamburg Germany: DNVGL.
- DUNJÓ, J., FTHENAKIS, V., VÍLCHEZ, J. A. & ARNALDOS, J. 2010. Hazard and operability (HAZOP) analysis. A literature review. *Journal of hazardous materials*, 173, 19-32.
- ESTEVEZ, A. S. & REIS PARISE, J. A. 2013. Mathematical modeling of cryogenic spills onto quiescent sea waters followed by pool fires of liquefied natural gas (LNG). *Applied Thermal Engineering*, 59, 587-598.
- EPRI 1995. *Advanced Light Water Reactor Utility Requirements Document (Volume III)*, California, USA, EPRI.
- KOCH, T. & CASTILLOF. F. 2017. SHIPLYS Project Deliverable Report 3.1 - Existing prototyping models and approaches.
- FRANK, T. 1980. *Industrial explosion prevention and protection*, New York USA, Mc Graw-Hill.
- FREEMAN, R. A. 1990. CCPS guidelines for chemical process quantitative risk analysis. *Process Safety Progress*, 9, 231-235.
- GAVELLI, F., DAVIS, S. G. & HANSEN, O. R. 2011. Evaluating the potential for overpressures from the ignition of an LNG vapor cloud during offloading. *Journal of Loss Prevention in the process industries*, 24, 908-915.
- Germany and Norway. 2012. HAZID report. London.
- GIASSI, A., BENNIS, F. & MAISONNEUVE, J.-J. 2004. Multidisciplinary design optimisation and robust design approaches applied to concurrent design. *Structural and Multidisciplinary Optimization*, 28, 356-371.
- GIARDINA, M. & MORALE, M. 2015. Safety study of an LNG regasification plant using an FMECA and HAZOP integrated methodology. *Journal of Loss Prevention in the Process Industries*, 35, 35-45.
- GOTHENBURG, P. O. 2015. LNG operating regulations including LNG bunkering.
- GOYAL, R. & KUGAN, S. Hazard and Operability Studies (HAZOP)--Best Practices Adopted by BAPCO (Bahrain Petroleum Company). SPE Middle East Health, Safety, Security, and Environment Conference and Exhibition, 2012. Society of Petroleum Engineers.
- GPO 1988. 33 CFR Part 127: Waterfront Facilities Handling Liquefied Natural Gas and Liquefied Hazardous Gas.
- GPO 1997. 18 CFR Part 153: Applications for authorization to construct, operate, or modify facilities used for the export or import of natural gas.
- GPO 2011. 49 CFR 193 Part 193: Liquefied Natural Gas Facilities
- GPO 2012. 46 CFR Part 154: Safety Standards for Self-Propelled Vessels Carrying Bulk Liquefied Gases.
- GUPTA, S. & CHAN, S. 2016. A CFD based explosion risk analysis methodology using time varying release rates in dispersion simulations. *Journal of Loss Prevention in the Process Industries*, 39, 59-67.
- HA, S-M. 2017. Comparative Analysis between IGF Code and IGC Code. Korean Register.
- HAMUTUK, L. O. 2008. Appendix 4. History of accidents in the LNG industry. Available from: <https://www.laohamutuk.org/Oil/LNG/app4.htm>.
- HIGHTOWER, L. G., ANAY LUKETA-HANLIN, JOHN COVAN, SHELDON TIESZEN, GERRY, WELLMAN, M. I., MIKE KANESHIGE, BRIAN MELOF, CHARLES MORROW, &



- RAGLAND, D. 2004. Guidance on Risk Analysis and Safety Implications of a Large Liquefied Natural Gas (LNG) Spill Over Water Sandia National Laboratories.
- HIRST, W. & EYRE, J. 1983. Maplin Sands experiments 1980: Combustion of large LNG and refrigerated liquid propane spills on the sea. *Heavy Gas and Risk Assessment—II*. Springer.
- HOFTIJZER, G. 1979. Heat radiation. *Chapter*, 6, 27.
- HSE 2001. Marine risk assessment - Offshore Technology Report 2001/063. HSE.
- IEC. 1985. Analysis techniques for system reliability—Procedure for failure mode and effects analysis (FMEA). *Bureau Central de la Commission Electrotechnique Internationale, Genève, Suisse*.
- IGU 2015. IGU World LNG Report - 2015 Edition. *World Gas Conference Edition*, . Fornebu, Norway: IGU.
- IGU 2017. 2017 World LNG Report. IGU.
- IMO 2002. MEPC/Circ.392: Guidelines for Formal Safety Assessment (FSA) for Use in the IMO Rule-making Process. London.
- IMO 2007. MSC 83/INF.3 FSA – Liquefied Natural Gas (LNG) Carriers Details of the Formal Safety Assessment London: IMO.
- IMO 2015. Third IMO Greenhouse Gas Study 2014. London: IMO.
- IMO 2017. International Code of Safety for Ships using Gases or other Low-flashpoint Fuels (IGF Code) London, UK: IMO.
- ISO 2010. ISO 28460: Installation and Equipment for Liquefied Natural Gas – Ship to shore interface and Port Operations.
- ISO 2012. ISO 10976: Refrigerated light hydrocarbon - measurement of cargoes on board LNG carriers.
- ISO 2013. 16903: Characteristics of LNG influencing design and material selection. Geneva Switzerland.
- ISO 2015a. Guidelines for systems and installations for supply of LNG as fuel to ships. Geneva Switzerland: ISO.
- ISO 2015b. ISO/TS 16901: Guidance on performing risk assessment in the design of onshore LNG installations including the ship/shore interface.
- ISO 2015c. ISO/TS 18683:2015 Guidelines for systems and installations for supply of LNG as fuel to ships. ISO.
- ISO 2017. ISO 20519: Ships and marine technology — Specification for bunkering of liquefied natural gas fuelled vessels. ISO.
- JAFARI, M. J., ZAREI, E. & BADRI, N. 2012. The quantitative risk assessment of a hydrogen generation unit. *international journal of hydrogen energy*, 37, 19241-19249.
- JIN, Y. & JANG, B.-S. 2015. Probabilistic fire risk analysis and structural safety assessment of FPSO topside module. *Ocean Engineering*, 104, 725-737.
- KIM, S. J., LEE, D. H., HONG, H. M., AHN, S. H., PARK, J. B., SEO, J. K., KIM, B. J. & PAIK, J. K. 2016. Methods for determining the optimal arrangement of water deluge systems on offshore installations. *Ocean Engineering*, 114, 236-249.
- KLETZ, T. 1991. *An engineer's view of human error*, Rugby UK, IChemE.
- KLETZ, T. A. 1997. Hazop—past and future. *Reliability Engineering & System Safety*, 55, 263-266.
- KLETZ, T. A. 1999. *HAZOP and HAZAN: identifying and assessing process industry hazards*, IChemE.

- KLIMENKO, V. 1981. Film boiling on a horizontal plate—new correlation. *International journal of heat and mass transfer*, 24, 69-79.
- LIMENKO, V. 1981. Film boiling on a horizontal plate—new correlation. *International journal of heat and mass transfer*, 24, 69-79.
- KR 2015a. LNG Fuelled Ready Ship For VLOC. Busan, South Korea.
- KR 2015b. HAZOP study report - LNG Regasification system. (2015) Project NO. 4800-4-104, Doc. No: KR-HSE-HAZP-RPT-002B. Busan: Korean Register.
- KR 2016. LNG Fuel-Ready Ship For 32K bulk carrier. Busan, South Korea: KR.
- LEE, S., SEO, S. & CHANG, D. 2015. Fire risk comparison of fuel gas supply systems for LNG fuelled ships. *Journal of Natural Gas Science and Engineering*, 27, 1788-1795.
- LEES, F. 2012. *Lees' Loss prevention in the process industries: Hazard identification, assessment and control*, Butterworth-Heinemann.
- Lasse, K. 2015. LNG (NG) fuelled shipping – experience and regulations. Haugesund, Norway: Norwegian Maritime Authority.
- LI, J. & HUANG, Z. 2012. Fire and explosion risk analysis and evaluation for LNG ships. *Procedia engineering*, 45, 70-76.
- LOBATO, J., RODRÍGUEZ, J., JIMÉNEZ, C., LLANOS, J., NIETO-MÁRQUEZ, A. & INAREJOS, A. 2009. Consequence analysis of an explosion by simple models: Texas refinery gasoline explosion case. *Afinidad*, 66.
- LR 2011. Rules and Regulations for the Classification of Natural Gas Fuelled Ships. Lloyd's Register: LR.
- LR 2012. LNG-fuelled deep sea shipping: The outlook for LNG bunker and LNG-fuelled newbuild demand up to 2025. London UK: Lloyd's Register.
- MAN Diesel. 2015. ME-GI Dual Fuel MAN B&W Engines: A Technical, Operational and Cost-effective Solution for Ships Fuelled by Gas. Copenhagen, Denmark.
- MANNAN, S. 2005. *Lees' loss prevention in the process industries*, Butterworth-Heinemann.
- MARY K. 2008. LNG Pool Fire Modeling Mary Kay O'Connor Process Safety Center.
- MARTINS, M., PESTANA, M., SOUZA, G. & SCHLEDER, A. 2016. Quantitative risk analysis of loading and offloading liquefied natural gas (LNG) on a floating storage and regasification unit (FSRU). *Journal of Loss Prevention in the Process Industries*, 43, 629-653.
- MAY, W. & MCQUEEN, W. 1973. Radiation from large liquefied natural gas fires. *Combustion Science and Technology*, 7, 51-56.
- MELTON, T. A. & MARX, J. D. 2009. Estimating flame speeds for use with the BST blast curves. *Process Safety Progress*, 28, 5-10.
- MIZNER, G. & EYRE, J. 1982. Large-Scale LNG and LPG pool fires. *EFCE Publication Series (European Federation of Chemical Engineering)*, 25, 147-1.
- MOHAMMADFAM, I. & ZAREI, E. 2015. Safety risk modeling and major accidents analysis of hydrogen and natural gas releases: A comprehensive risk analysis framework. *International Journal of Hydrogen Energy*, 40, 13653-13663.
- MUDAN, K. S. 1989. Evaluation of Fire and Flammability Hazards. *Encyclopedia of Environmental Control Technology*, 1, 416.
- NEDELKA, D., MOORHOUSE, J. & TUCKER, R. 1989. *The Montoir 35m diameter LNG pool fire experiments*, Midlands Research Station.
- NFPA 2004. NFPA 59: LNG Vehicular Fuel System Code.

- NFPA 2009. NFPA 59A: Standard for the production, storage, and handling of liquefied natural gas (LNG).
- NFPA 2015. NFPA 302: Fire Protection Standard for Pleasure and Commercial Motor Craft.
- NORSOK 2001. Standard Z-013 - Risk and emergency preparedness analysis. Norway: NORSOK.
- NORWAY 2000. Decision parameters including risk acceptance criteria. MSC 72/16, IMO: IMO.
- NORWAY2012. HAZID report. London.
- OGP 2010a. Report No.434-14.1: Risk Assessment Data Directory – Vulnerability of humans. London, UK: OGP.
- OGP 2010b. Risk Assessment Data Directory, Ignition probabilities. London, UK.
- OMAR BASHAA, Y. L., MARCELO CASTIERA, TOMASZ OLEWSKIA, LUC VECHOT, SAM MANNANB 2013. Modelling of LNG Pool Spreading on Land with Included Vapour-Liquid Equilibrium and Different Boiling Regimes *Chemical Engineering Transactions*, 31.
- OPSCHOOR, G. 1980. Investigation into the evaporation of liquefied gases spilled on water. *TNO Report*, 80-05624.
- OPSCHOOR, G. 1980. The spreading and evaporation of LNG-and Burning LNG-spills on water. *Journal of hazardous materials*, 3, 249-266.
- OREDA 2009. *Offshore Reliability Data Volume 1 Topside Equipment, 5th edn*, Trondheim, Norway, OREDA.
- PALTRINIERI, N., TUGNOLI, A. & COZZANI, V. 2015. Hazard identification for innovative LNG regasification technologies. *Reliability Engineering & System Safety*, 137, 18-28.
- PARK, S., JEONG, B., LEE, B. S., OTERKUS, S. & ZHOU, P. 2017. Potential risk of vapour cloud explosion in FLNG liquefaction modules. *Ocean Engineering*.
- PERKINS, H. C. 1974. *Air Pollution: Arizona*, Arizona, USA, McGRAW-HILL BOOK COMPANY.
- PIELLISCH, R. 2013. *Container Ship LNG? Plenty of Time* [Online]. Available: <http://hhpinsight.com/marine/2013/01/container-ship-lng-plenty-of-time/> [Accessed 18 January 2016].
- QI, R. 2011. *Liquefied Natural Gas (LNG) Vapor Dispersion Modeling with Computational Fluid Dynamics Codes*. Texas A&M University.
- QIAO, A. & ZHANG, S. 2010. Advanced CFD modeling on vapor dispersion and vapor cloud explosion. *Journal of Loss Prevention in the Process Industries*, 23, 843-848.
- RAJ, P. P., MOUSSA, A. N. & ARAVAMUDAN, K. 1979. Experiments involving pool and vapor fires from spills of liquefied natural gas on water. LITTLE (ARTHUR D) INC CAMBRIDGE MA.
- RAJ, P. K. 2007. LNG fires: A review of experimental results, models and hazard prediction challenges. *Journal of hazardous materials*, 140, 444-464.
- RAMIRO, J. S. & AISA, P. B. 2012. *Risk analysis and reduction in the chemical process industry*, Springer Science & Business Media.
- RAUSAND, M. & HØ YLAND, A. 2004. *System reliability theory: models, statistical methods, and applications*, John Wiley & Sons.
- REID, R. & WANG, R. 1978. The boiling rates of LNG on typical dike floor materials. *Cryogenics*, 18, 401-404.
- REPUBLIC OF KOREA 2014. Leakage analysis and gas explosion simulation in the LNG-fuelled ships. London.

- REPUBLIC OF KOREA 2015. Explosion analysis on the bunkering station for the LNG-fuelled ship. London: IMO CCC.
- REPUBLIC OF KOREA 2016. IMO CCC3/INF. 13: Evaluation of safety zone for LNG bunkering station for LNG-fuelled ships. . London IMO.
- RODEAN, H., HOGAN, W., URTIEW, P., GOLDWIRE JR, H., MCRAE, T. & MORGAN JR, D. 1984. Vapor burn analysis for the Coyote Series LNG spill experiments. Lawrence Livermore National Lab., CA (USA).
- SANTAMARÍA, J. & BRANA, P. 1998. Risk analysis and reduction in the chemical process industry. *Blackie Academic and Professional, London*.
- SCHNEIDER, A. L., LIND, C. D. & PARNAROUSKIS, M. C. 1980. US Coast Guard Liquefied Natural Gas Research at China Lake. COAST GUARD WASHINGTON DC.
- SCHMITZ, B. 2017. *What a Concept: The Importance of the Early Phase of Design* [Online]. PTC. Available: <http://www.ptc.com/cad-software-blog/what-a-concept-the-importance-of-the-early-phase-of-design> [Accessed 28 03 2017].
- SEMOLINOS, P. 2011 LNG as marine fuel: challenges to be overcome.
- SHIP&BUNKER. 2017. World Bunker Prices [Online]. Available: <https://shipandbunker.com/prices#MGO> [Accessed September 9th 2017].
- SIGTTO 2000. Liquefied Gas handling principles on ships and in Terminals.
- SIGTTO 2003. LNG operations in Port Areas.
- SIGTTO 2004. Liquefied Gas Fire Hazard Management.
- SIGTTO 2009. ESD Arrangements & Linked Ship/ Shore Systems for Liquefied Gas Carriers.
- SIGTTO 2013. Ship to Ship Transfer Guide for Petroleum, Chemicals and Liquefied Gases.
- SPOUGE, J. 1999. *A guide to quantitative risk assessment for offshore installations*, CMPT Aberdeen, SD.
- STEFANA, E., MARCIANO, F. & ALBERTI, M. 2016. Qualitative risk assessment of a Dual Fuel (LNG-Diesel) system for heavy-duty trucks. *Journal of Loss Prevention in the Process Industries*, 39, 39-58.
- THOMAS, P. 1965. FIRE SPREAD IN WOODEN CRIBS: PART III THE EFFECT OF WIND. *Fire Safety Science*, 600, -1--1.
- TUGNOLI, A., PALTRINIERI, N., LANDUCCI, G. & COZZANI, V. 2010. LNG regasification terminals: Comparing the inherent safety performance of innovative technologies. *Chemical Engineering Transactions*, 19, 391-396.
- TURBO, M. D. A. 2013. Flexible Dual Future: MAN B&W ME-GI Engine.
- TWEEDDALE, M. 2003. *Managing risk and reliability of process plants*, Gulf Professional Publishing.
- UNCTAD 2015. Review of Maritime transport. Geneva: United Nations.
- URBANSKI, S. 2013. Combustion efficiency and emission factors for wildfire-season fires in mixed conifer forests of the northern Rocky Mountains, US. *Atmospheric Chemistry and Physics*, 13, 7241-7262.
- VANDER MOLEN, R. & NICHOLLS, J. 1979. Blast wave initiation energy for the detonation of methane-ethane-air mixtures. *Combustion Science and Technology*, 21, 75-78.
- VANEM, E., ANTAO, P., Ø STVIK, I. & DE COMAS, F. D. C. 2008. Analysing the risk of LNG carrier operations. *Reliability Engineering & System Safety*, 93, 1328-1344.

- VERSTEEG, H. A. W. MALALASEKERA . 2007. *An Introduction to Computational Fluid Dynamics*, Essex UK, Pearson Education.
- VINNEM, J. E. 2007. *Offshore Risk Assessment Principles, Modeling and Applications of QRA studies*. Springer, London.
- WANG, J. 2001. The current status and future aspects in formal ship safety assessment. *Safety Science*, 38, 19-30.
- WEBBER, D. 1991. Source terms. *Journal of loss prevention in the process industries*, 4, 5-15.
- WINDFINDER. 2016. *wind&weather statistics, Kuta/Bali Airport* [Online]. Available: <http://www.eia.gov/todayinenergy/detail.cfm?id=20972> [Accessed 18 July 2016 2016].
- WITTER, R. E. 1992. Guidelines for hazard evaluation procedures. *Process Safety Progress*, 11, 50-52.
- WOODWARD, J. L. & PITBALDO, R. 2010. *LNG Risk Based Safety: modeling and consequence analysis*, John Wiley & Sons.
- WPCI. 2015. *LNG fuelled vessels - Tank types* [Online]. Available: <http://www.lngbunkering.org/lng/technical-solutions/tank-types> [Accessed 25.09.2017].
- YOON, J., HA J. AND PARK J 2008. LNG vapour dispersion from atmospheric relief valve. *International gas union research conference*. Paris.
- ZABETAKIS, M. G. 1965. Flammability characteristics of combustible gases and vapors. Bureau of Mines Washington DC.
- ZAREI, E., JAFARI, M., DORMOHAMMADI, A. & SARSANGI, V. 2013. The role of modeling and consequence evaluation in improving safety level of industrial hazardous installations: a case study: hydrogen production unit. *Iran Occupational Health*, 10, 54-69.

## APPENDIX A

### VALIDATION OF SOFTWARE

The reliability and accuracy of IQRA was investigated by comparing the results of the software to the values reported in existing publications based on the same techniques.

#### A.1. Flash fire

Using the analytical models discussed in Section 4 of Appendix A, several case studies were conducted for validation.

##### (a) Case study 1

Yoon et al. (2008) conducted a calculation of LNG vapour dispersion from atmospheric relief valve using Gaussian Plume Model. The case study was to find out the horizontal distance to reach 0.1 LEL (4,400 ppm) of natural gas released from the PSV. The results are compared to that of IQRA Software in Table A.. The profiles of vapour dispersion calculated by IQRA are shown in Figure A.1.

Table A.1 Gas dispersion model (Yoon et al. vs IQRA software).

Scenario	Wind Speed: 3.7 m/s	Stability: D	Hyundai Engineering Ltd.	IQRA Software	
	Effective Height	Leak Rate (kg/s)	(Yoon et al., 2008)	Briggs. Model	Von. Model
PSV on LNG Storage Tank	44m	10.3 kg/s	192 m	192 m	186 m
PSV on Vaporizer	27m	37.8 kg/s	392 m	392 m	411 m

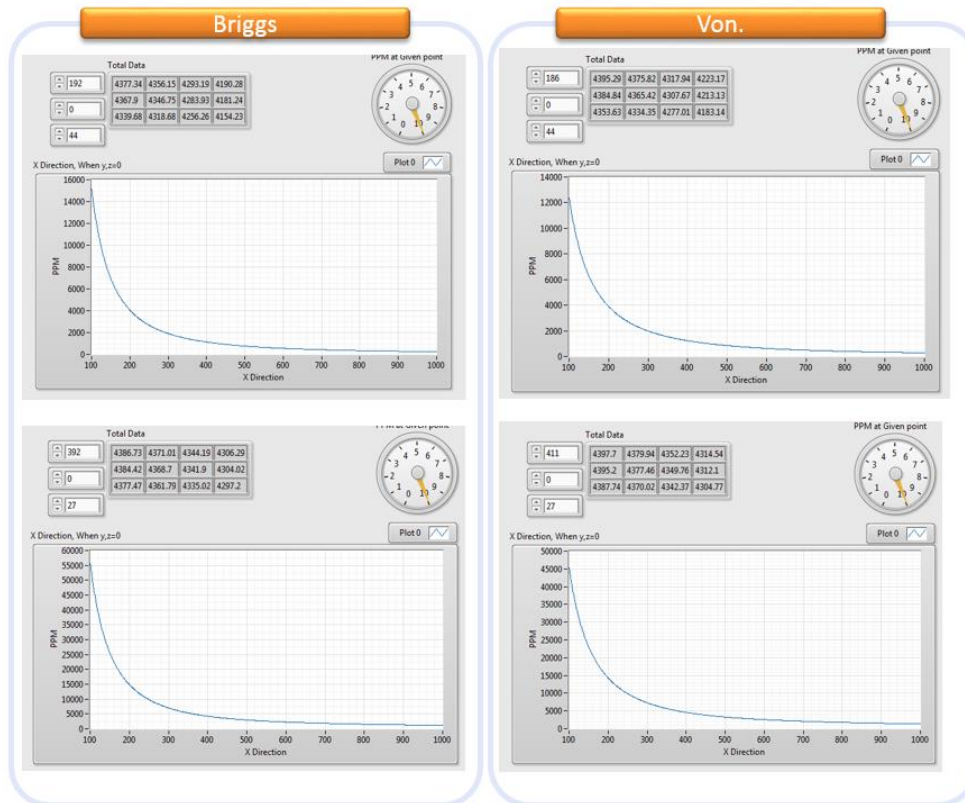


Figure A.1. Gas concentration in response to x-distance.

*(b) Case study 2*

Ramiro and Aisa (1998) calculated dispersion of ammonia released from a pipe of a chemical plant in the vapour phase and calculated the maximum concentration at a point situated 0.5 km from the source. Here the horizontal distance to reach the concentration of 11ppm or  $8.0E-6 \text{ kg/m}^3$  (which is 0.1 LEL) was estimated and the concentration at the co-ordinates (500, 50, 0) was also calculated. The results are compared with those produced by IQRA in Table A.2. The dispersion profile calculated by IQRA is given in Figure A. and A.3.

Table A.2 CHEMS-PLUS vs IQRA software.

Scenario	Wind Speed: 7m/s	Stability: D	CHEMS-PLUS 2.0 (Santamaria and Brana 1998)	IQRA Software		J.M (Santamaria and Brana 1998)
	Effective Height	Leak Rate (kg/s)		Van. Model	Briggs. Model	
Chemical Plant release (Ammonia)	15 m	0.2 kg/s	505m at 11ppm	500m at 11ppm	466m at 11ppm	500m at 11ppm
				3.38E- 6kg/m <sup>3</sup> (at 500, 50, 0)	3.64E- 6kg/m <sup>3</sup> (at 500, 50, 0)	3.38E-6kg/m <sup>3</sup> (at 500, 50, 0)

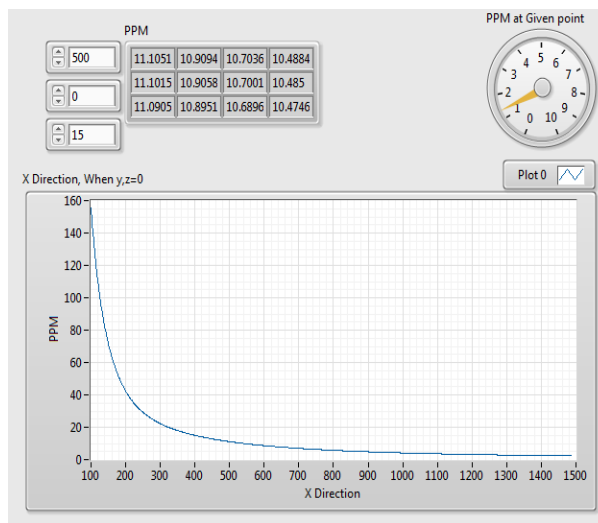


Figure A.2. Gas concentration in response to x-distance.



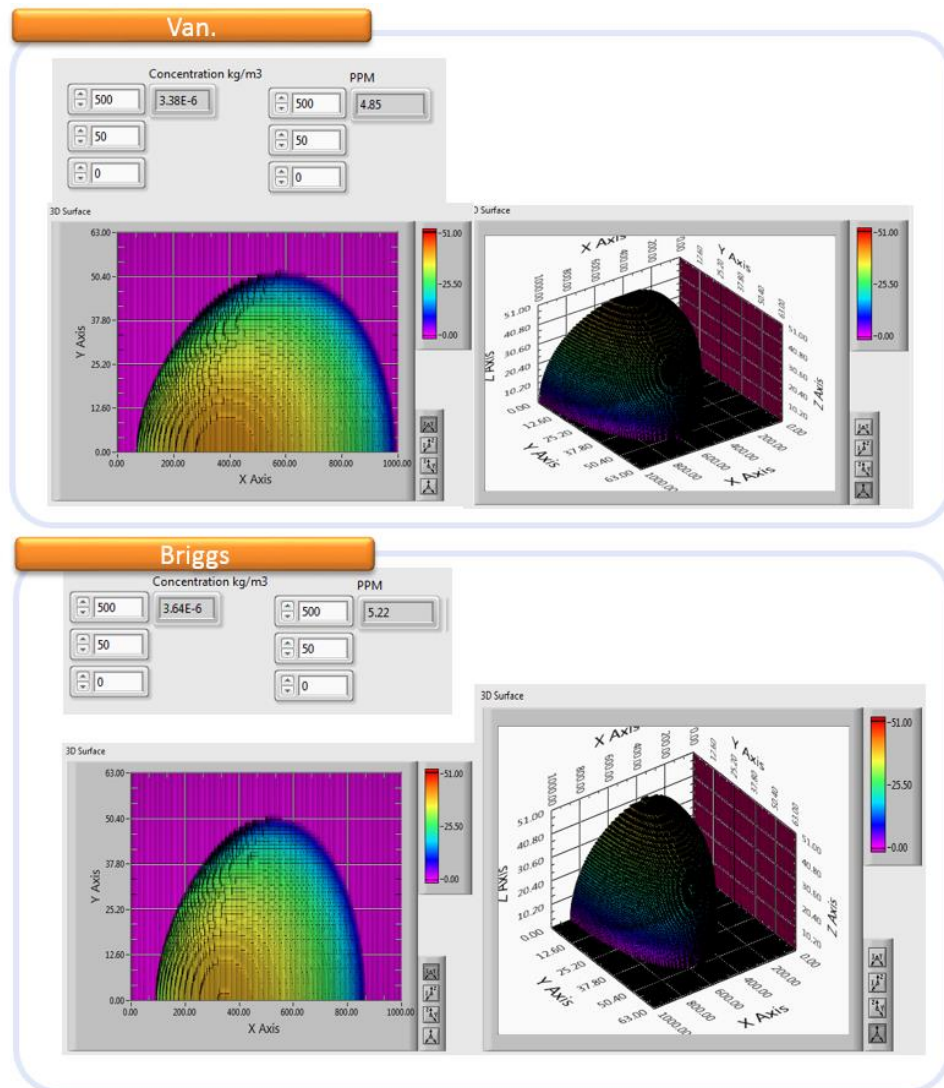


Figure A.3. Gas concentration (Briggs. vs Van.).

(c) *Case study 3*

Santamaria (2012) has conducted a puff model for ethane to investigate the safety distance from the VCE. The ethane was considered to be released vertically and the wind speed was 4 m/s. The result shows that the explosion can occur at distances less than 90.6 m, given that lower flammability limit is 3 % by volume (equivalent to 0.0375 kg/m<sup>3</sup>, taking a density of 1.25 kg/m<sup>3</sup> for ethane at 20 °C and atmospheric pressure). The ethane cloud centre travels the 90.6 m distance in 22.65 s (equal to 90.6m/4 m/s). The explosion will not occur if during approximately 23 s the cloud does not find

an ignition source in its path. IQRA software produced exactly the same value as shown in Table A.3.

Table A.3 Flash fire impact.

Scenario	Wind Speed: 4m/s	Stability: E	Santabria and Brana (1998)	IQRA Software
	Effective Height	Leak Rate (kg/s)		
Ethane release	0m	40kg	22.65s (90.6m)	22.65s (90.6m)

## A.2. Impact of explosion

### (a) *Case study 1*

Santamaria and Brana (1998) has calculated explosions equivalent to 500 and 5000 kg of TNT respectively. It calculated in both cases the radius within which it is probable that buildings become uninhabitable (partial demolition) (at 7 kPa) as a consequence of the explosion. It was 110 m for 500 kg of TNT and 240 m for 5000 kg of TNT. The results of IQRA software show 108 m for 500 kg of TNT and 233 m for 5,000 kg of TNT as shown in Figure A.4. The results are also shown in Table A.4.

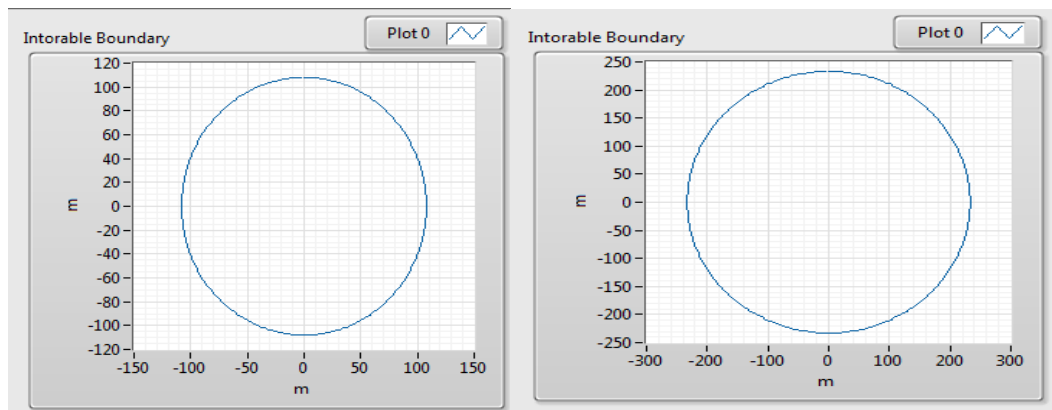


Figure A.4. Explosion impact.

Table A.4. Explosion impact.

Case	Tool	Distance (m)				
		100	200	400	700	1000
Case 1 (500 kg TNT)	Santa. 1998	7.5	3	1.3	0.72	0.45
	IQRA software	8	2.5	0.8	0.3	0.2
Case 2 (5000 kg TNT)	Santa. 1998	27.0	8.5	4.0	2.0	1.0
	IQRA software	29.2	9.1	2.8	1.1	0.6

The main reason of the discrepancies observed in pressure values is the fact that Santamaria and Brana used eye estimation in reading the original distance graph, while IQRA used fitted equation.

(b) Case study 2

Lobato et al. (2009) evaluated the effects of the explosion using simple models (TNT, TNO Multi-Energy, and BST). They showed that the empirical models can be used for risk assessment. Gasoline mass used for explosion in this case study was 4,881.9 kg. The results are compared in Table A.5 to Table A.6 and Figure A.5 and Figure A.6.

Table A.5 Explosion impact.

	90% lung	1% lung	Total build	1% eardrum
Overpressure (kPa)	169.2	101	68.9	16.2
TNT (1%)	16m	22m	27m	65m
TNT (5%)	27m	38m	47m	112m
TNT (10%)	35m	47m	59m	141m

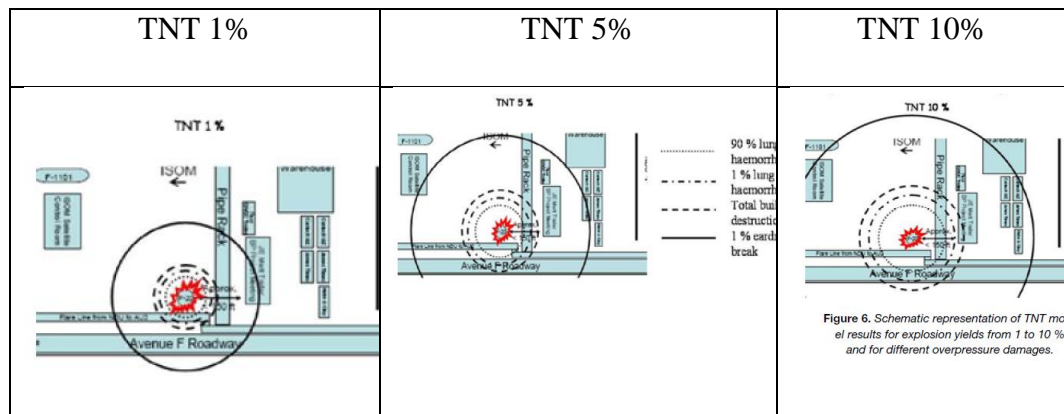


Figure A.5. Explosion impact (Lobato et al. 2009).

Table A.6 Explosion impact.

Reference (TNO 7)	Reference		IQRA Software		
	TNO 7	BST (0.588)	TNO 7	BST (1)	BST (0.5)
100m	Abt. 19KPa	Abt. 22KPa	19KPa	24KPa	15KPa
200m	Abt. 8 KPa	Abt.12.5KPa	8.3KPa	11KPa	7.7KPa
250m	Abt. 5 KPa	Abt.10 KPa	6.3KPa	9KPa	6KPa

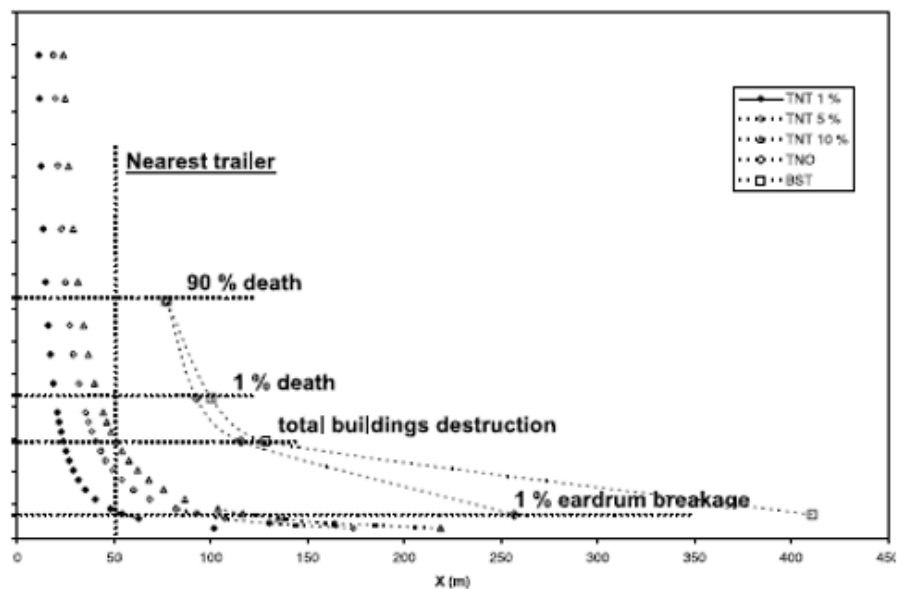


Figure A.6. Comparison of the results obtained with different models applied to standard damages (Lobato et al. 2009).

### A.3. Pool fire

The impact of pool fire was calculated with IQRA software and the results were compared with those given in a reference (Raj 2007). The results are shown in Table A.7 and Figure A.7.

Table A.7 Pool fire impact.

Fire Diameter (m)	Surface on which LNG boils	Mean SEP over the visible fire plume height(Eavg) (kW/m <sup>2</sup> )		
		IQRA Software	Reference (Raj 2007)	From field tests
15	water	171.688	172	185-224
20	Land	182.984	183	140-180
35	Land	176.299	177	175+-30
100	Land	112.49	113	-
300	water	89.2237	90	-

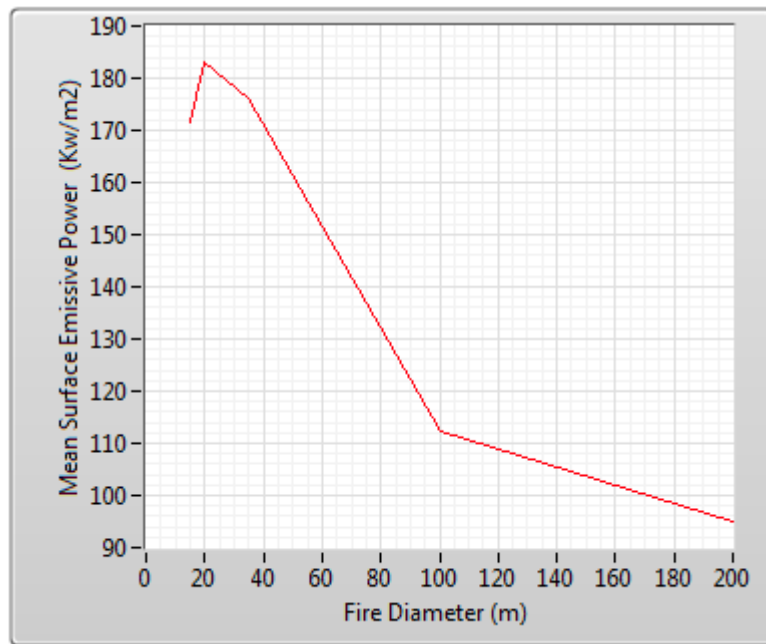


Figure A.7. Impact of pool fire.

## APPENDIX B

### CONSEQUENCE ANALYSIS RESULTS

Results of the study described in Chapter 10 are compared to the FEA results carried out based on static analysis with transient analysis. Table B. and Figure B.18 reveal that FEA for the static condition is more critical than the transient condition. However, the difference is negligibly small. For transient calculation, time step was 0.1 second. In addition, Figures B.2 to B.16 show the FEA results for the parametric analysis described for the study done in Chapter 10.

Table B.1 Comparison between static condition and transient condition.

Pressure	Stress (N/mm <sup>2</sup> )		Difference
	Static	Transient	
1 bar	491.06	490.43	0.13%
2 bar	982.13	980.82	0.13%
3 bar	1473.2	1470.8	0.16%

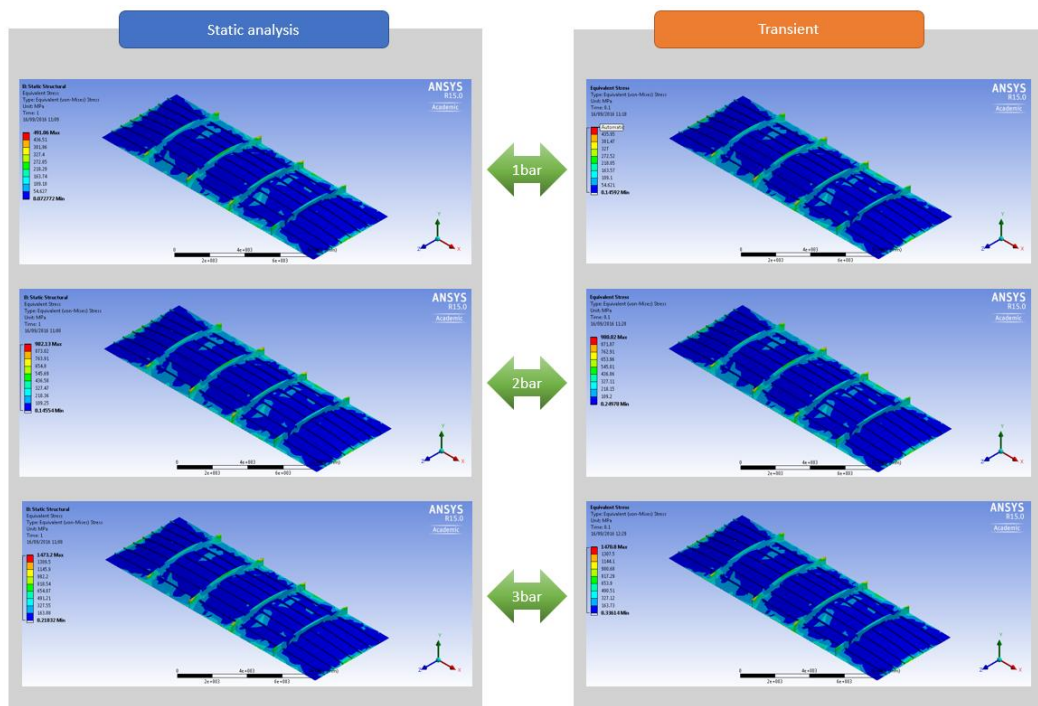


Figure B.18. Comparison between static condition and transient condition.

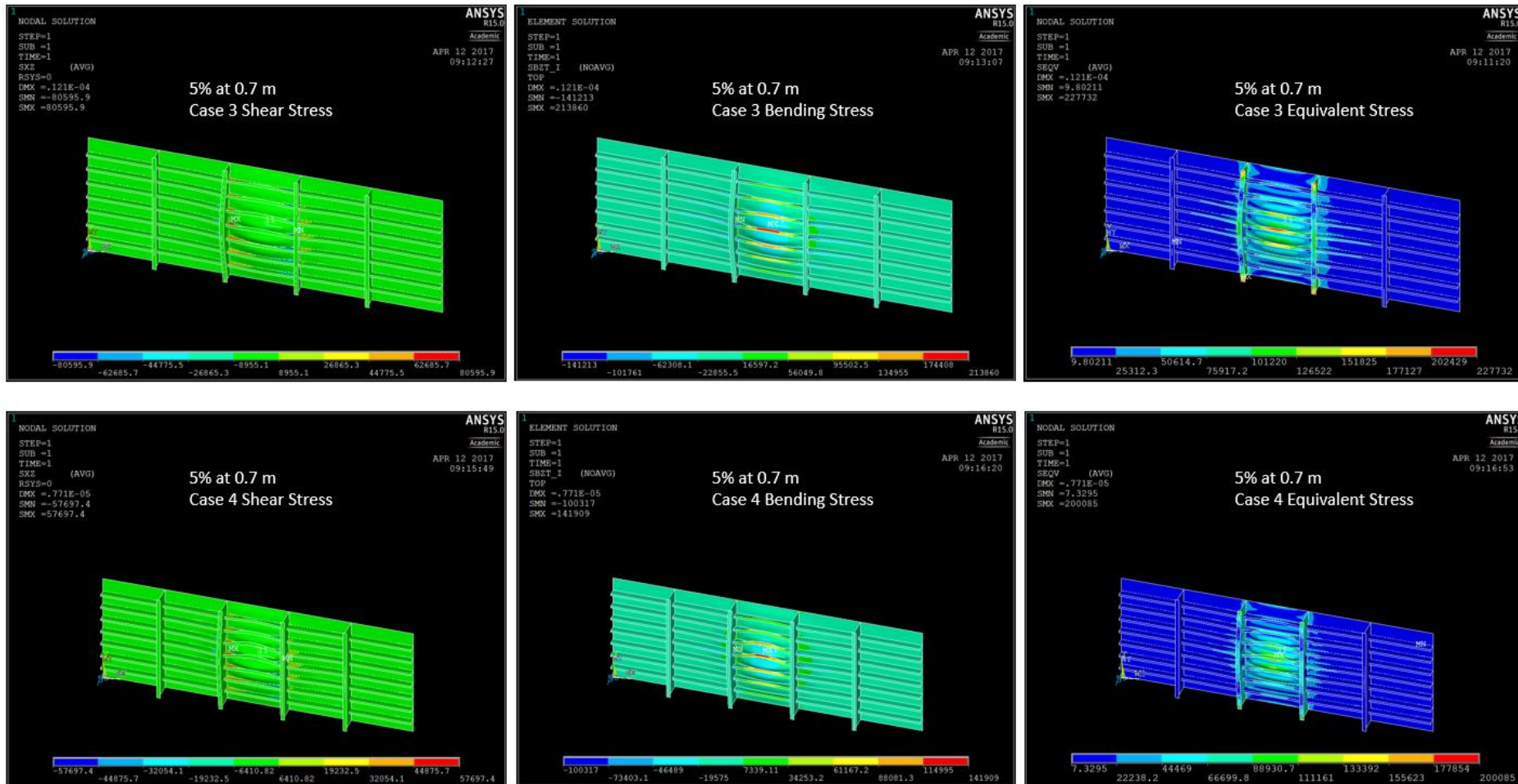


Figure B.2. Stresses of Case 1 and 2 at the condition of 5% of methane mixture and 0.7m ignition point.

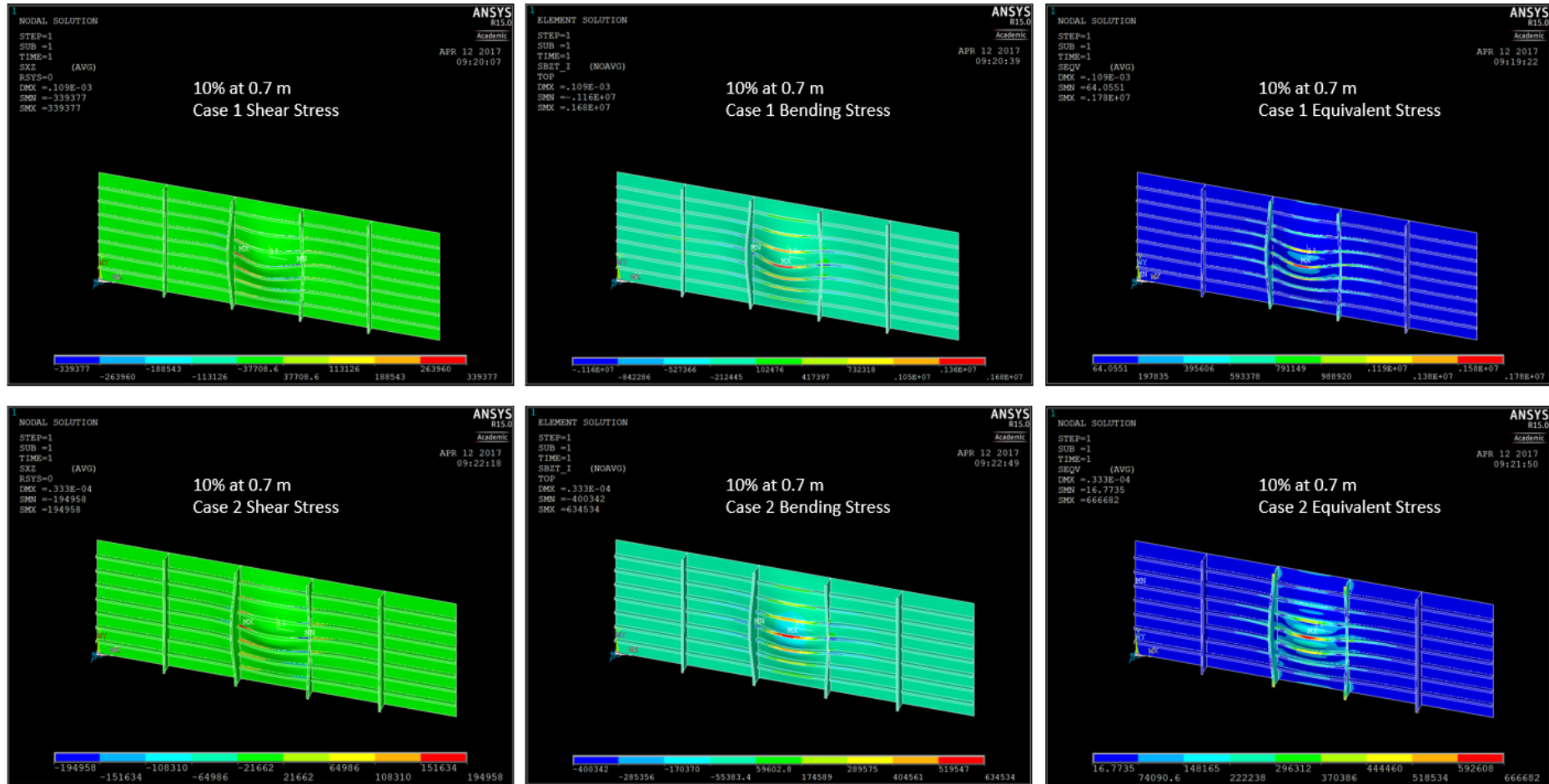


Figure B.3. Stresses of Case 3 and 4 at the condition of 5% of methane mixture and 0.7m ignition point.



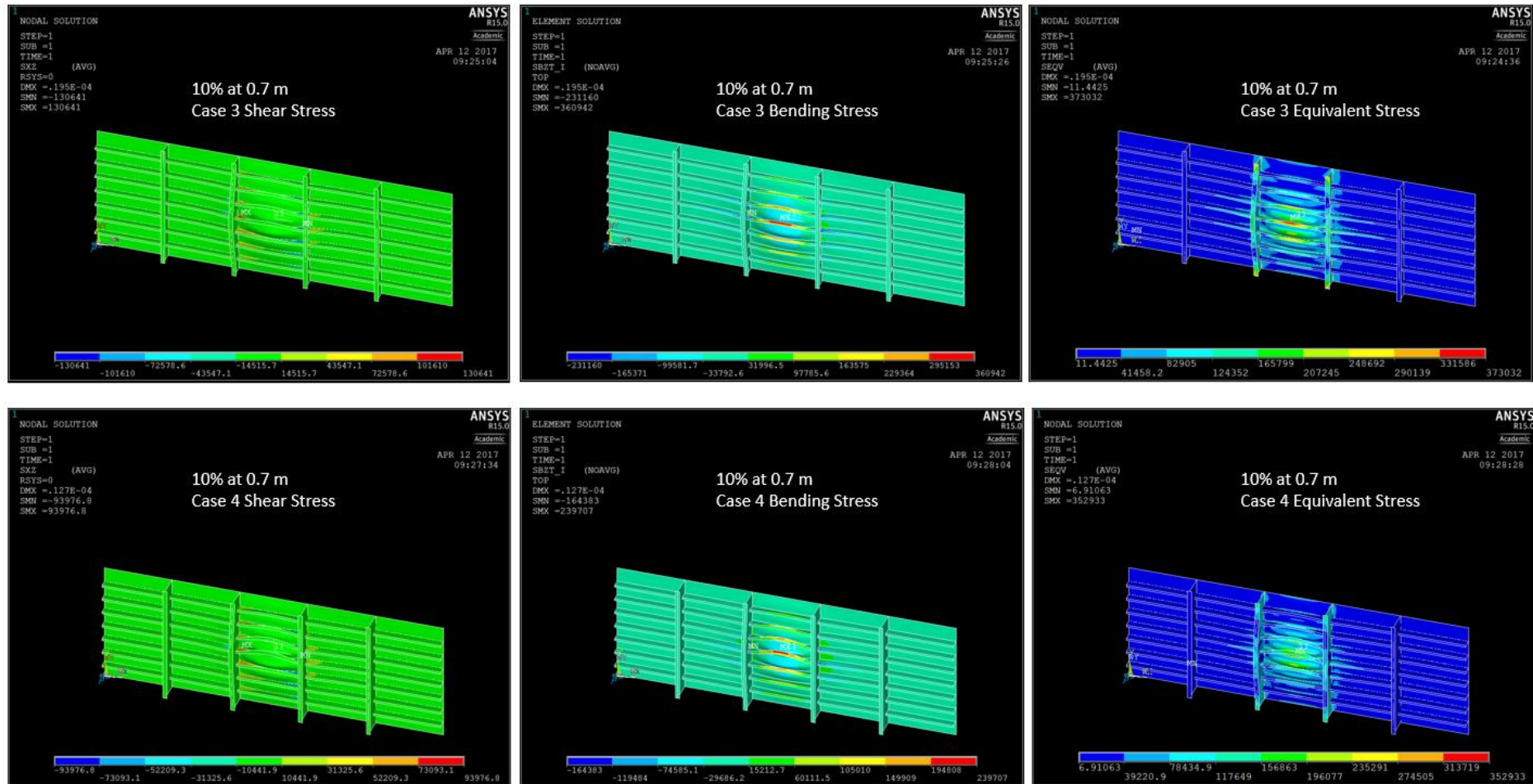


Figure B.4. Stresses of Case 1 and 2 at the condition of 10% of methane mixture and 0.7m ignition point.

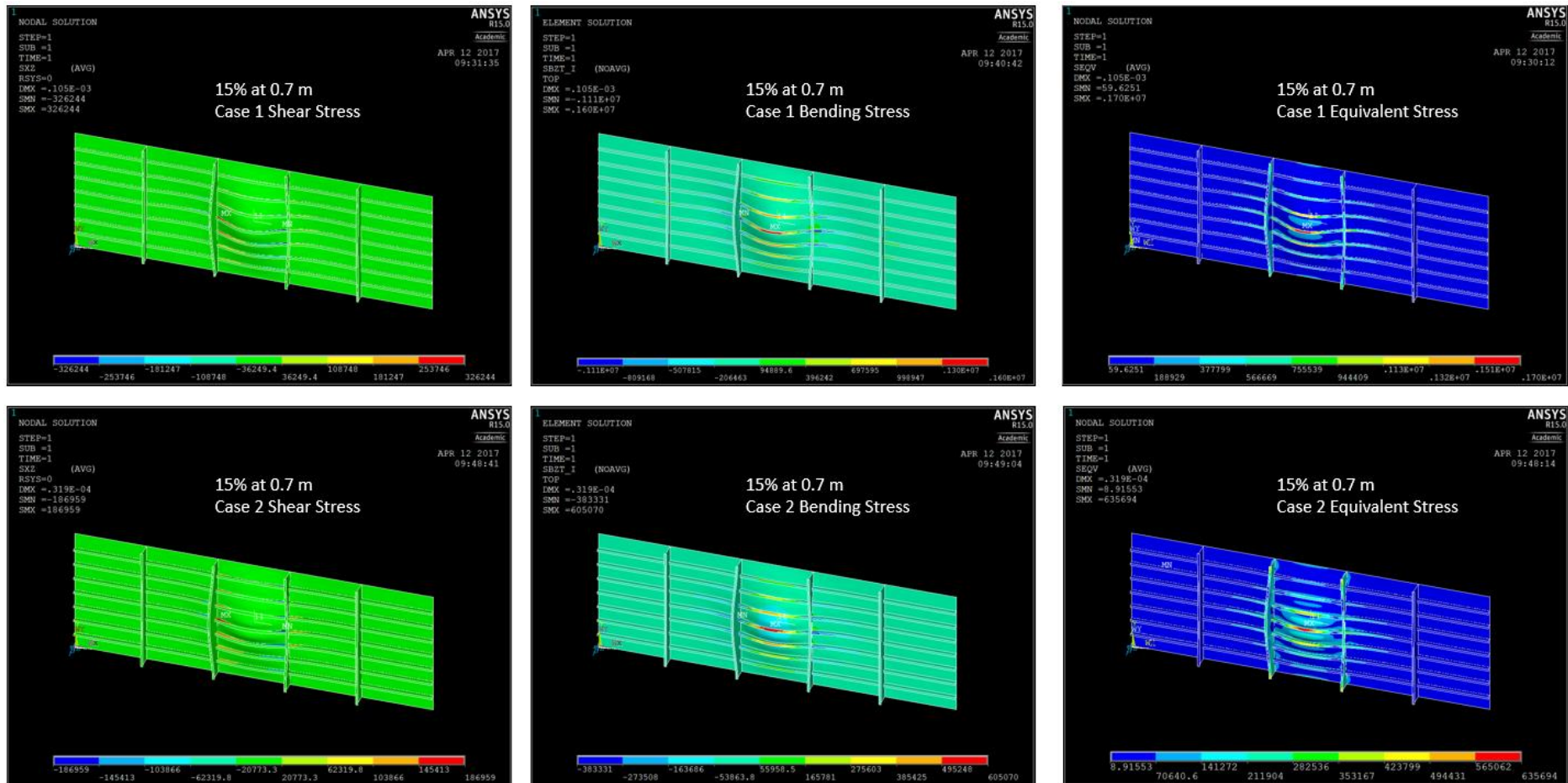


Figure B.5. Stresses of Case 3 and 4 at the condition of 10% of methane mixture and 0.7m ignition point.

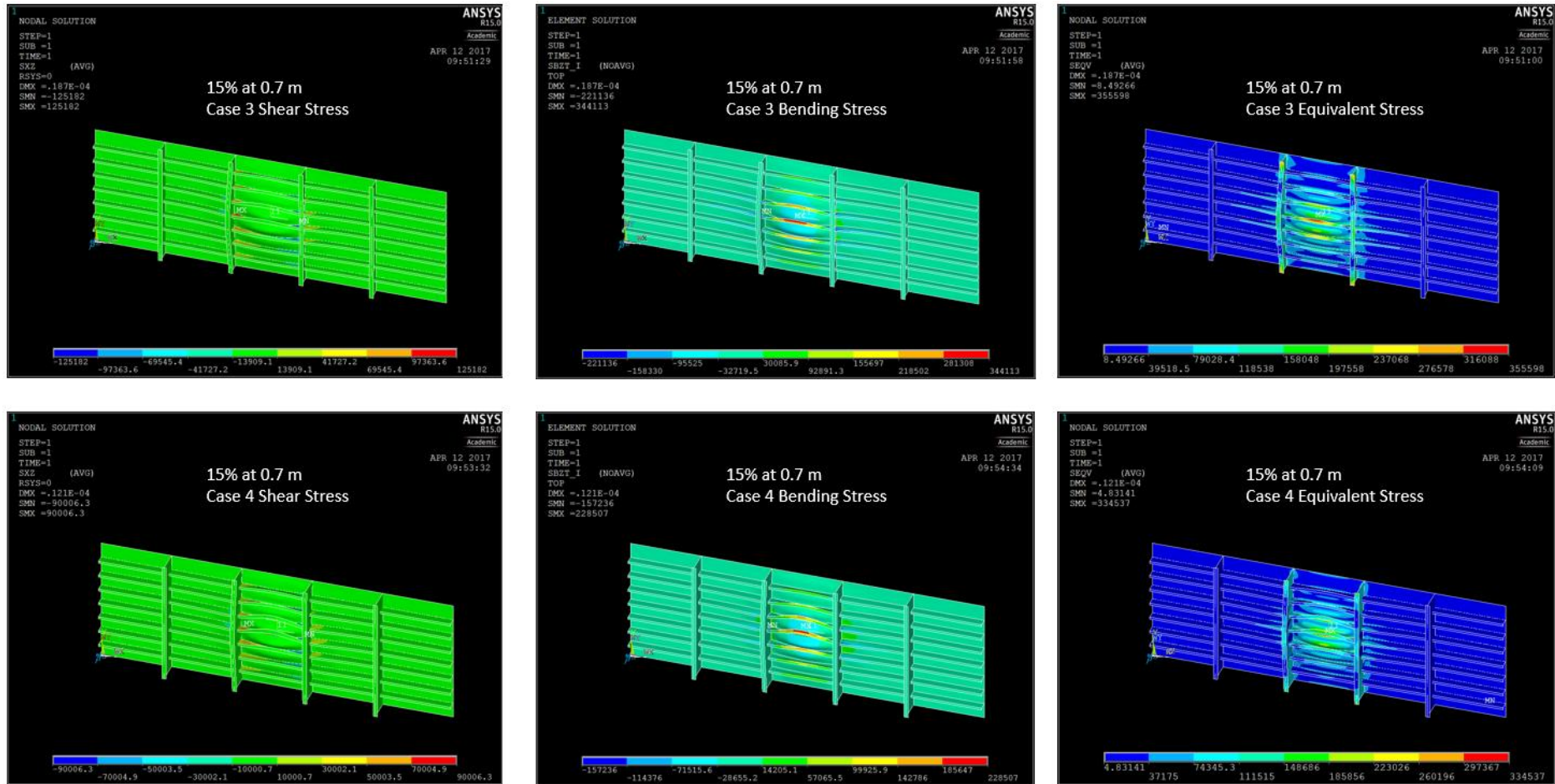


Figure B.6. Stresses of Case 1 and 2 at the condition of 15% of methane mixture and 0.7m ignition point.

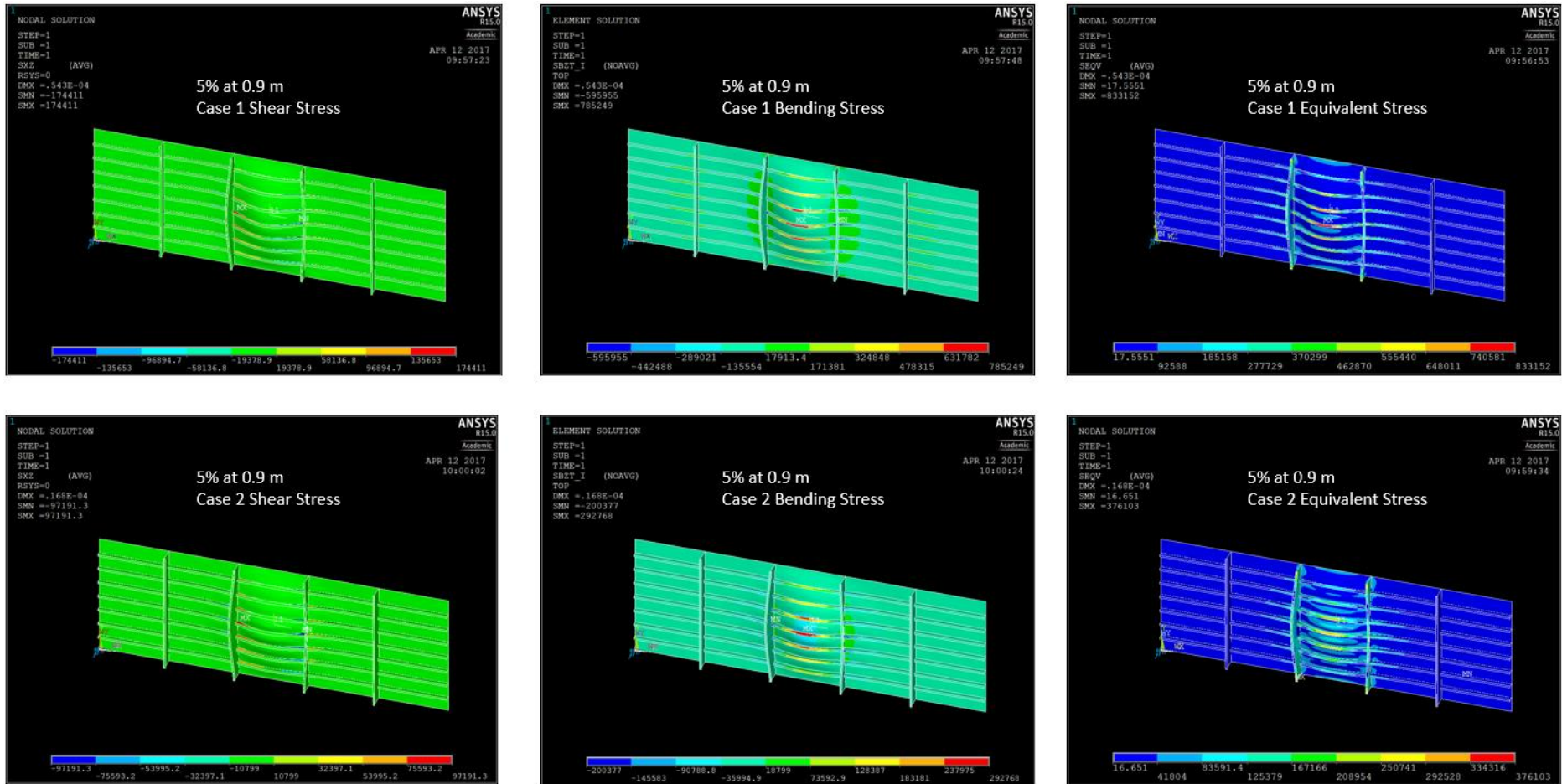


Figure B.7. Stresses of Case 3 and 4 at the condition of 15% of methane mixture and 0.7m ignition point.

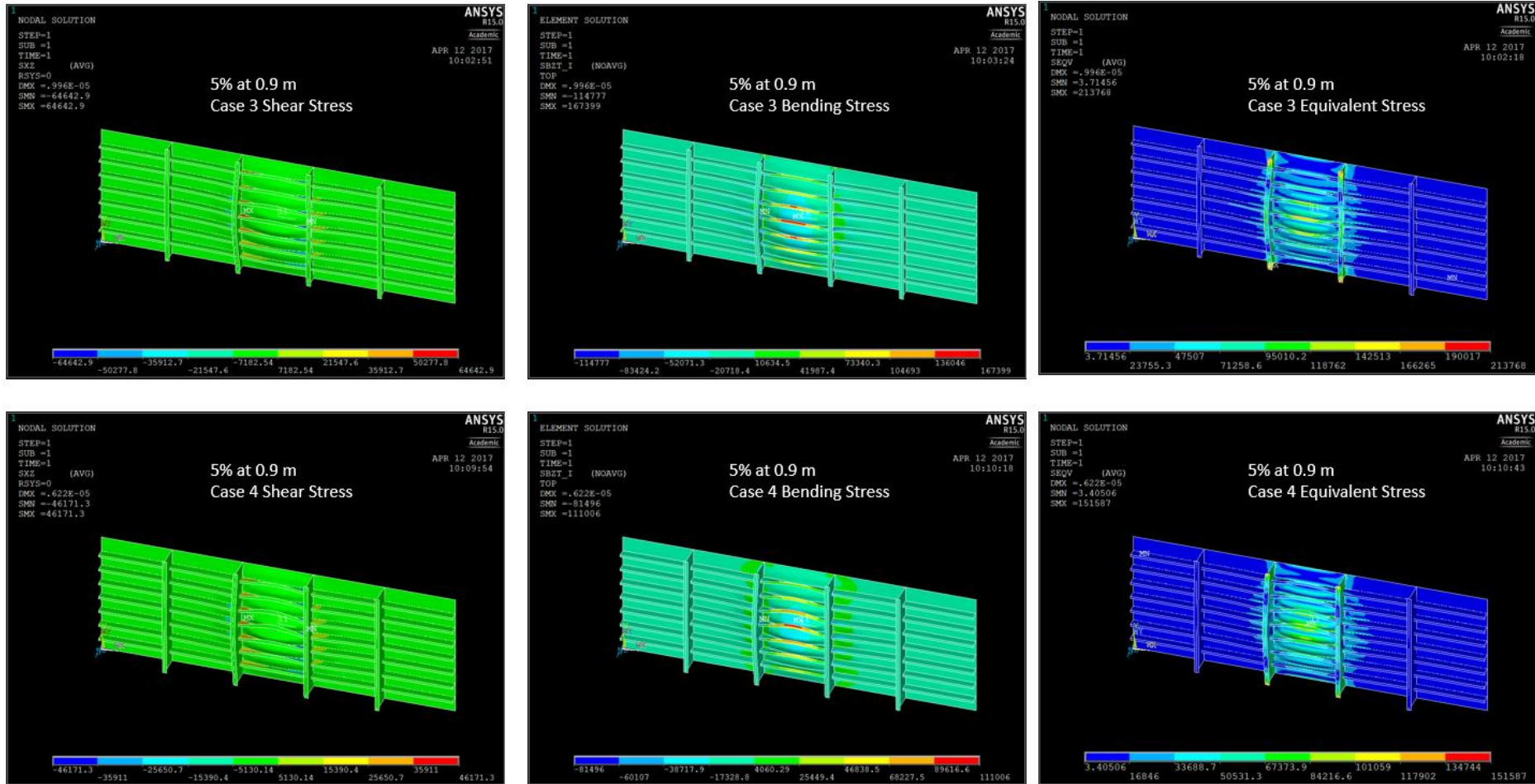


Figure B.8. Stresses of Case 1 and 2 at the condition of 5% of methane mixture and 0.9m ignition point.

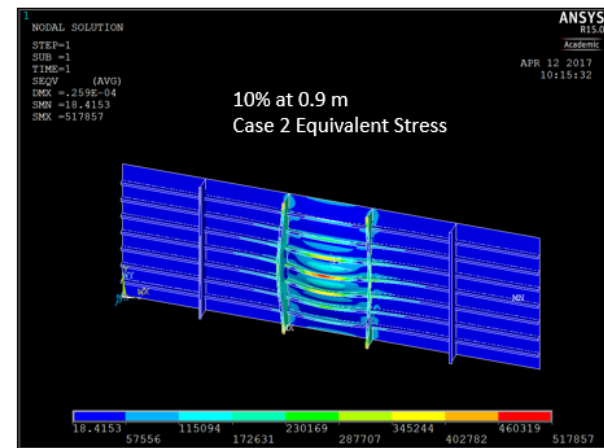
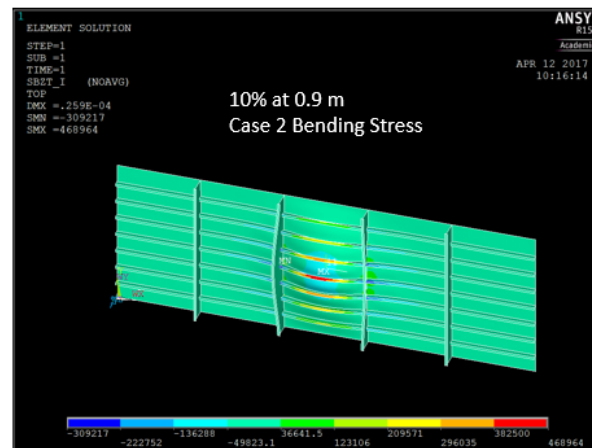
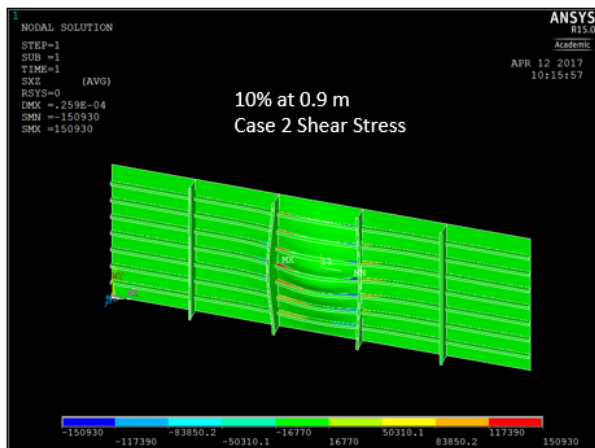
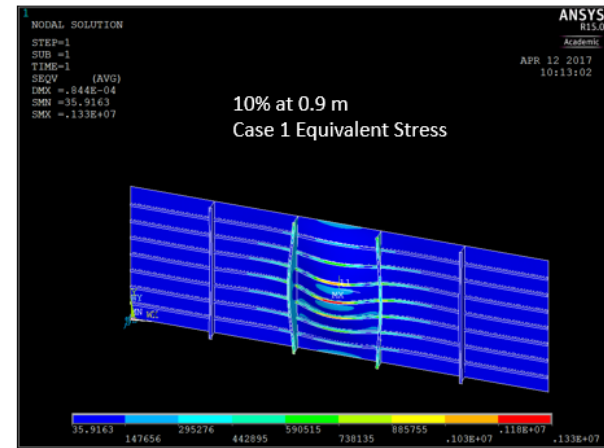
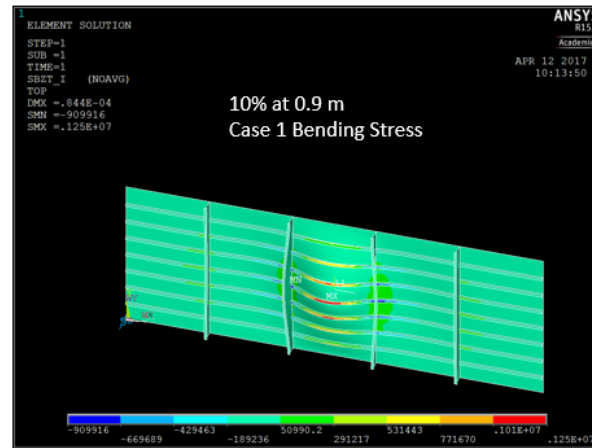
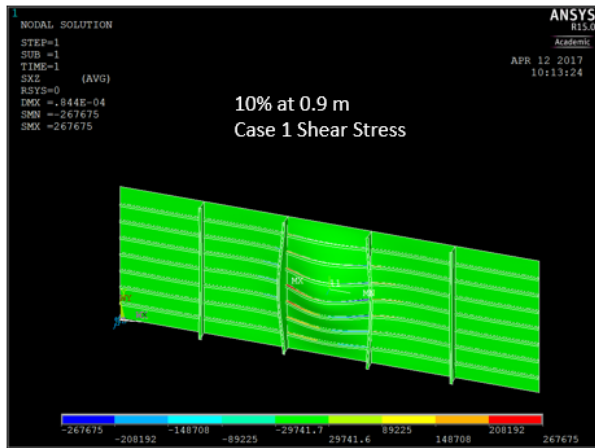


Figure B.9. Stresses of Case 3 and 4 at the condition of 5% of methane mixture and 0.9m ignition point.

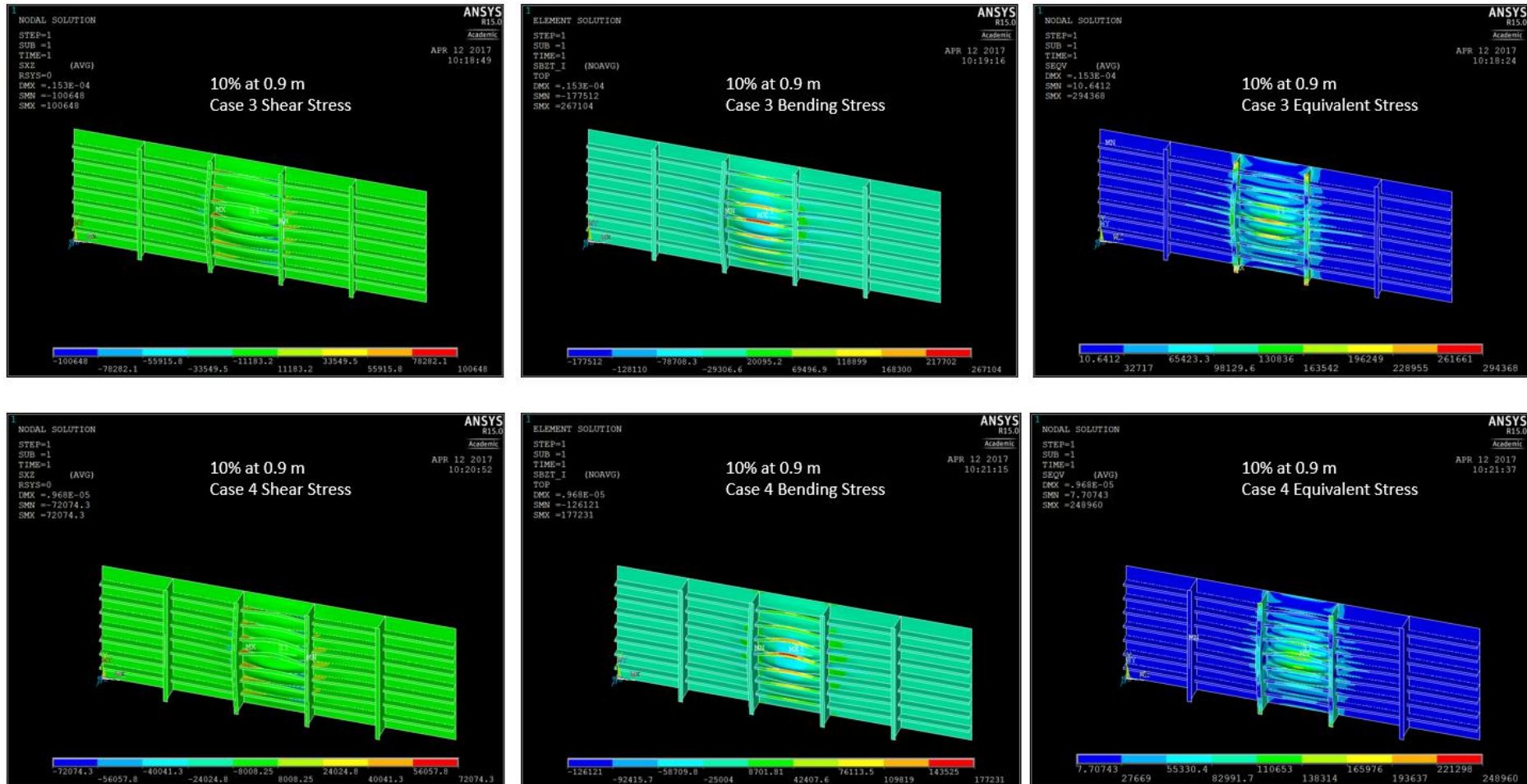


Figure B.10. Stresses of Case 1 and 2 at the condition of 10% of methane mixture and 0.9m ignition point.

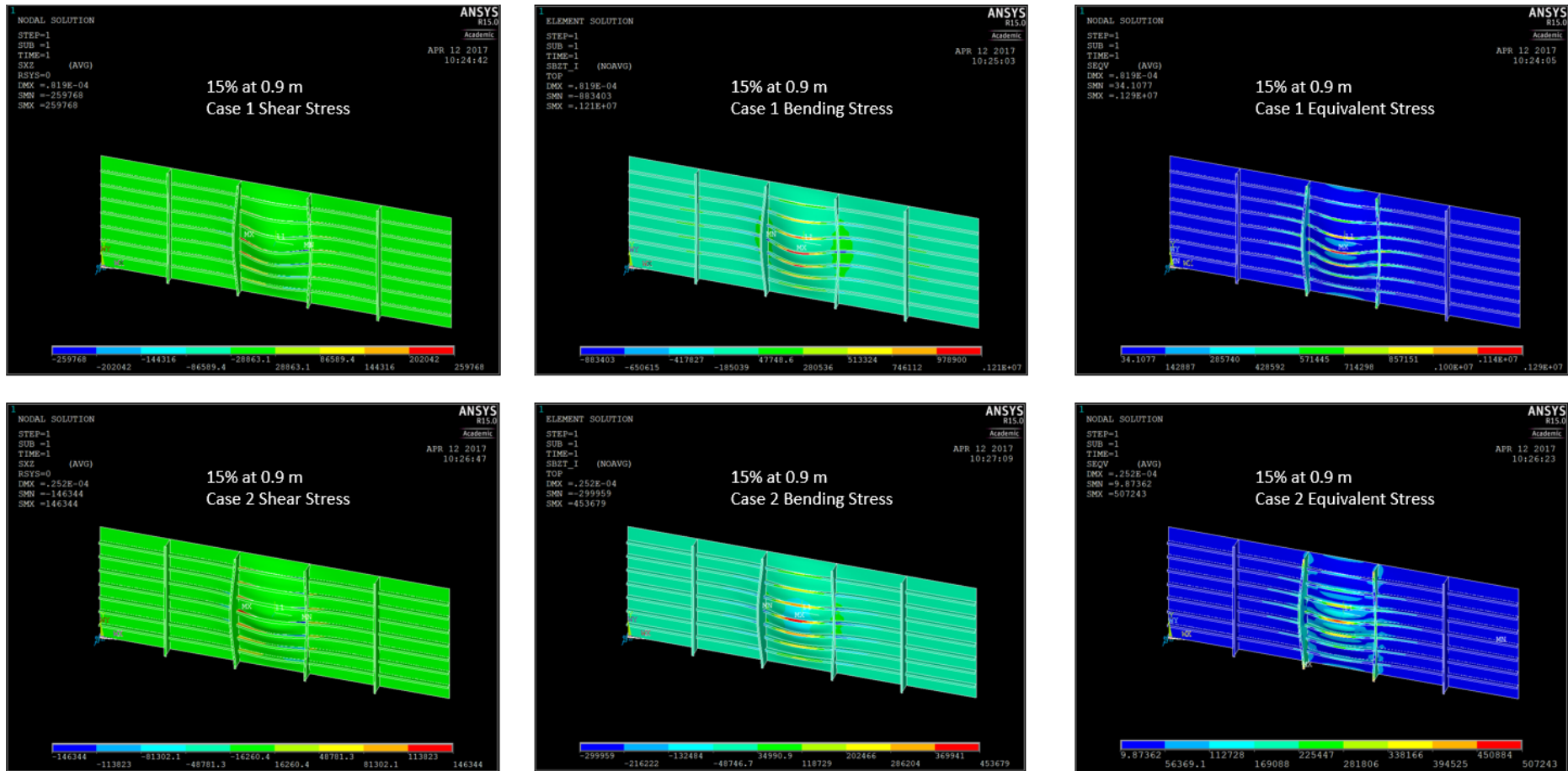


Figure B.11. Stresses of Case 3 and 4 at the condition of 10% of methane mixture and 0.9m ignition point.



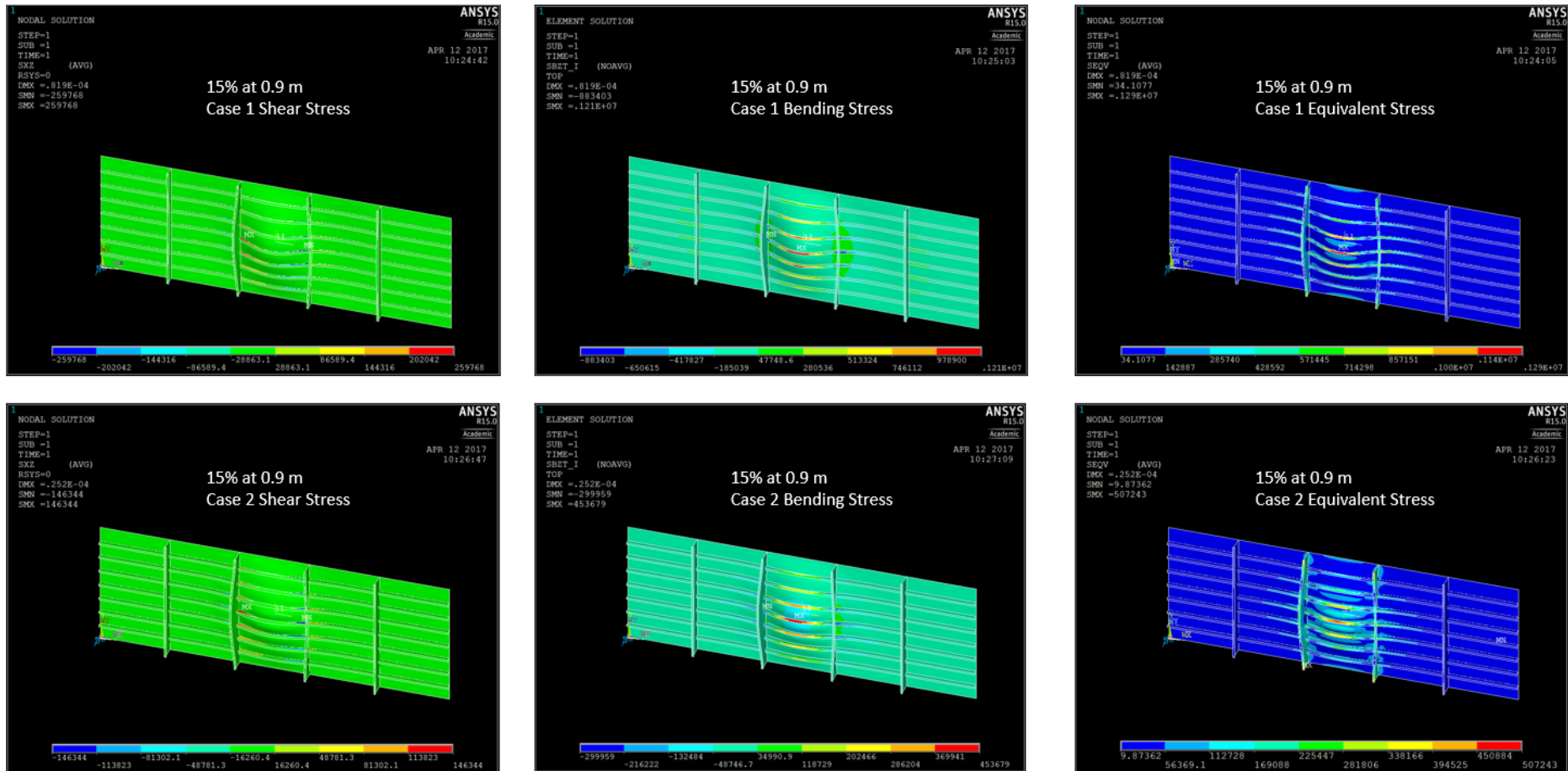


Figure B.12. Stresses of Case 1 and 2 at the condition of 15% of methane mixture and 0.9m ignition point.

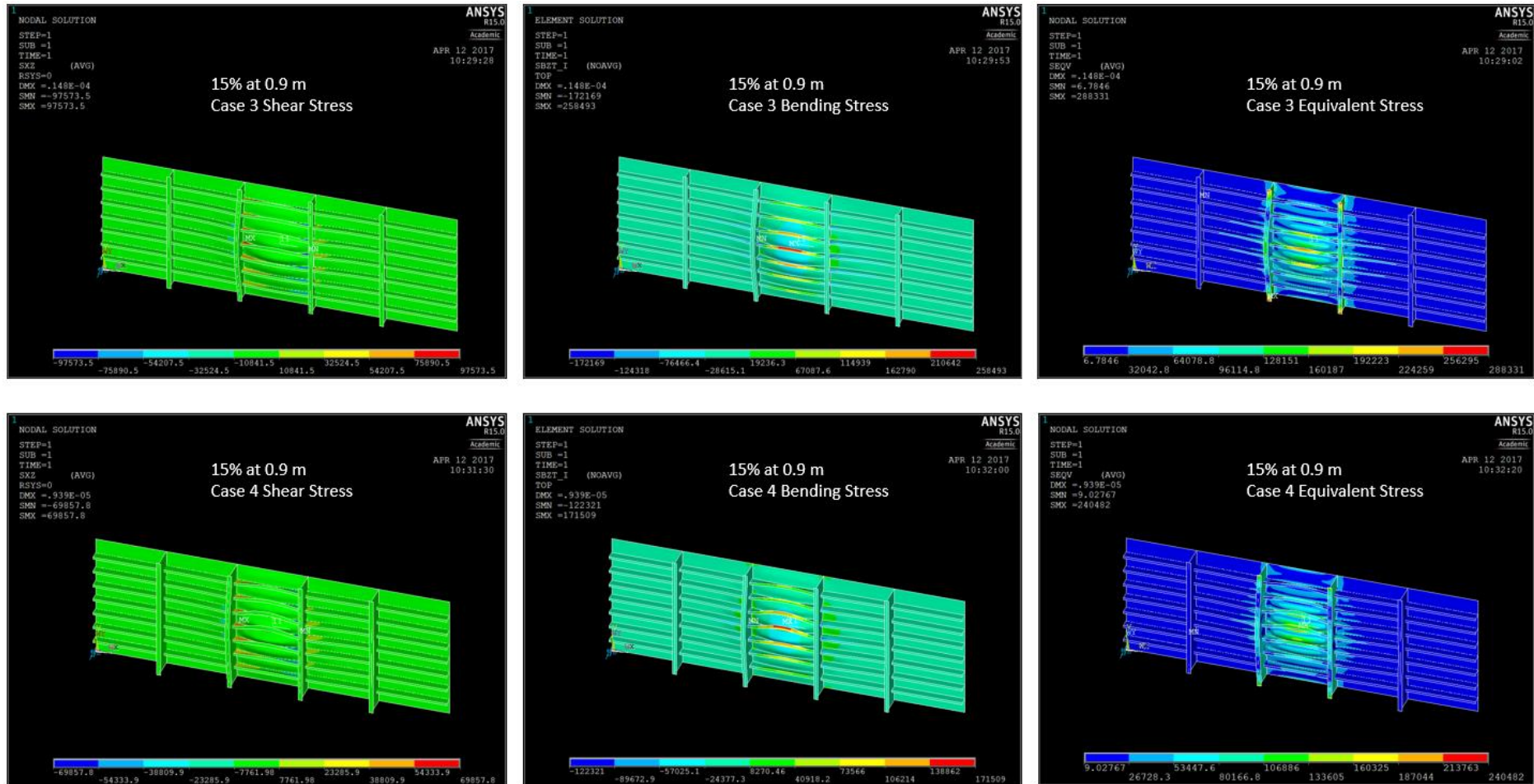


Figure B.13. Stresses of Case 3 and 4 at the condition of 15% of methane mixture and 0.9m ignition point.

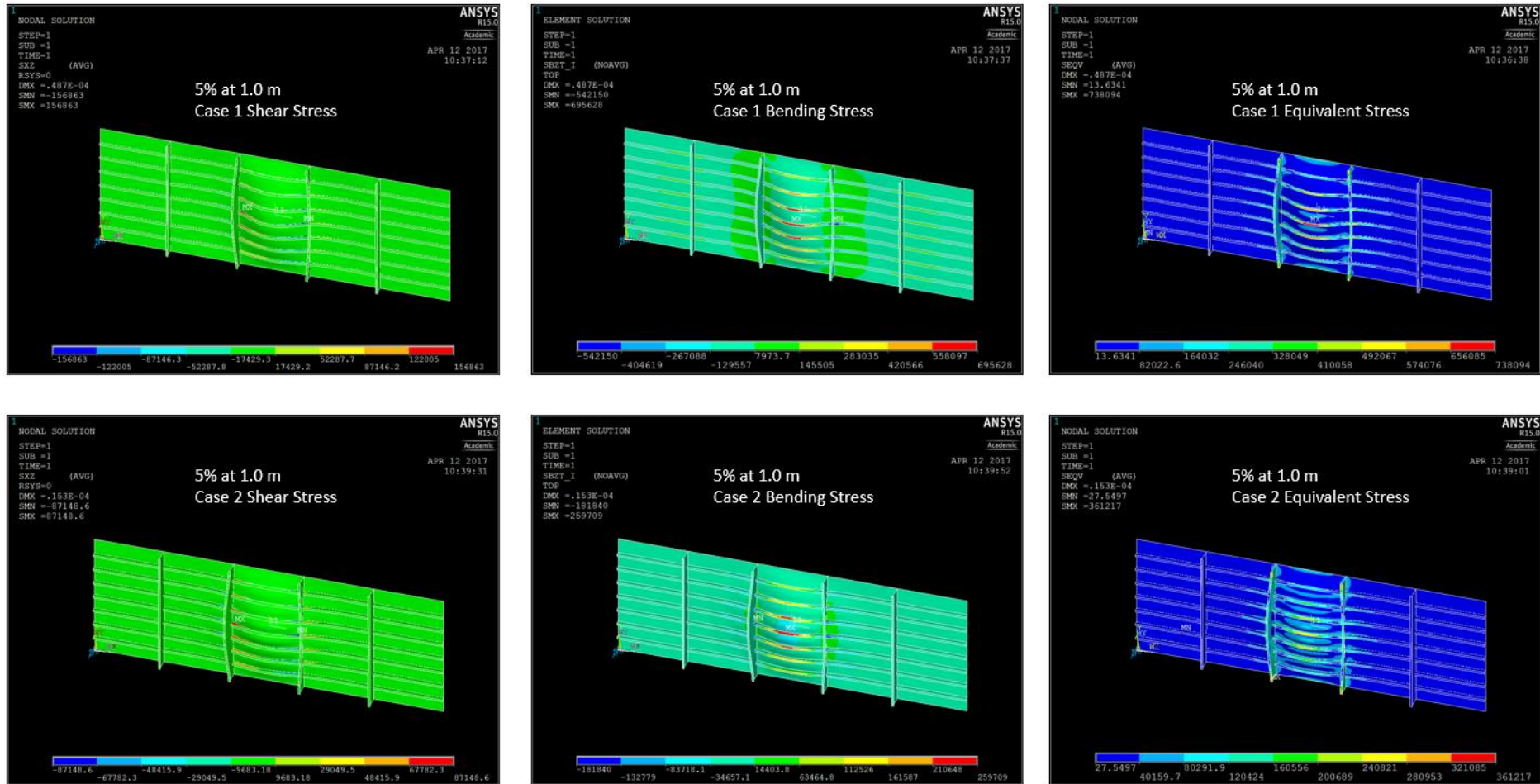


Figure B.14. Stresses of Case 1 and 2 at the condition of 15% of methane mixture and 1.0m ignition point.

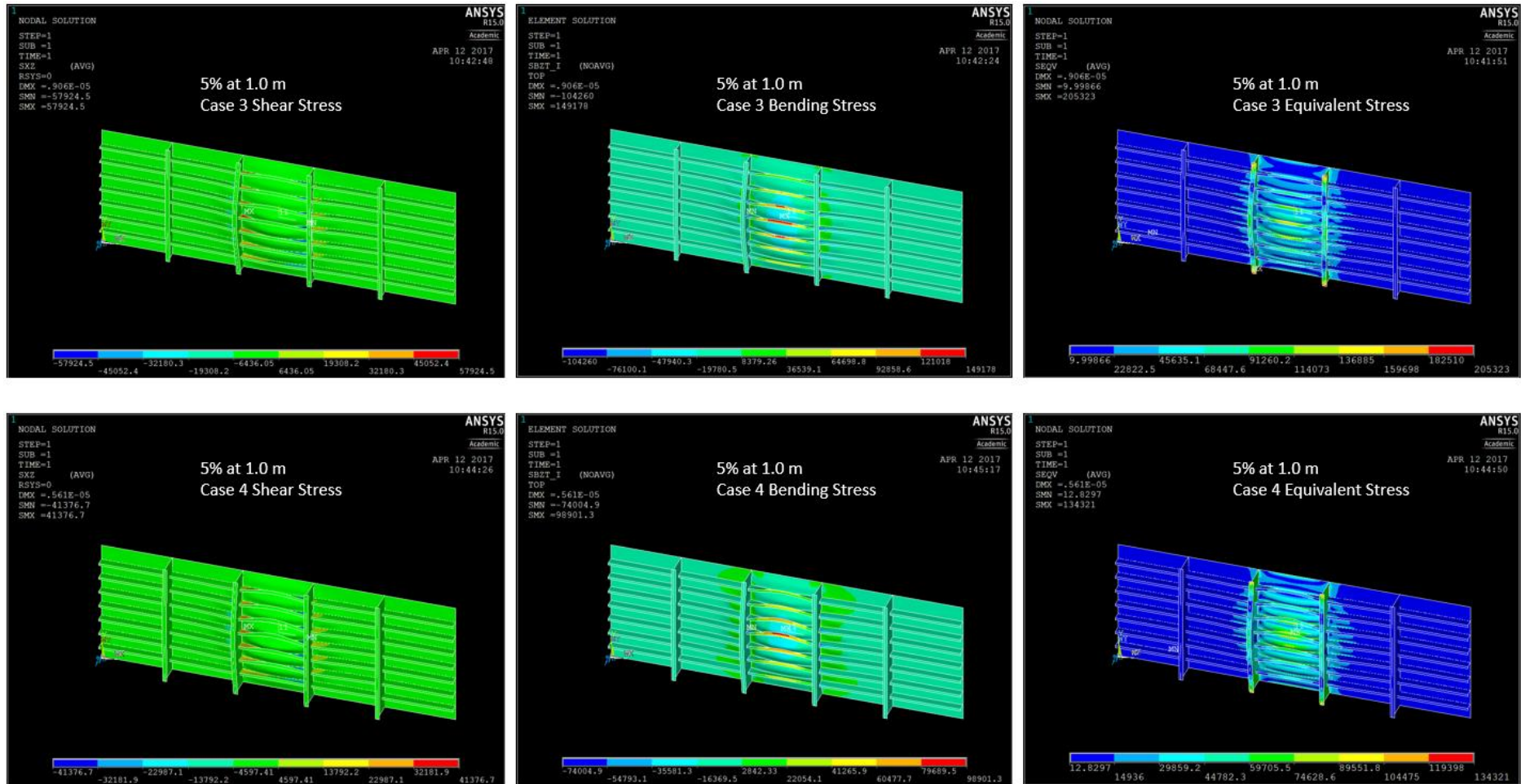


Figure B.15. Stresses of Case 3 and 4 at the condition of 5% of methane mixture and 1.0m ignition point.

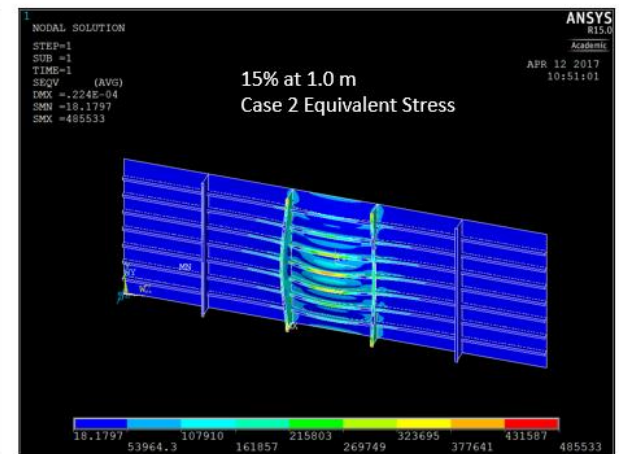
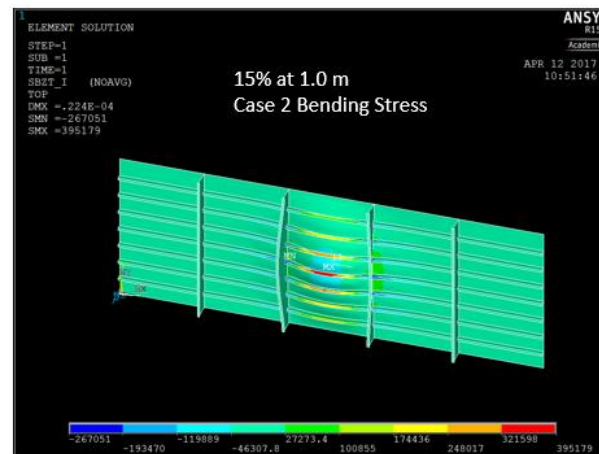
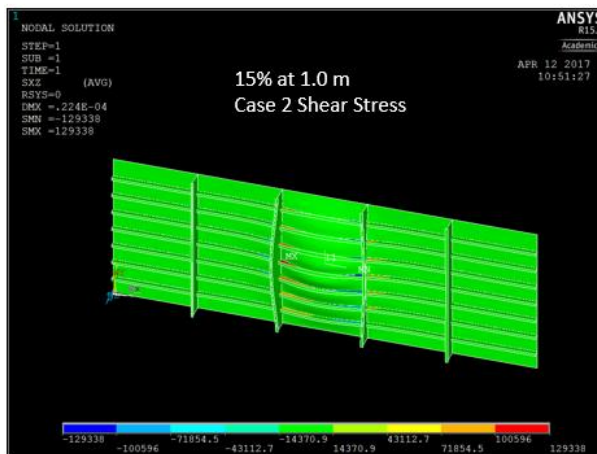
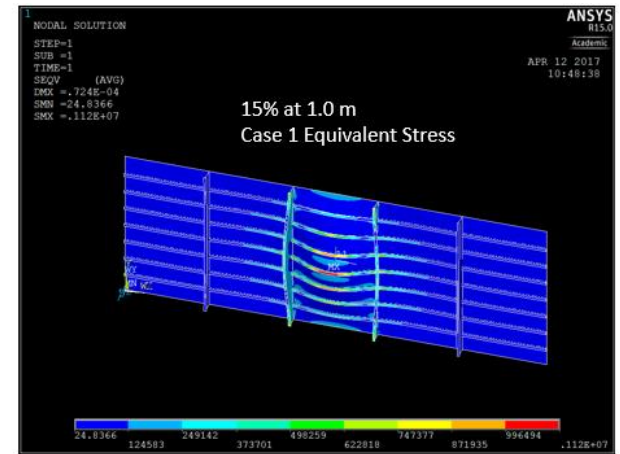


Figure B.16. Stresses of Case 3 and 4 at the condition of 5% of methane mixture and 1.0m ignition point.

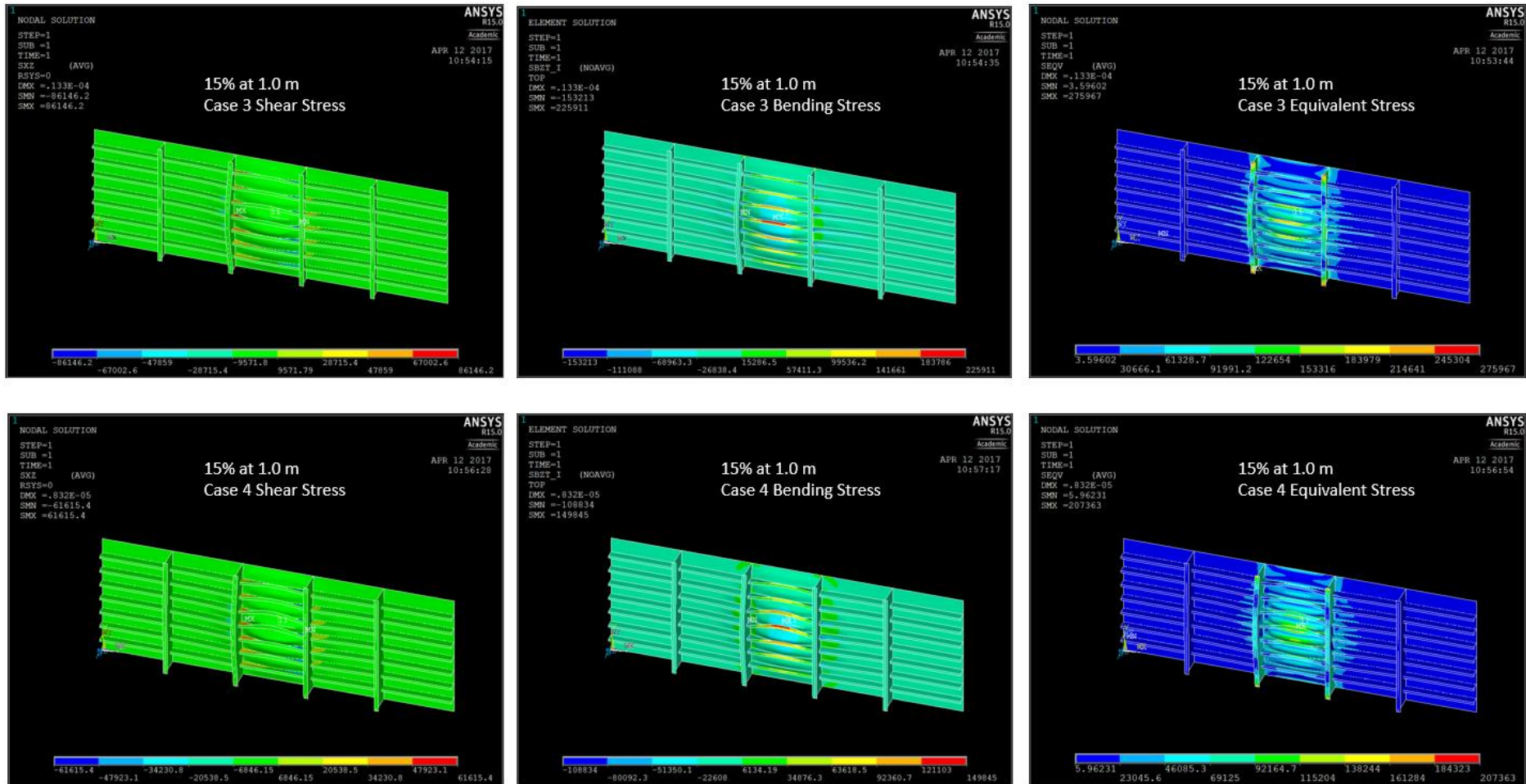


Figure B.17. Stresses of Case 3 and 4 at the condition of 15% of methane mixture and 1.0m ignition point.

## APPENDIX C

## LIST OF LNG-FUELLED SHIPS

Table C.1 shows the list of LNG-fuelled ships as of today, in 2018.

Table C.1. List of LNG-fuelled ships

No.	Ship name	Ship type	Delivery date	Owner
1	Glutra	Car pax ferry	2000	Fjord1
2	Bergensfjord	Car pax ferry	2006	Fjord1
3	Stavangerfjord	Car pax ferry	2007	Fjord1
4	Raunefjord	Car pax ferry	2007	Fjord1
5	Mastrafjord	Car pax ferry	2007	Fjord1
6	Fanafjord	Car pax ferry	2007	Fjord1
7	Tidekongen	Car pax ferry	2009	Tide Sjø
8	Tidedronnigen	Car pax ferry	2009	Tide Sjø
9	Tideprinsen	Car pax ferry	2009	Tide Sjø
10	Moldefjord	Car pax ferry	2009	Fjord1
11	Fannefjord	Car pax ferry	2010	Fjord1
12	Romsdalfjord	Car pax ferry	2010	Fjord1
13	Korsfjord	Car pax ferry	2010	Fjord1
14	Selbjørnsfjord	Car pax ferry	2010	Fosen Namsos Sjø
15	Tresfjord	Car pax ferry	2011	Fjord1
16	Boknafjord	Car pax ferry	2012	Fjord1
17	Landegode	Car pax ferry	2012	Torghatten Nord
18	Værøy	Car pax ferry	2012	Torghatten Nord
19	Barøy	Car pax ferry	2013	Torghatten Nord
20	Lødingen	Car pax ferry	2013	Torghatten Nord
21	Viking Grace	Car pax ferry	2013	Vking Line
22	Stavangerfjord	Car pax ferry	2013	Fjord Line
23	Bergensfjord	Car pax ferry	2013	Fjord Line
24	Francisco	High-speed ferry	2013	Buquebus
25	Hardanger	Car pax ferry	2013	Norled
26	Ryfylke	Car pax ferry	2013	Norled
27	FA Gauthier	Car pax ferry	2015	STQ Quebec
28	Ostfriesland*	Car pax ferry	2015	AG Ems
29	Helgoland	Car pax ferry	2015	AG Ems
30	Samsø	Car pax ferry	2015	Samsø Municipality

31	Stril Pioneer	PSV	2003	Møkster
32	Viking Energy	PSV	2003	Eidesvik
33	Viking Queen	PSV	2008	Eidesvik
34	Viking Lady	PSV	2009	Eidesvik
35	Barentshav	Patrol vessel	2009	Remøy
36	Bergen	Patrol vessel	2010	Remøy
37	Sortland	Patrol vessel	2010	Remøy
38	Skandi Gamma	PSV	2011	DOF
39	Normand Arctic	PSV	2011	Solstad
40	Viking Prince	PSV	2012	Eidesvik
41	Viking Princess	PSV	2012	Eidesvik
42	Island Crusader	PSV	2012	Solstad
43	Island Contender	PSV	2012	Solstad
44	Olympic Energy	PSV	2012	Solstad
45	Rem Leader	PSV	2013	Remøy Shipping
46	Econuri	Harbour vessel	2013	Incheon Port Authority
47	Hai Yang Shi You	Tug	2013	CNOOC
48	Hai Yang Shi You 521	Tug	2013	CNOOC
49	Borgøy	Tug	2014	Buksér og Berging
50	Bokn	Tug	2014	Buksér og Berging
51	Turva	Patrol vessel	2014	Finnish Border Guard
52	Stril Barents	PSV	2015	Møkster
53	Harvey Energy	PSV	2015	Harvey Gulf
54	Harvey Power	PSV	2015	Harvey Gulf
55	Harvey Liberty	PSV	2016	Harvey Gulf
56	Rem Eir	PSV	2015	Remøy Shipping
57	Hai Yang Shi You 525	Tug	2015	CNOOC
58	Siem Symphony	PSV	2015	Siem Offshore
59	Siem Pride	PSV	2015	Siem Offshore
60	Sakigaki	Tug	2015	NYK Line
61	Høydal	Fishfeed carrier	2012	Nordnorsk Shipping
62	Eidsvaag Pioneer	Fishfeed carrier	2013	Eidsvaag
63	With Harvest	Fishfeed carrier	2014	Egil Ulvan
64	With Marine	Fishfeed carrier	2014	Egil Ulvan
65	Kvitbjørn	Ro-ro cargo	2015	NorLines
66	Kvitnos	Ro-ro cargo	2015	NorLines
67	Isla Bella	Container ship	2015	TOTE
68	Perla del Caribe	Container ship	2016	TOTE
69	Bit Viking*	Product tanker	2011	Tarbit
70	Coral Star	Ethylene carrier	2014	Anthony Veder



71	Coral Sticho	Ethylene carrier	2014	Anthony Veder
72	Bergen Viking*	Product tanker	2015	Bergen Tankers
73	Sefarina	LPG carrier	2015	Chemgas Shipping
74	Greenland	Cement carrier	2015	JT Cement
75	Argonon*	Tank vessel	2011	Deen Shipping
76	Greenstream	Tank vessel	2013	Inter Barging
77	Greenrhine	Tank vessel	2013	Inter Barging
78	Sirocco	Gas tank vessel	2014	Chemgas Barging
79	Eiger-Nordwand*	Container vessel	2014	Danser
80	Green 6002	Bulk carrier vessel	2015	Shanghai Green Power
81	Armand-Imbeau II	Car pax ferry	2016	STQ Quebec
82	Jos-Deschênes II	Car pax ferry	2016	STQ Quebec
83	Abel Matutes*	Car pax ferry	2016	Baleària
84	unnamed	Car pax ferry	2016	Boreal Transport
85	unnamed	Car pax ferry	2016	Boreal Transport
86	unnamed	Car pax ferry	2016	Seaspan
87	unnamed	Car pax ferry	2016	Seaspan
88	Salish Orca	Car pax ferry	2016	BC Ferries
89	Salish Eagle	Car pax ferry	2017	BC Ferries
90	Salish Raven	Car pax ferry	2017	BC Ferries
91	unnamed	Car pax ferry	2017	Rederi AB Gotland
92	unnamed	Car pax ferry	2017	Rederi AB Gotland
93	Spirit of Vancouver Island*	Car pax ferry	2017	BC Ferries
94	Spirit of British Columbia*	Car pax ferry	2018	BC Ferries
95	Megastar	Car pax ferry	2017	Tallink
96	unnamed	Cruise ship	2019	AIDA (Carnival Group)
97	unnamed	Cruise ship	2020	AIDA (Carnival Group)
98	unnamed	Cruise ship	2019	Costa (Carnival Group)
99	unnamed	Cruise ship	2020	Costa (Carnival Group)
100	unnamed	Car pax ferry	2018	CalMac
101	unnamed	Car pax ferry	2018	CalMac
102	unnamed	Car pax ferry	2019	Baleària
103	unnamed	Car pax ferry	2019	Baleària
104	unnamed	Tug	2016	CNOOC
105	Elemaratayeh	Tug	2016	Dubai Maritime City
106	Harvey Freedom	PSV	2016	Harvey Gulf
107	Harvey America	PSV	2017	Harvey Gulf
108	Harvey Patriot	PSV	2017	Harvey Gulf
109	unnamed	PSV	2016	Siem Offshore

110	Siem Harmony	PSV	2016	Siem Offshore
111	Siem Melody	PSV	2016	Siem Offshore
112	Siem Rhapsody	PSV	2016	Siem Offshore
113	unnamed	Icebreaker	2016	Finnish Transport Agency
114	Scheldt River	Dredger	2016	DEME
115	Minerva	Dredger	2016	DEME
116	Bonny River	Dredger	2017	DEME
117	Apollo	Jack-up rig	2017	DEME
118	Livingstone	Cable-layer	2017	DEME
119	unnamed	Semisub crane vessel	2017	Heerema
120	unnamed	Tug	2017	Ø stensjø Rederi
121	unnamed	Tug	2017	Ø stensjø Rederi
122	unnamed	Tug	2017	Ø stensjø Rederi
123	unnamed	Tug	2017	Ningbo Port Company
124	unnamed	Container ship	2016	Brodosplit Navigation
125	unnamed	Container ship	2016	Brodosplit Navigation
126	unnamed	Container ship	2017	Brodosplit Navigation
127	unnamed	Container ship	2017	Brodosplit Navigation
128	unnamed	Ro-ro cargo	2016	SeaRoad
129	Wes Amelie*	Container ship	2016	Wessels Reederei
130	unnamed	Car carrier	2016	UECC
131	unnamed	Car carrier	2016	UECC
132	unnamed	Container ship	2016	Containerships
133	unnamed	Container ship	2016	Containerships
134	unnamed	Container ship	2017	Containerships
135	unnamed	Container ship	2017	Containerships
136	unnamed	Container ship	2017	Containerships
137	unnamed	Container ship	2017	Containerships
138	Taino	Container ro-ro	2017	Crowley Maritime
139	El Coqui	Container ro-ro	2017	Crowley Maritime
140	unnamed	Fishfeed carrier	2018	Nordnorsk Shipping
141	Daniel K Inouye	Container ship	2018	Matson Navigation
142	unnamed	Container ship	2018	Matson Navigation
143	Midnight Sun*	Container ship	2018	TOTE
144	North Star*	Container ship	2018	TOTE
145	Fure West*	Product tanker	2016	Furetank
146	Sundowner	LPG carrier	2016	Chemgas Shipping
147	Ternsund	Product/chemical tanker	2016	Terntank
148	unnamed	Product/chemical tanker	2016	Terntank

149	unnamed	Product/chemical tanker	2016	Terntank
150	unnamed	Product/chemical tanker	2017	Terntank
151	unnamed	CNG carrier	2016	CIMC Enric SZJ Gas
152	unnamed	Ethane carrier	2016	Ocean Yield
153	unnamed	Ethane carrier	2016	Ocean Yield
154	unnamed	Ethane carrier	2016	Ocean Yield
155	Damia Desgagnés	Bitumen tanker	2016	Groupe Desgagnés
156	Mia Desgagnés	Product/chemical tanker	2016	Groupe Desgagnés
157	unnamed	Product/chemical tanker	2017	Groupe Desgagnés
158	unnamed	Product/chemical tanker	2017	Groupe Desgagnés
159	unnamed	Ethane carrier	2016	Navigator Gas
160	unnamed	Ethane carrier	2016	Navigator Gas
161	unnamed	Ethane carrier	2016	Navigator Gas
162	unnamed	Ethane carrier	2016	Navigator Gas
163	unnamed	Bulk carrier	2018	ESL Shipping
164	unnamed	Bulk carrier	2018	ESL Shipping
165	unnamed	Ethane carrier	2018	Evergas
166	unnamed	Ethane carrier	2018	Evergas
167	unnamed	Ethane carrier	2018	Evergas
168	unnamed	Ethane carrier	2019	Evergas
169	Calypso*	Bulk carrier vessel	2016	Pro-Combi
170	EcoLiner No 1	Tank vessel	2016	Damen
171	unnamed	Hopper barge	2016	Bremenports
172	unnamed	Tank vessel	2016	Plouvier/Intertrans
173	unnamed	Tank vessel	2016	Plouvier/Intertrans
174	unnamed	Tank vessel	2016	Plouvier/Intertrans
175	unnamed	Tank vessel	2017	Plouvier/Intertrans
176	unnamed	Tank vessel	2017	Plouvier/Intertrans
177	unnamed	Tank vessel	2017	Plouvier/Intertrans
178	unnamed	Tank vessel	2017	Plouvier/Intertrans
179	unnamed	Tank vessel	2017	Plouvier/Intertrans
180	unnamed	Tank vessel	2017	Plouvier/Intertrans
181	unnamed	Tank vessel	2017	Plouvier/Intertrans
182	unnamed	Tank vessel	2018	Plouvier/Intertrans
183	unnamed	Tank vessel	2018	Plouvier/Intertrans
184	unnamed	Tank vessel	2018	Plouvier/Intertrans
185	unnamed	Tank vessel	2018	Plouvier/Intertrans
186	unnamed	Tank vessel	2018	Plouvier/Intertrans